Part I: Synthesis and Characterization of Sulfur-Bridged Oligothiophenes

Part II: Exploratory Syntheses Toward Dioxadiazinyl Radicals

by

Daniel John Talbot Myles
B.Sc., University of Waterloo, 2000

A Dissertation Submitted in Partial Fulfillment of the
Requirements for the Degree of

DOCTOR OF PHILOSOPHY

in the Department of Chemistry

Supervisor: Dr. Robin G. Hicks

ABSTRACT

A series of new model oligothiophenes capped with mesitylthio groups and bridged by divalent sulfur were prepared and characterized. The synthesis of the capped oligomers was accomplished by either convergent or divergent protocols. In the convergent approach, a series of unsymmetrical oligomers, bearing one mesitylthio group, with various conjugation lengths and substitution patterns of thiophene and 3,4-ethylenedioxythiophene (EDOT) were assembled by metal catalyzed cross coupling reactions. The internal sulfur bridge was inserted by reaction of the α-lithiated unsymmetrical oligothiophenes with bis(phenylsulfonyl)sulfide. In the divergent approach, the terminal mesitylthio groups were introduced by reactions of α-dilithiated or α-dibrominated bis(oligothienyl)sulfides with two equivalents of 2-mesitylenesulfenyl chloride or 2-mesitylenethiol, respectively. All of the oligothiophenes were characterized using elemental analysis, mass spectrometry, and $^{1}H/^{13}C$ NMR spectroscopies. The capped oligomers were either chemically or electrochemically oxidized to their corresponding radical cations and dications, and these were characterized by UV-Vis-NIR spectroscopy. The UV-Vis-NIR studies revealed that when electron-rich EDOTs are placed directly adjacent to the internal sulfur bridge then strong intramolecular electronic communication occurs for the cationic species. However, replacing the adjacent EDOTs with thiophene or by increasing the conjugation length leads to a weakening of the electronic communication through the internal sulfur bridge.

A new class of EDOT and thiophene containing sulfide polymers were then prepared by electrochemical anodic oxidation of α-uncapped monomer precursors. The polymers were expected to exhibit excellent charge transport properties and stability based on the model compound studies. Preliminary investigations on the electronic properties of the polymers have been achieved by *in-situ* spectroelectrochemistry on ITO electrodes. Further insights into their electronic structures have been made by appropriate comparisons to the α-capped model compounds.

The second part of this thesis describes synthetic routes to an unknown class of dioxadiazinyl radicals. The routes resemble those that have been established for the synthesis of the closely related verdazyl radicals. In this regard, an *O*-silylated chloroxime was prepared, fully characterized, and its reactions with hydroxylamine were investigated. Unfortunately, the targeted 6-siladioxadiazane was not formed, but rather *N*-hydroxy-*p*-toluamidoxime. The mechanistic details of this unexpected outcome were then briefly explored. The second approach involves the attempted ring-closing reactions of *O,O'*-bis(hydroxylamino)methane with a range of aldehydes. In all instances, mixtures of mono- and bis-imines were exclusively formed, and not the desired 6-membered ring products.

Supervisor: R. G. Hicks, (Department of Chemistry)

TABLE OF CONTENTS

List of Tables

List of Figures

List of Schemes

List of Abbreviations

a	hyperfine coupling constant
A	absorbance
Å	angstroms
Ag/AgCl	silver/silver chloride reference electrode
Ar	aryl substituent
BCO	bicyclo[2.2.2]octene
br	broad (IR and NMR descriptor)
bp	boiling point
Bu	butyl
^{o}C	degrees Celsius
CB	conduction band
cm	centimeter
CPDT	cyclopentadithiophene
CV	cyclic voltammetry
d	doublet (NMR descriptor)
dba	dibenzylacetone
DFT	density functional theory
DMF	dimethylformamide
DMSO	dimethylsulfoxide
DPPH	diphenylpicrylhydrazyl
dppp	diphenylphosphinopropane
E	3,4-ethylenedioxythiophene

E_g	band gap energy
E^o	formal potential
E_{pa}	peak anodic potential
E_{pc}	peak cathodic potential
EAS	electrophilic aromatic substitution
ECL	effective conjugation length
EDOT	3,4-ethylenedioxythiophene
EHMO	extended Hückel molecular orbital
EI	electron impact
EPR	electron paramagnetic resonance
ESR	electron spin resonance
Et	ethyl
Et_3N	triethylamine
EtOAc	ethyl acetate
EtOH	ethanol
Et_2O	diethyl ether
eV	electron volt
EWG	electron withdrawing group
FAB	fast atom bombardment
Fc	ferrocene
FCU	ferromagnetic coupling unit
FET	field effect transistor
G	gauss

H	hour(s)
HH	head to head
hfac	hexafluoroacetylacetonate
HMO	Hückel molecular orbital
HOMO	highest occupied molecular orbital
HRMS	high resolution mass spectrometry
HT	head to tail
Hz	Hertz
i_{pa}	peak anodic current
i_{pc}	peak cathodic current
im	imidazole
IR	infrared
ITO	indium thin oxide
J	coupling constant
K	Kelvin
kcal	kilocalorie
kJ	kilojoule
L	litre
LCAO	linear combination of atomic orbitals
LED	light emitting diode
LSIMS	liquid secondary ion mass spectrometry
LUMO	lowest unoccupied molecular orbital
m	multiplet (NMR descriptor) or medium (IR descriptor)

M	molarity
$M^{\bullet+}$	molecular ion
Me	methyl
MeOH	methanol
Mes	mesitylene
mg	milligram
MHz	megahertz
min	minute(s)
mL	milliliters
mol	mol
mmol	millimole
MO	molecular orbital
Mp	melting point
MS	mass spectrometry
mV	millivolt
m/z	mass per charge
n-BuLi	*normal*-butyllithium
NBS	*N*-bromosuccinimide
NCS	*N*-chlorosuccinimide
NIR	near infrared
nm	nanometer
NMR	nuclear magnetic resonance
[o]	oxidation

OLED	organic light emitting diode
P3AT	poly(3-alkyl)thiophene
PA	polyacetylene
PANI	polyaniline
PEDOT	polyethylenedioxythiophene
Ph	phenyl
ppm	parts per million
PPS	poly(*p*-phenylene)sulfide
PPy	polypyrrole
PT	polythiophene
q	quartet (NMR descriptor)
R	generic functional group
RT	room temperature
s	singlet (NMR descriptor) or strong (IR descriptor) or second(s)
SAM	self assembled monolayer
sh	shoulder
SCE	saturated calomel electrode
SOMO	singly occupied molecular orbital
t	triplet (NMR descriptor)
T	thiophene
T_c	critical temperature
TT	tail to tail
*t*Bu	tertiary butyl

THF	tetrahydrofuran
TLC	thin layer chromatography
TMEDA	tetramethylethylenediamine
UV	ultraviolet
V	volt
VB	valence band
vis	visible
vs	very strong (IR descriptor) or versus
vw	very weak (IR descriptor)
w	weak (IR descriptor)
δ	chemical shift in parts per million
ε	extinction coefficient (M^{-1} cm^{-1})
λ_{max}	maximum wavelength absorption
μ	mobility (cm^2 V^{-1} s^{-1})
ν	frequency

List of Numbered Compounds

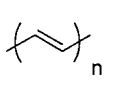

1.1

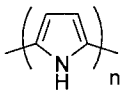

1.2

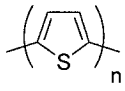

1.3

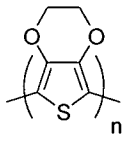

1.4

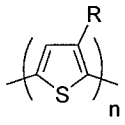

1.5

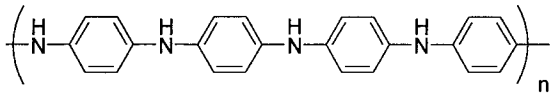

1.6

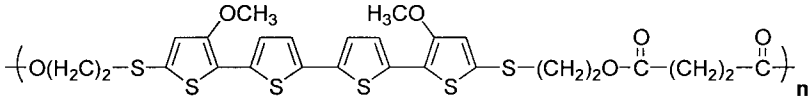

1.7

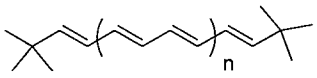

1.8 n = 1-3

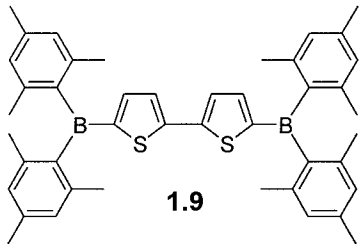

1.9

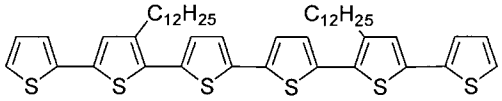

1.10

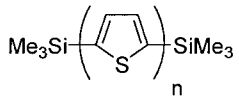

1.11 (n = 2)
1.12 (n = 3)

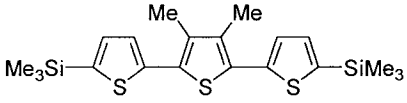

1.13

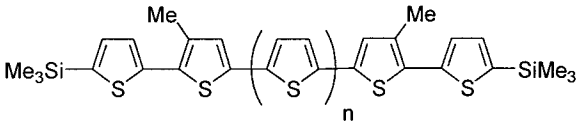

1.14 (n = 0)
1.15 (n = 1)

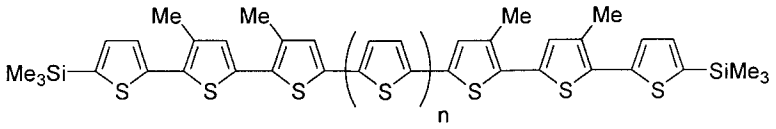

1.16 (n = 1)
1.17 (n = 2)

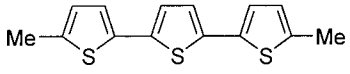

1.18

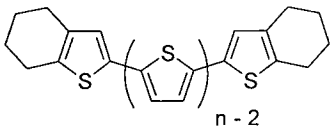

1.19 (n = 3)
1.20 (n = 4)
1.21 (n = 5)

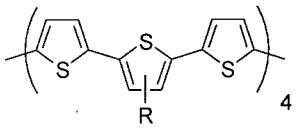

1.22 (R = $C_{10}H_{21}$)
1.23 (R = $C_{12}H_{25}$)

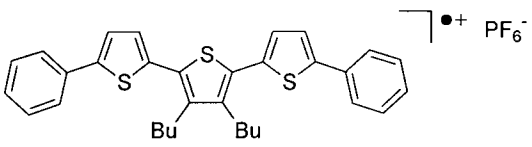

1.24

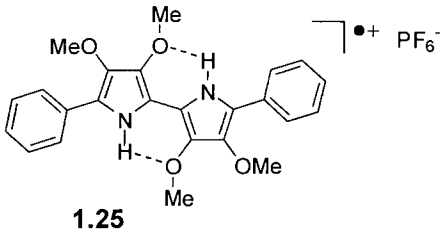

1.25

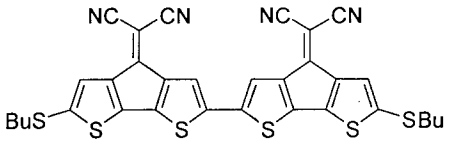

1.26

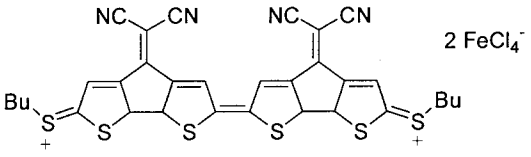

1.27

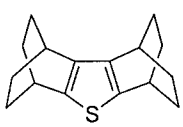

1.28

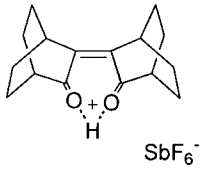

1.29

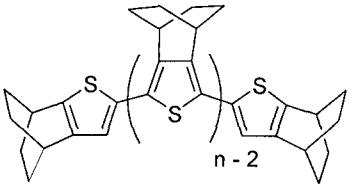

1.30 (n = 2)
1.31 (n = 3)
1.32 (n = 4)
1.33 (n = 6)

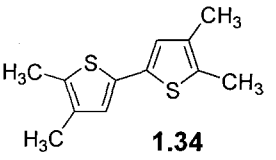

1.34

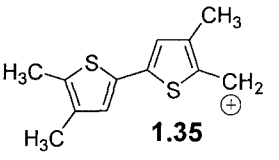

1.35

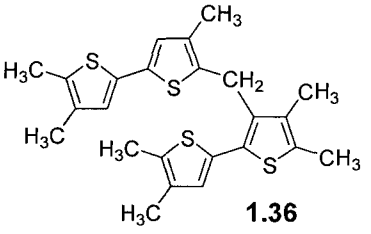

1.36

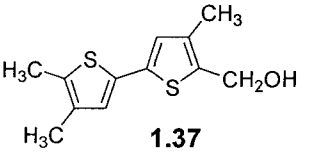

1.37

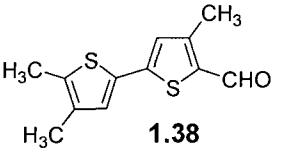

1.38

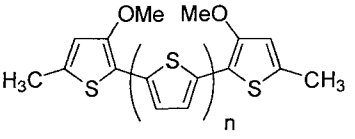

1.39 (n = 0)
1.40 (n = 1)
1.41 (n = 2)
1.42 (n = 3)

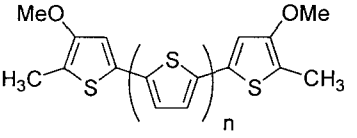

1.43 (n = 0)
1.44 (n = 1)
1.45 (n = 2)

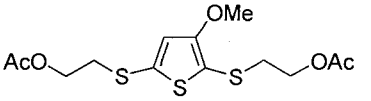

1.46

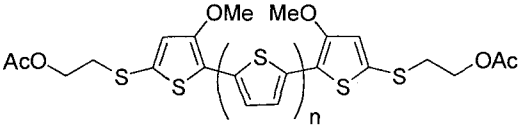

1.47 (n = 0)
1.48 (n = 1)
1.49 (n = 2)

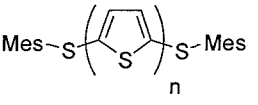

1.50 (n = 1)
1.51 (n = 2)
1.52 (n = 3)
1.53 (n = 4)

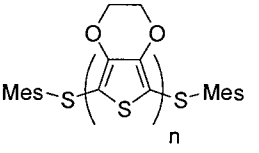

1.54 (n = 1)
1.55 (n = 2)
1.56 (n = 3)

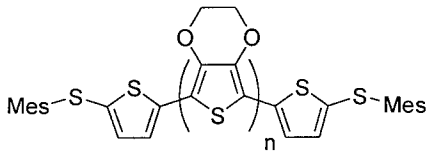

1.57 (n = 1)
1.58 (n = 2)

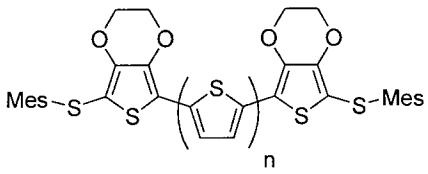

1.59 (n = 1)
1.60 (n = 2)

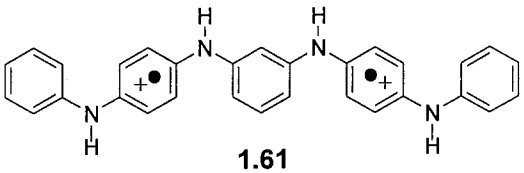

1.61

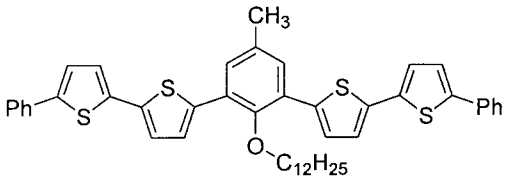

1.62

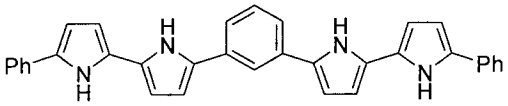

1.63

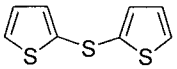

2.1

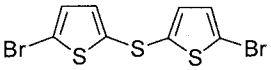

2.2

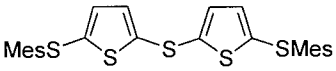

2.3

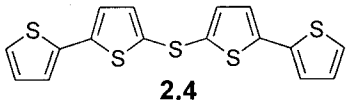

2.4

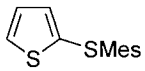

2.5

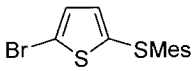

2.6

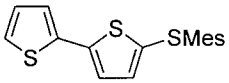

2.7

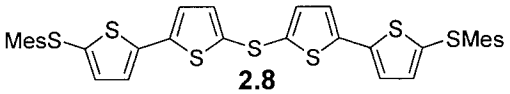

2.8

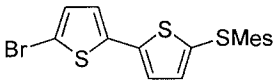

2.9

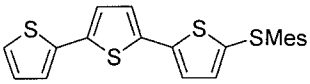

2.10

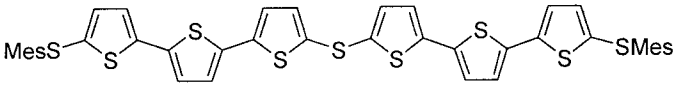

2.11

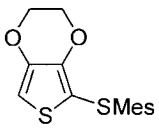

2.12

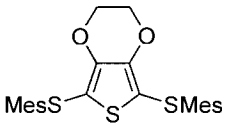

2.13

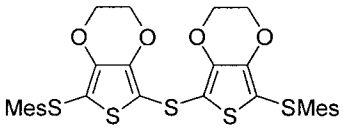

2.14

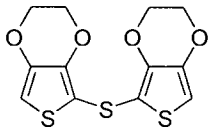

2.15

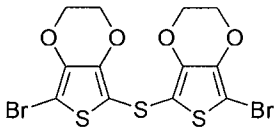

2.16

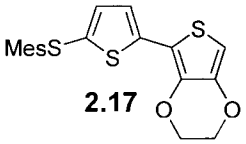

2.17

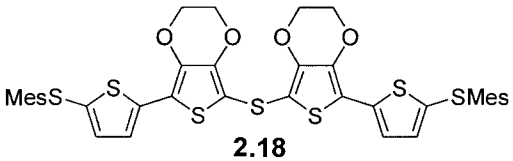

2.18

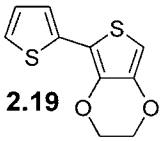

2.19

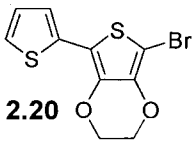

2.20

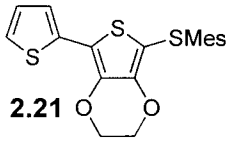

2.21

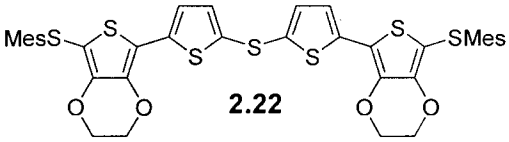

2.22

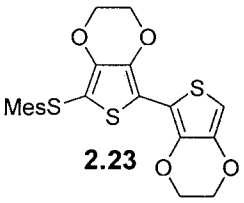

2.23

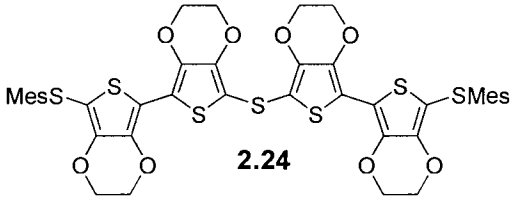

2.24

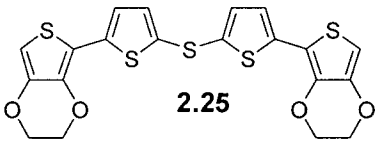

2.25

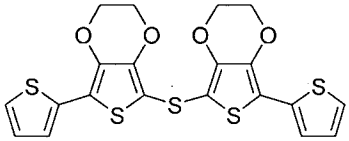

2.26

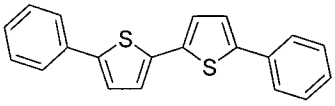

3.1

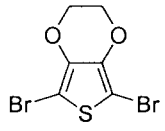

3.2

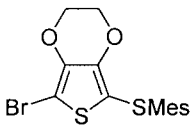

3.3

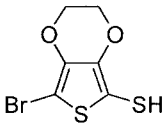

3.4

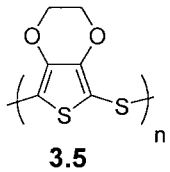

3.5

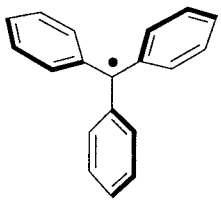

4.1

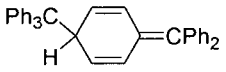

4.2

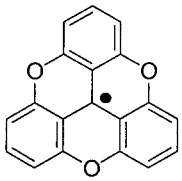

4.3

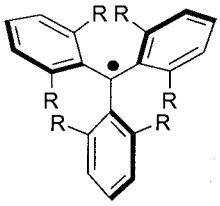

4.4 (R = OMe)

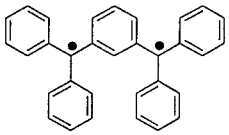

4.5

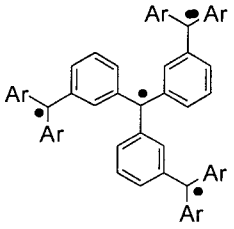

4.6 (Ar = *p*-^{t}BuC$_6$H$_4$)

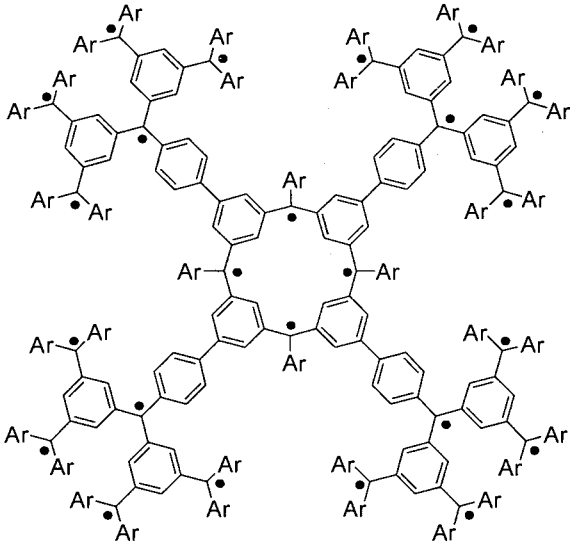

4.7 (Ar = *p*-^{t}BuC$_6$H$_4$)

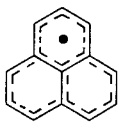

4.8

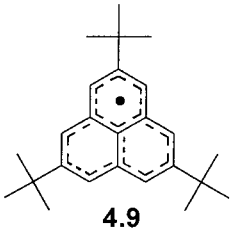

4.9

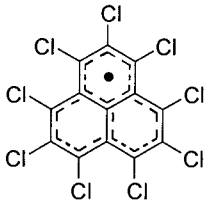

4.10

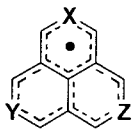

4.11 (X = N; Y, Z = CH)
4.12 (X, Y, Z = N)

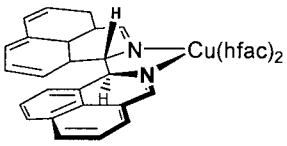

4.13

4.14

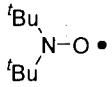

4.15

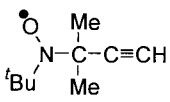

4.16

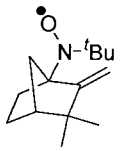

4.17

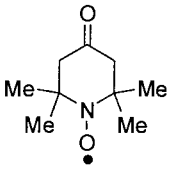

4.18

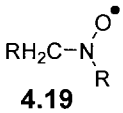

4.19

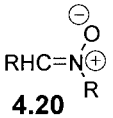

4.20

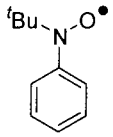

4.21

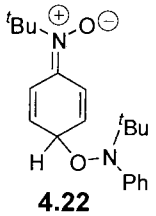

4.22

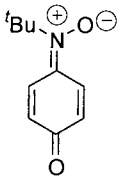

4.23

4.24

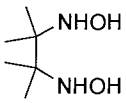

4.25

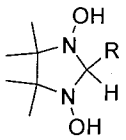

4.26

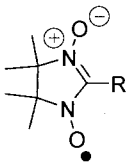

4.27

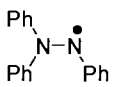

4.28

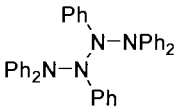

4.29

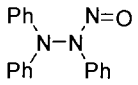

4.30

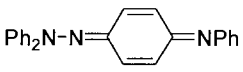

4.31

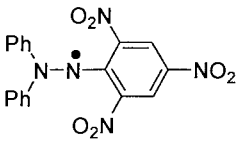

4.32

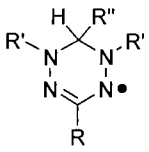

4.33

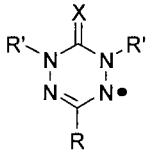

4.34

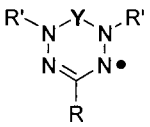

4.35

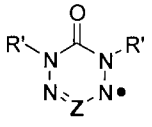

4.36

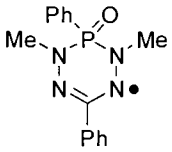

4.37

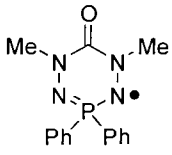

4.38

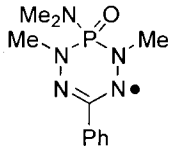

4.39

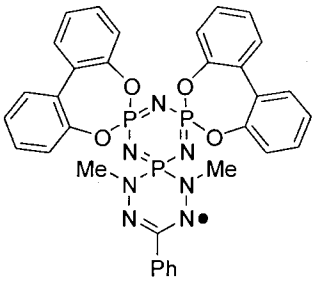

4.40

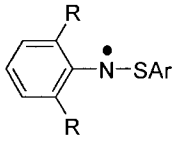

4.41

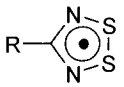

4.42

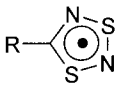

4.43

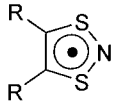

4.44

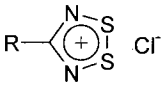

4.45

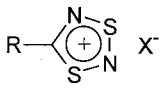

4.46

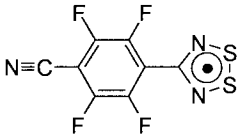

4.47

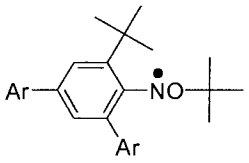

4.48

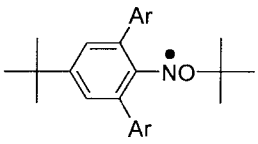

4.49

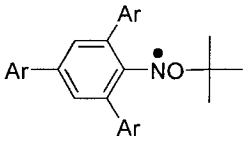

4.50

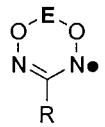

5.1

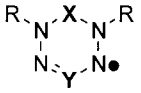

5.2

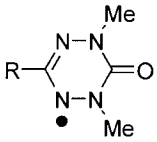

5.3

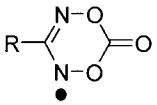

5.4

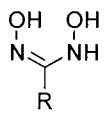

5.5

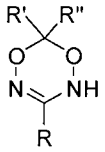

5.6

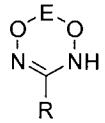

5.7

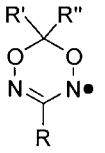

5.8

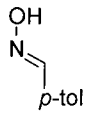

5.9

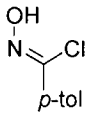

5.10

5.11

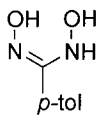

5.12

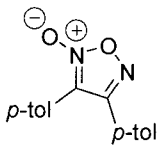

5.13

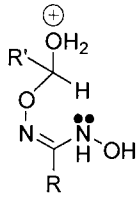

5.14

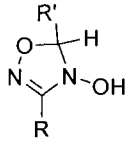

(**5.15**) R = Ph, R' = Et
(**5.16**) R = Ph, R' = *p*-NO_2
(**5.17**) R = *p*-tol, R' = Et
(**5.18**) R = *p*-tol, R' = *p*-tol

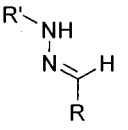

5.19

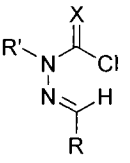

5.20

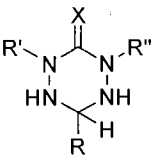

5.21

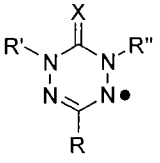

5.22

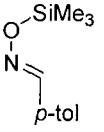

5.23

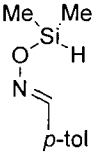

5.24

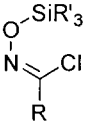

5.25

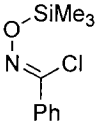

5.26

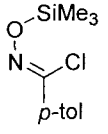

5.27

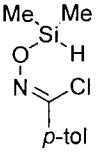

5.28

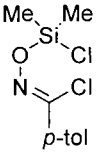

5.29

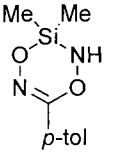

5.30

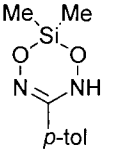

5.31

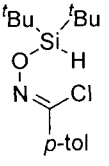

5.32

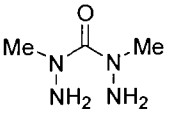

5.33

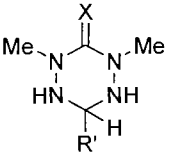

5.34

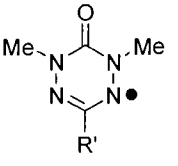

5.35

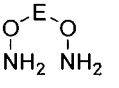

5.36

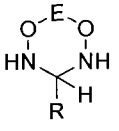

5.37

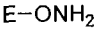

5.38

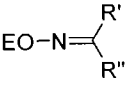

5.39

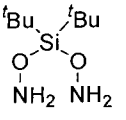

5.40

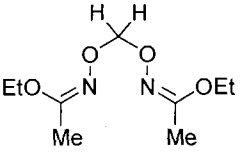

5.41

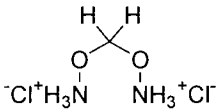

5.42

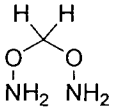

5.43

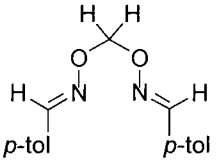

5.44

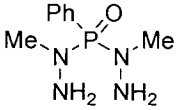

5.45

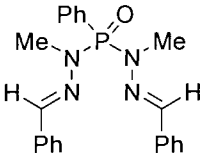

5.46

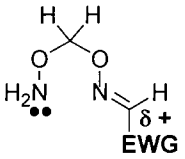

5.47

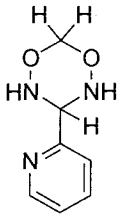

5.48

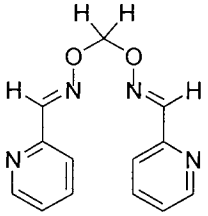

5.49

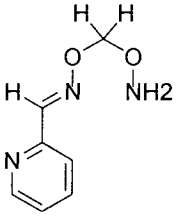

5.50

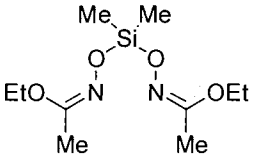

5.51

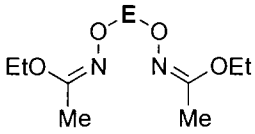

(**5.52**) E = C(O)
(**5.53**) E = PR_3
(**5.54**) E = RP(O)

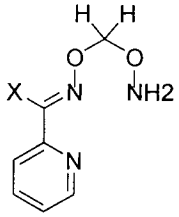

(**5.55**) X = Br
(**5.56**) X = Cl

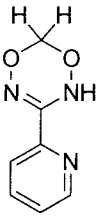

5.57

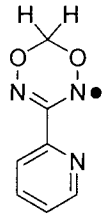

5.58

Acknowledgements

First and foremost I wish to acknowledge my supervisor, Professor Robin G. Hicks, for his guidance and support during my Ph.D. studies. His enthusiasm for science and his friendship has made my time here very enjoyable, and these will never be forgotten. I could not have asked for a better supervisor.

I wish to acknowledge a first class group of scientists and friends who have shared the lab with me over the years. Firstly, I would like to thank Dr. M'hamed Chahma, who was the only other individual working on thiophene chemistry during my time in the Hicks group. He taught me a great deal about electrochemistry, and helped considerably with the poly(thienyl)sulfide work. I would also like to thank Dr. Greg Patenaude, Dr. Martin Lemaire, Bryan Koivisto, Steve McKinnon, Dr. Rajsapan Jain, Dr. Kabir Khayrul, Dr. Peter Otieno, Joe Gilroy, Sharon Caldwell, Kevin Anderson, and Tyler Trefz, all of whom have provided a very pleasant environment to work in.

I wish to thank the members of my supervisory committee, Prof. Cornelia Bohne, Prof. Reginald Mitchell, and Prof. Chris Pritchet for all of their help and advice over the years.

Lastly, I would like to thank the technicians and secretaries in the chemistry department, especially Dave McGillivray for mass spectral analysis and Chris Greenwood for all of her help with the specialized NMR experiments.

To, for, and with Patrycja

Chapter 1

Introduction and Context for Part I

1.1 Introduction

It was during the late 1970s that the first highly conducting polymer comprised solely of organic fragments was discovered. Since that time an intense amount of research worldwide has been devoted to the study of organic based π-conjugated polymers for their inherent bulk physical properties, such as their magnetic responses and electrical conductivities. Unlike conventional inorganic conducting materials (e.g., copper and doped silicon), which tend to be brittle and dense, organic polymers offer the potential to be light, flexible, soluble, and more easily processed. These promising attributes have allowed for them to be fabricated into small electronic devices such as organic field-effect transistors (FETs),[1] light emitting diodes (LEDs),[2] and sensors.[3]

One drawback of studying polymers lies in the complexity of trying to correlate the polymer's structure with its physical properties. This stems from the traditional methods used to prepare these polymers. They are normally made by either chemical or electrochemical techniques, which provide polydisperse materials that often contain structural defects. Polymerization methods have been developed recently to minimize such structural anomalies and these are discussed later in this chapter. The inherent distribution in molecular weights makes molecular scale understanding difficult, as measurements on bulk polydisperse samples provide an average value of the property in question.

The dearth of structure/property information with respect to π-conjugated organic polymers has prompted synthetic chemists to prepare smaller more easily characterized

oligomer analogues that mimic the structure of their polymer counterparts. The main incentive is to gain a sound understanding of how the physical properties of a discrete/monodisperse oligomer relates to its chain length or size. Physical properties for a hypothetical defect-free polymer can generally be estimated by extrapolating those from the model oligomer systems. In addition to oligomers acting as model compounds for their polymer congeners, they are also being used as materials in their own right, for example, as organic semiconductors.

The intention of this introductory chapter is to first review the more heavily studied π-conjugated organic polymers and to describe their electronic structures by using band theory. The synthetic techniques employed for the preparation of these will also be briefly mentioned. This will be followed by a survey of the synthesis and electronic properties of smaller molecules, emphasizing the use of the "oligomer approach". The electronic and structural features of several thiophene oligomers will then be described. This will lead into a discussion of hybrid conjugated thiophene oligomers that incorporate main group elements into their chains, especially those that are linked by divalent sulfur. The thiophene oligomers with sulfur end-groups, which have been synthesized and studied for their electronic properties previously in our group, form the basis of the work presented herein and as such will be discussed in some detail. The chapter will close with the aims and objectives for the first part of this thesis.

1.2 Survey of Conducting Polymers

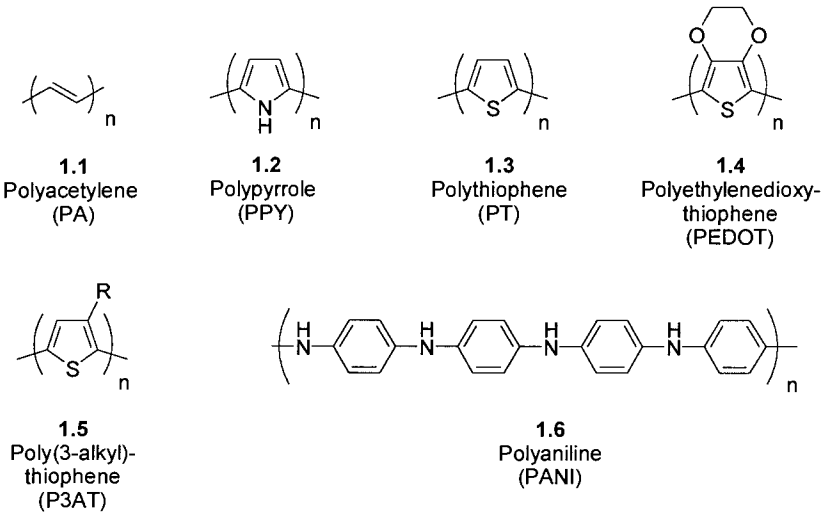

Figure 1.1. Most heavily studied conjugated organic polymers.

Polyacetylene (PA) (**1.1**) represents the earliest studied conducting organic polymer. PA itself can be prepared as a silvery compound by the polymerization of acetylene. It can exist in either the *cis* or *trans* form, but the latter is more thermodynamically stable. Neutral *trans*-PA can be p- or n-doped either chemically or electrochemically to the highly conducting state.[4] When iodine is used as the oxidant, an increase in conductivity from 10^{-5} S cm^{-1} to 10^{3} S cm^{-1} was observed.[5] Using arsenic pentafluoride (AsF_5) as the electron acceptor, an increased conductivity of 10^{5} S cm^{-1} (comparable to copper) has been obtained.[6] Reductive doping of *trans*-PA with alkali metals such as lithium, sodium, and potassium is also possible, but has received less attention because the resulting conductive polymers are extremely sensitive to moisture and air. More soluble hybrids of PA have also been prepared by substituting the acetylene backbone with various groups (e.g., CN, CF_3, Ph, etc.); however, the doped forms of these give lower conductivities with respect to the unsubstituted parent system.[7]

A common method for preparing polypyrroles (PPYs) (**1.2**) and polythiophenes (**1.3**) (PTs) is by electrochemical anodic oxidation of either a thiophene or pyrrole monomer, respectively.[8] The heterocycles couple predominantly through the more reactive 2- and 5-positions via highly reactive radical cation intermediates. The major advantage of this technique is that the doped polymer forms directly on the working electrode surface, which can be easily studied *in situ* (Figure 1.2). Unlike PA, the isolated

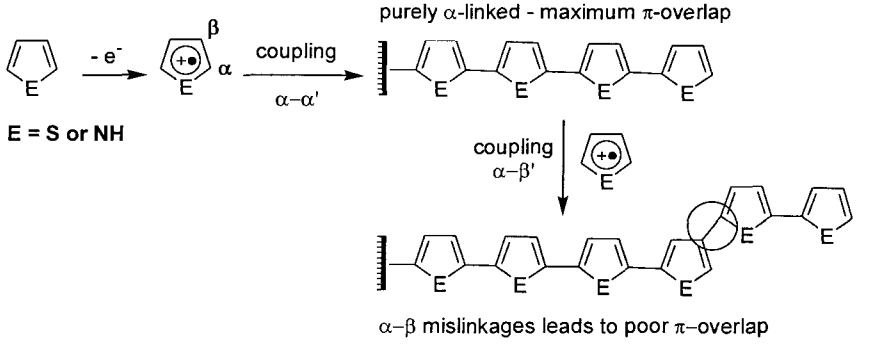

Figure 1.2. Electropolymerization pathways for the 5-membered heterocycles.

doped forms of PT and PPy exhibit good stability towards moisture and air; thereby rendering them easy to handle and use in real device applications. Their conductivities are typically on the order of 10^2 S cm^{-1}, considerably lower than PA, but largely dependent on the method of preparation.[9] Maximum conductivities for these two polymers are obtained when the heterocyclic rings are predominantly linked together in the α-positions, allowing for maximum π-overlap (Figure 1.2). Electropolymerization techniques suffer in that irregular α–β' couplings can also occur. These undesirable couplings become even more pronounced as the polymer length increases, which is detrimental to the polymers conductivity. Structural modifications have been made in attempts to avoid these structural mislinkages. For example, incorporation of an alkyl

group in the 3-position of a thiophene ring (i.e., 3-alkylthiophene) has been shown to remove unwanted α,β linkage defects upon polymerization.[10] The downside is that regiochemical defects can now form as a consequence of the unsymmetrical thiophene couplings (Figure 1.3). The undesirable head-to-head (HH) configuration disrupts the effective conjugation of the thiophene backbone by a severe steric interaction of the alkyl chains.

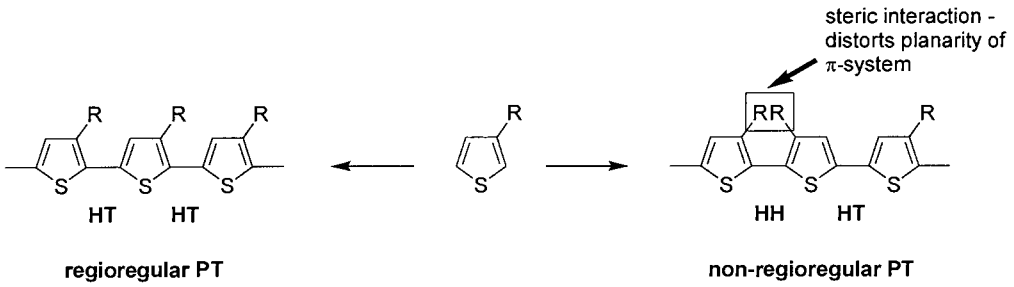

Figure 1.3. Polymerization of 3-alkylthiophene.

McCullough has used a chemical method to prepare a regioregular (approx. 100% HT-HT couplings) poly(3-alkyl)thiophene (P3AT) (**1.5**) via a Kumada polymerization (Scheme 1.1).[11] The resulting doped polymer shows significantly higher conductivity levels than those obtained by electrochemical methods.

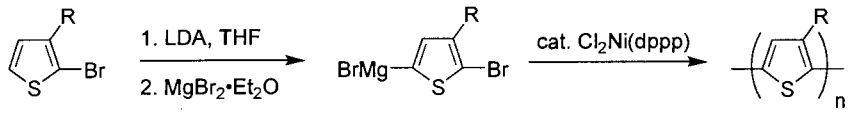

Scheme 1.1. Chemical polymerization to afford regioregular P3AT.

Another method used to avoid α–β mislinkages is by substituting both the 3- and 4-positions of the thiophene backbone. One important example of this is polyethylenedioxythiophene (PEDOT) (**1.4**). PEDOT can be prepared by chemical oxidation with $FeCl_3$ or by electrochemical methods to form a low band gap (E_g ~ 1.6 eV) polymer with exceptional environmental stability.[12] The enhanced stability is thought to arise from the electron-releasing ability of the oxygen atoms in the ethylenedioxy bridge to the positively charged polymer. The doped conductivities for the electrochemically generated polymers are typically on the order of 10^2 S cm^{-1}.[13]

The redox forms of polyaniline (PANI) (**1.6**) can be controlled by using acid-base chemistry.[14] The fully reduced form of PANI is referred to as "leuco-emeraldine" and in

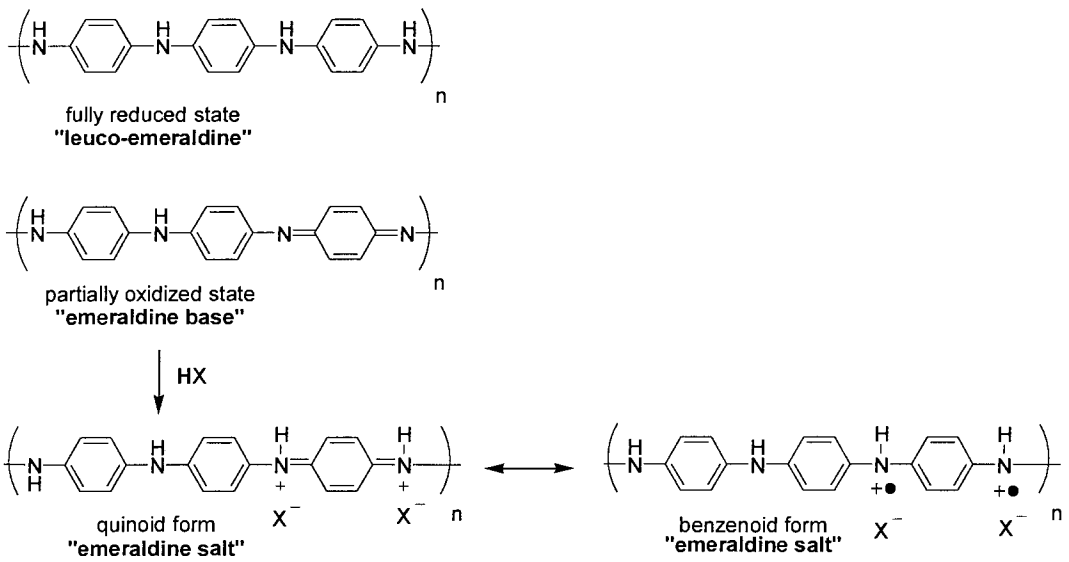

Figure 1.4. Various oxidation states of PANI.

this state the compound is an insulator (Figure 1.4). The polymer that is half-oxidized is called the "emeraldine base", and it is a semiconductor. The conductivity increases dramatically when the emeraldine base imine nitrogen atoms are protonated by strong

acid (e.g., aqueous HCl). The resulting "emeraldine salt" possesses delocalized radical cations and the material exhibits metallic-like conductivity as a result of a half filled π–band (see below). Conductivities as high as 10^5 S cm^{-1} have been obtained for the emeraldine salt form of PANI.[15]

1.3 Electronic Structure of π-Conjugated Polymers

The use of band theory for describing a molecular structure can be a complex task, as it brings together ideas from chemistry, solid-state physics, and mathematics. However, qualitative considerations based on Hückel molecular orbital (HMO) type semi-empirical methods allow for a basic picture of the electronic structure of conjugated polymers to be developed.

As a representative example, the band structure of an infinite chain of thiophenes is given (Figure 1.5). Thiophene itself possesses a π-bonding MO and a π*-antibonding MO within its frontier manifold. 2,2'-Bithiophene would then have a total of four MOs, which results from the linear combination of the MOs from two individual thiophene units. This process can be extrapolated to longer oligothiophenes, for instance, six thiophene units (i.e., sexithiophene) would contain a total of twelve MOs. An infinite chain length of thiophenes would then give rise to a fully occupied electronic band, as the energy levels become so closely spaced. This band is referred to as the valence band, whereas the band resulting from the combination of all the thiophene LUMOs is defined as the conduction band. These two bands are separated by an electronically forbidden region known as the band gap (E_g). The band picture shown in Figure 1.5 can also be used to describe several other neutral π-conjugated organic polymers (e.g., polypyrrole, poly(*p*-phenylene), polyacetylene, etc.).

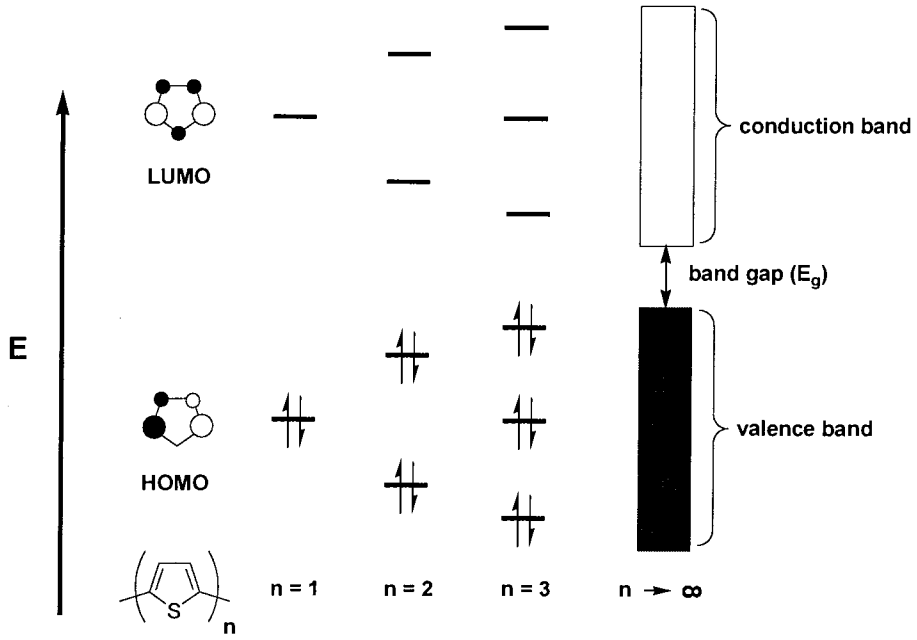

Figure 1.5. Band generation for an infinitely long thiophene.

The ability of a material to electrically conduct largely depends on the width of the band gap. Metallic like conductivity can be obtained when the band gap width is zero, thereby allowing electrons to be easily promoted into the conduction band (Figure 1.6). It

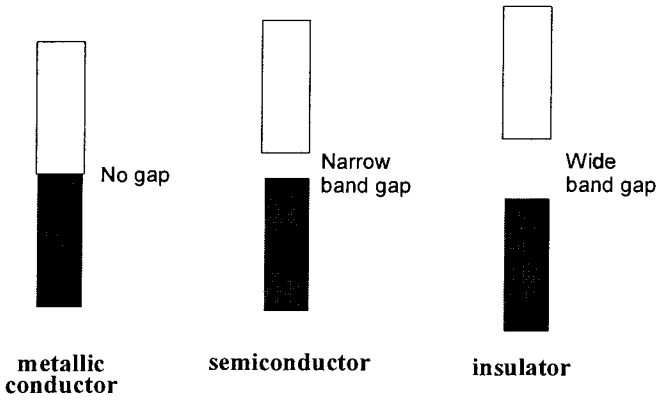

Figure 1.6. Electronic band structures.

is the resulting partially filled conduction and valence bands that give rise to the conductivity. A semiconductor has a non-zero band gap, and is usually defined by having

an energy gap of approximately 1 eV. In an intrinsic semiconductor the conduction band can be partially populated by thermally induced electronic excitations (Figure 1.7a). Increasing the temperature of an intrinsic semiconductor leads to an increase in the number of charge carriers followed by a concomitant increase in conductivity. Insulators are characterized by their wide band gaps (> 2 eV), and as such do not conduct because of the large energetic barrier to promote electrons from the valence to conduction band. The conductivity of a semiconductor can be further enhanced by increasing the number of charge carriers (holes or electrons) in the valence and/or conduction bands via chemical doping. Doping can be achieved by either removing electrons from the valence band, this being referred to as p-doping (oxidation) (Figure 1.7b) or by adding electrons to the conduction band via n-doping (reduction) processes (Figure 1.7c).

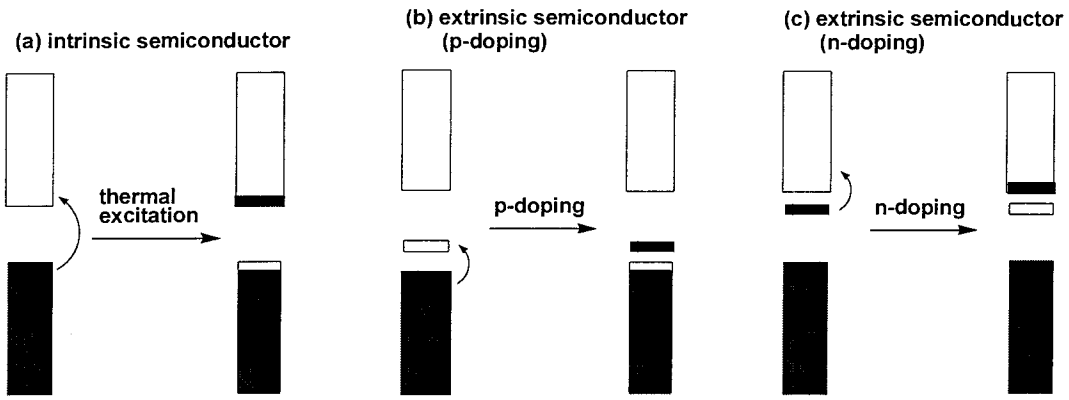

Figure 1.7. Intrinsic and extrinsic semiconductors.

All of the π-conjugated organic polymers, as discussed in §1.2, are insulators in their neutral forms, and must be doped to become conductive. Electron paramagnetic resonance (EPR) studies on several heavily doped π-conjugated polymers, such as polyacetylene, polyphenylene, and polypyrrole have confirmed that these materials

contain very low spin counts. Therefore, the high conductivity in these systems cannot be attributed to partially filled valence or conduction bands, as described by simple band theory (see above), but rather via spinless charge carriers.

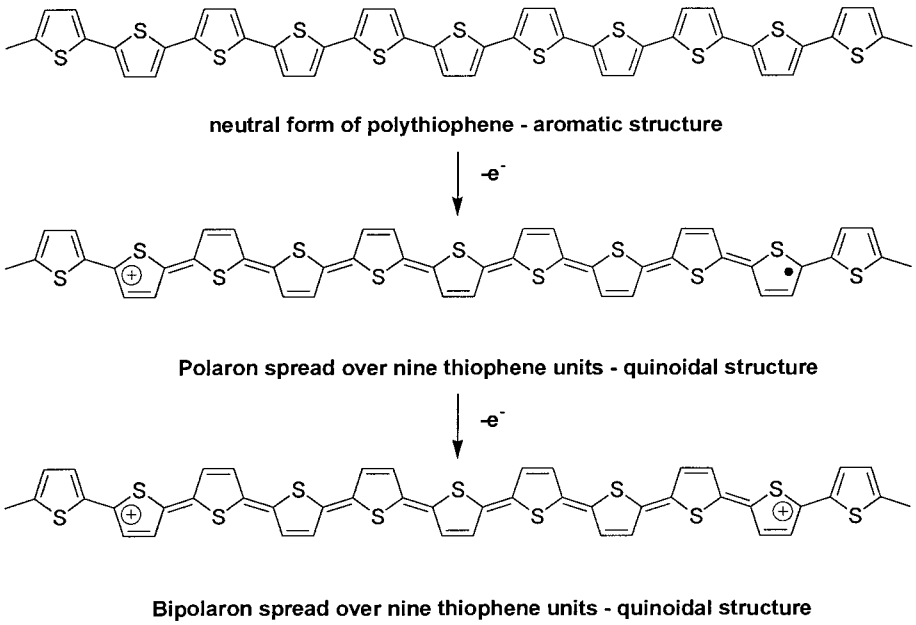

Figure 1.8. Polaron and bipolaron formation in polythiophene.

Removal of an electron from the top of the valence band of a conjugated polymer, for example polythiophene, results in the formation of a radical cation (Figure 1.8). The radical cation is free to delocalize over a few units which causes structural defects in the polymer. In solid-state physics, a radical cation that is confined to a small segment of a polymer is called a polaron. The energy associated with this polaron represents a destabilized bonding orbital, and thus appears as an electronic state at slightly higher energy than the valence band (Figure 1.9). Removal of a second electron forms a dication, which is referred to as a bipolaron. The polaron and bipolaron have an approximate delocalization length of nine thiophene units, which has been determined by

theory and model compound studies.[16] Heavy doping can then lead to bipolaron band formation, at the expense of removing states from the conduction and valence bands (Figure 1.9). It is the formation of these new subgap bands that are responsible for the conduction in organic polymers.

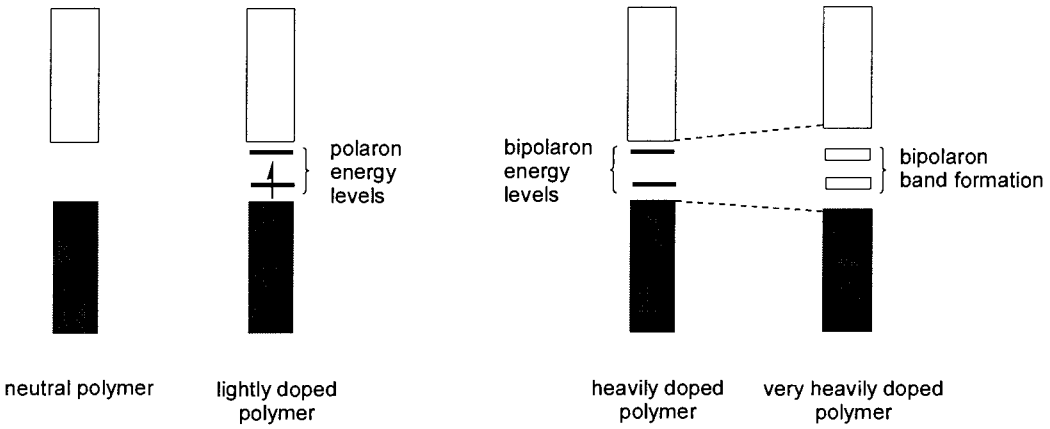

Figure 1.9. Band structures for doped π-conjugated organic polymers.

The theory of polaron/bipolaron formation is applicable to other π-conjugated organic polymers, such as poly(*p*-phenylene) and polypyrrole that contain non-degenerate ground state configurations. It should be noted that the polaron/bipolaron model is limited to describing conductivity in one dimension along the principal polymer chain. In the solid state, many doped organic polymers have higher conductivities than those predicted by the polaron/bipolaron theory. It is likely that in many of these materials interchain interactions along the π-stacking direction also contribute to their conductivity. Miller *et al.* have provided the first evidence of this possibility by determining the conductivity of an ester linked polythiophene (**1.7**).[17] The polymer cannot conduct via polarons or bipolarons because the π-conjugation of the short quaterthiophene units is

disrupted by the insulating ester linkers. Concentration dependent UV-visible studies on the *in-situ* generated radical cation showed that π-dimerization (see §1.51) was indeed occurring. The neutral polymer was then doped with iodine and the conductivity of a casted film was measured to be 0.8 S cm^{-1}. The authors concluded that the conductivity is primarily due to intermolecular oligothiophene π-stacks.

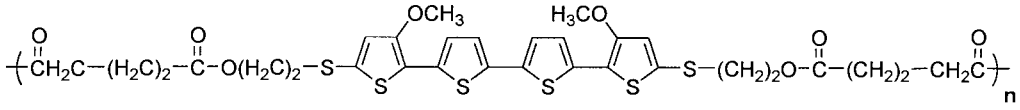

1.7

1.4 General Aspects of the Model Oligomer Approach

Although polydisperse materials often show desirable bulk properties, they can be troublesome when trying to evaluate how their exact structure correlates with an observable physical measurement. The inherent distribution in molecular weights makes microscopic/molecular scale understanding difficult, as measurements on bulk polydisperse samples provide an average value of the property in question. To gain a better understanding of structure/property relationships, synthetic chemists have set out to examine to what extent monodisperse conjugated oligomers can model their polymer analogs.[18] The "oligomer approach" of modeling a polymer typically involves the preparation of a homologous series of oligomers by sequentially increasing the chain length. By doing this, a saturation or convergence point is often observed for a specific physical property. This phenomenon is known as the effective conjugation length (ECL), that is, an oligomer containing so many monomeric units begins to behave (with respect to some property) like its polymer of infinite chain length. The ECL can be determined by extrapolation from a plot of an observable physical measurement (e.g., λ_{max}, oxidation

potential, etc.) versus the reciprocal of the number of monomeric repeat units (n^{-1}). Putting the "oligomer approach" to use, Müllen *et al.* prepared a homologous series of *t*-butyl capped oligoenes (**1.8**) and were able to estimate the band gap energy of a hypothetical defect-free *trans*-PA to be 1.7 eV.[19] This was achieved by plotting the HOMO-LUMO gap energies of each oligomer against the inverse number of double bonds, and then extrapolating to an infinite chain length. The determined band gap energy is an excellent agreement with the experimental value of 1.4 – 1.8 eV for a sample of *trans*-PA.

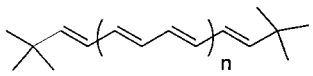

1.8 n = 1-3

In addition to oligomers acting as model compounds for their polymer congeners, they are also finding use in device applications because of their own interesting electrical and optical properties. One of the most promising organic molecules used to date in a FET is the p-type semiconductor α-sexithiophene (α-6T).[20] Record mobilities (μ) of 0.9 to 10 $cm^2\ V^{-1}\ s^{-1}$ have been measured on crystals of α-6T, these values being several orders of magnitude higher than those determined for polythiophene derived FETs. Oligothiophenes have also served in OLEDs, for instance, the n-doped dimesitylboryl end-capped oligomer **1.9** has been incorporated into a blue-emitting electroluminescent device.[21]

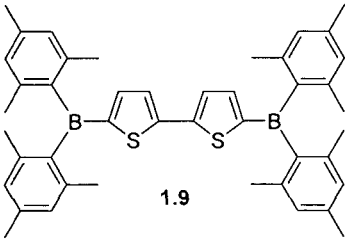

1.9

1.5 A Survey of Oligothiophenes

1.5.1 Oligothiophene Model Compounds

Oligothiophenes have received considerable attention in the past decade because they serve as effective models for polarons and bipolarons of conducting polythiophenes. The aim of this section is to highlight some of the scientific findings used to understand the conduction mechanism in doped polythiophenes.

Oligothiophenes that lack substituents in the 2- and 5-positions tend to be inadequate model systems for polythiophenes because they are normally highly reactive species when doped. That being said, there are a few examples of longer α-uncapped

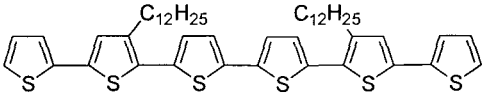

1.10

oligomers that have been shown to support stable radical cations and dications. Bäuerle *et al.* prepared the didodecylsexithiophene **1.10** and showed that this compound could be reversibly oxidized to the radical cation and dication (E_1° = 0.81 V, E_2° = 1.01 V vs. SCE).[22] The β-alkyl substituents help to stabilize the charge in the inner thiophene rings. Owing to its stability and enhanced solubility over its parent α-6T, **1.10** has found tremendous use as a component in FETs.[23]

Blocking the terminal α–positions with appropriate end-groups helps to suppress the polymerization of oxidized oligothiophenes, thereby permitting the study of discrete radical cations and dications. To this end, Tour and co-workers prepared a series of trimethylsilyl α-capped thiophene oligomers and probed their electronic structures by a combination of CV, EPR, and UV-Vis-NIR spectroscopy.[24] For the neutral series (**1.11** – **1.17**), λ_{max} was found to increase with thiophene chain length, a trend that is consistent with nearly all other oligothiophenes. All of the compounds except the dimer (**1.11**) and trimer (**1.12**) showed reversible one-electron oxidations by cyclic voltammetry (CV). All oligomers with four or more thiophene units could be subsequently converted to their dicationic states. One interesting outcome from these studies concerns the electrochemistry of the longer oligomers. The peak separation between the first and second oxidation potentials for **1.15**, **1.16**, and **1.17** saturate at 180 mV. This suggests that two discrete oxidation waves should also be viable for even longer monodisperse oligomers of these types, and possibly for a defect-free sample of polythiophene. However, cyclic voltammograms of real polythiophene films usually show a single broad wave, which may be attributed to structural variations and intermolecular chain interactions within the polymer during the electrochemical experiments. It should also be noted that π-dimerization does not occur within these silyl-capped oligomers; the authors attribute this to the steric bulk of the substituents. Therefore, these molecules can be thought of as models for understanding electronic communication in one-dimensional chains (i.e., polarons and bipolarons) for doped polythiophenes.

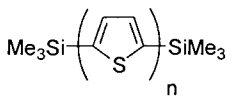

1.11 (n = 2)
1.12 (n = 3)

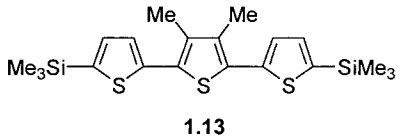

1.13

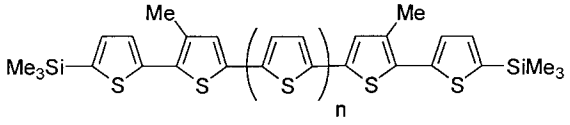

1.14 (n = 0)
1.15 (n = 1)

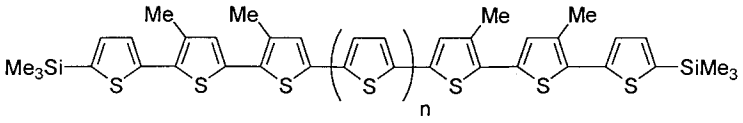

1.16 (n = 1)
1.17 (n = 2)

Miller *et al.* reported on the spectral and electrochemical properties of α-dimethylterthiophene (**1.18**) and showed that temperature and concentration dependent reversible π-dimerization of the radical cation occurs (see later).[25] While trying to elucidate the conduction mechanism in doped PTs they propose that the resulting diamagnetic dimer dication could serve as an alternative to a bipolaron. This can also explain why heavily doped PTs lack an appreciable EPR signal. Since this significant discovery, the polaron/bipolaron theory has been challenged by several others, who also observe reversible dimerization of radical cations in an array of other π-conjugated oligomers.[26] Although the one-electron oxidation process of compound **1.18** shows

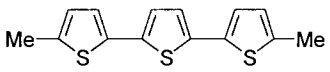

1.18

reversibility (E_1^o = 0.99 V vs. SCE at a scan rate of 100 mV s^{-1}) on the timescale of the CV experiment, the radical cation decomposes after several minutes at room temperature. Spectroelectrochemistry experiments had to be performed at -25 °C to avoid decomposition of the radical cation. During the bulk electrolysis the initial absorbance for the neutral species of **1.18** (λ_{max} = 360 nm) disappeared, while three new bands grew in at longer wavelengths. The band at 572 nm was due to the monomeric cation radical and the bands at 466 and 708 nm were assigned to the cation radical dimer. The dimer bands grow in at the expense of the monomeric radical cation band when either the concentration is increased or the temperature is decreased. Furthermore, the EPR signal vanishes for the radical cation species with a concentration increase or temperature decrease by virtue of the diamagnetic nature of the π-dimer formation.

Bäuerle and his coworkers looked at the electronic structures of mono- and dimeric radicals in a series of α,β-cyclohexyl end capped oligothiophenes (**1.19** – **1.21**).[27] The terminal cyclohexyl groups were used to shield the radical cations from undergoing polymerization reactions. Only the oligomers with at least three thiophene units could be reversibly oxidized to their corresponding radical cations; whereas, the oligomers with four or more thiophene units could be reversibly oxidized to dications. They were also able to show that reversible π-dimerization occurs upon cooling solutions of the radical cations by UV-Vis spectroscopy.

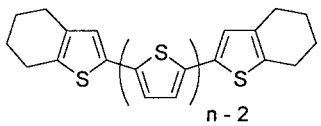

1.19 (n = 3)
1.20 (n = 4)
1.21 (n = 5)

In general, an oligothiophene radical cation shows four absorption bands in the UV-Vis-NIR region, which result from electronic transitions within three different energy levels (Φ_1 - Φ_3) (Figure 1.10). Φ_1 represents the HOMO-1, Φ_2 the SOMO, and Φ_3 the LUMO. The major optical bands M1 and M2 are due to transitions from Φ_2 to Φ_3, and Φ_1 to Φ_2, respectively. The bands on the higher-energy side of both M1 and M2 belong to the π-dimer and are denoted by D1 and D2. The MO diagram is in agreement with the general observation that the EPR signal of a radical cation diminishes upon dimer formation.

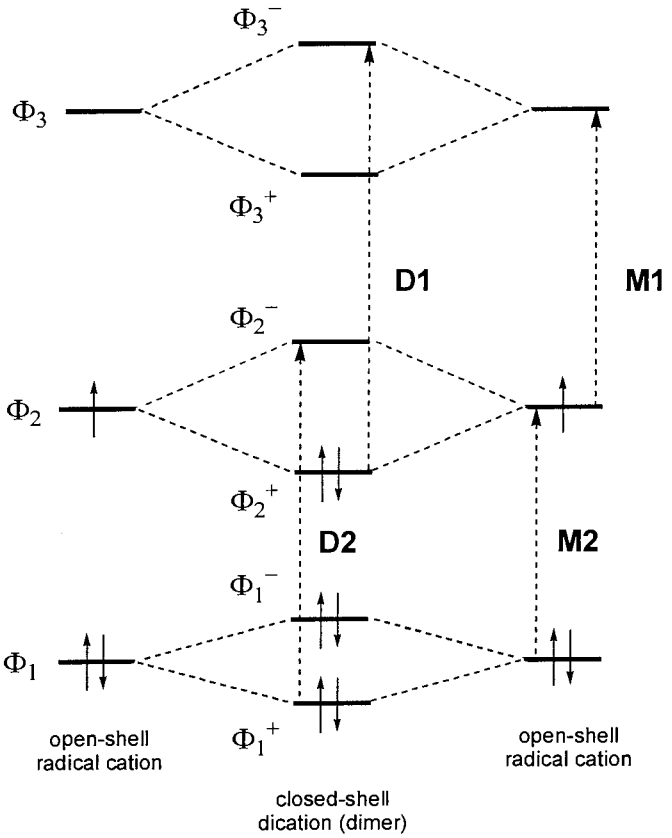

Figure 1.10. Frontier MO diagram and electronic transitions for radical cation and its corresponding π-dimer.

Garnier and co-workers have recently reported that π-dimerization occurs for even longer oligothiophenes (e.g., duodecithiophene (12T) **1.22**).[28] They claim that the doubly oxidized form of **1.22** results in the formation of a fourfold charged spinless π-dimer

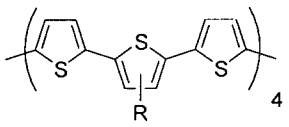

1.22 (R = $C_{10}H_{21}$)
1.23 (R = $C_{12}H_{25}$)

(Scheme 1.2). More recently, Janssen *et al.* examined a slightly different version of 12T (**1.23**).[29] Instead of a bipolaron or a π-dimer, as previously suggested, the authors state that the electronic configuration for the dication of **1.22** is that of a singlet ground state carrying two individual polarons. The UV results show that when **1.22** is oxidized to its dication, two equally intense electronic subgap transitions are observed, which they argue to be inconsistent with a bipolaron structure, but could explain two separate polarons on an oligothiophene chain. Furthermore, no peaks in the electrospray mass spectrum appeared for $(12T)_2^{4+}$, but peaks due to $12T^{2+}$ were observed. Although not conclusive, the EPR inactive nature for the dication of 12T is also in agreement with the proposed singlet ground state structure.

Scheme 1.2. Formation of a fourfold spinless π-dimer.

1.5.2 Structural Characterization of Cationic Oligothiophenes

To gain a better understanding of the role that π-dimerization plays in oligothiophenes, Miller and co-workers successfully prepared a pure radical cation sample of a terthiophene derivative (**1.24**) and determined its structure by x-ray diffraction.[30] The radical cation could be prepared by either chemical oxidation of **1.24** with $NOPF_6$ or by electrochemical oxidation. The structure consists of slipped columnar stacks of $[\mathbf{1.24}]^+$ cations, while the PF_6^- anions occupy the channels in between. There is

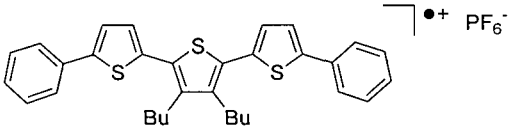

1.24

not a strong interaction between neighboring π-systems in this case, as the shortest interplanar contact distance between the cations is only 3.47 Å. Nevertheless, π-dimerization in the solid state has been determined by crystallography for oligopyrrole **1.25**; the neighboring radical cations of **1.25** stack as π dimers in a face-to-face manner with a minimum interplanar distance of 3.23 Å.[31]

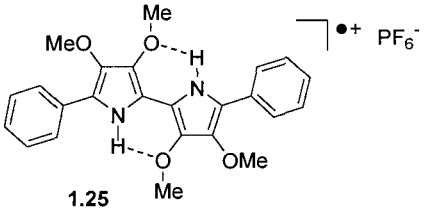

1.25

The first crystal structure of a dicationic oligothiophene was reported very recently. A dicyanovinylene-bridged CPDT oligomer (**1.26**) capped with butylthio groups has been converted to its dication (**1.27**) by constant current electrolysis in the presence of Et_4NFeCl_4 as supporting electrolyte (Scheme 1.3).[32] X-ray structural analysis shows that **1.27** is highly planar with a quinoid-like geometry. Furthermore, the terminal C-S bonds of **1.27** have more double-bond character as they are considerably shorter than the C-S bonds found in the neutral form (**1.26**). Furthermore, the lack of an EPR signal and the stability of **1.27** towards molecular oxygen provide evidence that it has a closed-shell singlet electronic ground state configuration.

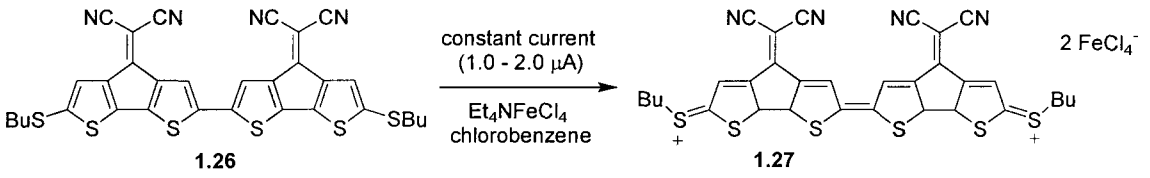

Scheme 1.3. Formation of a stable oligothiophene dication (**1.27**).

There are only a few examples of stable substituted monothiophene radical cations; most are extremely reactive and are difficult to observe, much less isolate. A radical cation of 3-alkoxy-2,5-bis(alkylthio)thiophene (**1.46**) has been previously prepared but its half-life was less than a few hours while in a solution of hexafluoropropan-2-ol.[33] Komatsu *et al.* have recently prepared an exceptionally stable radical cation from a monothiophene (**1.28**) annelated with two bicyclo[2.2.2]octene (BCO) units (Scheme 1.4).[34] The UV spectrum of $[\mathbf{1.28}]^{\bullet+}$ in dichloromethane showed two maximum absorptions at 350 and 271 nm, which are ascribed to the M2 and M1

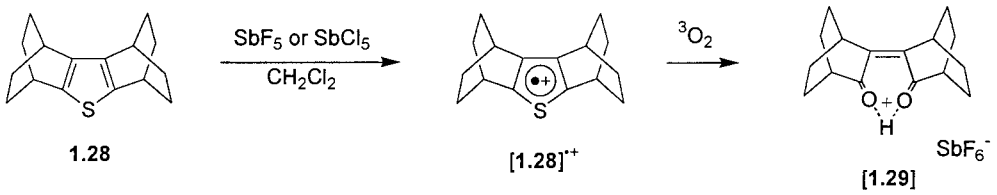

Scheme 1.4. Formation of a stable monothiophene radical cation $[\mathbf{1.28}]^{\bullet+}$.

transitions (see Figure 1.10), respectively. The steric bulk of the BCO units suppress any possibility of dimerization, and this feature is supported by the lack of dimer bands (i.e., D1 and D2 transitions) in the absorption spectrum. The crystal structure of $[\mathbf{1.28}]^{\bullet+}SbCl_6^-$ could not be unambiguously assigned due to disorder in the thiophene unit; however, the data was able to show that the thiophene moiety and hexachloroantimonate ion exist in a 1:1 ratio. Interestingly, they were able to obtain a crystal structure of **1.29**, which is the product derived from the reaction of $[\mathbf{1.28}]^{\bullet+}SbF_6^-$ with triplet oxygen.

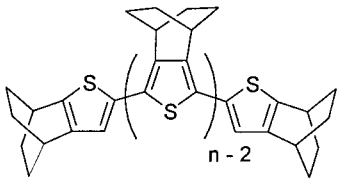

1.30 (n = 2)
1.31 (n = 3)
1.32 (n = 4)
1.33 (n = 6)

Motivated by the exceptional stabilizing ability of the BCO units on the radical cation of monothiophene **1.28**, Komatsu's group synthesized a homologous series of oligothiophenes (**1.30** – **1.33**) that were also fully annelated with BCO groups.[35] Radical cations of **1.30** and **1.31** could be prepared by chemical oxidation with one equivalent of $NOSbF_6$ and their structures were obtained by x-ray crystallography. The dication salts of **1.32** and **1.33** were prepared by using two equivalents of $NOSbF_6$ and their structures

were also determined. Interestingly, both the cationic and dicationic species are stable at room temperature in air. The radical cation molecules all take on quinoidal-like planar structures, where the sulfur atoms in the thiophene rings adopt a transoid orientation with respect to each other. The closest intermolecular contact distances between π-systems for **1.30** and **1.31** are 4.89 and 3.58 Å, respectively. Not only are the BCO units effective at prohibiting π–dimerization in the solid state, but also in solution, as was confirmed by low temperature UV-Vis-NIR and EPR spectroscopic studies. Of particular interest are the studies on the dications of **1.32** and **1.33**. Both dications display sharp single-line EPR signals in the solid state, suggesting the presence of paramagnetic species. Recent DFT calculations on a series of oligothiophene dications have shown that the open-shell two-polaron state is only 0.18 kcal mol^{-1} lower in energy with respect to the closed-shell bipolaron.[36] The authors claim that the open-shell paramagnetic species may be in equilibrium with the closed-shell state. Therefore, it seems surprising that Janssen *et al.* do not observe an EPR signal for their dicationic state of **1.22**, for which they claim consists of two polarons on the chain.

In summary, several model oligothiophenes have been prepared, characterized and used to elucidate the conduction mechanism in doped polythiophenes. Solution spectroscopic studies and solid state structural analyses have helped to shed light on this matter. The incorporation of bulky substituents have permitted detailed studies on the unimolecular (i.e., polarons and bipolarons) electronic properties in conjugated oligothiophenes; whereas, less sterically hindered structures have allowed for an understanding of how π-dimerization contributes to intermolecular electronic interactions.

1.5.3 Stabilizing Charged Oligothiophenes

Most efforts aimed at stabilizing charged oligothiophenes have involved the incorporation of terminal end-groups that protect the oligomer from undergoing dimerization and polymerization. However, most of the structural modifications mentioned thus far have only moderately improved the stability of oxidized oligothiophenes. Due to the inherently short lifetimes (i.e., half lives are usually on the order of several hours to minutes) of most charged oligothiophenes, the probing of their electronic structures is usually restricted to *in situ* spectroscopic techniques. Of the charged oligomers presented so far, the most stable are those that have been annelated with BCO units (**1.28** and **1.30–1.33**). The bulky BCO groups protect the thiophene radicals from undergoing dimerization and other decomposition pathways. The exceptional stability is also manifested in their ability to be left in air for several months without decomposition. Aside from these, only those with three or more thiophene units have been shown to produce stable radical cations. Clearly, there is room to warrant the design and synthesis of smaller and more stable cationic oligothiophenes. Within this context, the next sections deal with the efforts put forth to stabilize cationic thiophenes by substituent effects.

A few alkyl-substituted oligothiophenes are known to undergo reversible oxidations; for instance, α-diethylquaterthiophene and α-diethylquinquethiophene are both capable of generating stable radical cations, and the latter can also be converted to its dication on the CV timescale.[37] In general, alkyl groups are not particularly good for stabilizing cationic oligothiophenes, as undesirable couplings can occur within these groups. For example, Kossmehl and co-workers found that **1.34** rapidly decomposed to a

mixture of **1.36** and **1.38** when it was oxidized with $FeCl_3 \cdot H_2O$ (Scheme 1.5).[38] The methyl group in the 3-position of **1.34** activates the formation of a "benzylic-like" radical, which subsequently couples to the 3–β–position of another bithiophene molecule affording the dimer (**1.36**). The nucleophilic attack of water on the "benzylic" cation (**1.35**) results in the formation of the intermediate alcohol (**1.37**), which is then converted to the aldehyde (**1.38**) upon further oxidation.

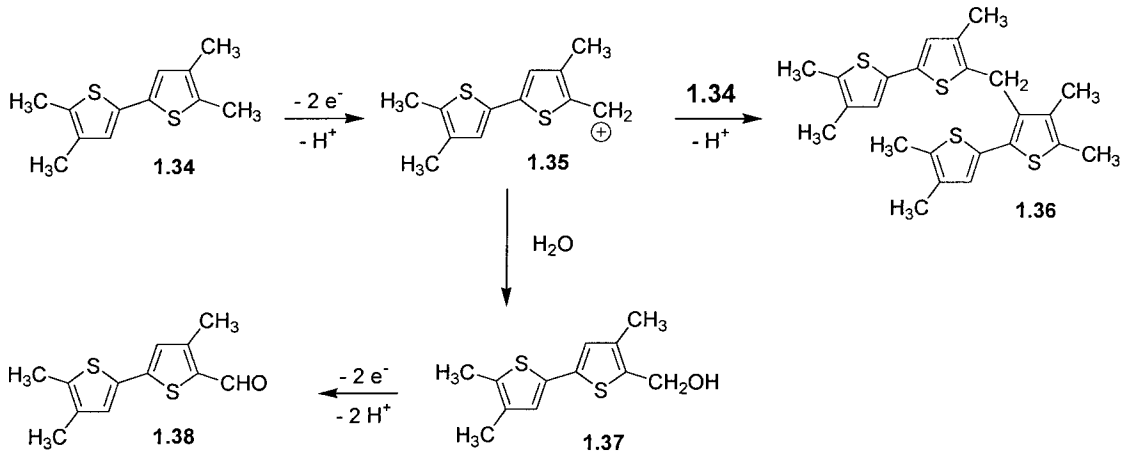

Scheme 1.5. Decomposition pathways in methylated oligothiophenes.

Miller *et al.* then investigated a class of methyl α–terminated oligothiophenes that contained strongly electron-donating methoxy substituents on the β-positions.[39] The methoxy groups were either placed on the "inside" (**1.39 – 1.42**) or the "outside" (**1.43 – 1.45**) of the thiophene oligomers and these were studied by CV.[40] The methoxy groups were effective at stabilizing the radical cations of **1.39 – 1.41**, as evidenced by their persistence in solution and in the solid state for more than one month. It is important to note that a stable radical cation could even be generated for the short bithiophene (**1.39**)

oligomer. Furthermore, repeated oxidative/reductive cycling did not lead to any detectable damage for compounds **1.39**, **1.40**, and **1.41**. On the other hand, the isomeric outside oligomers **1.43**, **1.44**, and **1.45** did not produce stable cation radicals. All of these decomposed upon oxidation in exactly the same way as **1.34**, affording dimerized products and aldehydes.

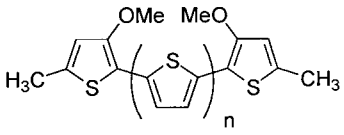

1.39 (n = 0)
1.40 (n = 1)
1.41 (n = 2)
1.42 (n = 3)

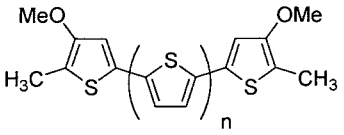

1.43 (n = 0)
1.44 (n = 1)
1.45 (n = 2)

In 1997, Miller's group then looked at a series of oligothiophenes (**1.46** – **1.49**) substituted with methoxy and thioalkyl groups.[41] The most interesting outcome from this report was that the first persistent cation radical $[\mathbf{1.46}]^{\bullet+}$ from a monothiophene was obtained. The authors attributed the stability and low oxidation potential (E_{pa} = 0.81 V; E_1^o = 0.78 V vs. SCE in CH_3CN) of **1.46** to the three donor substituents. All of the other oligomers (**1.47** – **1.49**) could be reversibly oxidized to both their cationic and dicationic states, as was shown by CV. For instance, the longest oligomer (**1.49**) was oxidized to its radical cation at a half-wave potential of 0.43 V (vs. SCE). The negative potential shift for **1.49** with respect to **1.46** was in agreement with the general trend that E_1^o decreases with increasing thiophene chain length.

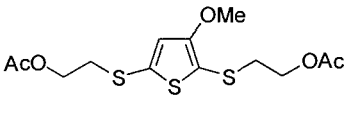

1.46

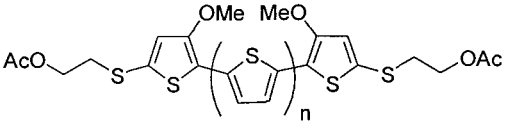

1.47 (n = 0)
1.48 (n = 1)
1.49 (n = 2)

1.5.4 α,ω-Bis(mesitylthio)oligothiophenes

Matt Nodwell, a previous graduate student in our group, prepared a series of α,ω-bis(mesitylthio)oligothiophenes **1.50-1.60** (Figure 1.11; Series III) and examined their electronic structures by a combination of UV-visible spectroscopy and CV.[42] The oligomers were prepared to gain a better understanding of how terminal sulfur donor substituents influence the electronic properties of charged oligothiophenes.

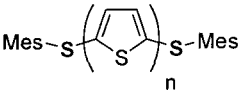

1.50 (n = 1)
1.51 (n = 2)
1.52 (n = 3)
1.53 (n = 4)

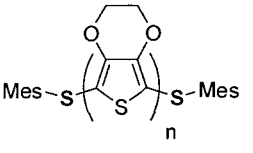

1.54 (n = 1)
1.55 (n = 2)
1.56 (n = 3)

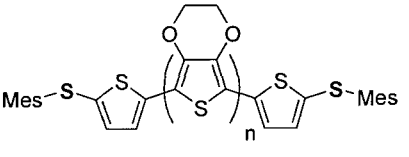

1.57 (n = 1)
1.58 (n = 2)

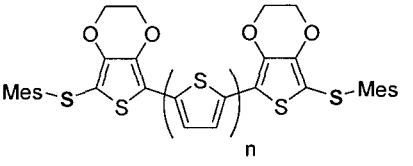

1.59 (n = 1)
1.60 (n = 2)

Figure 1.11. α,ω–Bis(mesitylthio)oligothiophenes (**Series III**).

A number of sulfur-terminated conjugated oligomers (e.g., those derived from 2-thienylacetylene,[43] *p*-phenylacetylene,[44] benzene,[45] thiophene,[46] etc.) have been synthesized in the past decade for the central purpose of using these as wires in molecular-scale electronic devices. The terminal sulfur atoms allow for attachment of the molecular wire to metal surfaces (i.e., electrodes) (Figure 1.12). The gold-sulfur (S-Au) system has been the most commonly studied primarily due to the robustness of the gold-thiol bond (50 kcal mol^{-1}).[47] In this vein, the majority of research has been devoted to

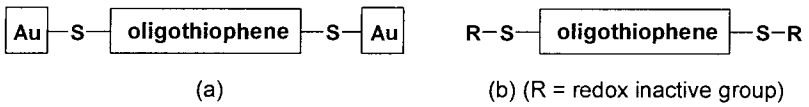

Figure 1.12. Schematic diagrams of (a) gold functionalized oligomer, and (b) thioether-capped oligomer.

understanding (a) the nature of the gold-sulfur interface,[48] and (b) the ordering properties of the surface-bound monolayers.[49] Surprisingly, there has been little to no work done on trying to assess how the terminal sulfur groups modulate the electronic features of the π-conjugated oligomer itself. Instead of using gold functionalized oligothiophenes, Nodwell incorporated redox-inactive mesityl (Mes) end groups (Figure 1.11), such that the properties of the sulfur-oligomer interactions could be independently addressed. The Mes groups also serve to protect the thiol (-SH) from undesirable oxidation reactions. Oligothiophenes were chosen as the conjugated backbone because they show exceptional stability when doped, and the synthetic aspects of assembling oligothiophenes are well documented throughout the scientific literature. Furthermore, the large amount of UV-Vis spectroscopic and electrochemical data for other substituted and unsubstituted oligothiophenes allowed for comparison with the compounds presented in Figure 1.11.

Along with the –SR donor groups, several of the oligomers were substituted in the β-positions with ethylenedioxy substituents in order to investigate the electronic structure of the oligothiophenes as a function of increased "electron richness".

Within the "pure" thiophene series (i.e., **1.50 – 1.53**) all of these can be reversibly oxidized to stable radical cations, whereas those that contain two or more thiophene units can also be reversibly oxidized to stable dications. It is important to stress here that even the monothiophene (**1.50**) affords a stable radical cation upon oxidation, which clearly shows the exceptional stabilizing ability of the terminal –SMes groups. The most important finding was that the oxidation potentials for the shorter oligomers are considerably lower with respect to those lacking terminal –SR groups. For example, this can be shown by comparing the first and second oxidation potentials for the sulfur- versus Bäuerle's cyclohexyl-capped[27] oligomers (Table 1.1). In accordance to the general trend, the first and second oxidation potentials decrease with increasing thiophene chain length for both series. However, the –SR groups have less of an effect at lowering the oxidation potential for the longer oligomers; for instance, the E_1^0 value for the cyclohexyl-capped tetramer (n = 4) is actually lower than the mesitylthio tetramer. The EDOT containing oligomers (**1.54 – 1.56**) are even more easily oxidized with respect to their parent thiophenes. The E_1^0 values for **1.54**, **1.55**, and **1.56** are +0.87, +0.57, and +0.42 V, respectively.

Table 1.1. Redox potentials of mesitylthio[42] and cyclohexyl capped[27] thiophene oligomers.

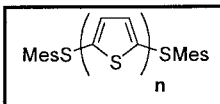 1.50-1.53	E_1^o (V) [a]	E_2^o (V) [a]	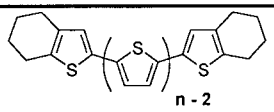	E_1^o (V) [a]	E_2^o (V) [a]
n = 1	+1.05	-	**n = 1**	+1.48 [b]	-
n = 2	+0.87	+1.25	**n = 2**	+1.00 [b]	+1.67 [b]
n = 3	+0.86	+1.02	**n = 3**	+0.85	+1.26 [b]
n = 4	+0.83	+0.91	**n = 4**	+0.79	+1.13

[a] All values are reported in V vs. SCE. [b] Anodic peak potential, irreversible oxidation.

The oxidation potentials further decrease with increasing the number of oxygen donor atoms on the oligothiophene backbone (Table 1.2). This is an excellent example of how the redox properties of the oligomers can be "fine-tuned" by subsituent effects.

Table 1.2. Potentials as a function of increasing the number of oxygen donor atoms.

Compound	Number of β-oxygen donor atoms	E_1^o (V) [a]	E_2^o (V) [a]
1.52	0	+0.86	+1.02
1.57	2	+0.67	+0.93
1.59	4	+0.57	+0.76
1.56	6	+0.42	+0.65

[a] All values are reported in V vs. SCE.

It is interesting to compare the redox behavior of the isomeric quaterthiophenes **1.58** and **1.60**. Both compounds contain the same number of oxygen and sulfur donor atoms, but exhibit significantly different electrochemical behavior (Table 1.3). Compound **1.60** is more difficult to oxidize than **1.58** to the radical cation, but easier to

oxidize to its dication. Essentially the radical cation of compound **1.60** is confined to one of the very electron-rich ends of the molecule, thereby allowing for the second electron to be relatively easily removed from the other end of the molecule. In other words, the electron-rich EDOT end-groups of **1.60** can be considered as two quasi-independent electrophores that are weakly coupled by a bithiophene spacer. On the other hand, it is slightly easier to oxidize **1.58** to its radical cation because there is a greater degree of charge delocalization in the central biEDOT unit. However, this increases the Coulombic repulsion to introduce a second charge, as can be seen by the larger ΔE^{o} (i.e., $E_2^{o} - E_1^{o}$) value for **1.58** with respect to **1.60**.

Table 1.3. Redox potentials for the isomeric quaterthiophenes.

Compound	E_1^{o} (V) [a]	E_2^{o} (V) [a]	ΔE^{o}
1.58	+0.49	+0.73	0.24
1.60	+0.61	+0.66	0.05

[a] All values are reported in V vs. SCE.

1.6 Aims and Objectives for Part I

Hybrid polymers that combine both organic and inorganic groups are becoming very attractive in materials science, due to their high stability and unique properties. Within this context, there have been two classes of hybrid polymers that have dominated the field. The first being conjugated metallopolymers,[50] which incorporate transition metals into the polymer backbone, whereas the second class is those that are bridged by main group elements (e.g., boron, silicon, nitrogen, phosphorus, and sulfur). With respect to the latter, polyaniline[51] and poly(*p*-phenylene)sulfide (PPS)[52] have been the most

heavily studied hybrid systems. Vinyl[53] and heteroaryl[54] sulfides have also been prepared, but have received far less attention because their doped polymers are exceptionally unstable.

Taking advantage of the well known chemistry of thiophenes and the stability of the corresponding polymers in their doped states, we thought it would be valuable to prepare and study a new class of thiophene polymers and model compounds bridged by divalent sulfur. Our group has already shown (see §1.54) that sulfur substituents are very effective at stabilizing charged oligothiophenes. Combining this aforementioned feature with the exceptional properties of polythiophenes might provide entry into a new class of *stable* hybrid polymers. We and others have shown that the more electron rich EDOT also aids in the stability of oligomers and polymers derived from this unit.[55] The latter part of the second chapter deals with the synthesis of various EDOT and thiophene-sulfide monomers to be used as polymer precursors. The synthetic details and electronic features of the polymers are briefly discussed in chapter three. The target monomer compounds are depicted in Figure 1.13 (Series I).

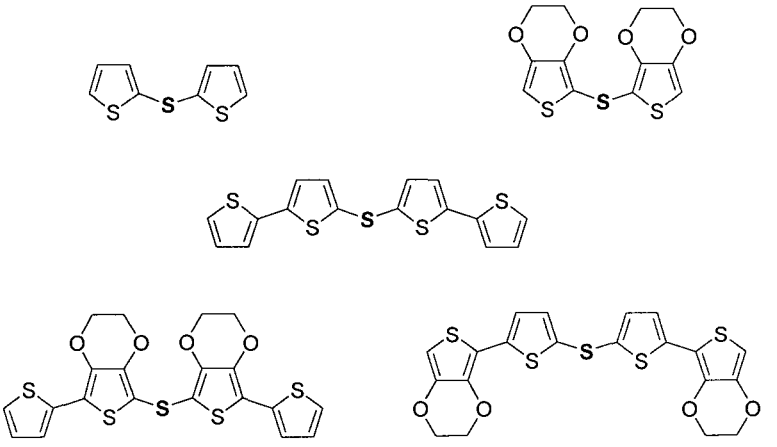

Figure 1.13. Proposed EDOT and thiophene-sulfide uncapped polymer precursors **(Series I)**.

Although it is anticipated that the non-conjugated polymers derived from the Series I type compounds will provide interesting physical properties, it may be difficult to accurately asses their electronic structures when doped due to potential solubility problems and structural defects. For example, one fundamentally important question pertains to these polymers ability to communicate electrical charge between the flanking thiophenes by way of the bridging sulfur groups. It should be possible to address some of these issues by preparing some model compounds that also consist of discrete thiophene and EDOT units bridged by divalent sulfur. The studies on these model oligomer compounds form the main thrust of the work presented in this thesis.

Most studies on cationic model oligothiophene compounds have been restricted to those that are fully π-conjugated. Surprisingly, there has been far less work done on systems in which the π-conjugated units are separated by various linkers (Figure 1.14). The linker group can be a metal fragment, a different organic group, or a main group

element. A prototypical polymer example of this is polyaniline, which can be thought of as a hybrid for polyphenylene that has nitrogen atoms placed between the phenyl rings.

Figure 1.14. π-Conjugated segments connected by a linker.

Consequently, the chemistry of polyaniline differs drastically with respect to that of polyphenylene. For instance, the bridging nitrogen atoms allow for the doping of polyaniline to be controlled by acid-base chemistry. The incorporation of linker groups is exciting because they offer the possibility of also modulating the electronic features of the π-conjugated segment; thus providing access to materials with novel physical properties.

Recently, there has been some interest in studying hybrid oligomers and polymers for their potential use in high-spin polaronic ferromagnets.[56] The basic idea is to have two spin containing groups that are bridged by a ferromagnetic coupling unit (FCU) (Figure 1.15). The most commonly used FCU is *meta*-phenylene. Janssen *et al.* have used this

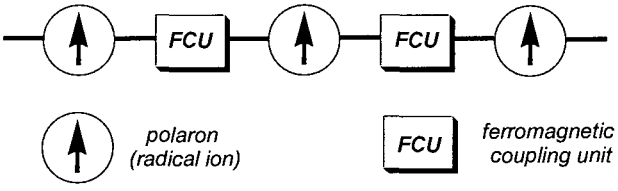

Figure 1.15. Schematic design for high-spin oligomers/polymers.

design strategy to prepare a stable triplet-state diradical of a meta-para aniline oligomer (**1.61**).[57] The radicals are stabilized in the *p*-phenylenediamine units and were shown to

couple ferromagnetically via the *m*-phenylene link. Oligothiophene (**1.62**) and oligopyrrole (**1.63**) have also been investigated as high-spin polaronic oligomers.[58] However, these two compounds do not couple ferromagnetically as π-dimerization of the charged species inhibits the formation of high-spin states.

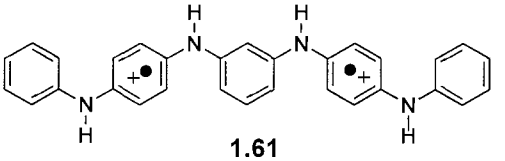

1.61

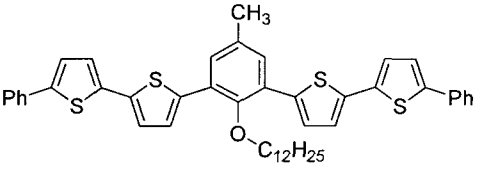

1.62

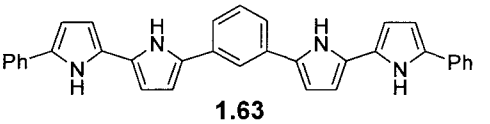

1.63

We propose to prepare a series of π-conjugated model oligomers that are linked by a main group element, namely, divalent sulfur, but for an entirely different reason than using them as high-spin polaronic materials. The target compounds (referred to as "Series II") are depicted in Figure 1.16. This study aims at understanding how internal sulfur substituents communicate charge between oligothiophenes. This is particularly important

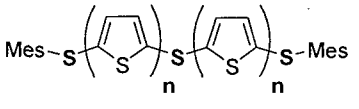

n = 1 - 3

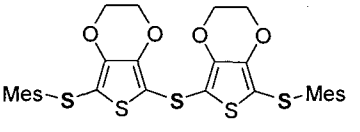

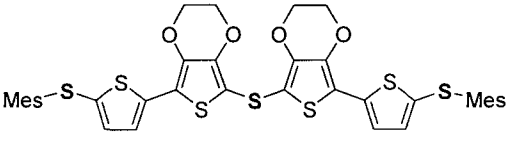

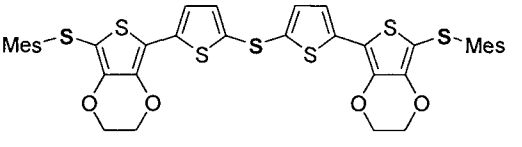

Figure 1.16. Proposed EDOT and thiophene-sulfide capped oligomers (**Series II**).

in trying to elucidate the conduction mechanism in doped thienyl-sulfide polymers. Thus, the first part of chapter two deals with the synthetic strategies employed for the preparation of the Series II type compounds that contain both EDOT and thiophene bridged by divalent sulfur, whereas the latter part provides the synthetic details for the α-uncapped thiophene oligomers (Figure 1.13; Series I) to be used as polymer precursors. With respect to the former, the compounds have the general topology as shown in Figure 1.17. Redox-inactive mesityl (Mes) groups were chosen to protect the terminal sulfur groups. Oligothiophenes were chosen as the π-conjugated portion, because they generally exhibit electrochemical reversibility. The extent of electronic communication of the charged oligomers is to be probed as a function of electron richness (i.e., EDOT versus thiophene) and the oligomer chain length.

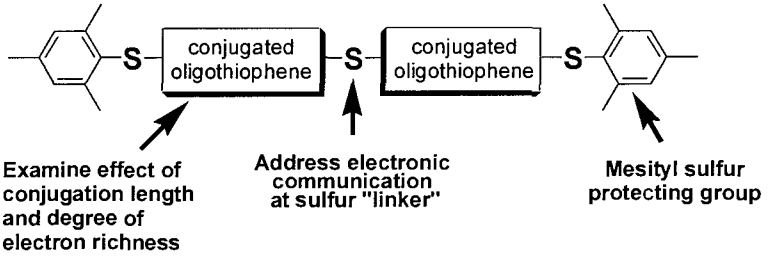

Figure 1.17. Schematic representation for the capped thienyl-sulfide oligomers.

The proposed compounds, as shown in Figure 1.16 (Series II), are very similar in structure to Nodwell's Series III compounds, with the exception that these now contain not only *terminal* sulfur groups, but also *internal* bridging ones. The structural resemblance between the two series and the availability of UV-Vis spectroscopic and electrochemical data for the α,ω-bis(mesitylthio)oligothiophenes will allow for their

comparisons. The new compounds can be thought of as discrete thienyl-sulfide polymer pieces that are capped with redox inactive mesityl groups.

Chapter 2

Synthesis of Sulfur-Bridged Oligothiophenes

2.1 Introduction

Thiophene, furan, and pyrrole are members of a class of aromatic 5-membered ring heterocycles (Figure 2.1). The degree of aromaticity of these compounds is manifested in their experimentally determined resonance energies. The resonance energies of thiophene, pyrrole and furan are 29, 21, and 16 kcal mol^{-1}, respectively.[59] Amongst these, furan has the lowest resonance energy and this is consistent with its chemical reactivity: furan is more susceptible to undergo addition rather than substitution reactions. For example, the greater diene character of furan allows it to undergo Diels-Alder cycloaddition reactions. On the other hand, thiophene and pyrrole behave more similarly to benzene in that they readily react via substitution reactions (see §2.1.2).

E	Compound
S	Thiophene
O	Furan
NH	Pyrrole

Figure 2.1. 5-Membered heterocycles.

2.1.1 Nomenclature

The numbering scheme for thiophene is represented in Figure 2.2. The heteroatom is given priority and is labeled position 1. The remaining positions are labeled by numbering around the ring in a clockwise fashion. The 2- and 5- positions are also referred to as the α-positions, whereas the 3- and 4- are termed the β- positions.

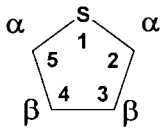

Figure 2.2. Thiophene labeling scheme.

Thiophene oligomers are named in accordance to the IUPAC rules. A few examples are represented below (Figure 2.3). The first ring attachment is through a 2- or 3- position and the remaining rings are given increasing number of primes (').

2,2':5',2"-terthiophene 3',4'-ethylenedioxy-2,2':5',2"-terthiophene bis(3',4'-ethylenedioxy-5,2'-bithiophene-2-yl)sulfide

Figure 2.3. Nomenclature of thiophenes.

Since the oligothiophenes presented herein are all α-linked we have found it easier to adopt a shorthand notation. Thiophene rings will be represented by a **T**, and 3,4-ethylenedioxythiophene units by an **E**. Therefore, 3'4'-ethylenedioxy-2,2':5',2"-terthiophene would be expressed as **TET** using this notation, and bis(3',4'-ethylenedioxy-5,2'-bithiophene-2-yl)sulfide would be **ET-S-TE**.

2.1.2 Electrophilic Aromatic Substitution

Electron-rich thiophene undergoes electrophilic aromatic substitution (EAS) much more readily than benzene, and in most cases does not require the use of a catalyst. The ease of EAS has rendered this method one of the most important for functionalizing thiophenes. Thiophenes are predominantly substituted in the α-positions upon treating them with electrophiles. An explanation for this regiochemical outcome can be understood by examining the HOMO of thiophene (Figure 2.4). The largest orbital coefficients are found to be directly adjacent to the sulfur atom in thiophene. In other words, these are the sites with the greatest amount of electron density,

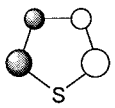

Figure 2.4. HOMO of thiophene.

making them most susceptible to electrophiles. An example of this is the direct bromination of thiophene with molecular bromine in carbon tetrachloride (Scheme 2.1). A mixture of 2-bromothiophene and 2,5-dibromothiophene is obtained.

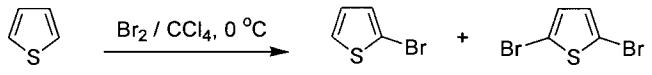

Scheme 2.1. Synthesis of α-brominated thiophenes.

The 3- and 4- positions can also be substituted if harsher brominating conditions are employed. Thiophene can be treated with a large excess of bromine in the presence of acetic acid at reflux to furnish 2,3,4,5-tetrabromothiophene (Scheme 2.2).[60] 3,4-dibromothiophene can be made by selective dilithiation of the tetrabromo compound followed by protonation with water.

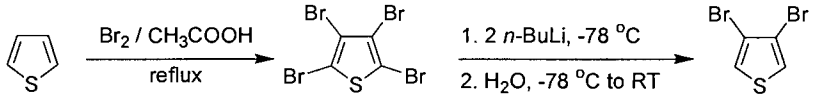

Scheme 2.2. Synthesis of β-brominated thiophenes.

2.1.3 Metallation of Thiophenes

Treatment of thiophene with strong bases (e.g., *n*-butyllithium or LDA) usually results in selective metallation at the α-positions.[61] The α-protons on the thiophene ring

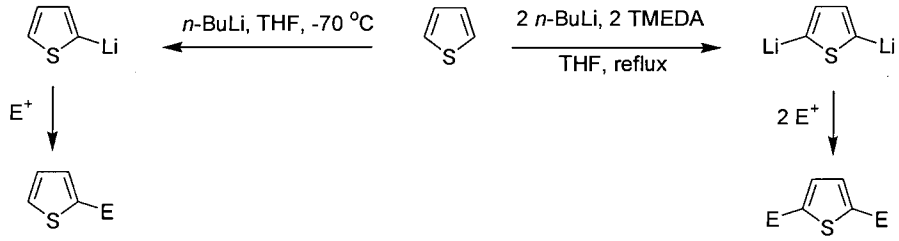

Scheme 2.3. Lithiation of thiophenes followed by electrophilic quenching.

are more acidic than the β-protons, this being attributed to the inductive electron-withdrawing nature of the adjacent sulfur atom. The monolithiation of thiophene is achieved by treating thiophene with one equivalent of *n*-butyllithium in THF (Scheme 2.3). The dilithiation of thiophene requires two equivalents of *n*-butyllithium and is most effective when carried out in the presence of TMEDA in THF. The resulting carbanions can then be quenched with various electrophiles (E^+; e.g., TMSCl, MeI, Bu_3SnCl, $B(OMe)_3$, I_2, etc.) to afford 2- and 2,5- substituted thiophenes (Scheme 2.3). An alternative method to access metallated thiophenes is via lithium-halogen exchange reactions at low temperature. This is particularly useful for the preparation of β-metallated thiophenes. For instance, careful treatment of 3,4-dibromothiophene (generated according to Scheme 2.2) with one equivalent of *n*-butyllithium at -78 °C in Et_2O affords 3-lithiothiophene. Reynolds *et al.* have successfully prepared 3,4-bis(isopropylthio)thiophene by a stepwise lithiation-electrophilic quenching protocol (Scheme 2.4).[62]

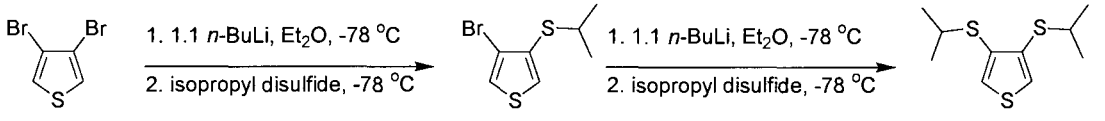

Scheme 2.4. β-Lithiation - Preparation of 3,4-bis(isopropylthio)thiophene.

Grignard reagents of thiophene can also be prepared by reacting an appropriate bromothiophene with magnesium metal in an ethereal solvent. For example, 2-

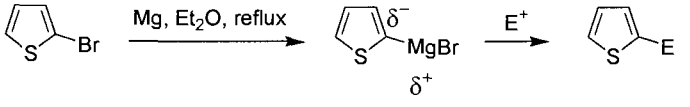

Scheme 2.5. A Grignard reagent of 2-bromothiophene.

thienylmagnesium bromide can be prepared by the action of magnesium on 2-bromothiophene in Et_2O (Scheme 2.5). The resulting carbanion can then be subjected to a wide range of electrophiles, just as in the case of the thienyllithium reagents.

2.1.4 Metal Mediated Coupling of Thiophenes

The main thrust of this section is to discuss the ways in which oligothiophenes can be assembled via metal promoted carbon-carbon bond forming reactions.

The Ullmann reaction represents one of the earliest methods used for the synthesis of symmetrical biaryl compounds.[63] The reaction involves the reductive homocoupling of an aryl halide while in the presence of a stoichiometric amount of finely divided copper. This method requires reaction temperatures above 200 °C, and in most cases provides the homocoupled product in low yield. For example, 2,2'-bithiophene was obtained in less than 20% by an Ullmann coupling of 2-iodothiophene with copper bronze.[64] It was later found that lithiated thiophenes could be coupled to each other by using a variety of copper salts. 2,2'-Bithiophene can now be prepared in 85% yield by reacting 2-thienyllithium with a twofold excess of cupric chloride.[65] Other transition metals have also been employed in the symmetrical coupling of thiophenes. For instance, nickel(0) tris(triphenylphosphine) (prepared *in situ* by the combination of $NiCl_2$, Zn, and PPh_3) is found to be an extremely powerful catalyst in promoting the coupling of α-monobrominated thiophenes (Scheme 2.6).[66]

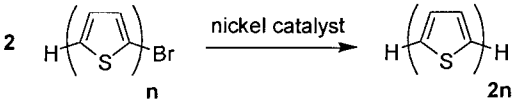

Scheme 2.6. Nickel catalyzed homocoupling of α-brominated thiophenes.

During the past decade a large library of monodisperse conjugated thiophene oligomers have been prepared by using highly efficient late transition metal-catalyzed cross-coupling reactions. These reactions are useful in preparing both homo- and heterocoupled products. Transformations of this type have found tremendous use due to the mild reaction conditions, tolerance of a wide range of functional groups, and high reaction conversions. Although there are many different coupling methods, only the Stille and Kumada reactions will be discussed in some detail, since they are the only ones to be applied in this thesis.

The Stille reaction involves the cross-coupling of an organic halide with an organotin reagent in the presence of a palladium catalyst (Scheme 2.7).[67]

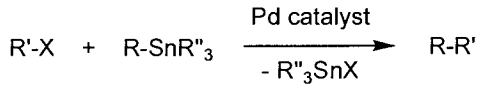

R = alkenyl, alkynyl, aryl, benzyl, allyl;

R" = Bu, Me; **X** = OTf, I, Br;

Scheme 2.7. General Stille reaction.

Organotin compounds can be prepared by several different routes, are relatively inert to water and oxygen (thereby allowing their handling without special precaution), and tolerate many functional groups (e.g., CN, OH, CHO, NO_2 and CO_2R) on either coupling partner. Organostannane derivatives are also tolerant to strong oxidants (e.g., $KMnO_4$, CrO_3, etc.) and various nucleophiles (e.g., $LiAlH_4$, Wittig reagents, and Grignard reagents). The disadvantage of the Stille reaction is that organostannane compounds are extremely toxic. The organometallic substrates (R-SnR"$_3$) used in the Stille reaction are often prepared by the reaction of lithiated derivatives (R-Li) with trialkylstannyl chlorides R"$_3$SnCl. In general, it has been found that aryl iodides,

bromides, and triflates are most effective towards cross coupling with organotin reagents, since they readily add across Pd(0) complexes. Aryl chlorides typically do not undergo coupling (this is ascribed to a reluctance of such reagents to oxidatively add to Pd(0) complexes) and only a few examples of electron-poor aryl chlorides have actually been shown to effect this type of reaction.[68] Although several palladium(0) catalysts have been used, the most common ones include: $Pd(PPh_3)_4$, $Pd(PPh_3)_2Cl_2$, $Pd(dppp)Cl_2$, $Pd(OAc)_2/P(o\text{-tolyl})_3$ (generation of Pd(0) *in situ*), and $Pd_2(dba)_3$.

In the early 1980s, at the time when extensive research was directed towards preparing conducting polymers, Kumada discovered the mild and efficient cross-coupling reaction of Grignard reagents with various heterocyclic systems using nickel-based catalysts (Scheme 2.8).[69] The most commonly used coupling reagent for this reaction is $Cl_2Ni(dppp)$. Typical catalyst loadings fall within the range of 0.1 – 1 mol % with respect to the organic halide. The coupling is performed by treating an *in situ* prepared Grignard reagent with a second organic halide and the nickel catalyst in an ethereal solvent.

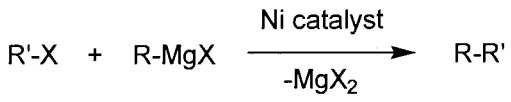

Scheme 2.8. General Kumada reaction.

2.2 The Synthesis of Oligothiophenes Bridged by Sulfur

2.2.1 Synthesis of Sulfur-Bridged Oligomers by a Divergent Approach (Series II)

The syntheses of uncapped thiophene oligomers bridged by divalent sulfur have been reported sporadically throughout the literature. The most common route involves the coupling of a thiophenethiol with a bromothiophene in the presence of a copper salt. The major drawback of this procedure is the preparation and use of smelly and toxic thiols. Nevertheless, Nakayama *et al.* have successfully used this method to prepare a series of

oligo(thio-2,5-thienylenes).[70] They were able to prepare bis(2-thienyl)sulfide **2.1** in decent yield by reacting 2-bromothiophene with the cuprous salt of 2-thiophenethiol in DMF (Scheme 2.9). The α-dibromination of **2.1** was then achieved by treating it with two equivalents of NBS, providing **2.2** in good yield. Compound **2.2** was then used as a building block to prepare longer oligo(thio-2,5-thienylenes), but no physical properties on these compounds were reported by Nakayama.[70]

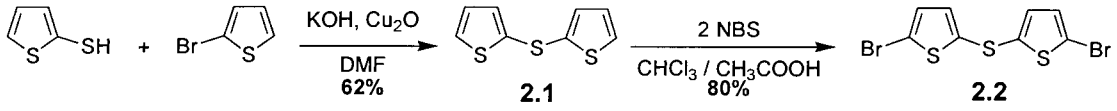

Scheme 2.9. Nakayama's synthesis of **2.1** and its α-dibrominated derivative **2.2**.

Our goal was to synthesize a series of oligomers of the general form MesS-(**T**)$_n$-S-(**T**)$_n$-SMes, with n = 1 to 3. Our initial approach was to use an iterative divergent protocol which would enable us to either cap a dibromo compound with 2-mesitylenethiol or to extend the conjugation length by a metal catalyzed cross-coupling reaction (Scheme 2.10). Once the chain length extension was made, the resulting compound could be dibrominated and then subjected again to either a capping reaction or an extension reaction. In general, the mesitylthio protecting group can be introduced in one of two ways, including (a) the reaction of α–lithiated thiophenes with 2-mesitylenesulfenyl chloride (MesSCl), or (b) by the reaction of 2-mesitylenethiol (MesSH) with a bromothiophene. The mesitylthio group was chosen because of its solubilizing ability and also because it serves as a simple NMR probe.

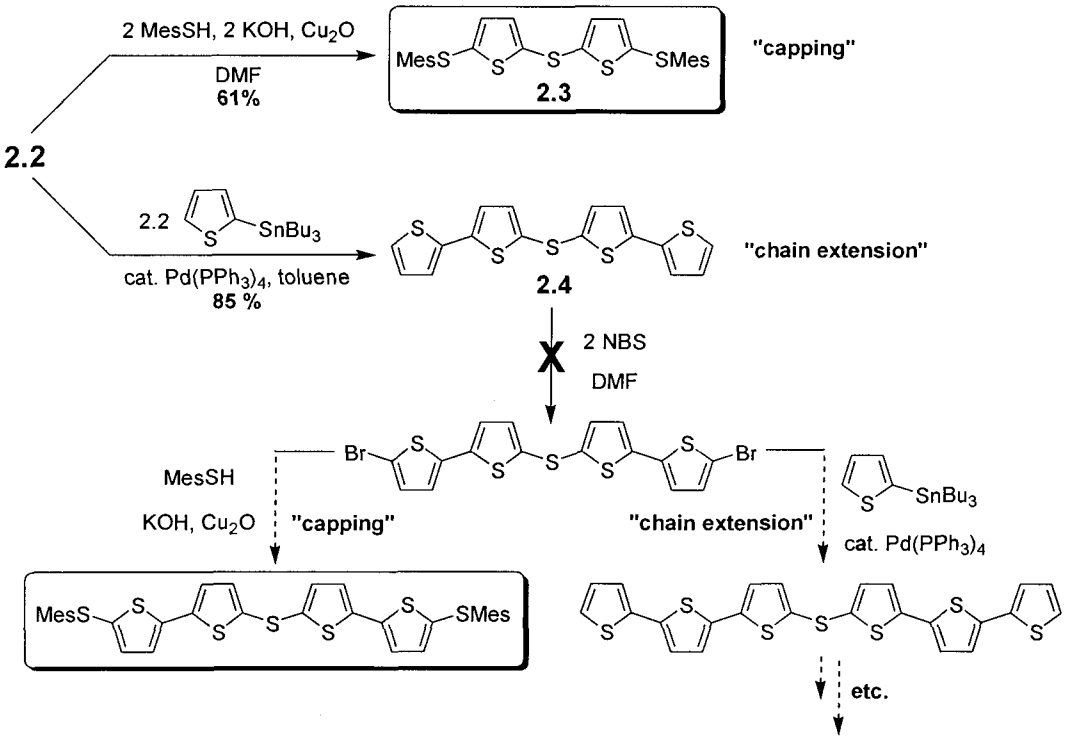

Scheme 2.10. Synthesis of MesS-$(\mathbf{T})_n$-S-$(\mathbf{T})_n$-SMes oligomers using a divergent protocol.

The first step in the process involved capping the literature compound **2.2** by treating it with two equivalents of 2-mesitylenethiol in the presence of KOH and Cu_2O (Scheme 2.10). This provided the α–mesitylthio capped bis(thiophene)sulfide **2.3** in 61% yield. Initial attempts at increasing the chain length of **2.2** involved reacting it with a slight excess of 2-thienylmagnesium bromide in the presence of [$NiCl_2$(dppp)] as catalyst under Kumada conditions. To our surprise, 2,2':5',2"-terthiophene was obtained as the only isolable product, which may suggest metal-mediated desulfurization of the internal C-S bond. A control experiment showed that the dibromide did not react with the Grignard reagent in the absence of the nickel catalyst. This phenomenon in not unprecedented, as García and co-workers have recently shown that catalytic amounts of

$[(dippe)NiH]_2$ induced the desulfurization of dibenzothiophene while in the presence of Grignard reagents such as methylmagnesium bromide (Scheme 2.11).[71] Fortunately, a

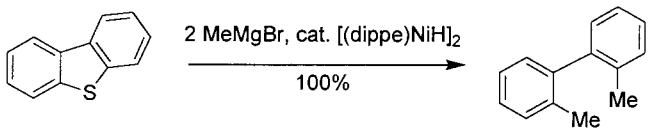

Scheme 2.11. Desulfurization of dibenzothiophene.

palladium-catalyzed Stille type reaction between **2.2** and 2-tributylstannylthiophene worked remarkably well to form the desired bis(bithiophene)sulfide derivative **2.4**. Difficulties were encountered directly after during attempts to dibrominate this compound. Addition of NBS to a dilute solution of **2.4** in DMF at room temperature resulted in immediate precipitation of a yellow solid. Analysis of this crude compound by NMR spectroscopy suggests that it is predominantly the α-monobrominated product. Warming the DMF reaction mixture to 100 °C enabled us to dissolve the monobrominated intermediate. The reaction was held at 100 °C for one hour, during which time large amounts of yellow solid had precipitated from the mixture. Solution characterization of this solid was hampered due to its insoluble nature in organic solvents. These solubility problems prompted the development of a new synthetic strategy that would introduce the internal bridging sulfur unit last. We also thought that it would be advantageous to introduce the mesitylthio end groups early on, as they may impart greater solubility to the oligomer precursors.

2.2.2 Synthesis of Sulfur-Bridged Oligomers by a Convergent Approach (Series II)

The new general approach for the convergent synthesis of MesS-$(\mathbf{T})_n$-S-$(\mathbf{T})_n$-SMes (n = 1 – 3) is outlined in Scheme 2.12. The reaction of two equivalents of a

metallated thiophene with one equivalent of a main group transfer reagent (EX_2; E = S) is deemed the convergent step. One additional desirable feature of this protocol is that the

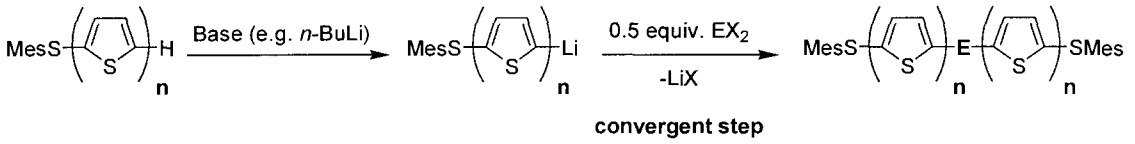

Scheme 2.12. Synthesis of main group element bridged oligomers by a convergent protocol.

bridging group could in principle be modulated by treating the intermediate α-lithiated thiophene with other main group substrates EX_2 (e.g., $PhBCl_2$, Me_2SiCl_2, $PhPCl_2$, $(PhSO_2)_2S$, etc.). Attempts have been made to prepare some bis(thienyl)sulfides by reaction of lithiated thiophenes with sulfur dichloride (SCl_2); however, these reactions typically proceeded in very low yield.[72] Bis(phenylsulfonyl) sulfide has been shown to be a highly effective alternative sulfur transfer reagent to both aryllithium and Grignard reagents.[73]

Compound **2.3** was previously prepared according to Scheme 2.10. We thought it would be beneficial to prepare this same compound using the convergent strategy, as outlined in Scheme 2.13. Firstly, 2-mesitylthiothiophene **2.5** was prepared in 77% by the reaction of 2-thienylmagnesium bromide with MesSCl. Subsequent lithiation of **2.5** with one equivalent of *n*-BuLi, followed by treatment with $(PhSO_2)_2S$ provided the desired sulfide **2.3** in 80% yield. Spectroscopic data were identical to those for material prepared by Scheme 2.10. Bromination of **2.5** with NBS yielded monobromothiophene **2.6** in 87%. This compound was previously prepared in 57% by treating 2,5-dibromothiophene with one equivalent of *n*-BuLi, followed by trapping the 2-lithio derivative with MesSCl.[42]

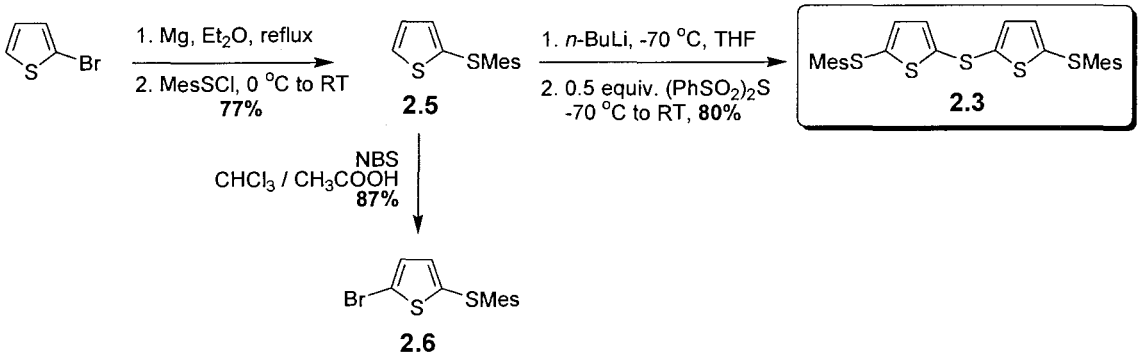

Scheme 2.13. Convergent synthesis of MesS-**T**-S-**T**-SMes (**2.3**).

By analogy, the bis(bithiophene)sulfide derivative **2.8** was prepared by lithiation of **2.7** followed by the introduction of sulfur with $(PhSO_2)_2S$ (Scheme 2.14).

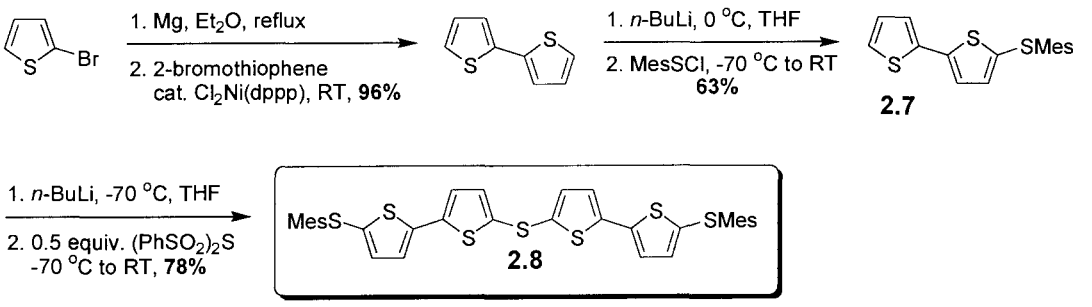

Scheme 2.14. Synthesis of MesS-$\mathbf{T_2}$-S-$\mathbf{T_2}$-SMes (**2.8**).

The bis(terthiophene)sulfide compound **2.11** required a slightly more elaborate route (Scheme 2.15). Selective bromination[74] of **2.7** at the α-position with NBS in DMF was performed at room temperature, thus providing **2.9** in 90% yield. A Stille reaction between **2.9** and 2-tributylstannylthiophene with $Pd(PPh_3)_4$ as the catalyst in toluene provided 5-mesitylthio-2,2':5',2"-terthiophene **2.10** in 88% yield. Terthiophene **2.10** was converted to the desired sulfide **2.11** in 50% by lithiation and quenching the anion with $(PhSO_2)_2S$.

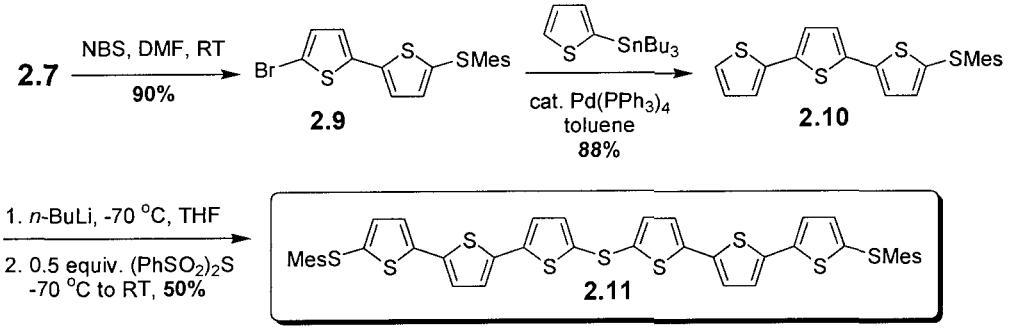

Scheme 2.15. Synthesis of MesS-$\mathbf{T_3}$-S-$\mathbf{T_3}$-SMes (**2.11**).

2.2.3 Synthesis of 3,4-Ethylenedioxythiophene Containing Oligomers (Series II)

The next sections deal with the synthesis of some "mixed" sulfur bridged oligomers that contain both thiophene and 3,4-ethylenedioxythiophene (EDOT) rings.

As a starting point, we sought to prepare a more electron-rich version of **2.3** by incorporating ethylenedioxy substituents on the β-positions of the thiophene rings. The

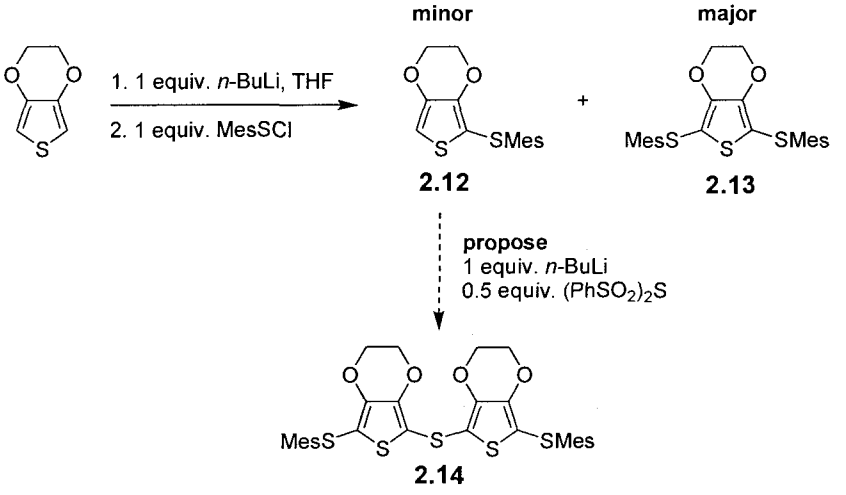

Scheme 2.16. Reaction of 2-lithioEDOT with MesSCl.

initial idea was to mimic the convergent synthesis of **2.3** (Scheme 2.16). However, this idea was quickly abandoned due to difficulties in preparing large amounts of pure 2-mesitylthio-3,4-ethylenedioxythiophene **2.12**. Nodwell has shown that the reaction of lithioEDOT with MesSCl preferentially gives the bisubstituted EDOT **2.13** over the monosubstituted compound **2.12**.[42]

We were able to prepare bis(3,4-ethylenedioxy-2-thienyl)sulfide **2.15** in 79% by treating 2-lithioEDOT with $(PhSO_2)_2S$ in THF (Scheme 2.17). By analogy to the divergent synthesis of parent thiophene **2.3**, dibromination of **2.15**, followed by capping with MesSH may provide entry into the desired compound **2.14**. Dibromination of **2.15**

with two equivalents of NBS in acetonitrile at -20 °C afforded a white solid. Conversion to the dibromide was confirmed by ^{1}H NMR spectroscopy. The signal at 6.33 ppm for the α-protons of **2.15** completely vanishes, while a new multiplet at 4.25 ppm appears for the ethylenedioxy protons of the dibromide product. Even when stored in an inert atmosphere, the isolated white solid of **2.16** rapidly converts to a dark blue compound. Wudl *et al.* have recently shown that prolonged storage of 2,5-dibromo-3,4-ethylenedioxythiophene in the solid state at room temperature results in the formation of a highly conducting blue-black crystalline polymer.[75] We believe that monomer **2.16** may also be undergoing a similar solid state polymerization reaction. No further studies have been carried out on the polymer resulting from **2.16**, but it would be interesting to probe the conductivity of this material, and compare it to that of Wudl's. The tendency of **2.16** to polymerize has hampered its use in subsequent chemistry. Fortunately, the introduction of MesS units onto **2.15** could be accomplished by trapping the bright red dianion of **2.15** with two equivalents of MesSCl in THF, giving **2.14** in moderate yield (Scheme 2.17).

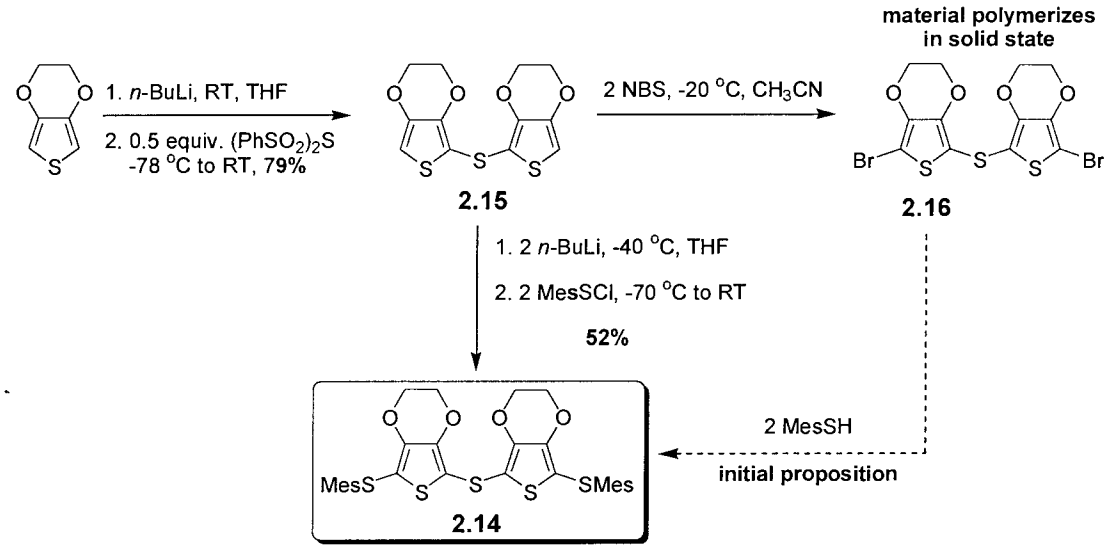

Scheme 2.17. Synthesis of MesS-E-S-E-SMes (**2.14**).

A pair of isomeric EDOT containing bis(bithiophene)sulfide derivatives (**2.18** and **2.22**) were then prepared. The system with the EDOTs located on the "inside" of the oligomer was prepared by Scheme 2.18. Stille coupling of 2-tributylstannyl-3,4-ethylenedioxythiophene with the monobromide **2.6** using $Pd(PPh_3)_4$ afforded **2.17** in decent yield. Lithiation of **2.17** with *n*-BuLi, followed by quenching with $(PhSO_2)_2S$ gave **2.18** in 68% yield (Scheme 2.18).

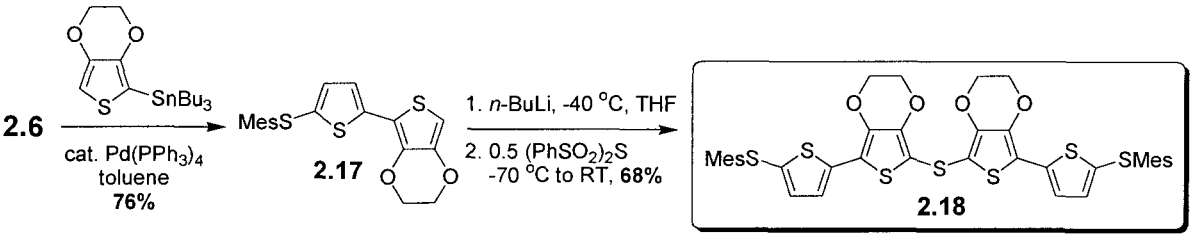

Scheme 2.18. Synthesis of MesS-**TE**-S-**ET**-SMes (**2.18**).

The isomeric bis(bithiophene)sulfide **2.22** with the EDOTs on the "outside" was prepared according to Scheme 2.19. The Grignard reagent of EDOT was prepared *in situ* by the action of $MgBr_2 \cdot Et_2O$ on 2-lithioEDOT. Subsequent coupling of the Grignard reagent to 2-bromothiophene was effected by a Kumada reaction, affording bithiophene **2.19** in good yield. Selective bromination of **2.19** with NBS in DMF at -20 °C provided **2.20** in 85% yield. This reaction takes advantage of the fact that the more electron-rich EDOT ring is more susceptible to electrophilic aromatic substitution. Treatment of **2.20** with *n*-BuLi directed the lithium to the EDOT ring, which could then be reacted with MesSCl to give the capped monomer **2.21** in 66% yield. Finally, lithiation of **2.21**, followed by introduction of sulfur with $(PhSO_2)_2S$ gave **22** in 72% yield.

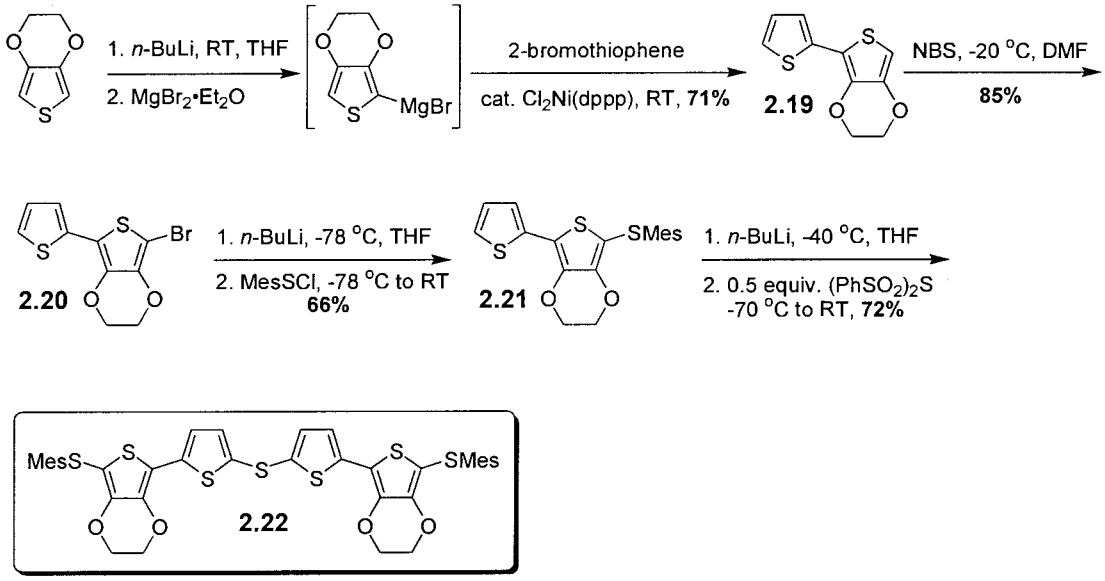

Scheme 2.19. Synthesis of MesS-**ET**-S-**TE**-SMes (**2.22**).

Nodwell has reported the synthesis of 5-mesitylthio-2,2'-bis(3,4-ethylenedioxythiophene) (**2.23**), but showed that it was unreactive towards deprotonation with strong bases (e.g., *n*-butyllithium).[42] Thus, we were unable to prepare the bis(biEDOT)sulfide derivative because the necessary lithio-biEDOT intermediate was unattainable (Scheme 2.20). An alternative would be to use our divergent protocol starting with **2.16**, but we have already demonstrated that this compound is unstable as it undergoes rapid polymerization.

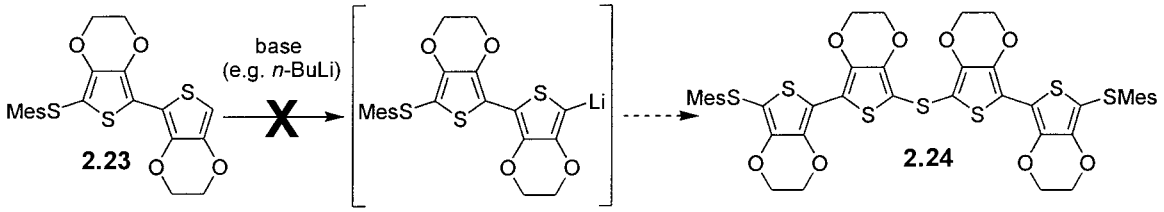

Scheme 2.20. Proposed Synthesis of MesS-**EE**-S-**EE**-SMes (**2.24**).

The ^{1}H NMR spectrum of **2.21** in $CDCl_3$ is shown in Figure 2.5 as a representative example. The doublet of doublets at 7.15, 7.08, and 6.94 ppm are due to the three inequivalent thiophene protons. The sharp singlet at 6.92 ppm is assigned to the protons that are directly attached to the mesitylene ring. The multiplet at 4.29 ppm is attributed to the ethylenedioxy protons, and the two singlets at 2.56 and 2.25 ppm (2:1 ratio, respectively) are assigned to the methyl protons on the mesitylene ring. The ^{1}H NMR spectrum of **2.22** in d_8-THF is shown in Figure 2.6. The NMR spectrum of **2.22** is simplified considerably with respect to that of **2.21**. This is due to the fact that the terminal α-proton found in **2.21** is replaced by a sulfur atom, giving rise to only two inequivalent thiophene protons for **2.22**. The thiophene protons in **2.22** now appear as two doublets, one at 7.05 ppm, and the other at 6.91 ppm. All other peaks are consistent with the proposed structure of **2.22**.

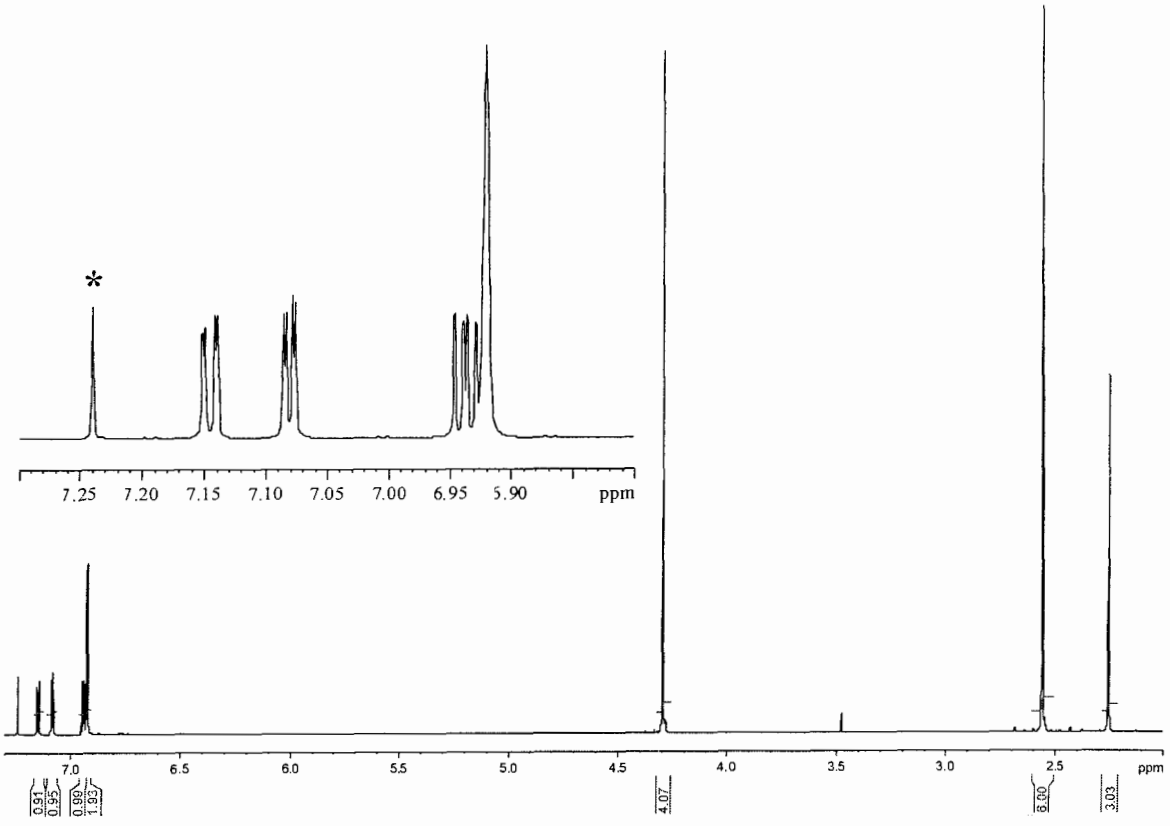

Figure 2.5. ^{1}H NMR spectrum of **2.21** in $CDCl_3$. The peak with an asterisk is due to $CHCl_3$.

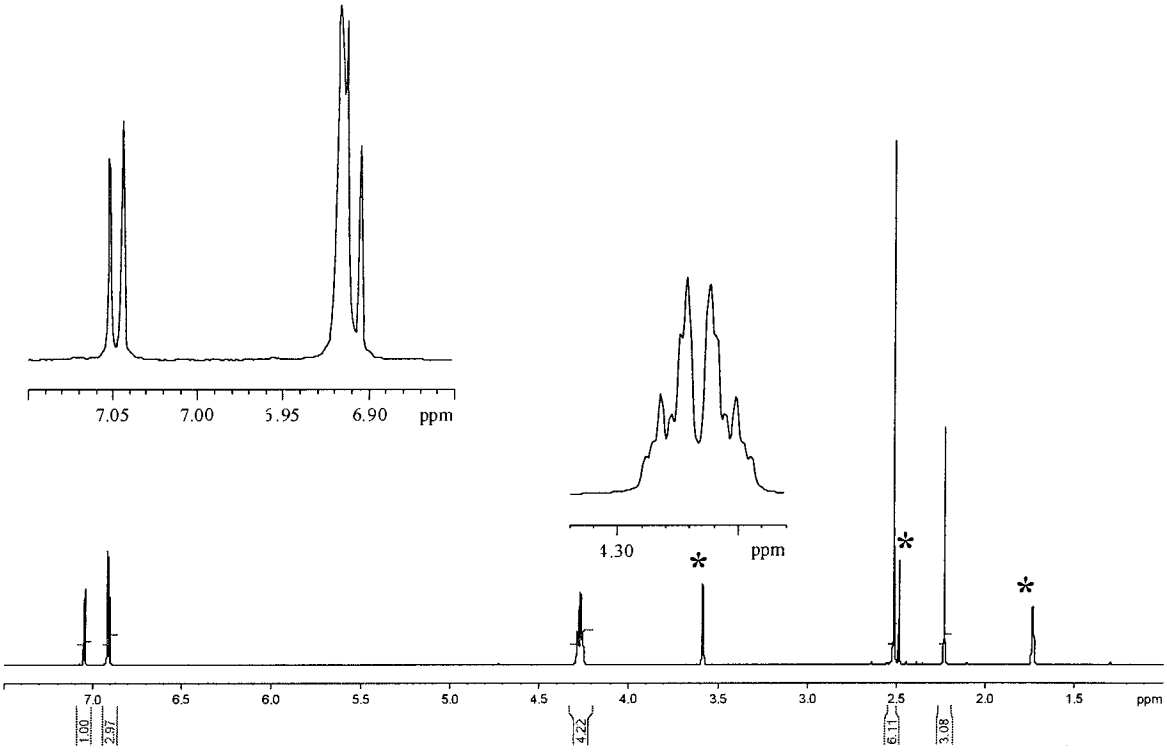

Figure 2.6. ^{1}H NMR spectrum of **2.22** in d_8-THF. The peaks with asterisks at 3.58 and 1.73 ppm are due to THF, whereas the peak at 2.49 ppm is due to water.

2.2.4 Synthesis of α– Uncapped Bis(bithiophene) Sulfide Oligomers (Series I)

Compounds **2.1**, **2.4**, and **2.15** are all α-uncapped thiophene oligomers that can be oxidatively polymerized by either chemical or electrochemical methods. To extend this series, the isomeric bis(bithiophene)sulfide oligomers **2.25** and **2.26** have been synthesized by two independent procedures (Scheme 2.21). By analogy with the synthesis of **2.4**, the Stille coupling of 2-tributylstannyl-3,4-ethylenedioxythiophene and **2.2** in the presence of $Pd(PPh_3)_4$ afforded bis(bithiophene) **2.25** in 77%. Isomer **2.26** was prepared in 66% by lithium-halogen exchange of **2.20** with one equivalent of *n*-BuLi, followed by treating the anion with $(PhSO_2)_2S$ in THF.

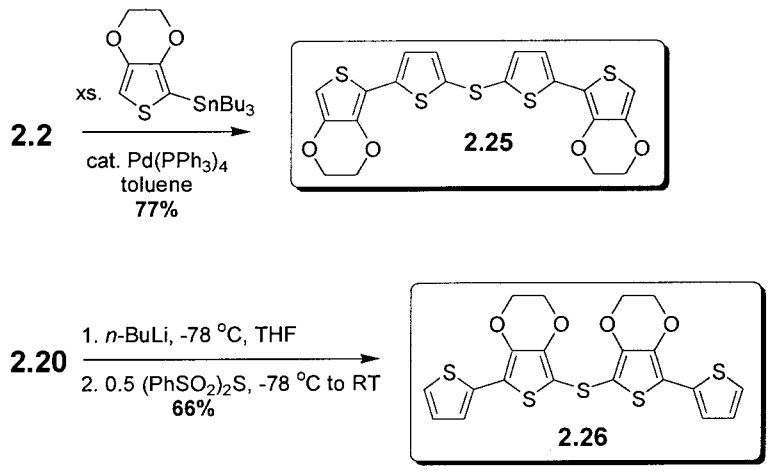

Scheme 2.21. Synthesis of **ET-S-TE (2.25)** and **TE-S-ET (2.26)**.

2.3 Summary

A series of thiophene oligomers bridged by divalent sulfur and capped with mesitylthio (MesS) groups have successfully been prepared. The initial strategy made use of a divergent synthetic procedure. The internal bridging sulfur group was introduced in the first step by a copper mediated carbon-sulfur bond forming reaction between 2-bromothiophene and 2-thiophenethiol. Once the bridging unit was in place, the resulting **T-S-T (2.1)** monomer was subjected to dibromination with NBS to provide the necessary precursor Br-**T**-S-**T**-Br (**2.2**). Compound **2.2** could either be capped with MesSH or its chain length extended by a Stille type cross-coupling reaction with 2-tributylstannylthiophene. The process was terminated after this first iteration due to solubility problems that were encountered during the attempted synthesis of Br-**TT**-S-**TT**-Br. Therefore, an alternative convergent protocol was developed to avoid such solubility problems. The new method takes advantage of the fact that the terminal solubilizing groups (MesS) are introduced early on in the synthesis. A series of thiophene oligomers (**2.5**, **2.7**, **2.10**, **2.17**, and **2.21**) capped at one of the α-terminal position with a

MesS group and uncapped at the other end, were successively metallated and coupled to sulfur by using $(PhSO_2)_2S$. Compound **2.14** could only be prepared by double deprotonation of **2.15**, followed by anion trapping with two equivalents of MesSCl. All resulting sulfide compounds have been fully characterized by standard spectroscopic techniques and all show good solubility in organic solvents. The electronic properties of these molecules are presented in the following chapter.

A series of α-uncapped thiophene sulfide oligomers (**2.1**, **2.4**, **2.15**, **2.25**, and **2.26**) have also been synthesized. Several of these monomers underwent electrochemical oxidative polymerization affording a new class of conducting thiophene-sulfide hybrid polymers. The polymer results are briefly discussed in the following chapter.

2.4 Experimental Section

General Experimental

Unless stated otherwise, all reactions and manipulations were carried out under an argon atmosphere using standard Schlenk or glovebox techniques. Glassware was oven dried at 125 °C for 24 h prior to use. Diethyl ether, tetrahydrofuran (THF), and toluene were distilled under argon from sodium benzophenone ketyl. Acetonitrile, dichloromethane, and hexanes were distilled over calcium hydride. All reagents were purchased from Aldrich and used as received except as otherwise stated.

All ^1H and ^{13}C NMR spectra were recorded on a Bruker AC300 instrument (300 MHz for ^1H, and 75.47 MHz for ^{13}C), unless otherwise noted. ^1H and ^{13}C NMR spectra were referenced to the central solvent line, relative to tetramethylsilane. UV-visible spectra were recorded on a Varian Cary 5 instrument. Elemental analyses were carried out by Canadian Microanalytical Services Ltd., Vancouver, BC, Canada. Mass spectra

were recorded on a Finnigan 3300 or a Kratos Concept H spectrometer using electron impact (EI) or liquid secondary ion (LSI) sources. Melting points were taken on a Gallenkamp melting point apparatus and are uncorrected.

Purification of sulfur dichloride: SCl_2

Commercially available SCl_2 is usually contaminated with a minimum of 20 % sulfur monochloride (S_2Cl_2; bpt. 138 °C). This results from the disproportionation of SCl_2 to S_2Cl_2 and chlorine gas. Small amounts of SCl_2 were purified by the following method directly prior to use. In the absence of light, 2 mL of PCl_3 was added rapidly to 20 mL of commercially available SCl_2. The dark red mixture was then stirred for 10 minutes at room temperature. The product was distilled (under an atmosphere of argon) to afford 10 mL of dark red SCl_2, bp 59 °C.

Bis(phenylsulfonyl)sulfide: $(PhSO_2)_2S$

Prepared by a modification of the literature method.[72] To a slurry of sodium benzenesulfinate (50 g, 0.30 mol) in freshly distilled toluene (700 mL) was added dropwise a solution of SCl_2 (10 mL) in toluene (40 mL) over 1 h. After the addition was complete, the mixture was stirred overnight at room temperature. The sodium chloride was filtered off and washed with toluene (3 x 75 mL). The solvent was then removed from the filtrate by rotary evaporation to leave a pale yellow solid that was recrystallized from benzene to give white needles of the title compound, yield 36 g (75 %). Mp: 132 °C (Lit.[72] mp 128 – 130 °C).

2-Mesitylenethiol. This compound was prepared by the literature route.[76] A slurry of magnesium powder (2.79 g, 0.11 mmol) and one crystal of iodine in THF (40 mL) were brought to a gentle reflux. A solution of 2-bromomesitylene (14.7 mL, 0.10 mol) in THF (20 mL) was then added dropwise to the above refluxing suspension over a period of 2 h. Once the addition was complete, the brown mixture was left to reflux overnight. The reaction mixture was cooled to 0 °C, and solid sulfur (3.20 g, 0.10 mol) was added portionwise over 10 min. The grayish mixture was then warmed to room temperature and stirred for an additional 1 h. This was recooled to 0 °C and the mixture was carefully quenched by the addition of water (20 mL). The mixture was then acidified by the slow addition of 6 M HCl (25 mL). The organic layer was separated and immediately dried over anhydrous magnesium sulfate. After filtration of the drying agent, the solvent was removed from the filtrate by rotary evaporation to leave a clear yellow oil. Vacuum distillation at 75 °C/10^{-3} Torr afforded the title compound as a colorless oil, yield 11.5 g (72 %). ^{1}H NMR ($CDCl_3$): δ 6.81 (s, 2H), 3.09 (s, 1H), 2.25 (s, 6H), 2.18 (s, 3H).

2-Mesitylenesulfenyl chloride. This compound was prepared by the literature route.[42] To a slurry of NCS (9.20 g, 68.9 mmol) in THF (40 mL) was added dropwise a solution of 2-mesitylenethiol (10.0 g, 65.7 mmol) in THF (30 mL). After stirring at room temperature for 1 h, the solvent was removed in vacuo to leave a bright orange solid. Addition of hexanes (30 mL) to this solid resulted in the precipitation of the succinimide by-product, which was removed by filtration, and washed with additional hexanes (3 x 10 mL). The volatiles were then flash distilled from the filtrate to a leave an orange crystalline solid,

yield 12.0 g (98 %). This material was stored in the glovebox at -30 ^{0}C and was used without further purification. ^{1}H NMR ($CDCl_3$): δ 6.98 (s, 2H), 2.60 (s, 6H), 2.29 (s, 3H).

2-Thiophenethiol. This compound was prepared by the literature route.[77] *n*-Butyllithium (100 mL, 0.16 mol, 1.6 M in hexanes) was added dropwise to a solution of thiophene (13.5 g, 0.16 mol) at -40 °C over a 30 min. period. After the addition, the temperature of the reaction mixture was held between -30 °C and -20 °C for 1 h, and then lowered to -70 °C. Solid sulfur (5.12 g, 0.16 mol) was then added to the cold solution in one aliquot. After stirring for 30 min the temperature of the mixture was allowed to rise to -10 °C by removing the cooling bath, whereupon the yellow solution was carefully poured into 100 mL of rapidly stirring ice-water. The upper organic phase was removed and the aqueous layer was made acidic by the slow addition of 2 M H_2SO_4. The aqueous phase was immediately extracted with Et_2O (2 x 50 mL). The combined ether extracts were washed with water (2 x 100 mL) and dried over anhydrous sodium sulfate. After filtration of the drying agent, the solvent was removed from the filtrate by rotary evaporation to leave a golden yellow oil. Vacuum distillation at 58 °C/5 mmHg afforded 2-thiophenethiol as a colorless oil, yield 11.3 g (61 %). ^{1}H NMR ($CDCl_3$): δ 7.21 (dd, J = 5.1, 1.5 Hz, 1H), 6.99 (dd, J = 3.7, 1.5 Hz, 1H), 6.82 (dd, J = 5.1, 3.7 Hz, 1H), 3.42 (s, 1H). This compound was stored at -20 °C in a sealed ampule.

Bis(2-thienyl)sulfide (2.1). This compound was prepared by the literature route.[70] A solution of 2-thiophenethiol (6.58 g, 56.6 mmol) in DMF (10 mL) was added dropwise to a stirred slurry of 2-bromothiophene (9.23 g, 56.6 mmol), KOH (3.84 g, 68.4 mmol), and

copper (I) oxide (4.06 g, 28.4 mmol) in DMF (30 mL) at room temperature. The mixture was warmed slowly and heated between 140 - 150 °C for 20 h. The resulting mixture was poured into 6 M HCl (60 mL), and benzene (200 mL) was added to it. The resulting two-phase mixture was stirred for 20 min., and then filtered through a plug of Celite. The organic layer was separated, washed with water (3 x 50 mL), and dried over anhydrous $MgSO_4$. After filtration of the drying agent, the solvent was removed from the filtrate by rotary evaporation to leave an orange oil. Vacuum distillation at 118 – 120 °C/10^{-3} Torr afforded the title compound as a pale yellow oil, yield 7.0 g (62 %). ^{1}H NMR ($CDCl_3$): δ 7.35 (dd, J = 5.1, 1.5 Hz, 2H), 7.22 (dd, J = 3.7, 1.5 Hz, 2H), 7.00 (dd, J = 5.1, 3.7 Hz, 2H).

Bis(5-bromo-2-thienyl)sulfide (2.2). Prepared by a modification of the literature method.[70] Bis(2-thienyl)sulfide **2.1** (5.04 g, 25.4 mmol) was dissolved in CH_2Cl_2/CH_3COOH (100 mL, 3:2 v/v). NBS (9.05 g, 50.8 mmol) was added portionwise to the solution at 0 °C, and the resulting mixture was stirred at this temperature for 4 h. The mixture was poured into water (100 mL), and the organic phase was separated. The organic layer was washed with water (3 x 40 mL), saturated sodium bicarbonate (3 x 40 mL), and dried over anhydrous magnesium sulfate. After filtration, the solvent was removed by rotary evaporation, and the red residue was purified by column chromatography (silica gel, hexane/dichloromethane (7:3 v/v)) to provide 7.23 g (80%) of the title compound as a yellow oil. ^{1}H NMR ($CDCl_3$): δ 6.96 (d, J = 3.7 Hz, 2H), 6.90 (d, J = 3.7 Hz, 2H). ^{13}C NMR ($CDCl_3$): δ 135.74, 133.70, 130.52, 115.80.

Bis(5-mesitylthio-2-thienyl)sulfide (2.3). A solution of 2-mesitylenethiol (1.12 g, 7.36 mmol) in DMF (15 mL) was added dropwise to a stirred slurry of the dibromide **2.2** (1.31 g, 3.68 mmol), KOH (0.49 g, 8.73 mmol), and copper (I) oxide (0.53 g, 3.70 mmol) in DMF (15 mL) at room temperature. The mixture was warmed slowly and heated between 140 - 150 °C for 20 h. The resulting mixture was poured into 6 M HCl (15 mL), and benzene (250 mL) was added to it. The resulting two-phase mixture was stirred for a while and then filtered through a plug of Celite. The organic layer was separated, washed with water (3 x 50 mL), and dried over anhydrous $MgSO_4$. After filtration, removal of the solvent gave an orange oil, which was purified by column chromatography (silica gel, hexanes/ethyl acetate (9:1 v/v)) to provide a slightly yellow solid. Recrystallization from methanol/chloroform produced white crystalline flakes of the title compound, yield 1.12 g (61%). Mp: 92 °C. UV-Vis (CH_2Cl_2) λ_{max} 310 nm (ε 1.9 x 10^4). ^{1}H NMR ($CDCl_3$): δ 6.94 (s, 4H), 6.89 (d, J = 3.7 Hz, 2H), 6.66 (d, J = 3.7 Hz, 2H), 2.46 (s, 12H), 2.28 (s, 6H). ^{13}C NMR ($CDCl_3$): δ 142.85, 142.34, 139.60, 134.35, 132.96, 129.46, 129.01, 127.48, 21.72, 21.10. MS (LSI): *m/z* 498 (M^+, 100%). Anal. Calcd $C_{26}H_{26}S_5$: C, 62.61; H, 5.25; S, 32.14%. Found: C, 62.40; H, 5.29; S, 31.83%.

Bis(5,2'-bithien-2-yl)sulfide (2.4). A solution containing 2-(tributylstannyl)thiophene (1.85 g, 4.95 mmol), **2.2** (800 mg, 2.25 mmol) and $Pd(PPh_3)_4$ (130 mg) in toluene (10 mL) was refluxed in the dark for 20 h. After cooling to room temperature, the black mixture was diluted with ether (100 mL) and poured into saturated potassium fluoride (100 mL). The resulting tributyltin fluoride was filtered off and washed with cold ether (3 x 15 mL). The organic phase was collected, washed with brine and dried (Na_2SO_4). The

solvent was removed by rotary evaporation and the residue was purified by column chromatography (silica, 1:1 hexane/diethyl ether) to provide a bright yellow solid. This was recrystallized from hexanes/dichloromethane to give **2.4** as yellow plates, yield 692 mg (85 %). Mp: 96 °C. ^{1}H NMR ($CDCl_3$): δ 6.96 – 7.20 (m). ^{13}C NMR ($CDCl_3$): δ 141.58, 136.66, 133.85, 133.67, 127.91, 124.94, 124.17, 123.83. MS (LSI): *m/z* 362 (M^+, 100%). Anal. Calcd for $C_{16}H_{10}S_5$: C, 53.00; H, 2.78; S, 44.22%. Found: C, 52.80; H, 2.81; S, 44.43%.

2-(Mesitylthio)thiophene (2.5). 2-bromothiophene (4.00 g, 24.5 mmol) was added to a slurry of magnesium powder (0.90 g, 37.0 mmol) in diethyl ether (20 mL). The reaction was initiated with a small amount of the bromo reagent and a crystal of iodine. Once the exothermic reaction had started, the remaining bromo reagent was added dropwise to the ice-cooled magnesium slurry over the course of 20 min. The solution was allowed to warm to room temperature, and then refluxed for 1 h. After which time the brown Grignard solution was recooled to 0 °C, and a solution of 2-mesitylenesulfenyl chloride (4.57 g, 24.5 mmol) in hexanes (25 mL) was added dropwise via cannula. The resulting pale brown solution was stirred at 0 °C for an additional 30 min. The mixture was then warmed to room temperature and poured into brine (100 mL). The aqueous layer was extracted with ether (3 x 50 mL), and the combined organic extracts were further washed with water (3 x 50 mL) and dried over anhydrous sodium sulfate. After filtration, removal of the solvent gave a dark brown oil, which was purified by flash chromatography (silica gel, hexanes) to provide a pale yellow liquid, yield 4.41 g (77 %). ^{1}H NMR (CD_2Cl_2): δ 7.16 (dd, J = 5.1, 1.5 Hz, 1H), 6.95 (s, 2H), 6.92 (dd, J = 3.7, 1.5 Hz, 1H), 6.88 (dd, J =

5.1, 3.7 Hz, 1H), 2.49 (s, 6H), 2.25 (s, 3H). ^{13}C NMR ($CDCl_3$): δ 142.82, 139.27, 137.42, 130.03, 129.36, 128.24, 127.09, 126.07, 21.82, 21.09. HRMS (EI) for $C_{13}H_{14}S_2$ [M^+]: Calcd: 234.0537. Found: 234.0541.

Bis(5-mesitylthio-2-thienyl)sulfide (2.3). A solution of 2-(mesitylthio)thiophene **2.5** (5.00 g, 21.3 mmol) in THF (100 mL) cooled to –70 °C was treated dropwise with *n*-butyllithium (13.3 mL, 21.3 mmol, 1.6 M in hexanes). The resulting yellow solution was stirred at –70 °C for 1 h. After which time, a solution of bis(phenylsulfonyl) sulfide (3.34 g, 10.6 mmol) in THF (20 mL) was added dropwise via cannula, and the resulting golden yellow solution was stirred at –70 °C for an additional 1 h. The mixture was warmed to room temperature and poured into water (100 mL). The aqueous layer was extracted with ether (3 x 50 mL), and the combined organic extracts were further washed with water (3 x 50 mL) and dried over anhydrous sodium sulfate. After filtration, removal of the solvent gave a yellow oil, which was purified by column chromatography (silica gel, hexanes/ethyl acetate (9:1 v/v)) to provide a slightly yellow solid. Recrystallization from methanol/chloroform produced white crystalline flakes of the title compound, yield 4.26 g (80 %). Spectroscopic data were identical to those for material prepared by Scheme 2.8.

2-Bromo-5-(mesitylthio)thiophene (2.6). This compound has been prepared previously by a different route.[42] 2-(Mesitylthio)thiophene **2.5** (4.36 g, 18.6 mmol) was dissolved in a mixture of chloroform (20 mL) and glacial acetic acid (20 mL). To this was added solid NBS in small portions. After stirring at room temperature for 3 h, the golden yellow solution was poured onto 100 mL of water, and the organic phase was separated. The

organic layer was washed with saturated sodium bicarbonate (3 x 75 mL), water (3 x 75 mL), and then dried over anhydrous sodium sulfate. After filtration of the drying agent, the solvent was removed by rotary evaporation to provide a pale yellow solid. This was recrystallized from absolute ethanol to afford the title compound as white needles, yield 5.05 g (87 %). Mp: 49 °C (Lit.[42] mp 47 – 48 °C). ^{1}H NMR ($CDCl_3$): δ 6.95 (s, 2H), 6.80 (d, J = 3.7 Hz, 1H), 6.70 (d, J = 3.7 Hz, 1H), 2.49 (s, 6H), 2.25 (s, 3H). MS (EI): *m/z* 312 (M^+, ^{79}Br, 90%), 314 (M^+, ^{81}Br, 100%).

2,2'-Bithiophene. This compound was prepared by the literature route.[78] A slurry of magnesium powder (4.59 g, 0.19 mmol) and one crystal of iodine in Et_2O (40 mL) were combined at room temperature. 2-bromothiophene (12.1 mL, 0.13 mol) was then added dropwise to the above suspension at room temperature over a period of 1 h. The solution was heated to a gentle reflux and stirred for a further 2 h. The mixture was then cooled to room temperature and transferred via cannula to a solution of 2-bromothiophene (9.7 mL, 0.10 mol) and catalytic Ni(dppp)Cl_2 (105 mg) in Et_2O (50 mL) at 0 °C. After the addition, the mixture was warmed to room temperature and left to stir overnight. The dark brown mixture was then poured into 300 mL of ice-water and extracted with Et_2O (3 x 150 mL). The organic extracts were combined, washed once with water (100 mL), and dried over anhydrous sodium sulfate. The solvent was removed by rotary evaporation and the residue was purified by flash chromatography (silica, hexanes) to afford 2,2'-bithiophene as a white crystalline solid, yield 16 g (96 %). ^{1}H NMR ($CDCl_3$): δ 7.22 (dd, J = 5.1, 1.1 Hz, 2H), 7.18 (dd, J = 3.6, 1.1 Hz, 2H), 7.00 (dd, J = 5.1, 3.6 Hz, 2H).

5-Mesitylthio-2,2'-bithiophene (2.7). To a solution of bithiophene (3.00 g, 18.0 mmol) in THF (60 mL) was added dropwise *n*-butyllithium (11.3 mL, 18.1 mmol, 1.6 M in hexanes) at 0 °C. The mixture was warmed to room temperature and stirred for 1.5 h. The mixture was cooled to –70 °C, and a solution 2-mesitylenesulfenyl chloride (3.38 g, 18.1 mmol) in hexanes (25 mL) was then added dropwise via cannula. Stirring was continued at –70 °C for 0.5 h, then the mixture was allowed to warm to room temperature, and water (50 mL) was added. The aqueous layer was washed with ether (50 mL), and the organic extracts were washed with brine (3 x 50 mL) and dried over anhydrous magnesium sulfate. The solvent was removed by rotary evaporation, and the green oily residue was purified by column chromatography (silica gel, hexanes) to provide a slightly yellow solid. Subsequent recrystallization from methanol produced white crystalline flakes of the title compound, yield 3.60 g (63 %). Mp: 46 °C. ^{1}H NMR (500 MHz, $CDCl_3$): δ 7.13 (dd, J = 5.1, 1.1 Hz, 1H), 7.01 (dd, J = 3.6, 1.1 Hz, 1H), 6.96 (s, 2H), 6.94 – 6.92 (m, 2H), 6.81 (d, J = 3.7 Hz, 1H), 2.53 (s, 6H), 2.28 (s, 3H). ^{13}C NMR ($CDCl_3$): δ 142.82, 139.46, 137.77, 137.17, 136.74, 129.55, 129.44, 128.82, 127.71, 124.15, 123.56, 123.44, 21.84, 21.11. MS (LSI): *m/z* 316 (M^+, 100%). Anal. Calcd $C_{17}H_{16}S_3$: C, 64.51; H, 5.10; S, 30.39%. Found: C, 64.58; H, 5.29; S, 30.07%.

Bis(5'-mesitylthio-5,2'-bithien-2-yl)sulfide (2.8). A solution of **2.7** (6.00 g, 18.9 mmol) in THF (150 mL) cooled to –70 °C was treated dropwise with *n*-butyllithium (11.9 mL, 19.0 mmol, 1.6 M in hexanes). The resulting bright yellow solution was stirred at –70 °C for 1 h. After which time, a solution of bis(phenylsulfonyl) sulfide (2.98 g, 9.48 mmol) in THF (20 mL) was added dropwise via cannula, and the resulting orange solution was

stirred at –70 °C for an additional 1 h. The mixture was warmed to room temperature and poured into water (100 mL). The fine yellow precipitate was filtered off and washed with cold methanol (3 x 50 mL). This solid was recrystallized from a mixture of chloroform and methanol (120 mL, 1:1 v/v) to afford **2.8** (4.90 g, 78%) as pale yellow needles. Mp: 154 °C. UV-Vis (CH_2Cl_2) λ_{max} 360 nm (ε 3.9 x 10^4). ^{1}H NMR ($CDCl_3$): δ 7.00 (d, J = 3.7 Hz, 2H), 6.94 (s, 4H), 6.86 (d, J = 4.4 Hz, 2H), 6.80 (d, J = 3.7 Hz, 2H), 6.74 (d, J = 4.4 Hz, 2H), 2.48 (s, 12H), 2.27 (s, 6H). ^{13}C NMR ($CDCl_3$): δ 142.82, 141.33, 139.57, 137.89, 136.72, 133.58, 133.48, 129.46, 129.27, 128.38, 124.02, 123.28, 21.78, 21.10. MS (EI): *m/z* 662 (M^+, 100%). Anal. Calcd. for $C_{34}H_{30}S_7$: C, 61.59; H, 4.56; S, 33.85%. Found: C, 61.40; H, 4.49; S, 33.85%.

5-Bromo-5'-mesitylthio-2,2'-bithiophene (2.9). 5-Mesitylthio-2,2'-bithiophene **2.7** (6.32 g, 20.0 mmol) was dissolved in DMF (100 mL). In the absence of light, NBS (3.91 g, 22.0 mmol) was added portionwise to the solution at room temperature. After addition, the solution was stirred at room temperature overnight in the dark. The resulting pale yellow solution was diluted with dichloromethane (100 mL) and poured into brine (100 mL). The aqueous phase was collected and washed with a second portion of dichloromethane (100 mL). All organics were collected and extracted with water (5 x 100 mL) to remove any remaining DMF. The dichloromethane layer was dried over anhydrous sodium sulfate, filtered and evaporated. The obtained pale orange liquid was purified by column chromatography (silica gel, hexanes/dichloromethane (4:1 v/v)) to provide the title compound as a yellow liquid, yield 7.10 g (90 %). ^{1}H NMR ($CDCl_3$): δ 6.94 (s, 2H), 6.87 (d, J = 4.4 Hz, 1H), 6.84 (d, J = 3.7 Hz, 1H), 6.75 (d, J = 3.7 Hz, 1H),

6.72 (d, J = 3.7 Hz, 1H), 2.49 (s, 6H), 2.26 (s, 3H). MS (LSI): *m/z* 394 (M^+, ^{79}Br, 90%), 395 (M + 1, ^{79}Br, 28%), 396 (M^+, ^{81}Br, 100%), 397 (M + 1, ^{81}Br, 27%).

5-Mesitylthio-2,2':5',2"-terthiophene (2.10). A flask was charged with 2-(tributylstannyl)thiophene (3.05 mL, 9.59 mmol), **2.9** (3.79 g, 9.59 mmol), $Pd(PPh_3)_4$ (554 mg), and toluene (20 mL). The mixture was heated to reflux for 20 h. After cooling to room temperature, the black mixture was diluted with ether (100 mL) and poured into saturated potassium fluoride (100 mL). The resulting tributyltin fluoride was filtered off, and washed with cold ether (3 x 15 mL). The organic phase was collected, washed with brine (3 x 100 mL) and dried over anhydrous sodium sulfate. The solvent was removed by rotary evaporation, and the dark yellow residue was purified by column chromatography (silica gel, hexane/EtOAc (9:1 v/v)) to provide a bright yellow solid. Recrystallization from ethanol produced yellow crystalline plates of the title compound, yield 3.36 g (88 %). Mp: 80 °C. ^1H NMR (500 MHz, $CDCl_3$): δ 7.18 (dd, J = 5.1, 1.1 Hz, 1H), 7.11 (dd, J = 3.6, 1.1 Hz, 1H), 6.99 (d, J = 3.8 Hz, 1H), 6.98 (dd, J = 5.1, 3.6 Hz, 1H), 6.96 (s, 2H), 6.92 (d, J = 3.7 Hz, 1H), 6.90 (d, J = 3.8 Hz, 1H), 6.80 (d, J = 3.8 Hz, 1H), 2.52 (s, 6H), 2.28 (s, 3H). MS (LSI): *m/z* 398 (M^+, 100%). Anal. Calcd $C_{21}H_{18}S_4$: C, 63.27; H, 4.55; S, 32.18%. Found: C, 63.47; H, 4.51; S, 31.92%.

Bis(5"-mesitylthio-5,2':5',2"-terthien-2-yl)sulfide (2.11). A solution of 5-mesitylthio-2,2':5',2"-terthiophene **2.10** (765 mg, 1.92 mmol) in THF (25 mL) cooled to –70 °C was treated dropwise with *n*-butyllithium (1.20 mL, 1.92 mmol, 1.6 M in hexanes). The resulting bright orange solution was stirred at –70 °C for 1 h. After which time, a solution

of bis(phenylsulfonyl) sulfide (302 mg, 0.96 mmol) in THF (10 mL) was added dropwise via cannula, and the resulting orange solution was stirred at –70 °C for an additional 1 h. The mixture was then warmed to room temperature and poured into a cold mixture of diethyl ether and water (120 mL, 1:5 v/v). The fine yellow precipitate was filtered off and washed with cold methanol (3 x 15 mL). This solid was recrystallized from a mixture of tetrahydrofuran and methanol (40 mL, 1:1 v/v) to afford **2.11** (400 mg, 50%) as dark golden yellow crystals. Mp: 156 °C. UV-Vis (CH_2Cl_2) λ_{max} 395 nm (ε 6.5 x 10^4). ^{1}H NMR (500 MHz, $CDCl_3$): δ 7.08 (d, J = 3.7 Hz, 2H), 6.93 – 6.95 (m, 8H), 6.90 (d, J = 3.7 Hz, 2H), 6.86 (d, J = 3.8 Hz, 2H), 6.78 (d, J = 3.7 Hz, 2H), 2.50 (s, 12H), 2.27 (s, 6H). ^{13}C NMR (125 MHz, $CDCl_3$): δ 143.06, 141.51, 139.78, 137.74, 137.22, 136.82, 135.30, 134.07, 133.89, 129.68, 129.54, 128.77, 124.91, 124.14, 123.94, 123.77, 22.01, 21.32. MS (LSI): *m/z* 826 (M^+, 10%). Anal. Calcd $C_{42}H_{34}S_9$: C, 60.97; H, 4.14; S, 34.88%. Found: C, 60.67; H, 4.17; S, 34.27%.

Bis(3,4-ethylenedioxy-2-thienyl)sulfide (2.15). To a solution of 3,4-ethylenedioxythiophene (2.50 g, 17.6 mmol) in THF (75 mL) was added dropwise *n*-butyllithium (11.0 mL, 17.6 mmol, 1.6 M in hexanes) at room temperature. The mixture was stirred at this temperature for 45 min, and then cooled to –78 °C. A solution of bis(phenylsulfonyl) sulfide (2.76 g, 8.78 mmol) in THF (20 mL) was then added dropwise via cannula. After stirring at -78 °C for 1 h, the reaction mixture was allowed to warm to room temperature and stirred for an additional 30 min. The mixture was poured into water (100 mL), and the aqueous layer was extracted with ether (3 x 100 mL). The combined organic extracts were washed with water (3 x 100 mL) and dried over

anhydrous sodium sulfate. The solvent was removed by rotary evaporation, and the residue was purified by column chromatography (silica gel, hexane/ethyl acetate (1:1 v/v)) to provide a slightly yellow solid. Recrystallization from methanol/chloroform produced off-white crystals of the title compound, yield 2.17 g (79%). Mp: 141 °C. ^{1}H NMR ($CDCl_3$): δ 6.33 (s, 2H), 4.26 (m, 4H), 4.15 (m, 4H). ^{13}C NMR ($CDCl_3$): δ 143.44, 141.12, 107.46, 102.99, 64.96, 64.29. MS (LSI): *m/z* 314 (M^+, 100%). Anal. Calcd $C_{12}H_{10}O_4S_3$: C, 45.85; H, 3.21; S, 30.59%. Found: C, 45.61; H, 3.11; S, 29.86%.

Bis(5-mesitylthio-3,4-ethylenedioxy-2-thienyl)sulfide (2.14). A solution of **2.15** (2.06 g, 6.55 mmol) was cooled to -40 °C and treated slowly with *n*-butyllithium (8.19 mL, 13.1 mmol, 1.6 M in hexanes). The bright red solution was stirred for 1.5 h at -40 °C. After which time the solution was cooled to -70 °C, and a freshly prepared solution of 2-mesitylenesulfenyl chloride (2.45 g, 13.1 mmol) in hexanes (15 mL) was added dropwise via cannula. The resulting pale brown solution was stirred at -70 °C for an additional 30 min. The mixture was then warmed to room temperature and poured into water (100 mL). The fine white precipitate was filtered off, washed with cold methanol (3 x 20 mL), and dried *in vacuo*. Yield: 2.10 g (52%). Mp: 206 °C. UV-Vis (CH_2Cl_2) λ_{max} 309 nm (ε 2.3 x 10^4). ^{1}H NMR ($CDCl_3$): δ 6.90 (s, 4H), 4.19 (m, 8H), 2.48 (s, 12H), 2.25 (s, 6H). ^{13}C NMR ($CDCl_3$): δ 143.13, 142.92, 140.55, 139.40, 129.53, 128.99, 113.53, 107.17, 64.95, 64.77, 22.19, 21.27. MS (LSI): *m/z* 614 (M^+, 18%), 463 {$(M - C_9H_{11}S)^+$, 100%}. Anal. Calcd $C_{30}H_{30}O_4S_5$: C, 58.60; H, 4.92; S, 26.07%. Found: C, 58.21; H, 4.72; S, 26.07%.

2-Tributylstannyl-3,4-ethylenedioxythiophene. This compound was prepared by modification of the literature procedure.[79] A solution of 3,4-ethylenedioxythiophene (3.00 g, 21.1 mmol) in THF (25 mL) was treated with *n*-butyllithium (13.2 mL, 21.1 mmol, 1.6 M in hexanes) at room temperature. The mixture was stirred at room temperature for 1.5 h and then cooled to -40 °C. Chlorotributylstannane (5.72 mL, 21.1 mmol) was then added dropwise by syringe to the above cold solution. After the addition, the mixture was slowly warmed to room temperature and then stirred overnight. The solvent was removed by rotary evaporation and the remaining residue was suspended in hexanes (50 mL). The white precipitate of lithium chloride was filtered off and washed with hexanes (3 x 15 mL). The solvent was removed from the filtrate under vacuum to afford the title compound as a pale yellow liquid, yield 7.95 g (87 %). The compound was used without further purification. ^{1}H NMR ($CDCl_3$): δ 6.54 (s, 1H), 4.15 (m, 4H), 1.60 – 1.48 (m, 6H), 1.39 – 1.22 (m, 6H), 1.08 (t, 9H), 0.89 (q, 6H).

3,4-Ethylenedioxy-5'-mesitylthio-2,2'-bithiophene (2.17). Prepared by a modification of the literature procedure.[42] A solution of **2.6** (2.31 g, 7.37 mmol), 2-tributylstannyl-3,4-ethylenedioxythiophene (3.20 g, 7.42 mmol) and $Pd(PPh_3)_4$ (148 mg) in toluene (25 mL) was refluxed for 20 h. After cooling to room temperature, the dark mixture was diluted with Et_2O (100 mL) and poured into saturated potassium fluoride (100 mL). The resulting tributyltin fluoride was filtered off, and washed with cold Et_2O (3 x 15 mL). The organic phase was separated, washed with brine (3 x 100 mL), and dried over anhydrous sodium sulfate. The solvent was removed by rotary evaporation, and the dark yellow residue was purified by column chromatography (silica gel, hexane/EtOAc (5:1 v/v)) to provide a

yellow solid. Recrystallization from chloroform/MeOH produced bright yellow crystalline needles of the title compound, yield 2.10 g (76 %). Mp: 102 °C (Lit.[42] mp 101 – 102 °C).

Bis(5'-mesitylthio-3,4-ethylenedioxy-5,2'-bithien-2-yl)sulfide (2.18). A solution of 3,4-ethylenedioxy-5'-mesitylthio-2,2'-bithiophene **2.17** (0.85 g, 2.27 mmol) in THF (15 mL) cooled to –40 °C was treated dropwise with *n*-butyllithium (1.42 mL, 2.27 mmol, 1.6 M in hexanes). The bright orange solution was stirred at –40 °C for 1.5 h. After which time the solution was cooled to -70 °C, and a solution of bis(phenylsulfonyl) sulfide (0.36 g, 1.15 mmol) in THF (10 mL) was added dropwise via cannula. The resulting yellow solution was stirred at -70 °C for an additional 30 min. The mixture was then warmed to room temperature and poured into a cold mixture of diethyl ether and water (120 mL, 1:5 v/v). The fine yellow precipitate was filtered off and washed with cold water (3 x 15 mL). This solid was recrystallized from a mixture of chloroform and methanol (80 mL, 3:5 v/v) to afford **2.18** (0.60 g, 68%) as yellow flakes. Mp: 198 °C. UV-Vis (CH_2Cl_2) λ_{max} 375 nm (ε 4.2 x 10^4).. ^{1}H NMR ($CDCl_3$): δ 6.93 (d, J = 3.7 Hz, 2H), 6.92 (s, 4H), 6.76 (d, J = 3.7 Hz, 2H), 4.26 (m, 8H), 2.48 (s, 12H), 2.25 (s, 6H). ^{13}C NMR ($CDCl_3$): δ 143.70, 142.94, 139.45, 136.82, 136.70, 134.90, 129.85, 129.60, 128.86, 123.55, 115.51, 104.47, 65.14, 64.85, 22.07, 21.29. HRMS (LSI) for $C_{38}H_{34}O_4S_7$ [M^+]: Calcd: 778.0502. Found: 778.0502. Anal. Calcd $C_{38}H_{34}O_4S_7$: C, 58.58; H, 4.40; S, 28.81%. Found: C, 58.47; H, 4.39; S, 28.38%.

3,4-Ethylenedioxy-2,2'-bithiophene (2.19). This compound has been prepared previously by a different route.[80] To a solution of 3,4-ethylenedioxythiophene (5.09 g, 35.8 mmol) in THF (80 mL) was added dropwise *n*-butyllithium (22.4 mL, 35.8 mmol, 1.6 M in hexanes) at room temperature. After 45 min, the reaction mixture was cooled to 0 °C by an ice bath, after which 9.25 g (35.8 mmol) of $MgBr_2 \cdot Et_2O$ was added in one portion. The solution was warmed slowly to room temperature and was stirred for a further 1 h. After which time the solution was recooled to 0 °C, and 2-bromothiophene (5.84 g, 3.47 mL, 35.8 mmol) was added in one portion via syringe, followed by the addition of the coupling reagent $Ni(dppp)Cl_2$ (194 mg, 1 mol %). The reaction mixture was allowed to warm to room temperature and stirred for an additional 48 h. This was then poured into water (200 mL), and the insoluble brown residue was filtered off and washed with ether (2 x 30 mL). The aqueous phase was collected and washed with ether (3 x 100 mL). The organic layers were combined and dried over anhydrous $MgSO_4$. After filtration, removal of the solvent gave a brown oil, which was purified by fractional distillation under reduced pressure (135 – 137 °C/10^{-3} Torr) yielding a viscous yellow oil. Yield: 5.71 g (71%). ^{1}H NMR ($CDCl_3$): δ 7.20 (dd, J = 3.7, 1.5 Hz, 1H), 7.19 (dd, J = 5.2, 1.5 Hz, 1H), 6.99 (dd, J = 5.2, 3.7 Hz, 1H), 6.21 (s, 1H), 4.32 (m, 2H), 4.23 (m, 2H). HRMS (EI) for $C_{10}H_8O_2S_2$ [M^+]: Calcd: 223.9966. Found: 223.9966.

3,4-Ethylenedioxy-5-bromo-2,2'-bithiophene (2.20). Prepared by a modification of the literature method.[80] A solution of **2.19** (5.59 g, 24.9 mmol) in DMF (50 mL) was cooled to –20 °C. NBS (4.44 g, 24.9 mmol) was then added portionwise over 45 min. After the addition was complete, stirring was continued at –20 °C for 4 h, then the red/orange

mixture was allowed to warm to room temperature, and water (150 mL) was added. The aqueous layer was washed with dichloromethane (2 x 100 mL), and the combined organic extracts were washed with water (8 x 100 mL) and dried over anhydrous sodium sulfate. After filtration, removal of solvent gave a grayish solid, which was purified by recrystallization from methanol/chloroform (3:2 v/v) to produce pale yellow crystals, yield 6.45 g (85 %). Mp: 84 °C (Lit.[80] mp 83 °C). ^{1}H NMR (500 MHz, $CDCl_3$): δ 7.20 (dd, J = 5.1, 1.2 Hz, 1H), 7.13 (dd, J = 3.7, 1.1 Hz, 1H), 6.99 (dd, J = 5.1, 3.7 Hz, 1H), 4.30 (m, 4H).

3,4-Ethylenedioxy-5-mesitylthio-2,2'-bithiophene (2.21). A solution of **2.20** (3.90 g, 12.9 mmol) in THF (40 mL) cooled to –78 °C was treated dropwise with *n*-butyllithium (8.04 mL, 12.9 mmol, 1.6 M in hexanes). The resulting bright red solution was stirred for 1.5 h at –78 °C. A solution of 2-mesitylenesulfenyl chloride (2.41 g, 12.9 mmol) in hexanes (20 mL) was added dropwise via cannula, and the resulting rusty red solution was stirred at –78 °C for an additional 30 min. The mixture was warmed to room temperature and poured into water (100 mL). The aqueous layer was extracted with ether (3 x 50 mL), and the combined organic extracts were further washed with water (3 x 50 mL) and dried over anhydrous sodium sulfate. After filtration, removal of the solvent gave a dark yellow solid, which was purified by column chromatography (silica gel, hexanes/dichloromethane (1:1 v/v)) to provide a bright yellow solid. Recrystallization from methanol/chloroform produced bright yellow needles of the title compound, yield 3.20 g (66 %). Mp: 120 °C. ^{1}H NMR (500 MHz, $CDCl_3$): δ 7.15 (dd, J = 5.1, 1.1 Hz, 1H), 7.08 (dd, J = 3.7, 1.1 Hz, 1H), 6.94 (dd, J = 5.1, 3.7 Hz, 1H), 6.92 (s, 2H), 4.29 (m, 4H),

2.56 (s, 6H), 2.25 (s, 3H). ^{13}C NMR (125 MHz, $CDCl_3$): δ 142.68, 141.51, 138.91, 136.52, 134.25, 129.44, 129.23, 126.93, 123.74, 122.74, 113.00, 107.07, 64.76, 64.69, 21.97, 20.95. MS (EI): *m/z* 374 (M^+, 100%). Anal. Calcd $C_{19}H_{18}O_2S_3$: C, 60.93; H, 4.84; S, 25.68%. Found: C, 60.75; H, 4.92; S, 25.67%.

Bis(5'-mesitylthio-3',4'-ethylenedioxy-5-2'-bithien-2-yl)sulfide (2.22). A solution of **2.21** (1.00 g, 2.67 mmol) in THF (30 mL) cooled to –40 °C was treated dropwise with *n*-butyllithium (1.67 mL, 2.67 mmol, 1.6 M in hexanes). The dark red solution was stirred at –40 °C for 1 h. After which time the solution was cooled to -70 °C, and a solution of bis(phenylsulfonyl) sulfide (0.42 g, 1.34 mmol) in THF (10 mL) was added dropwise via cannula. The resulting pale red solution was stirred at -70 °C for an additional 30 min. The mixture was then warmed to room temperature and poured into water (75 mL). The fine yellow precipitate was filtered off and washed with cold methanol (3 x 20 mL). This solid was recrystallized from a mixture of chloroform and methanol (80 mL, 3:5 v/v) to afford **2.22** (0.75 g, 72%) as white needles. Mp: 213 °C. UV-Vis (CH_2Cl_2) λ_{max} 375 nm (ε 4.4 x 10^4). ^{1}H NMR (500 MHz, THF-d_8): δ 7.05 (d, J = 3.9 Hz, 2H), 6.92 (s, 4H), 6.91 (d, J = 3.9 Hz, 2H), 4.27 (m, 8H), 2.51 (s, 12H), 2.22 (s, 6H). ^{13}C NMR (125 MHz, THF-d_8): δ 143.48, 142.99, 139.84, 139.78, 138.69, 134.03, 133.77, 130.35, 130.10, 123.03, 112.90, 108.54, 65.96, 65.78, 22.26, 21.11. HRMS (LSI) for $C_{38}H_{34}O_4S_7$ [M^+]: Calcd: 778.0502. Found: 778.0490.

Bis(3',4'-ethylenedioxy-5,2'-bithien-2-yl)sulfide (2.25). A solution of 2-(tributylstannyl)-3,4-(ethylenedioxy)thiophene (2.50 g, 5.80 mmol), **2.2** (860 mg, 2.41

mmol) and $Pd(PPh_3)_4$ (140 mg) in toluene (15 mL) was refluxed for 20 h. The toluene was removed under vacuum, and the remaining dark yellow residue was dissolved in a minimal amount of dichloromethane. The crude product was precipitated by the addition of hexanes. This material was further purified by column chromatography (silica, 1:1 hexanes/chloroform) to give **2.25** as a bright yellow solid, yield 890 mg (77 %). Mp: 130 °C. ^{1}H NMR ($CDCl_3$): δ 7.10 (d, J = 3.7 Hz, 2H), 7.01 (d, J = 3.7 Hz, 2H), 6.20 (s, 2H), 4.30 – 4.28 (m, 4H), 4.27 – 4.18 (m, 4H). ^{13}C NMR ($CDCl_3$): δ 142.0, 139.3, 138.1, 133.5, 133.2, 122.8, 109.7, 97.7, 65.2, 64.8. MS (LSI): *m/z* 478 (M^+, 100%). Anal. Calcd for $C_{20}H_{14}O_4S_5$: C, 50.19; H, 2.95; S, 33.50%. Found: C, 50.01; H, 2.99; S, 33.68%.

Bis(3,4-ethylenedioxy-5-2'-bithien-2-yl)sulfide (2.26). A solution of **2.20** (2.00 g, 6.60 mmol) in THF (30 mL) cooled to –78 °C was treated dropwise with a 1.6M hexanes solution of *n*-butyllithium (4.12 mL, 6.60 mmol). The resulting bright red solution was stirred for 1.5 h at –78 °C. A solution of bis(phenylsulfonyl) sulfide (1.04 g, 3.30 mmol) in THF (10 mL) was added dropwise via cannula and the resulting yellow solution was stirred at –78 °C for an additional 30 min. The mixture was warmed to room temperature and poured into water (100 mL). The aqueous layer was extracted with ether (3 x 75 mL), and the combined organic extracts were further washed with water (3 x 75 mL) and dried over anhydrous sodium sulfate. After filtration, the solvent was removed by rotary evaporation and the residue was purified by column chromatography (silica, 1:1 hexanes/chloroform) to afford a yellow solid. This was recrystallized from methanol/chloroform to give **2.26** as yellow needles, yield 1.04 g (66%). Mp: 176 °C. ^{1}H NMR ($CDCl_3$): δ 7.25 (dd, J = 5.1, 1.5 Hz, 2H), 7.22 (dd, J = 3.7, 1.5 Hz, 2H), 7.01 (dd,

J = 5.1, 3.7 Hz, 2H), 4.33 (m, 8H). ^{13}C NMR ($CDCl_3$): δ 143.9, 136.9, 134.3, 127.3, 124.7, 123.7, 115.7, 104.6, 65.2, 64.9. HRMS (EI) for $C_{20}H_{14}O_4S_5$ [M^+]: Calcd: 477.9496. Found: 477.9495. Anal. Calcd. For $C_{20}H_{14}O_4S_5$: C, 50.19; H, 2.95%. Found: C, 49.94; H, 2.80%.

Chapter 3

Physical Properties of Oligothiophenes

3.1 Introduction

The purpose of this chapter is to address some physical properties of the uncapped (Series I) and α–capped bis(thienyl)sulfide oligomers (Series II) in both their neutral and oxidized forms, using the parent α,ω-bis(mesitylthio)oligothiophenes (Series III) as a comparative benchmark. The electronic structures of the Series I and II oligomers are probed by using a combination of cyclic voltammetry and UV-Vis-NIR spectroscopy. The cyclic voltammetry studies provide information on the stability, charge-spin delocalization, and the relative ease at which the oligomers are oxidized. The UV studies on the neutral oligomers allow for a perspective of how the internal sulfur bridge contributes to the overall conjugation length and also gives access to their HOMO-LUMO gap energies. UV-Vis-NIR spectroscopy is used to characterize the charged Series II oligomers, and these spectra are compared to those of the Series III model compounds. All of these characterization tools are used to determine how electronic coupling occurs via the internal sulfur bridge as a function of (a) thiophene conjugation length and (b) EDOT and thiophene substitution patterns. The aforementioned points also play an important role on the stability of the charged Series II oligomers. Lastly, all of the uncapped Series I compounds could be electropolymerized to afford new PPS-like polymers with high stability. The electrochemistry of the monomers is presented and the properties of the polymers are briefly discussed.

3.2 Electronic Absorption Spectroscopy of Neutral Oligomers

The lowest-energy electronic transitions for both the uncapped (Series I) and α–capped thienyl-sulfide oligomers (Series II) in their neutral states are presented in Table 3.1, along with the data for the parent α,ω-bis(mesitylthio)oligothiophenes (Series III). The λ_{max} values for all three series are found to increase with increasing the number of thiophene rings, a trend that is consistent with nearly all other oligothiophenes. An example of this is represented in Figure 3.1.

Table 3.1. Lowest-energy electronic transitions for neutral oligothiophenes.[a]

Series I	λ_{max} (nm)	Series II	λ_{max} (nm)	Series III	λ_{max} (nm)
T-S-T (2.1)	268	MesS-**T**-**S**-**T**-SMes **(2.3)**	310	MesS-**T**-SMes **(1.50)**	302
E-S-E (2.15)	270	MesS-**E**-**S**-**E**-SMes **(2.14)**	309	MesS-**E**-SMes **(1.54)**	305
T_2-S-T_2 (2.4)	335	MesS-**T_2**-**S**-**T_2**-SMes **(2.8)**	360	MesS-**T_2**-SMes **(1.51)**	358
ET-S-TE (2.25)	345	MesS-**ET**-**S**-**TE**-SMes **(2.22)**	375		
TE-S-ET (2.26)	345	MesS-**TE**-**S**-**ET**-SMes **(2.18)**	375		
		MesS-**T_3**-**S**-**T_3**-S-Mes **(2.11)**	395	MesS-**T_3**-SMes **(1.52)**	386

[a] The shorthand notation for labeling compounds is defined in §2.1.1.

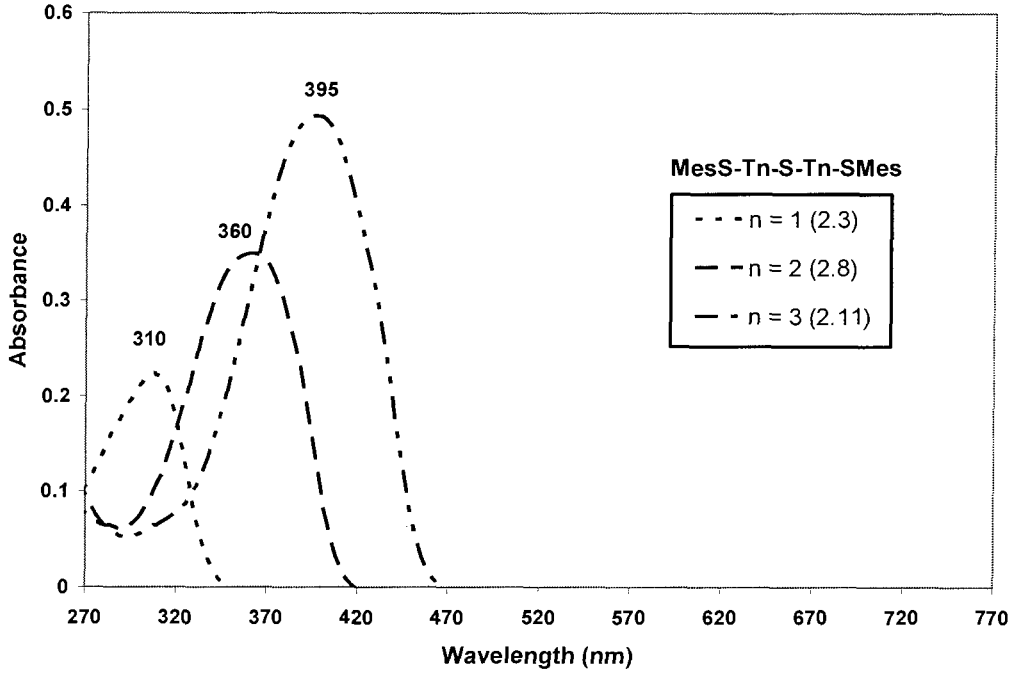

Figure 3.1. UV-Vis spectra of **2.3**, **2.8**, and **2.11** in dichloromethane at constant concentration (1 x 10^{-5} M).

The next important observation that can be made pertains to the position of λ_{max} for those compounds in Series I versus II. All of the λ_{max} values for the compounds in Series II are significantly bathochromically shifted (25 – 42 nm) with respect to their unsubstituted parent systems in series I. This shift is primarily attributed to the conjugative overlap of the *terminal* mesitylthio sulfur lone pairs with the oligothiophene π system. This same trend has been observed when comparing the Series III type compounds with their unsubstituted analogues. For example, the longest wavelength absorption of thiophene is at 243 nm, whereas 2,5-bis(mesitylthio)thiophene (**1.50**) is at 302 nm.[42]

On the other hand, the *internal* bridging sulfur units have little effect on extending the overall conjugation length, as can be seen by comparing the UV data of Series II with III. For example, comparison of **2.8** with **1.51**, which both have bithiophene units flanked by sulfurs, shows that their maximum wavelength absorptions are nearly identical, despite the fact that **2.8** is considerably longer. The optimized geometry structure of bis(bithiophene) (**2.8**) shows that the conjugation of the four thiophene unit backbone is highly disrupted upon inserting the sulfur bridge (Figure 3.2).[81] As a result, compound **2.8** behaves like two independent bithiophenes terminated with sulfur groups. All other Series II neutral compounds are believed to adopt similar geometries at the internal sulfur bridge based on similarities of the UV-Vis data with respect to their parallel Series III compounds.

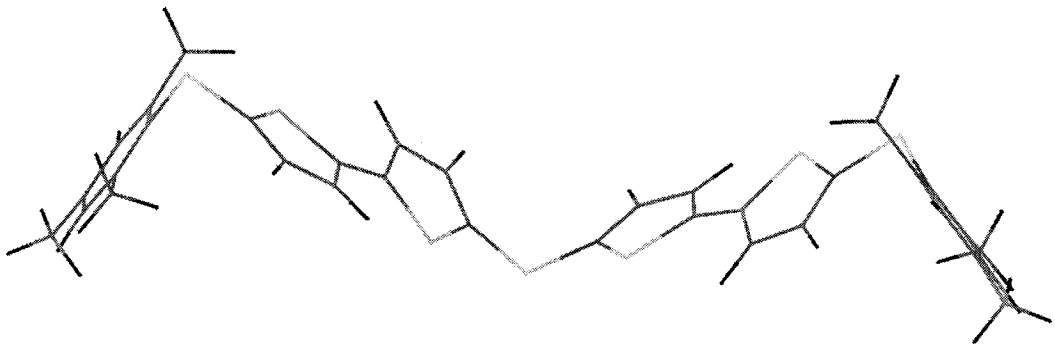

Figure 3.2. Optimized molecular structure of **2.8** calculated at the B3LYP/6-31G** level.[81]

The λ_{max} values for bis(methylthio)bithiophene (MeS-T_2-SMe)[82] and MesS-T_2-SMes (**1.51**) are 345 and 358 nm, respectively. Replacing the terminal methyl groups with mesityl groups appear to have a small effect on the position of λ_{max}. A DFT calculation on **1.51** has shown that the terminal thiophene-sulfur bond is almost planar with respect to the mesityl *ipso* carbon, but the mesityl ring itself is nearly perpendicular to the central bithiophene moiety.[83] Therefore, this twisting inhibits the mesityl groups to engage in the overall conjugation with the thiophene backbone. For the same reasons, the mesityl groups do not contribute very much to λ_{max} for the Series II type compounds.

The lone pair electrons on the oxygen atoms of the ethylenedioxy residues can also participate in conjugative overlap with the π-system of the thiophene backbone. However, these β–substituents have less of an effect on the position of λ_{max} than the terminal α-substituents. This can be seen by comparing either compounds **1.50** versus **1.54** or **2.8** versus **2.18** or **2.22**. This trend is expected, since the largest orbital coefficients of the thiophene π-HOMO reside on the α-carbon atoms (see Figure 2.4). Therefore, the energy of the HOMO is predominantly influenced by substituents that are directly attached to the α-positions. In actual fact, the terminal sulfur donor substituents lower the energy of the HOMO, much more so than the β-ethylenedioxy substituents.

3.3 Cyclic Voltammetry Studies

3.3.1 A Primer to Cyclic Voltammetry

Cyclic voltammetry (CV) is used here to investigate the redox properties of the target compounds described in the second chapter. The main advantage of CV over linear techniques (e.g., linear sweep voltammetry) is that it allows for the observation of a reverse scan, which can be a direct probe of the compounds stability for a specific redox couple. That is, a stable electrogenerated species should have a current wave of opposite direction with respect to the initial scan. The absence of a reverse scan suggests that the electrogenerated species is prone to decomposition. This is referred to as an *irreversible* process. A typical CV for a *reversible* one-electron process is represented in Figure 3.3. For example, a neutral compound might be oxidized to a cation in the forward scan, which is subsequently reduced back to the neutral form during the reverse scan at more negative potential. The reversibility is further manifested in the following requirements:

(i) The ratio of the anodic (i_{pa}) and cathodic (i_{pc}) peak currents should be equal to one.

(ii) For a one-electron redox process, the difference between the anodic (E_{pa}) and the cathodic (E_{pc}) peak potentials should be 59 mV at room temperature, which can be derived from the Nernst equation.

(iii) E_{pa} and E_{pc} should be independent of scan rate.

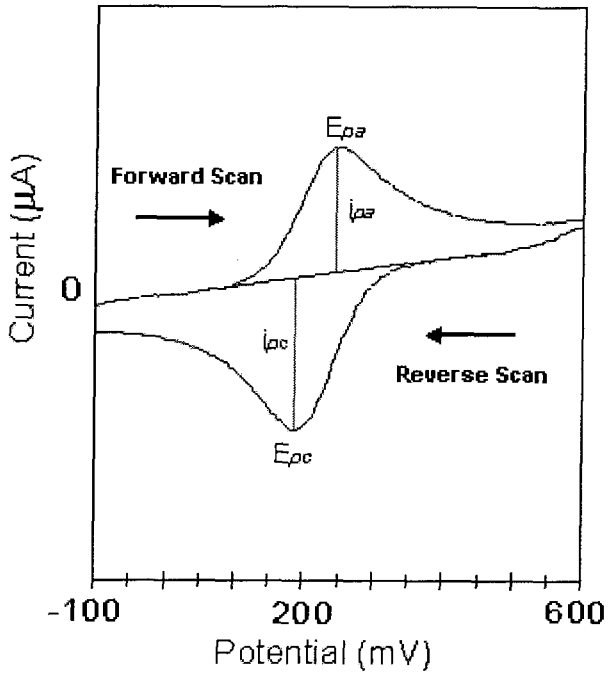

Figure 3.3. Representative CV for a reversible one-electron redox process.

The formal potential (E^o) for a reversible system is determined from the average of the peak potentials (i.e., $E^o = (E_{pa} + E_{pc})/2$).

3.3.2 *Electrochemistry Studies on the Series II Oligomers*

The oxidation potentials and reversibility of the redox processes for compounds **2.3**, **2.8**, and **2.11** were determined by cyclic voltammetry. The voltammograms are presented in Figure 3.4 and the data is summarized in Table 3.2.

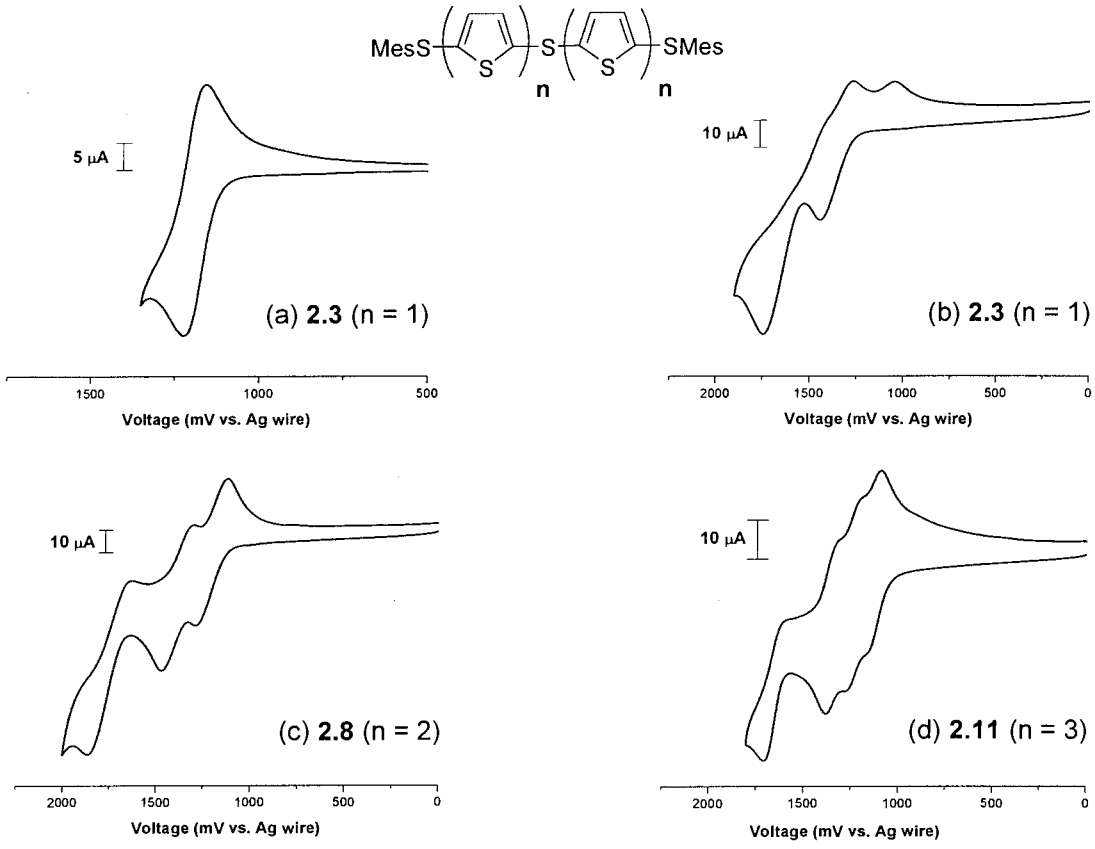

Figure 3.4. Cyclic voltammograms of (a) **2.3** showing the first reversible oxidation, (b) **2.3** showing the second irreversible oxidation, (c) **2.8**, and (d) **2.11** in dichloromethane containing 0.1 M *n*-Bu_4NBF_4. Scan rate = 100 mV/s.

Table 3.2. Oxidation potentials of Series II thiophene oligomers.

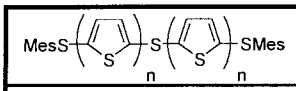	E_1° (V)[a]	E_2° (V)[a]	E_3° (V)[a]	E_4° (V)[a]
n = 1 (**2.3**)	1.34	1.73[b]		
n = 2 (**2.8**)	1.07	1.26	1.74[b]	
n = 3 (**2.11**)	0.92	1.04	1.15	1.49[b]

[a] Volts vs SCE at 100 mV/s. [b] Anodic peak potential, irreversible oxidation.

All of the compounds presented in Table 3.2 display a fully reversible first oxidation. This is consistent with Nodwell's finding that terminal sulfur substituents are highly effective towards stabilizing radical cations of oligothiophenes.[42] As the chain length increases, E_1° decreases along the series **2.3**→**2.8**→**2.11** (1.34→1.07→0.92 V), a trend that is consistent with nearly all other oligothiophenes. Furthermore, increasing the thiophene chain length permits the formation of additional reversible redox states, and these oxidation potentials (i.e., E_2° and E_3°) also decrease with increasing thiophene conjugation length. The anodic and cathodic peak separations for each reversible couple are in the range of 62 – 70 mV, suggesting that these all result from single one-electron oxidations.

These electrochemical results provide evidence that the internal sulfur bridge is indeed providing an electronic coupling pathway between the flanking thiophene units. If the sulfur link were completely insulating, then we would expect the electrochemical behavior to be very similar to the Series III compounds. For instance, if the two thiophene units were completely non-interacting, then the diradical dication of **2.3** would look very much like the radical cation of the parent compound **1.50**. It might also be

expected that the removal of the two electrons would occur at the same potential, thereby, resulting in a two-electron redox wave. This phenomenon has been seen in Janssen's *m*-phenylene bridged system (**1.62**), where the capped bithiophene (**3.1**) serves as a useful model compound.[58] Compound **3.1** has two well-defined reversible one-electron

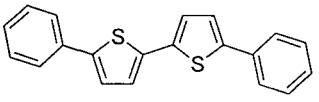

3.1

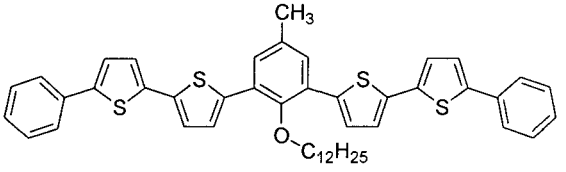

1.62

oxidations at half-wave potentials of 1.10 and 1.61 V vs. SCE. On the other hand, compound **1.62** with a *m*-phenylene bridge has two redox waves (E_1^o = 1.01 V and E_2^o = 1.18 V), each of which corresponds to a two-electron process affording the diradical dication $\mathbf{1.62}^{2\bullet 2+}$ and the tetracation $\mathbf{1.62}^{4+}$. These two redox couples each have anodic and cathodic peak separations of 150 mV, which is ascribed to two consecutive, but unresolved one-electron oxidation waves. Therefore, the *m*-phenylene bridge is ineffective at communicating charge due to its insulating/nonresonant nature. The fact that the first redox couple for **2.3** only corresponds to a one-electron oxidation and that it is much more difficult to remove a second electron provides evidence that the sulfur bridge is not insulating, as in the *m*-phenylene system, but rather it is providing a communication pathway for the charged thiophenes. Further support for this is gleaned by comparing **2.8** with **1.51**. A stable dication can be generated for parent **1.51**, while at most a stable dication can be generated for **2.8**. Thus, if the sulfur bridge were completely insulating, it should also be possible to generate a stable tetracation for **2.8**; however, this is not the case.

Closer examination of the electrochemical behavior of **2.3** reveals that it has a second irreversible oxidation (Table 3.2). The first oxidation most likely results from the removal of an electron from one of the thiophene rings, whereas the second electron is removed from the other thiophene ring affording a diradical dication. A new reduction wave appears at more negative potential after the first scan past the irreversible oxidation wave (Figure 3.4b). This reduction wave is not observed if the switching potential is kept below 1.73 V (E_2^{pa}) vs SCE (Figure 3.4a), signifying that it arises after the second oxidation. This second irreversible oxidation, along with the formation of a new redox couple at more negative potential is also observed for compounds **2.14** and **2.18** (Table 3.3).

Table 3.3. Oxidation potentials of Series II EDOT containing oligomers.

Compound	E_1^0 (V)[a]	E_2^0 (V)[a]	E_3^0 (V)[a]	E_4^0 (V)[a]
MesS-**E-S-E**-SMes (**2.14**)	0.95	1.19[b]		
MesS-**TE-S-ET**-SMes (**2.18**)	0.79	0.98[b]		
MesS-**ET-S-TE**-SMes (**2.22**)	0.79	0.94	1.31[c]	1.71[b]

[a] Volts vs SCE at 100 mV/s. [b] Anodic peak potential, irreversible oxidation. [c] Quasi-reversible.

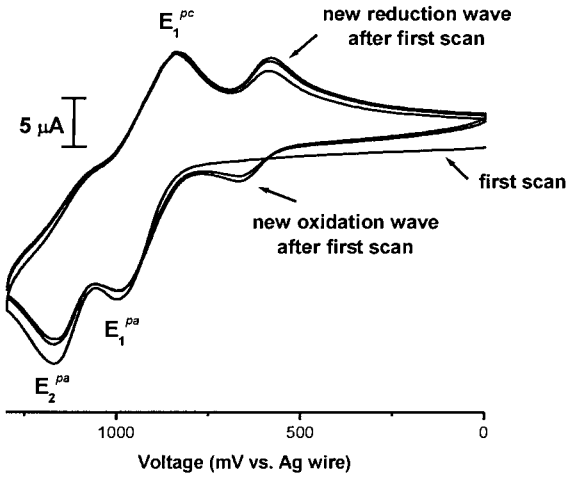

Figure 3.5. Cyclic voltammogram of **2.18** (MesS-**TE-S-ET**-SMes) showing the first three scans. Scan rate = 1000 mV/s.

A representative CV of **2.18** is shown above in Figure 3.5. In subsequent scans for **2.14** and **2.18**, the new reduction waves develop corresponding oxidation waves, which support the formation of a new redox active species. We propose that the diradical dications of **2.14** and **2.18** are decomposing to the known biEDOT **1.55** and quaterthiophene derivative **1.58**, respectively. A possible decomposition pathway for the diradical dication of **2.18** is depicted in Scheme 3.1. The internal carbon-sulfur bond of $\mathbf{2.18}^{2\bullet 2+}$ may be homolytically cleaved, followed by dimerization of the diradical cation to provide $\mathbf{1.58}^{2\bullet 2+}$. Neutral **1.58** is then formed by a two-electron reduction of this intermediate diradical dication. The determined formal potentials (**2.14**: E^o = 0.59 V and **2.18**: E^o = 0.50 V) of these new redox couples correspond very well to the literature values (**1.55**: E_1^o = 0.57 V and **1.58**: E_1^o = 0.49 V) that were reported by Nodwell.[42] It should be noted that additional experiments would be required to confirm the formation of the tentatively assigned decomposition products **1.55** and **1.58**. Further light can be shed on this second irreversible oxidation by comparing **2.18** with its isomeric

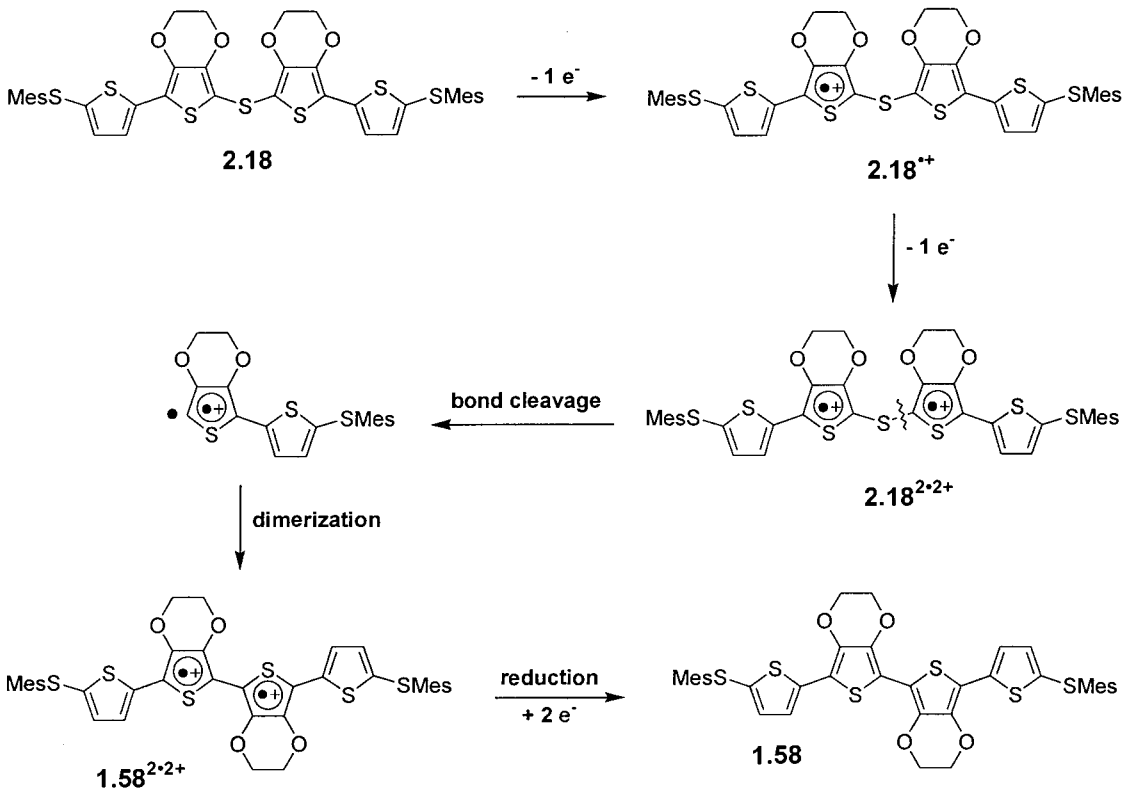

Scheme 3.1. Possible decomposition pathway for the diradical dication of **2.18**.

counterpart **2.22**. Compounds **2.18** and **2.22** both undergo reversible one-electron oxidations, but only the latter exhibits subsequent reversible redox processes. We believe that the charge distribution in **2.18** and **2.22** is confined to the more electron rich EDOT rings rather than the β-unsubstituted thiophenes. The ability of sulfur-terminated EDOT rings to localize charge has also been observed in Nodwell's isomeric quaterthiophenes **1.58** and **1.60** (see §1.5.4). Thus, the dicationic state of compound **2.18** experiences a buildup of charge in the EDOT rings directly adjacent to the sulfur bridge, which leads to its irreversible decomposition (Scheme 3.1). This destructive charge buildup around the internal sulfur bridge can be relieved by increasing the conjugation length, allowing for charge delocalization or by placing the more electron rich EDOT rings away from the

internal sulfur bridge. The bis(bithiophene) (**2.8**), bis(terthiophene) (**2.11**), and the bis(bithiophene) oligomer (**2.22**) with the EDOTs on the outside accommodate these requirements. Both compounds **2.8** and **2.11** can be reversibly oxidized to their dicationic states (Figure 3.4). This second reversible oxidation is now feasible because the charge is able to delocalize in the flanking bi- and terthiophene units. The increased conjugation length for the bis(terthiophene) (**2.11**) also permits the formation of a stable trication.

As expected, the oxidation potentials for all the EDOT containing oligomers are significantly lower than their analogous thiophene counterparts, this being attributed to the electron-donating capacity of the ethylenedioxy substituents. This can be seen by comparing **2.3** with **2.14**, or by comparing **2.8** with either **2.18** or **2.22**.

The fact that the electron-rich EDOT rings have a strong tendency to localize charge may be detrimental to EDOT-containing oligomers and polymers to transport this charge. However, interesting observations can be made when comparing **2.22** with **1.60**. Both compounds contain terminal EDOT groups that are bridged by either a bis(thienyl)sulfide linker or by bithiophene, respectively. It has been previously shown that the dication structure of **1.60** is one in which the two charges are localized on the electron-rich EDOT ends. In other words, the dication of **1.60** can be thought of as two independent electrophores that are *weakly* coupled by a bithiophene spacer. The lack of delocalization in the bithiophene spacer is confirmed by the ease at which the second electron is removed from **1.60** with respect to the first. This is further manifested in the small difference (i.e., $\Delta E_{2\text{-}1}^{o} = E_2^{o} - E_1^{o} = 0.05$ V) between the first and second formal potentials. The increased Coulombic repulsion to introduce a second charge for **2.22** ($\Delta E_{2\text{-}1}^{o} = 0.15$ V) with respect to **1.60**, suggests that there is a slightly greater degree of

delocalization for the radical cation in the bis(thienyl)sulfide bridge. This is probably because the internal sulfur bridge pulls some of the charge away from the electron-rich EDOT ends. Thus, the sulfur bridge in **2.22** appears to be valuable in transporting the charge away from the electron-rich EDOT ends. A quasi reversible trication can even be generated for **2.22** (Figure 3.6). The irreversible oxidation at 1.71 V vs SCE is again most likely due to carbon-sulfur bond cleavage.

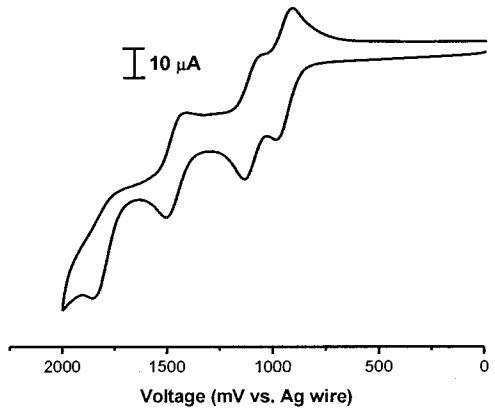

Figure 3.6. Cyclic voltammogram of **2.2** (MesS-**ET-S-TE**-SMes) in dichloromethane containing 0.1 M nBu$_4$NBF$_4$. Scan rate = 100 mV/s.

3.3.3 Electrochemistry Studies on the Series I Oligomers

The electrochemical data for the α-uncapped thienyl-sulfide monomers (Series I) are summarized in Table 3.4. All of the monomers displayed irreversible oxidation waves as expected for α-unsubstituted thiophenes, which is a prerequisite for electropolymerization reactions.

Table 3.4. Oxidation potentials of Series I monomers.

Monomer	**T-S-T (2.1)**	**E-S-E [85] (2.15)**	**TT-S-TT (2.4)**	**ET-S-TE (2.25)**	**TE-S-ET (2.26)**
E_1^o (V)[a]	1.150[b]	1.180[b]	1.370[b]	1.015[b]	0.960[b]

[a] Volts vs Ag/AgCl at 100 mV/s. [b] Anodic peak potential, irreversible oxidation.

The electropolymerization experiments were performed in dichloromethane containing 1 M *n*-Bu_4NBF_4 by repeated scans slightly beyond the first anodic peak potential for each of the monomers. The polymerization potentials were kept as low as possible to avoid possible damage (e.g., internal carbon-sulfur bond cleavage, as was observed in the model compound studies) of the developing polymers. Electropolymerization of all monomers was confirmed by the observation that the peak current increased with increasing the number of scans, and that highly colored polymer films formed in all cases on the working electrode surface.

As a representative example, Figure 3.7 shows the CV of monomer **2.25** as a function of the number of scans. The first scan shows the irreversible process with the anodic peak potential at 1.015 V vs Ag/AgCl; whereas, the fifth and tenth scans show the

formation of a new redox couple with anodic and cathodic peak potentials at 660 and 600 mV, respectively. The growth of the reduction peak indicates that the polymer can be reversibly oxidized and reduced.

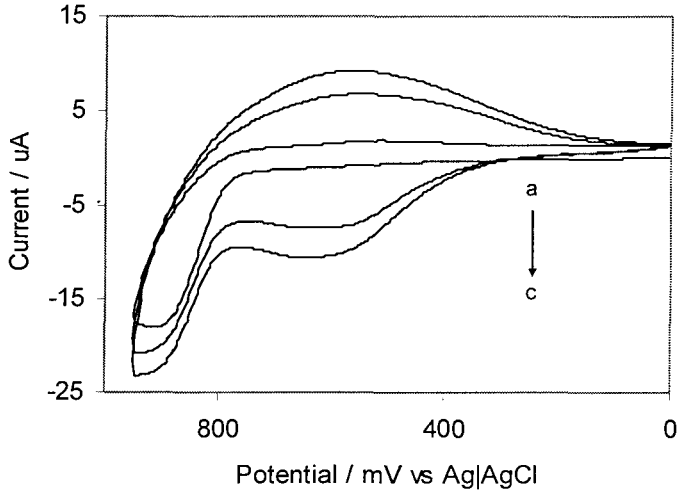

Figure 3.7. Electropolymerization of **2.25** in dichloromethane at 100 mV/s: (a) 1st scan, (b) 5th scan, and (c) 10th scan.

The platinum modified electrode for **2.25** in a monomer free electrolyte solution showed a broad reversible oxidation at more negative potential (Figure 3.8). The oxidation potentials for all of the deposited polymers are presented in Table 3.5. The variation of peak current of the modified electrodes was found to be linearly dependent on scan rate, which is indicative of surface-bound species. No changes were observed in the electrochemical properties of all polymers either after repeated cycling several hundred times or by exposing the polymers to air. The stability of the polymers is attributed to the excellent electrochemical properties of the thiophene and EDOT moieties, and also the presence of the divalent sulfur bridges that stabilize cationic thiophenes.

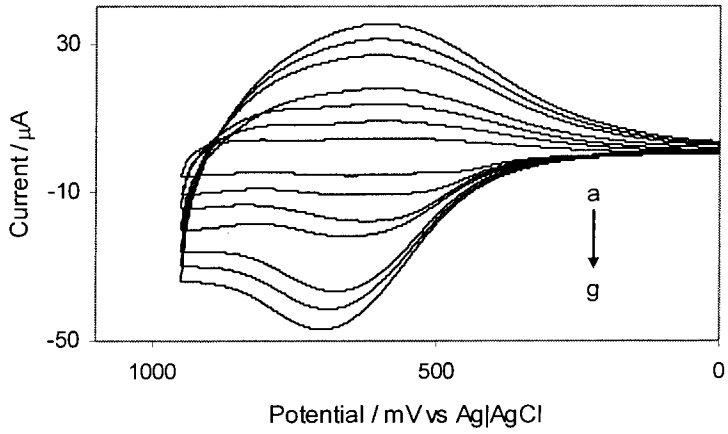

Figure 3.8. CV of the film of Poly(**2.25**) at different scan rates: (a) 0.025, (b) 0.050, (c) 0.075, (d) 0.100, (e) 0.150, (f) 0.175, and (g) 0.200 V/s.

Table 3.5. Oxidation potentials of Series I polymers.

Polymer	(-**T**-**S**-**T**-)$_n$ poly(**2.1**)	(-**E**-**S**-**E**-)$_n$ [85] poly(**2.15**)	(-**TT**-**S**-**TT**-)$_n$ poly(**2.4**)	(-**ET**-**S**-**TE**-)$_n$ poly(**2.25**)	(-**TE**-**S**-**ET**-)$_n$ poly(**2.26**)
E_1° (V)[a]	1.460	0.600	1.310	0.630	0.870

[a] Volts vs Ag/AgCl at 100 mV/s.

3.4 UV-Vis-NIR Spectroscopy

3.4.1 UV-Vis-NIR Spectroscopy of Selected Series III Oligomers

As a reference point, UV-Vis-NIR spectra for the cationic α,ω-bis-(mesitylthio)oligothiophenes (Series III) were obtained, and the corresponding data is summarized in Table 3.6. Dilute solutions of the oligomers were chemically oxidized by the stepwise addition of nitrosonium tetrafluoroborate ($NOBF_4$; E_1° = 1.00 V vs Fc/Fc^+ in CH_2Cl_2)[84] in dichloromethane at room temperature. Stable radical cations could be generated for compounds **1.50** – **1.54** and dications for **1.52** and **1.53**. Only radical

cations could be produced for monothiophenes **1.50** and **1.54** because they both only posses one reversible oxidation, as was shown by CV. The second oxidation potential of **1.51** is too high to obtain its dication by chemical oxidation, even when using a very strong oxidizing reagent such as $NOBF_4$. However, a spectrum of the dication was acquired by bulk electrolysis of **1.51** beyond its second anodic peak potential. In actual fact, all of the radical cations and dications could be generated by bulk electrolysis by holding the potential slightly beyond their first and second anodic peak potentials, respectively. Furthermore, the spectral data for all of the electrochemically generated cations using *n*-Bu_4NBF_4 as supporting electrolyte match exactly with those obtained by chemical oxidations with $NOBF_4$.

Table 3.6. Electronic absorption maxima for selected oxidized oligothiophenes.[a]

	RS-T_1-SR **(1.50)**	RS-T_2-SR **(1.51)**	RS-T_3-SR **(1.52)**	RS-T_4-SR **(1.53)**	RS-**E**-SR **(1.54)**
neutral	302	358	386	420	305
radical cation	412 (M1) 638 (M2)	*500*, 572 (M1) *805*, 905 (M2)	676 (M1) *1015*, 1170 (M2)	*654*, 756 (M1) *1190*, 1420 (M2)	405 (M1) 551 (M2)
dication		520	*654*, 696	*806*, 893	

[a] Absorption maxima are measured in nanometers. Values in italics are due to vibronic transitions. The M1 and M2 electronic transitions are defined in Figure 1.10. R = Mes.

Both monothiophenes **1.50** and **1.54** could be converted to radical cations by the addition of one equivalent of $NOBF_4$. Upon oxidation, the dichloromethane solutions

change from colorless to an intense violet color. The electronic absorption spectrum for the radical cation of **1.50** shows two absorption maxima at 412 and 638 nm, which are assigned to the SOMO→LUMO (M1 transition; see Figure 1.10) and HOMO-1→SOMO (M2) transitions, respectively. Similarly, the radical cation of the EDOT derivative **1.54** exhibits two intense transitions at 405 (M1) and 551 nm (M2).

In agreement with their increasing conjugation lengths, the principal radical cation transitions (i.e., M1 and M2) shift to lower energies in going from **1.50** to **1.53**. The radical cation solution colors in dichloromethane range from violet to blue to green along the series **1.51**→**1.52**→**1.53**. A representative UV-Vis-NIR spectrum of **1.52** is displayed in Figure 3.9. For compounds **1.51** to **1.53** additional higher energy bands with respect to M1 and M2 are observed. For other oligothiophenes these higher energy features have been ascribed to dimer transitions (i.e., D1 and D2; Figure 1.10), in which their intensities are dependent on temperature, concentration and solvent polarity. The higher energy bands for the compounds presented in Table 3.6 do not show a dependence on either solvent polarity or concentration, suggesting that the phenomenon of π-dimerization does not occur within these molecules. Dimer formation is most likely suppressed because of the steric hindrance of the capping mesityl groups. We believe that these higher energy features are due to vibronic transitions because the difference in energy between each of the M1 and M2 transitions with their corresponding high energy bands are in the range of vibrational energies.[83] For example, the energy differences for **1.51** are 2517 cm^{-1} (572→500 nm) and 1373 cm^{-1} (905→805 nm).

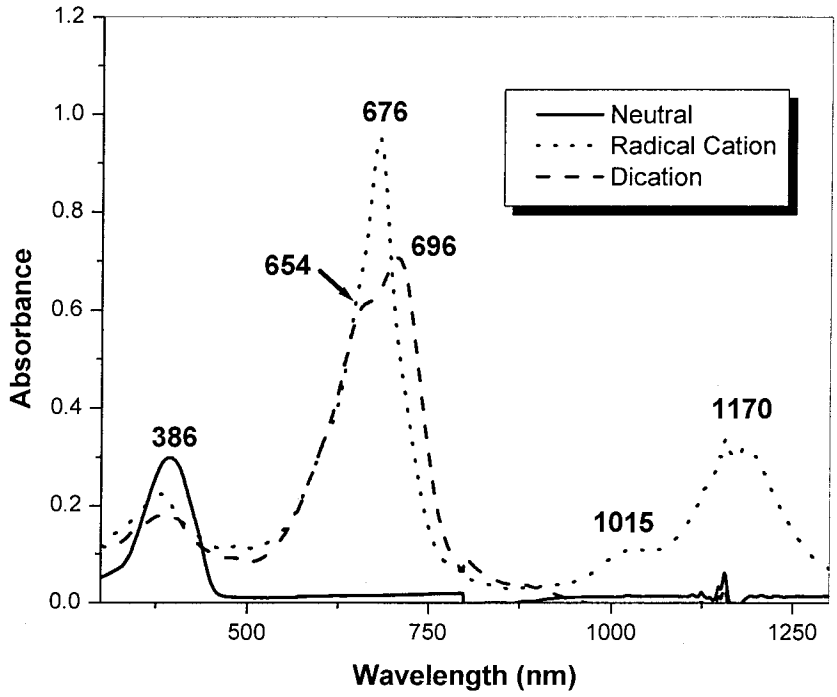

Figure 3.9. UV-Vis-NIR spectra of the radical cation and dication of **1.52**.

Dications of **1.52** and **1.53** could be generated by treating them with two equivalents of $NOBF_4$ in dichloromethane. The dication of **1.52** exhibits a dark blue color in solution, while **1.53** is dark green. The dark purple dication of **1.51** was not accessible by chemical oxidation with $NOBF_4$, so it was produced by electrolysis at 1.3 V vs Ag/AgCl using n-Bu_4NBF_4 as supporting electrolyte. As expected, the longest wavelength absorptions of these dications ((**1.51**$^{2+}$, 520 nm (2.38 eV); **1.52**$^{2+}$, 696 nm (1.78 eV); **1.53**$^{2+}$, 893 nm (1.39 eV)) are bathochromically shifted with increasing conjugation length. A linear correlation is observed between the principal absorption energy and the inverse chain length, as shown in Figure 3.10. These principal absorption bands are due to HOMO→LUMO transitions. The higher energy bands for **1.52** and **1.53** (654 and 806 nm, respectively) are assigned again to vibronic transitions.

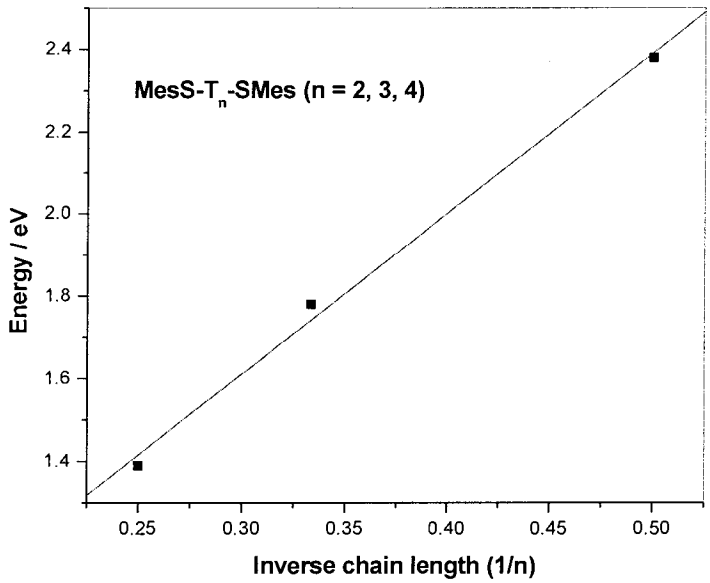

Figure 3.10. Correlation of the longest wavelength absorptions for the dications of **1.51**, **1.52**, and **1.53** with their inverse chain lengths.

3.4.2 UV-Vis-NIR Spectroscopy of Series II Oligomers

The α–capped bis(thienyl)sulfide (Series II) oligomers were electrochemically oxidized and the resulting radical cations and dications were characterized by UV-Vis-NIR spectroscopy. The UV-Vis-NIR data is summarized in Table 3.7. Chemical methods (i.e., $NOBF_4$) were avoided because in most cases the small differences in sequential oxidations did not permit for a discrete redox couple to be accurately addressed.

Table 3.7. Electronic absorption maxima for Series II oxidized oligothiophenes.[a]

	2.3	**2.14**	**2.8**	**2.22**	**2.18**	**2.11**
neutral	310	309	360	375	375	395
radical cation	*508* 555 (M1) *816* 896 (M2)	520 (M1) 570 (sh) 660 *765* 860 (M2)	*497* 563 (M1) *784* 865 (M2)		*634* 725 (M1) *1077* 1241 (M2)	
dication			581	*788*, 892		680

[a] Absorption maxima are measured in nanometers. Values in italics are due to vibronic transitions. The M1 and M2 electronic transitions are defined in Figure 1.10. sh = shoulder.

Compound **2.3** was oxidized by bulk electrolysis at its first anodic peak potential in dichloromethane. During the electrolysis the solution changes from colorless to an intense violet color. Complete conversion to the radical cation is observed by the loss of the neutral band at 310 nm in the UV-Vis-NIR spectrum and by the onset of two new major bands at 555 (M1) and 896 nm (M2). Each of these bands is accompanied by higher energy absorptions, which are again assigned to vibronic fine structure. Insights into the electronic structure of **2.3** can be further made by comparing it to **1.50**, because both compounds contain monothiophene units flanked by sulfur atoms. The longest wavelength absorptions for the radical cation of **1.50** appear at 412 (M1) and 638 nm (M2), which are significantly hypsochromically shifted with respect to the M1 and M2 transitions for **2.3**. These observations suggest that there may be a strong intrachain interaction between the thiophene units via the sulfur bridge for compound **2.3**, while in

its monoradical cationic state. Interchain contributions are neglected based on the premise that the bulky mesityl groups do not permit close radical interactions between neighboring molecules, and also because π-dimerization is not observed in the optical spectra. This same phenomenon can be seen by comparing the analogous EDOT derivatives **1.54** and **2.14**. The radical cation bands for **1.54** are at 405 (M1) and 551 nm (M2); whereas M1 and M2 for **2.14** are at 520 and 860 nm, respectively. It should be noted that the M1 and M2 bands for **2.14** cannot be definitively assigned because other atypical bands appear in its spectrum (Figure 3.11). They were tentatively chosen as M1 and M2 since they appear around the same position for those observed for the radical cation of **2.3**. The nature of the additional bands at 570 and 660 nm is unclear at this point, but they might be due to a large structural change when **2.14** is converted to its radical cation. The band at 765 nm might be a vibronic transition that accompanies M2 (860 nm), since they have an energy difference of 1444 cm^{-1}. However, dimer bands can be ruled out based on the fact that the intensities of the 570, 660, and 765 nm peaks show neither a concentration nor solvent polarity dependence. Despite these unassigned features, the principal absorption bands for **2.14** are considerably bathochromically shifted compared to those for **1.54**, giving further support that the EDOT rings in **2.14** are electronically coupled by way of the sulfur bridge.

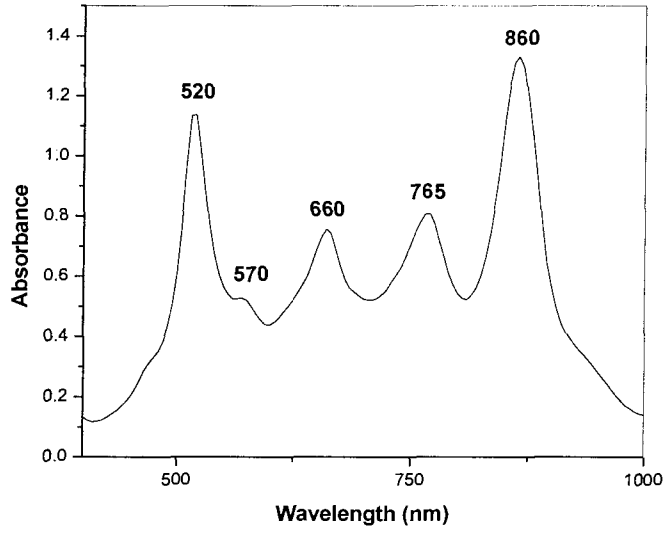

Figure 3.11. UV-Vis-NIR spectrum of the radical cation of **2.14**.

Interesting observations can be made for the bis(bithiophene) derivatives **2.8**, **2.18** and **2.22**. Comparisons between **2.8** and **1.51** can be made since they both contain bithiophene units flanked by sulfurs. Compound **2.8** was converted to its radical cation (E_1^{pa} = 0.8 V vs Ag/AgCl) and subsequent dication (E_2^{pa} = 1.3 V) by controlling the potential of the electrolysis. The radical cation exhibits a pale purple color, while the dication is dark purple in dichloromethane. The spectroscopic features for the radical cations of **2.8** and **1.51** are qualitatively the same; however, all of the absorption maxima for **2.8** (M1 = 563 nm and M2 = 865 nm) are in this case slightly blue-shifted with respect to those for **1.51** (M1 = 572 nm and M2 = 905 nm). This contrasts the behavior of the monothiophene sulfur-bridged compounds (**2.3** and **2.4**) in which their radical cation absorptions are red-shifted with respect to their parent non-bridged (**1.50** and **1.54**) counterparts. This data indicates that little to no electronic coupling occurs between

adjacent bithiophenes via the sulfur bridge, presumably because the radical cations are strongly localized in the bithiophene cores. Thus, polymers made up of bithiophene units bridged by divalent sulfur may not be good charge carries, which may be detrimental to the polymers overall conductivity. The corresponding bithiophene-sulfide polymer has been prepared by electrochemical polymerization of the **T-S-T** (**2.1**) monomer (see § 3.3.3); however, we were unable to compare its solution spectral data to the model compounds (i.e., **2.8** and **1.51**) due to the poor solubility of the polymer. Alternatively, spectral data can be obtained by growing a thin polymer film on a transparent electrode (e.g., ITO); unfortunately, the polymer did not adhere very well to the ITO electrode.

The UV-Vis-NIR spectrum of the radical cation of the bis(bithiophene)sulfide (**2.18**) derivative with internal EDOTs is presented in Figure 3.12. Interestingly, the electronic spectrum for the radical cation of **2.18** has its principal absorption maxima at 725 (M1) and 1241 nm (M2), values that are remarkably red-shifted compared to its parent bithiophene **2.8**. The MesS-**TE-S-ET**-SMes (**2.18**) compound behaves similarly to MesS-**E-S-E**-SMes (**2.14**), whereby the monoradical cation is predominantly localized on the electron rich EDOT rings, allowing for strong electronic coupling through the sulfur bridge.

The radical cation for the isomeric bis(bithiophene)sulfide (**2.22**) compound with the EDOTs on the outside could not be generated by either chemical or electrochemical techniques. The electrochemical oxidation of **2.22** proceeded directly to the dication due to the small potential difference between the cationic and dicationic states. For the same reason, only the dication could be obtained for Nodwell's quaterthiophene **1.60**.[42] The main dication bands for **2.22** and **1.60** are at 892 and 860 nm, respectively. The red-shift

may result from a slightly greater degree of electronic communication in the bis(thienyl)sulfide bridge for **2.22** than the bithiophene bridge for **1.60**.

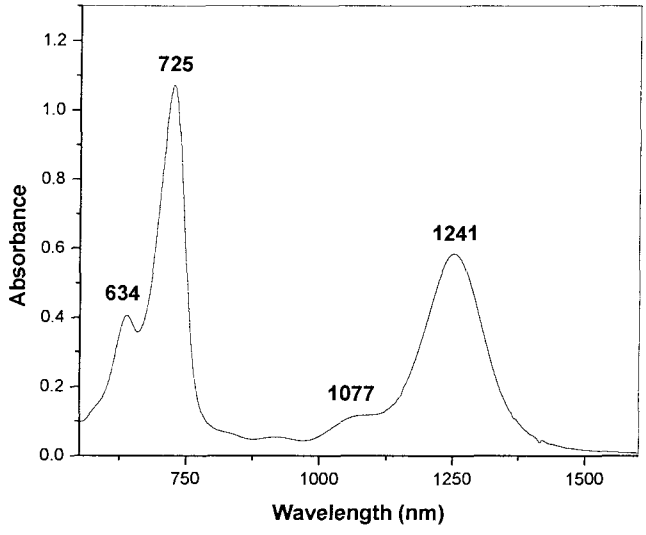

Figure 3.12. UV-Vis-NIR spectrum of the radical cation of **2.18**.

It was not feasible to obtain UV spectra for each of the three reversible redox couples for the bis(terthiophene)sulfide (**2.11**) compound because successive oxidations were too close together in potential. Even holding the potential just below the first anodic peak potential (E_1^{pa} = 0.9 V vs Ag/AgCl) resulted in what we believe is the dication for **2.11**. The dication exhibits a dark green color in dichloromethane with an absorption maximum at 680 nm.

3.4.3 UV-Vis-NIR Spectroscopy of a Polymer Derived from a Series I Monomer

Since all of the polymers (see Table 3.5) are insoluble in standard organic solvents, the spectroelectrochemical properties of films of the polymers were examined on transparent indium thin oxide (ITO) electrodes. As an example of an ITO-deposited film, poly(**2.15**) (Figure 3.13) shows various electronic spectra as a function of applied potential.[85] At 1.3 V (vs Ag/AgCl), poly(**2.15**) is deep blue and exhibits two maximum absorptions at 605 and 1020 nm. As the potential is lowered to a maximum of -0.2 V, the dark yellow neutral form of poly(**2.15**) appears and shows two peaks at 455 and 484 nm. The doping/de-doping processes are fully reversible, which confirm the excellent stability of the polymer in both reduced and oxidized states. All of the other polymers exhibit similar spectroelectrochemical properties.

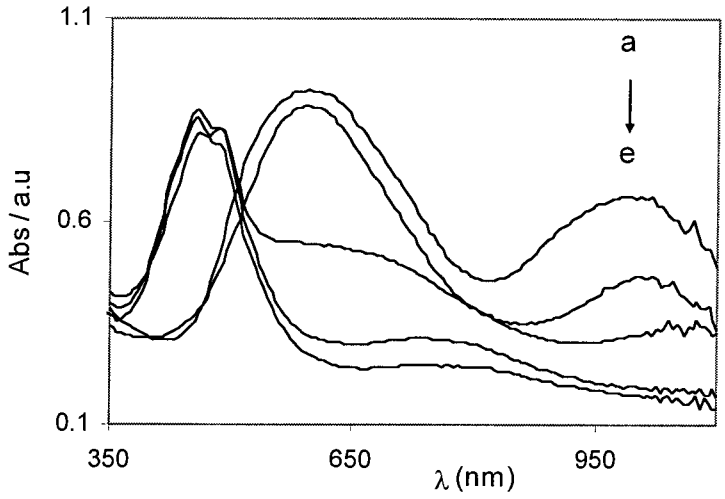

Figure 3.13. Electronic spectra of poly(**2.15**) at different potentials: (a) +1.3, (b) +0.5, (c) +0.2, (d) 0, (e) -0.2 V vs Ag/AgCl.

The mesityl capped model compounds can also be used to gain an understanding of how electronic communication occurs in their polymer counterparts. As a representative example, compound **1.55** (MesS-**EE**-SMes) serves as an effective model for poly(**2.15**) ((-**E**-**S**-**E**-)$_n$) because both contain biEDOT units flanked by sulfur atoms. Neutral poly(**2.15**) has its absorption maxima at 455 and 484 nm, whereas model compound **1.55** absorbs at 362 nm. The fact that poly(**2.15**) has its absorptions red-shifted with respect to **1.55**, provides evidence that the biEDOT units are electronically coupled in the neutral polymer. Furthermore, the doped polymer has its longest wavelength absorptions at 605 and 1020 nm, and the radical cation of **1.55** has two bands at 509 and 900 nm. The red-shift is most likely due to strong intrachain electronic coupling of the biEDOT groups in the polymer. The mesityl-capped model compounds prohibited an understanding of how interchain interactions may contribute to electronic coupling because the steric hindrance of the mesityl groups did not allow for neighboring molecules to come in close contact with each other. However, interchain interactions in the polymers might serve as a secondary pathway for electronic coupling, since they lack mesityl end-groups. Regardless of the exact conduction mechanism, all of the polymers show excellent charge transport properties, and this can be seen for poly(**2.15**), which has a maximum conductivity of 1.5×10^{-3} S cm^{-1}. This conductivity value is comparable to those obtained for doped polyacetylenes[86] and poly(phenylene)sulfides.[52]

3.5 Conclusions and General Remarks for Part I

The first part of this chapter dealt with the electrochemistry of the thiophene-sulfide capped oligomers (Series II), which revealed some interesting observations. All of the Series II compounds could be reversibly oxidized to at least a monoradical cation by CV, illustrating the stabilizing ability of the divalent sulfur bridges. For compounds **2.8** (MesS-$\mathbf{T_2}$-**S**-$\mathbf{T_2}$-SMes), **2.11** (MesS-$\mathbf{T_3}$-**S**-$\mathbf{T_3}$-SMes), and **2.22** (MesS-**ET-S-TE**-SMes) higher oxidation states could also be reversibly obtained. A reversible dication could be generated for **2.8** and reversible trications for **2.11** and **2.22**. Compounds **2.3** (MesS-**T-S-T**-SMes), **2.14** (MesS-**E-S-E**-SMes) and **2.18** (MesS-**TE-S-ET**-SMes) could only be reversibly oxidized to monoradical cations, whereas attempts to introduce a second charge resulted in irreversible decomposition of the oligomers. In all of these compounds a new redox couple appears at most negative potential after scanning past the second irreversible oxidation (see Figure 3.5). For **2.3** and **2.14** it is believed that the first electron is removed from one of the thiophene rings and then a second electron is removed from the adjacent ring. Irreversible decomposition results from the large charge buildup around the sulfur bridge. Although compound **2.18** contains bis(bithiophene) units, it is believed that the charge is localized in the electron-rich EDOT rings that are directly adjacent to the sulfur-bridge, causing it to electrochemically behave analogously to **2.14**. Presumably the internal carbon-sulfur bond is cleaved providing new dimerized products. The increased conjugation lengths for **2.8** and **2.11** allows for the charge to strongly delocalize in the flanking bi- and terthiophene units, respectively. The extended delocalization in these compounds helps to pull the charge away from the internal sulfur bridge.

Comparative UV-Vis-NIR studies on the Series II compounds with those of Series III showed that strong electronic coupling via the internal sulfur bridge occurred only for compounds **2.3**, **2.14**, and **2.18**. Therefore, it is anticipated that polymers made up of either –**T-S-T**-, -**E-S-E**-, or –**TE-S-ET**- units would also show good electronic transport properties. Poly(thio-2,5-thienylene) (i.e., (-**T-S**-)$_n$) has received some attention, but the electrochemically doped polymer is quite unstable and prone to irreversible changes via cross-linking processes.[87] The EDOT polymer analog (i.e., (-**E-S**-)$_n$) has never been prepared, but it is expected to exhibit better stability than its parent β-unsubstituted thiophene because (a) the β-positions are blocked from undergoing cross-linking reactions, (b) the ethylenedioxy substituents stabilize cationic thiophenes by an electron-donating effect, and (c) the bridging sulfur substituents should also help stabilize the doped polymer. Poly(**2.26**) (i.e., (-**TE-S-ET**-)$_n$) has been prepared in this thesis and no changes were observed in the electrochemical properties of the polymer either after repeated oxidative/reductive cycling several hundred times or after exposure to air. The stability of the polymer is due to the excellent electrochemical properties of the thiophene groups and also the presence of divalent sulfur that stabilize the charged thiophenes.

We have prepared poly(**2.15**), which also exhibits excellent electrochemical stability and electronic transport properties for a formally non-conjugated polymer. The maximum conductivity of this polymer was measured to be 1.5×10^{-3} S cm^{-1}. This moderately high conductivity further supports that sulfur bridges are effective at communicating charge between oxidized thiophenes. The polymer also exhibits good electrochromic properties, that is, the polymer is dark yellow-orange in its neutral state and is dark blue in its fully oxidized form. The electrochromic behavior is fully

reversible, as expected on the basis of the electrochemical stability mentioned above. This compliments the electrochemical behavior of PEDOT (**1.4**), which is dark blue in its neutral form due to it being a low band gap polymer, and almost transparent in its doped form. This is an example of how the bridging sulfur groups greatly modulate the electronic properties of the thiophene polymers.

In summary, we have prepared a series of oligomers that are bridged by sulfur and capped with redox-inactive mesityl groups. These compounds were shown to be highly effective model compounds for thienyl-sulfide polymers. The model compounds allowed for an understanding of how substitution patterns of thiophene and electron-rich EDOT blends related to the stability of the compounds in their doped states, and also how these substitution patterns related to electronic communication. The model studies motivated the synthesis of some new sulfur-bridged thiophene polymers. Several of these polymers exhibited high stability in both their neutral and doped states, and showed excellent electrochromic and charge transport properties.

3.6 Future Directions for Part I

From the model compound studies, it is anticipated that a polymer made of alternating EDOT and sulfur bridges (**3.5**) should exhibit excellent charge transport properties and stability when doped; however, no such polymer has been prepared to date. It might be possible to prepare this polymer from a difunctional monomer, such as compound **3.4**. Nodwell has shown that 2,5-dibromo-3,4-ethylenedioxythiophene (**3.2**) can be converted to **3.3** by treating it with one equivalent of *n*-butyllithium, followed by reacting the intermediate lithio species with MesSCl. Using a similar approach, the monolithiated intermediate could be trapped with electrophilic sulfur, and the resulting lithium-thiolate could be protonated by aqueous acid to afford the desired monomer **3.4** (Scheme 3.2). Due to the fact that brominated EDOTs are not very reactive towards

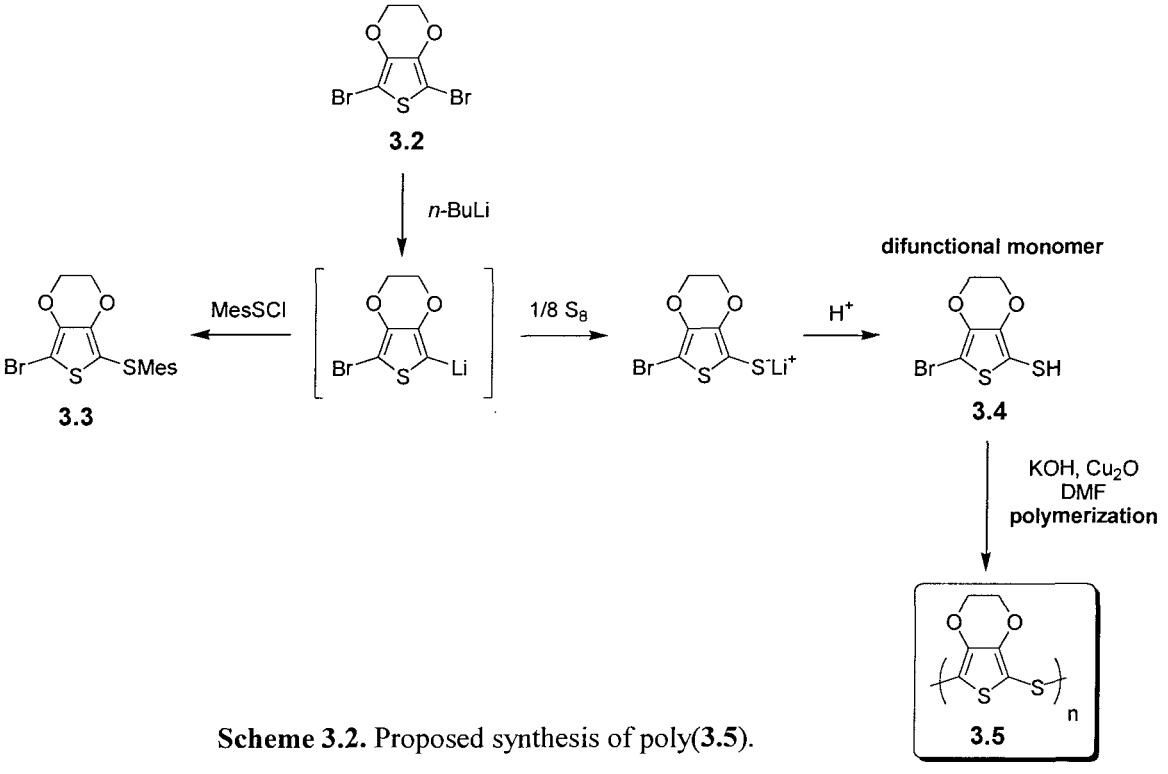

Scheme 3.2. Proposed synthesis of poly(**3.5**).

nucleophilic substitution, it might be necessary to persuade the polymerization reaction by a copper mediated coupling strategy, as initially outlined in §2.2.1. The doping of the neutral polymer (**3.5**) could in principal be done either chemically (e.g., $FeCl_3$, $NOBF_4$, etc.) or electrochemically.

A second offspring from this work would be to exchange the central bridging sulfur groups with other main group elements (e.g., phosphorus, silicon, or boron). This can easily be achieved by applying our convergent protocol, as outlined in Scheme 2.12. The incorporation of electron-deficient boron is particularly interesting because not only will the electronics of the flanking thiophenes be influenced by the boron atom itself, but can also be modulated by changing the pendant R group (Scheme 3.3). The boron atom is also susceptible to reaction with Lewis bases (e.g., amines (R_3N:) and phosphines (R_3P:)), which can serve as a secondary pathway to alter the electronic properties.

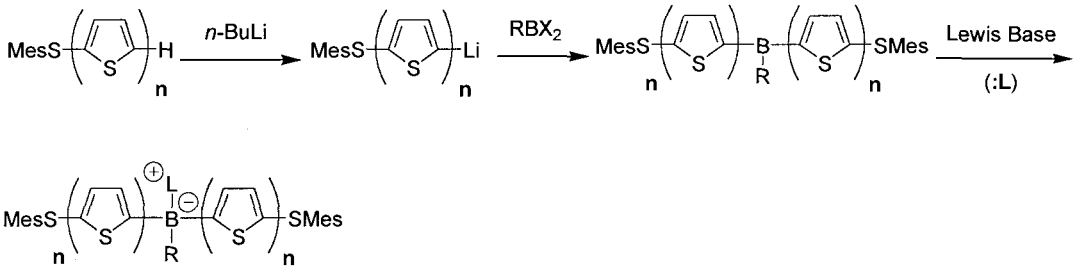

Scheme 3.3. Proposed synthesis of boron-bridged thiophene oligomers.

3.7 Experimental Section

General Experimental

Cyclic voltammetry measurements were conducted on a BAS CV-50W instrument in three-electrode electrochemical cells. The working electrode was a glassy carbon disk, the counter electrode was a platinum wire, and the reference electrode was a silver wire. Dichloromethane was dried by heating at reflux over calcium hydride, followed by distillation. Ferrocene (0.470 V vs SCE in dichloromethane)[28] was used as an internal standard for the electrochemical experiments. Cyclic voltammograms were obtained under argon at room temperature in a dichloromethane solution containing approximately 1 mmol of analyte and 0.1 M of *n*-Bu_4NBF_4 as supporting electrolyte. The E_{pa}-E_{pc} separations of the reversible couples were within 10% of that of the Fc/Fc^+ couple.

Electrolyses of **2.3**, **2.8**, **2.11**, **2.14**, **2.18**, and **2.22** were performed in dichloromethane containing 0.1 M *n*-Bu_4NBF_4 at constant potential (anodic peak potentials of oligomers) in a cell with two compartments. The anode and cathode were platinum plates (3 cm^2). The electrolysis potential was applied versus Ag/AgCl reference. Electrolyses of **2.1**, **2.4**, **2.15**, **2.25**, and **2.26** were conducted in dichloromethane containing 1 M *n*-Bu_4NBF_4 using platinum plate (3 cm^2) electrodes in a one compartment cell. Ag/AgCl was used as the reference electrode and was calibrated versus the Fc/Fc^+ redox (E^o = 0.580 V vs Ag/AgCl)[88] internal reference.

Chemical oxidation experiments were performed by adding aliquots of $NOBF_4$ in dichloromethane from a gas-tight syringe to a solution of the neutral oligomer also in dichloromethane. The resulting oxidized solutions were transferred to sealed quartz

cuvettes by stainless steel cannulas. Cuvettes were oven dried for 24 h prior to use. UV-Vis-NIR spectra were obtained on a Varian Cary 5 spectrometer at room temperature.

Chapter 4

Introduction and Context for Part II

4.1 Introduction

A radical is defined as a species that contains one or more unpaired electrons. Most radicals are transient and highly reactive intermediates since they have a strong preference to form closed-shell configurations by pairing up in either bonds or in non-bonding sets. Stable open-shell species are intriguing because (a) they contradict typical bonding conventions and (b) they do not demonstrate the reactivity patterns (e.g., facile dimerization, H• or R• abstraction, autoxidation, etc.) normally associated with radicals. In describing radicals, the terms *persistent* and *stable* are often used interchangeably, and so here it is imperative to decipher between the two. According to Power, "A *persistent* radical has a relatively long lifetime under the conditions it is generated, whereas a *stable* radical is inherently stable as an isolated species and shows no sign of decomposition under an inert atmosphere at room temperature".[89] From a practical perspective, the term *stable* will be used to describe those radicals that can be isolated in the solid state and stored for a minimum of several days without decomposition. A radical that has a sufficient lifetime to be characterized by conventional techniques (e.g., chemically or spectroscopically) will be defined as a *persistent* one.

Stable radicals are not only interesting from a fundamental standpoint, but also from a practical one. They have potential use in the area of molecular-based magnetic and electronic materials.[90] This is because most technologically important materials require unpaired electrons for magnetic and charge transport properties. Structural, dynamic, and mechanistic details for biological systems have been probed by using stable

radicals as spin labels in conjunction with ESR spectroscopy.[91] They have also found use as reagents for selective cross-coupling reactions and as additives for radical based polymerizations.[92] These synthetic applications require the use of stable radicals, because they tend to have more controlled chemical reactivity than typical radicals. Thus, the purpose of this introductory chapter is to give a brief survey on the general classes of stable radicals and to describe the features that govern their stability (e.g., spin delocalization, use of heteroatoms and steric protection).

4.2 Survey on Persistent and Stable Radicals

Most radicals exist only as transient intermediates during the course of reactions, thus making them extremely difficult to observe, much less isolate. One method used to detect the presence of reactive radicals is by spin trapping. This technique is briefly described in *§4.2.3*. Direct spectral data can be obtained in some instances for short lived radical species by freezing them in the crystal lattices of other molecules. For example, the methyl radical survives with a half-life of 10 – 15 minutes in a methanol lattice at 77 K, which allows for its detection by ESR spectroscopy.[93] When not frozen, the transient methyl radical undergoes dimerization and is prone to abstraction reactions with its surroundings (Scheme 4.1).[94] The driving forces for these reactions are the formation of

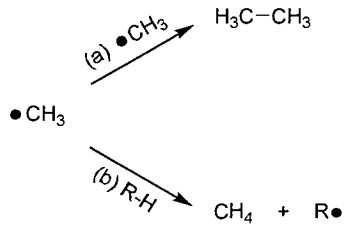

Scheme 4.1. Possible fates of the methyl radical: (a) dimerization and (b) hydrogen abstraction.

strong carbon-carbon (345 – 355 kJ mol^{-1}) and carbon-hydrogen (400 – 415 kJ mol^{-1}) bonds in the ethane and methane products, respectively. In addition, the generation of ethane and methane from the methyl radical are also kinetically favored. Unlike primary alkyls, several secondary and tertiary radicals are known to be persistent. For example, under standard conditions (25 °C, [radical] = 10^{-5} M) the half-lives of $(Me_3C)_2CH\bullet$ and $(Me_3C)_3C\bullet$ are on the order of minutes.[95] The persistency of these radicals is primarily due to the steric protection that the bulky *tert*-butyl groups offer. As will be seen throughout this chapter, steric protection is one of the most common methods used for stabilizing radicals.

4.2.1 Triarylmethyl Radicals

In 1900, Moses Gomberg serendipitously discovered the triphenylmethyl (commonly referred to as "trityl") radical **4.1** while trying to synthesize hexaphenylethane from triphenylmethyl chloride and silver metal (Scheme 4.2).[96] For a long time it was believed that **4.1** was in equilibrium with hexaphenylethane, but in 1968

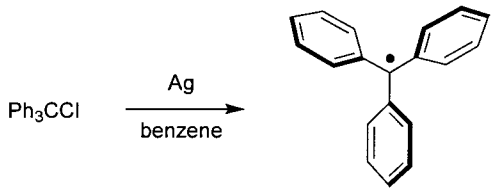

4.1

Scheme 4.2. Synthesis of Gomberg's triphenylmethyl radical (**4.1**).

the exact structure of the dimer (**4.2**) was deduced by NMR spectroscopy.[97] In fact, hexaphenylethane cannot form due to severe steric interactions between the phenyl groups in the approaching trityl radicals. Radical **4.1** is best described as persistent because it dimerizes in solution, and also exists as a dimer in the solid state.

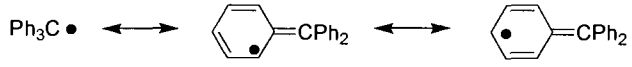

Figure 4.1. The canonical forms of the triphenylmethyl radical.

ESR spectroscopy of **4.1** shows that the majority of spin density resides on the central carbon ($a(^{13}C)$ = 26 ± 3 G) with much smaller amounts on the phenyl rings ($a(H_o)$ = 2.55, $a(H_p)$ = 2.78 G). The fact that spin resides on the *para*-positions (see Figure 4.1) of **4.1** corroborates well with the formation of **4.2**. Thus, dimer **4.2** results from the head-to-tail coupling of the two trityl radicals according to Scheme 4.3. In general, the

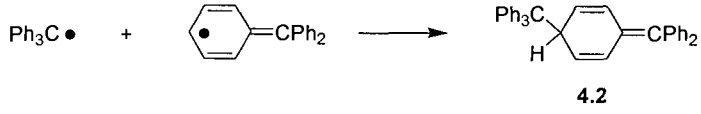

4.2

Scheme 4.3. Formation of dimer **4.2**.

persistent nature of triarylmethyl radicals is ascribed predominantly to steric factors more than spin delocalization. To prove this, radicals **4.3** and **4.4** were prepared and studied.[98] The former has a fully planar structure allowing for maximum delocalization of the radical, whereas the latter adopts a propeller-like structure by virtue of the sterically crowding *ortho* methoxy substituents. If delocalization is the major contributing factor to stability, then dimerization of **4.3** should be difficult. The opposite holds true if steric hindrance plays the dominant role; that is, association of **4.4** should become more difficult. Experimentally it was found that no dimerization occurs for **4.4** in the solid state or in solution, while the dimer of **4.3** only dissociates into radicals on heating in solution (1 – 2% dissociation in xylene (10^{-3} M) at 140 °C).[98]

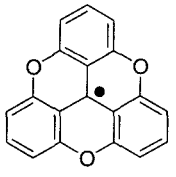

4.3

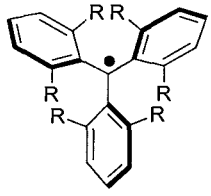

4.4 (R = OMe)

Several other substituted triarylmethyl radicals have been reported in the literature, some of which have been structurally characterized by X-ray crystallography. For example, tris(*p*-nitrophenyl)methyl, an exceptionally stable organic radical, was determined by crystallography to be monomeric in the solid state with its phenyl rings twisted by about 30° from each other.[99]

Gomberg's discovery has motivated the syntheses of diradical **4.5** (S = 1),[100] tetraradical **4.6** ($S = 2$)[101] and even polyradical **4.7** (S ≈ 10).[102] Polyradicals of the latter type are being extensively studied by Rajca's group as building blocks for high-spin magnetic materials.[103]

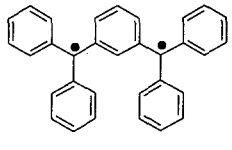

4.5

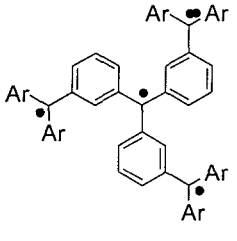

4.6 (Ar = *p*-^{t}BuC$_6$H$_4$)

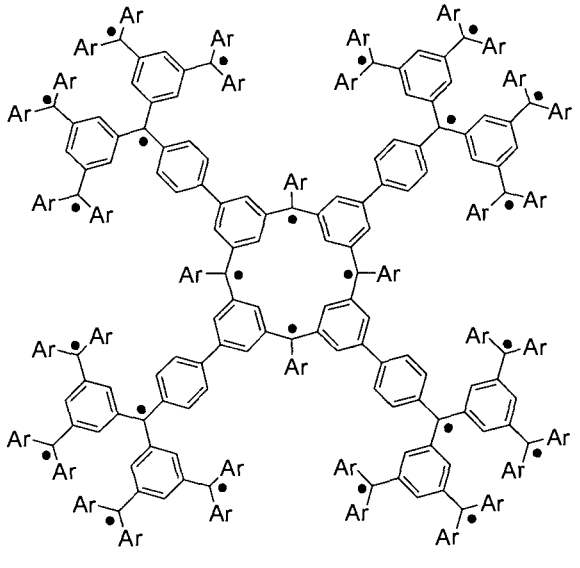

4.7 (Ar = *p*-^{t}BuC$_6$H$_4$)

4.2.2 Phenalenyl Radicals

Phenalene reacts readily with methoxide to give the corresponding anion, which can be subsequently oxidized to phenalenyl radical **4.8** (Scheme 4.4).[104] The highly delocalized phenalenyl radical persists in dilute solution as long as oxygen remains

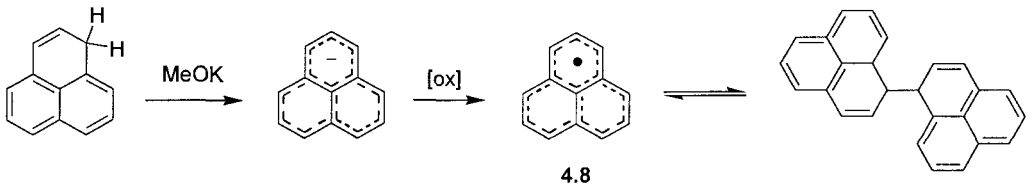

4.8

Scheme 4.4. Synthesis of phenalenyl radical **4.8**.

absent. A temperature dependent equilibrium exists between radical **4.8** and its corresponding σ-dimer. At low temperature the dimer is favored, while at higher temperatures the dimer reverts back to radical **4.8**. The tendency for **4.8** to undergo σ-dimerization has prevented its structure to be determined by crystallography. However, Yamamoto and co-workers recently synthesized 2,5,8-tri-*tert*-butyl-phenalenyl radical **4.9** and were successful in obtaining its crystal structure.[105] The *tert*-butyl groups were placed at the three β-positions to aid in the stability of the phenalenyl radical and to prevent σ-dimerization. Solid radical **4.9** is stable indefinitely in an inert atmosphere. The molecules form discreet face-to-face π-dimers with an interplanar contact distance ranging from 3.2 to 3.3 Å. The molecules are staggered by 60 ° from one another to avoid steric interaction of *tert*-butyl groups (Figure 4.2). The ESR spectrum of **4.9** shows seven lines, as expected for the radical coupling to the six equivalent ring protons.

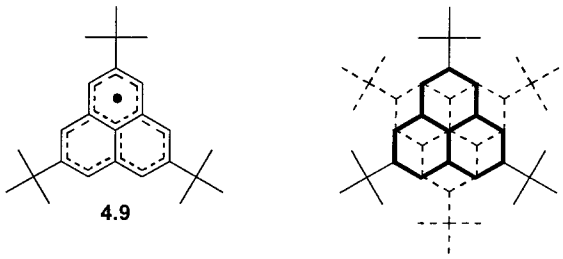

4.9

Figure 4.2. Compound **4.9** and a diagram of its solid-state structure showing the face-to-face π-dimer.

Haddon *et al.* have also reported the synthesis and structural properties of a perchlorinated phenalenyl derivative (**4.10**).[106] The monomeric radicals of **4.10** stack in one-dimensional columns in the solid state with a minimum interplanar contact distance of 3.78 Å. The peri-chlorine atoms prohibit the molecules from coming in close contact with each other. Phenalenyl **4.10** and its derivatives are actively being pursued as neutral radical conductors.[107]

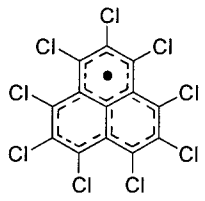

4.10

Azaphenalenyl radicals are also beginning to appear in the literature, and these systems are exciting because the Lewis basic nitrogen atoms can potentially be used as coordination sites; for example, to paramagnetic metal centers (Figure 4.3). The incentive here is to design functional magnetic materials by taking advantage of the so-called "metal-radical" approach.

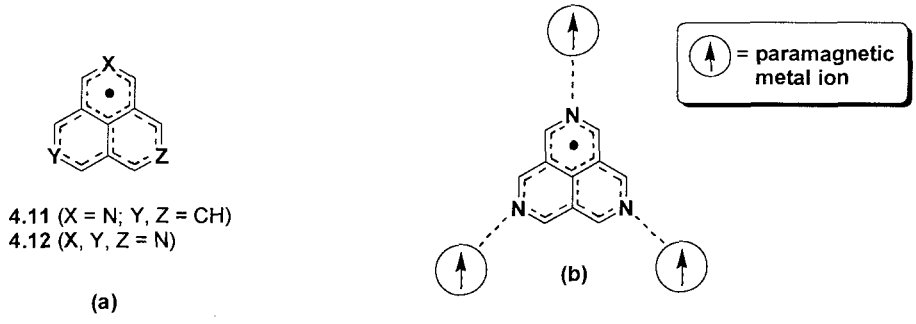

Figure 4.3. (a) Azaphenalenyl radicals **4.11** and **4.12** and (b) a possible coordination mode of **4.12** to paramagnetic metal centers.

In contrast to the persistent parent phenalenyl **4.8**, azaphenalenyl radical **4.11** is more stable as it does not dimerize in solution or in the solid state under normal conditions.[108] Interestingly, an attempted complexation of **4.11** with $Cu(hfac)_2$ (hfac = hexafluoroacetylacetonate) lead to the formation of a σ–dimer (**4.13**), which was characterized by X-ray crystallography (Scheme 4.5).[108] Complex **4.13** is important because it represents the first example of a structurally characterized σ-dimer of a phenalenyl radical.

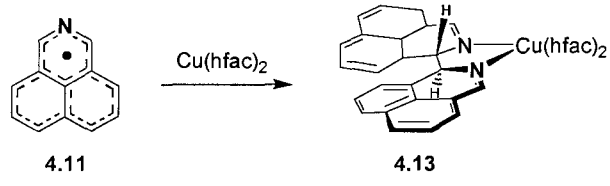

Scheme 4.5. Synthesis of an azaphenalenyl σ-dimer copper complex (**4.13**).

4.2.3 Nitroxide and Nitronyl Nitroxide Radicals

One of the simplest inorganic radicals is nitric oxide (NO). The unpaired electron is fully delocalized (see canonical forms in Figure 4.4) over the NO framework and resides in an antibonding π* SOMO. The stability is in part due to its electron-rich hybrid

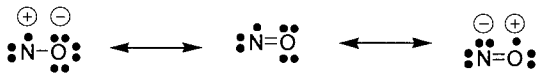

Figure 4.4. Canonical forms of nitric oxide.

structure, but also because of the lone pair repulsions which disfavor σ-dimerization. A purely inorganic derivative of nitric oxide is Fremy's salt ($(KSO_3)_2NO•$), which was isolated in 1845 as the first free radical.[109] The related nitroxide radicals have the NO radical flanked by organic groups, as represented in **4.14**. The stability of nitroxides rely little if it all on steric protection, but rather the inherent electronic properties of the NO group itself (see above). Analogous to nitric oxide, self-association of nitroxide radicals is unfavorable because of the lone pair repulsions in the resulting σ-dimer (Figure 4.5).

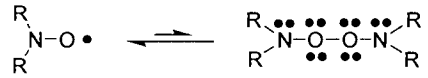

4.14

Figure 4.5. Unfavorable σ-dimerization of generic nitroxide radical **4.14**.

Di-*tert*-alkyl nitroxide radicals **4.15-4.18** are stable and all show three dominant lines in their ESR spectra.[110] The lines are split by 15–16 G as a result of the unpaired electron coupling to the nitrogen atom. Interestingly, compound **4.18** is so stable that it

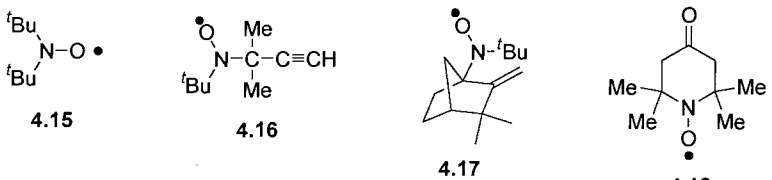

4.15 **4.16** **4.17** **4.18**

has been shown to react with Grignard reagents without causing any damage to the nitroxide radical (Scheme 4.6).[111]

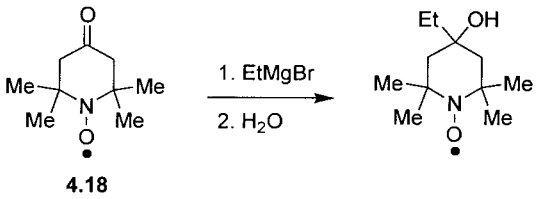

4.18

Scheme 4.6. Reaction of nitroxide **4.18** with a Grignard reagent.

On the other hand, alkyl nitroxides that have hydrogen atoms on their α-carbons are subject to decomposition. The intermediate dialkylnitroxides (**4.19**) can be prepared by the oxidation (e.g., using PbO_2) of *N,N*-dialkylhydroxylamines, which then undergo rapid conversion to nitrones (**4.20**) via α-hydrogen elimination (Scheme 4.7).[112] Nitroxides of the type **4.19** are not sufficiently long-lived to be isolated.[113]

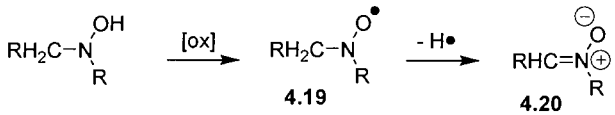

4.19 4.20

Scheme 4.7. Formation of nitrones (**4.20**) via α-hydrogen elimination of alkylnitroxides (**4.19**).

There are also several examples of phenyl substituted nitroxide radicals, but these usually require adequate blocking groups (e.g., ^{t}Bu, OMe, NO_2, etc.) at the *para* positions to aid in their stability. One reason for this is exemplified by the decomposition of *tert*-butylphenylnitroxide (Scheme 4.8).[114] Even though nitroxide **4.21** does persist for several

days in dilute solution, delocalization of spin onto the *para* position of the phenyl ring results in the slow formation of **4.23** and **4.24** via intermediate **4.22**.

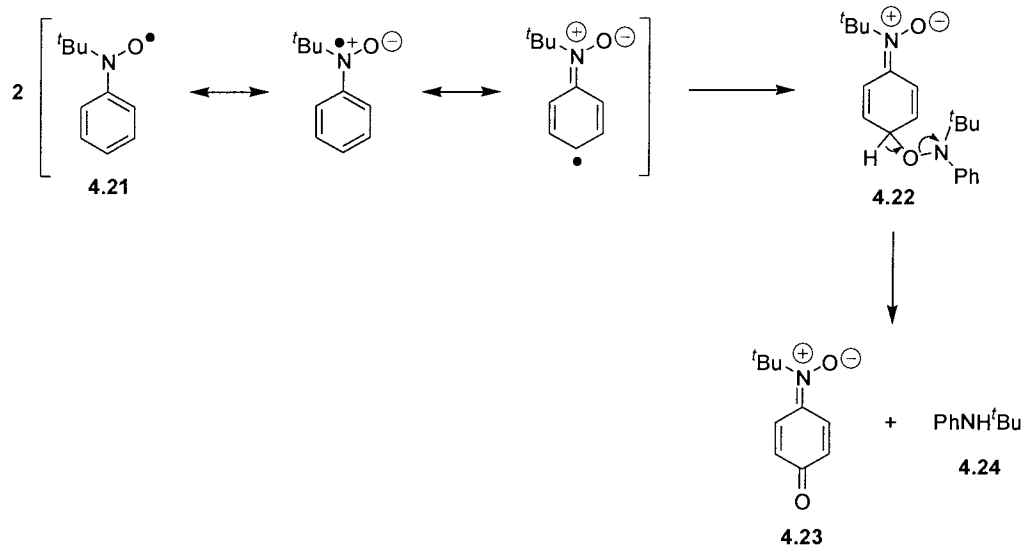

Scheme 4.8. Decomposition pathway for a phenyl substituted nitroxide radical (**4.21**).

Nitroxide radicals are important products in spin trapping reactions.[115] Spin trapping is a technique often used in conjunction with ESR spectroscopy to detect the presence of reactive radicals. In essence, a particular compound interacts with a reactive radical to make a more persistent or stable radical. For example, nitroso compounds (RN=O) are particularly good spin traps because they react rapidly with radicals (•R') to make stable nitroxide radicals (R'RN-O•). The resulting nitroxides are then easily detected by ESR.

Closely related to the nitroxides are the nitronyl nitroxide radicals (**4.27**). Bis(hydroxylamino) **4.25** can be condensed with a range of aldehydes to give **4.26** (Scheme 4.9).[116] The latter can be oxidized (PbO_2 is most commonly used) to give the corresponding nitronyl nitroxides **4.27**. ESR studies show that the spin is delocalized on

the two equivalent N-O fragments giving rise to a prominent five line pattern with ^{14}N coupling constants on the order of 16–17 G.

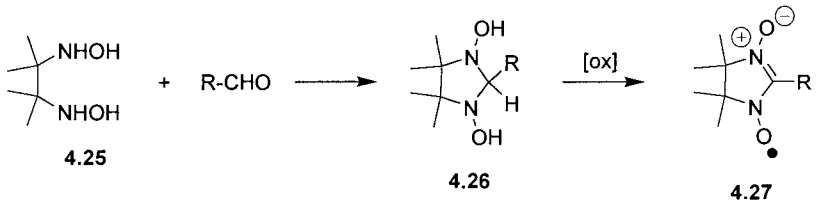

Scheme 4.9. Synthesis of nitronyl nitroxide radicals (**4.27**).

4.2.4 Hydrazyl Radicals

During the period of 1920-9, Goldschmidt and co-workers discovered and investigated a new class of hydrazyl radicals.[117] The parent triphenylhydrazyl radical **4.28** was prepared by oxidation of triphenylhydrazine with lead dioxide (Scheme 4.10). The

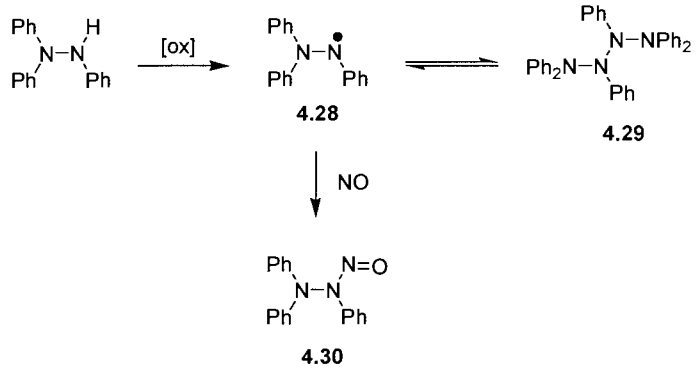

Scheme 4.10. Formation, dimerization, and nitrosation of hydrazyl radical **4.28**.

green radical could be stored in the solid state at -80 °C for several days without decomposition. Blue ether solutions of the radical slowly decompose to its dark red dimer **4.29**. Presence of persistent **4.28** could also be confirmed by its conversion to nitrosoamine **4.30** upon treatment with nitric oxide. Amongst dimer formation, hydrazyl

4.28 also decomposes to diimine **4.31** and diphenylamine according to Scheme 4.11.[118] Most other hydrazyls (triaryl or otherwise) experience similar decomposition fates (see

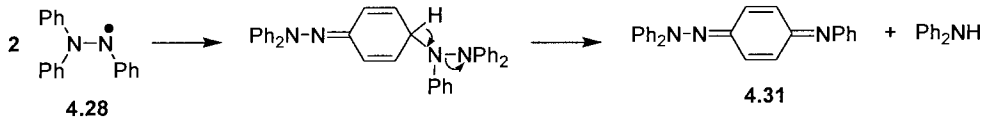

Scheme 4.11. A decomposition pathway for hydrazyl radical **4.28**.

Schemes 4.10 and 4.11), and as such they are generally perceived as a class of short-lived radicals. That being said, there are a few examples of stable hydrazyls that take advantage of steric protection. An example of this is 2,2-diphenyl-1-picrylhydrazyl (DPPH) radical **4.32** that has sterically protecting *ortho*-nitro substituents.[117] DPPH is stable indefinitely in the solid state and in dilute solution. It is commonly used as an ESR standard for determining radical concentrations. The ESR spectrum of **4.32** shows that the unpaired electron resides primarily on the two nitrogens with a coupling constant of 9.35 G to the picryl nitrogen, and 7.85 G to the other nitrogen atom.

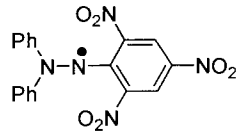

4.32

4.2.5 Verdazyl Radicals

In contrast to hydrazyls, the structurally related verdazyl radicals (**4.33** and **4.34**) generally display good stability. The verdazyls were first discovered, serendipitously, by Kuhn and Trischmann in the early 1960s while attempting to alkylate formazans (see *§5.2.1*).[119] Since this landmark discovery several other synthetic strategies to verdazyls have been developed, and these are described in Chapter 5.

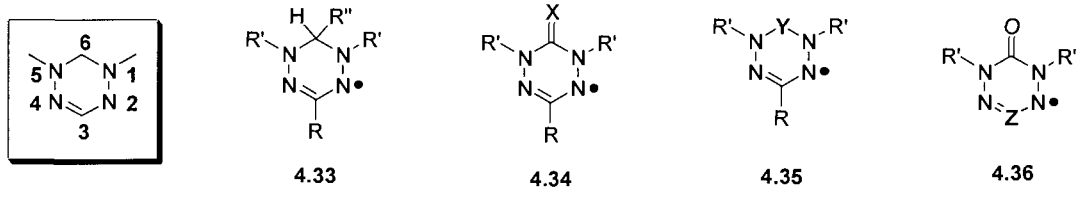

Figure 4.6. Numbering scheme and generic structures of verdazyl radicals **4.33-4.36**.

The two most heavily studied verdazyls (**4.33** and **4.34**) have generic structures as represented in Figure 4.6. Both are stabilized by delocalization of the unpaired electron over the four nitrogen atoms (see canonical forms in Figure 4.7). Verdazyls of type **4.33**

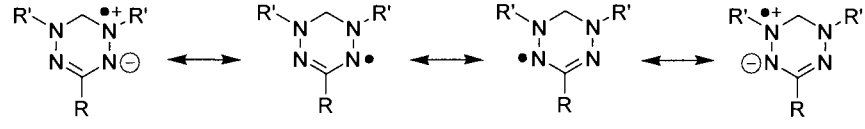

Figure 4.7. Canonical forms of a generic verdazyl radical.

generally adopt a half-boat conformation with the C6 group raised slightly from the plane of the rest of the molecule (Figure 4.8a). A crystal structure of the triphenylverdazyl radical **4.33** (R = R' = Ph and R" = H) shows that the methylene bridge is raised by 0.62 Å.[120] On the other hand, verdazyls of type **4.34** (i.e., those containing a carbonyl or

thiocarbonyl group at C6) adopt fully planar structures (Figure 4.8b). The planarity is due to an amide-type resonance of the carbonyl or thiocarbonyl group with the adjacent N1 and N5 nitrogen atoms.

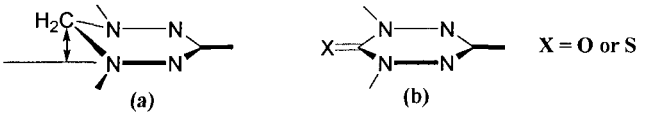

Figure 4.8. Schematic diagrams of (a) showing the nonplanar geometry of **4.33** at the methylene carbon, and (b) showing the planar structure of **4.34**.

The ESR spectra of parent verdazyls **4.33** and **4.34** each show a prominent nine line pattern that arises from coupling of the unpaired electron to the four nearly equivalent nitrogen atoms. The coupling pattern is in agreement with (a) the four resonance forms of verdazyls, as shown in Figure 4.7, and (b) the extended Hückel calculations that show the unpaired electron residing in a delocalized π-molecular orbital spanning the four nitrogen atoms (Figure 4.9).[121] Coupling of the electron to each of the nitrogen atoms are usually on the order of 5-6 G.

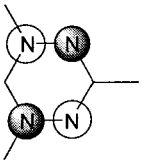

Figure 4.9. π SOMO of a generic verdazyl.

The parent verdazyls show extraordinary stability in both the solid state and in dilute solution. In fact, many solid verdazyl derivatives can be left out in air for several years without decomposition.

4.2.6 Phosphaverdazyl Radicals

Synthetic routes to verdazyl radicals **4.33** and **4.34** with a plethora of substituents on the carbon and nitrogen ring atoms have been well established. The alteration of these peripheral substituents generally has little consequence on the overall stability and electronic properties of the verdazyl radical itself. This is largely due to the radical being confined to the central electron-rich π-system (vide supra). Surprisingly, there have been no studies on how the electronic and structural properties are influenced by skeletal atom substitutions at the **Y** and/or **Z** positions of verdazyls **4.35** and **4.36**, respectively. In this respect, previous research in our group has focused on the incorporation of phosphorus at these **Y** and **Z** positions. Phosphorus is appealing because its spin-active nucleus (^{31}P; I = ½) is 100% abundant; thus providing an additional handle on the electronic structure by ESR spectroscopy.

In 1999, Hicks and Hooper reported the synthesis (Scheme 4.12) and ESR results of 6-phosphaverdazyl **4.37** and 3-phosphaverdazyl **4.38**.[122] Unfortunately, the stability of

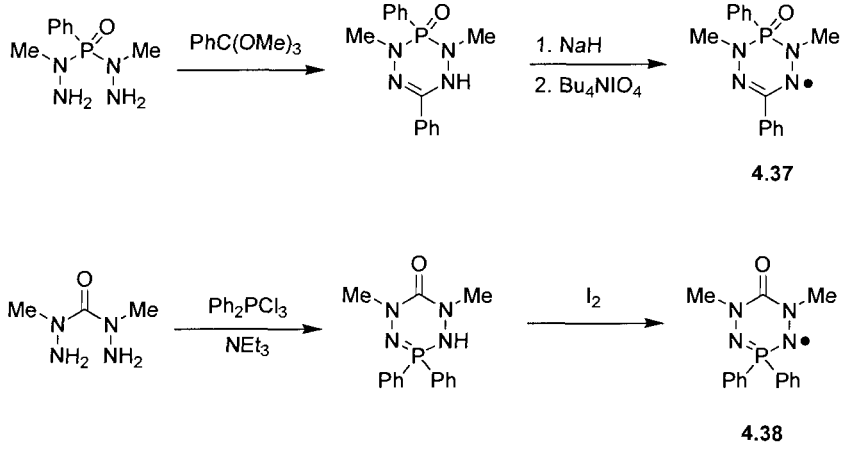

Scheme 4.12. Synthesis of phosphaverdazyls **4.37** and **4.38**.

these is not as high as their carbon analogues. They survive for several days to weeks as solids at -30 °C, but at room temperature or in solution they decompose more rapidly. Decomposition of these radicals has precluded their structures to be determined by X-ray crystallography. Therefore, insights into their electronic and molecular structures have been accomplished by a combination of DFT calculations and ESR spectroscopy.

The ESR spectrum for phosphaverdazyl **4.38** is almost identical to that of parent verdazyl **4.34** (R = Ph, R' = Me, and X = O), except for a small coupling of 0.2 G to the phosphorus atom. The coupling is in close agreement with Hückel calculations for the SOMO of **4.38**, which predicts zero spin density on phosphorus by the fact that a nodal plane bisects the 3- and 6-positions. By analogy to verdazyl **4.34**, it is inferred that **4.38** also adopts a planar geometry. In contrast, the 6-phosphaverdazyl (**4.37**) was observed to have a relatively stronger coupling of 5.2 G to its phosphorus atom. At first glance this seems surprising since there are no exocyclic orbitals of proper symmetry to overlap with the verdazyl π system. The non-planar geometry of **4.37** does, however, permit for sufficient mixing of the σ and π systems, thereby resulting in spin leakage onto the phosphorus.

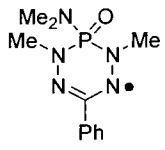

4.39

The intriguing results obtained for **4.37** motivated the synthesis of a verdazyl radical with a dimethylamino group attached to the phosphorus. Radical **4.39** was deliberately designed by Hicks and co-workers to examine if spin could leak out onto the exocyclic nitrogen group.[123] Indeed a relatively strong coupling of 4.6 G to the exocyclic nitrogen was observed by ESR, but in this instance there was no coupling to the phosphorus atom. Since X-ray structural information could not be obtained for **4.39**, high level DFT

calculations were performed to gain insight on the electronic and molecular structures. Briefly, the DFT calculations revealed that the lowest energy conformation for **4.39** is one in which the phosphaverdazyl ring system is nearly planar and that the NMe_2 has its p-orbital sitting above the verdazyl π SOMO. The planarity of the system, as inferred by DFT calculations, agrees well with there being no spin density on phosphorus, and this is again a consequence of a nodal plane passing through that position for the SOMO. The through-space interaction between the nitrogen p-orbital and the verdazyl π SOMO is what causes the spin to leak onto the nitrogen atom (Figure 4.10). This phenomenon is

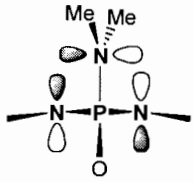

Figure 4.10. End-on view of **4.39** showing the overlap of the nitrogen p-orbital with the verdazyl π system.

referred to as "spiroconjugation". Hicks *et al.* later reported that spiroconjugation also occurs in phosphazene **4.40**.[124] This system is particularly interesting because it represents a rare instance of spin injection into a phosphazene ring.

4.40

4.2.7 Sulfur-Nitrogen Radicals

Nitrogen sulfide (NS•), unlike nitric oxide, is exceptionally unstable and decomposes rapidly to polythiazyl $(SN)_x$.[125] Nitrogen sulfide has been detected in a frozen argon matrix at 12 K.[126] However, thioaminyl radicals are known to be persistent and in some instances stable. The bis(alkyl) substituted thioaminyl radicals are at best persistent, but a few bis(aryl) (**4.41**) derivatives show considerably higher degrees of stability.[127] The thioaminyls are commonly prepared by oxidation of sulfenamides (Scheme 4.13).[128] Sulfenamides themselves are made by the reaction of aryl amines with aryl sulfenyl chlorides in the presence of an auxiliary base. Aryl substituted thioaminyls

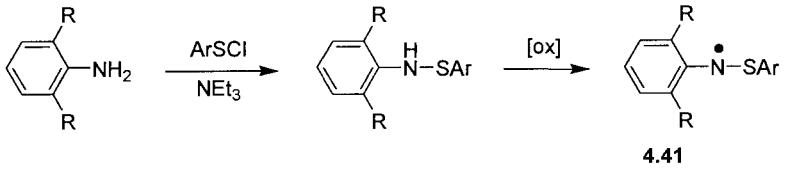

4.41

Scheme 4.13. Synthesis of thioaminyl radicals (**4.41**).

are stabilized by delocalization of the electron, not only within the electron-rich SN bridge (Figure 4.11), but also in the aryl substituents. Bulky *ortho* substituents (e.g., R = ^{t}Bu or Ph for **4.41**) also aid in stability by protecting the radical from undergoing dimerization and other decomposition reactions.[129]

Figure 4.11. Resonance structures of the thioaminyl radical.

A large number of radicals based on sulfur-nitrogen ring systems have been developed, and many of these enjoy a high degree of stability.[130] A few select examples (**4.42-4.44**) of thiazyl radicals will be described herein, but is by no means meant to be exhaustive.

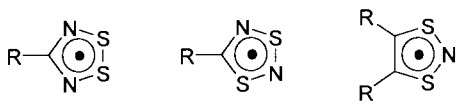

4.42 **4.43** **4.44**

The isomeric dithiadiazolyls **4.42** and **4.43** are 5-membered ring heterocycles each containing 7π electrons. 1,2,3,5-dithiadiazolyl radical **4.42** can be prepared by the reduction (e.g., zinc metal or triphenylphosphine) of dithiadiazolium cation **4.45** (Scheme 4.14).[131] The cations are commonly made by the reaction of persilylated amidines[132] with sulfur dichloride. Similarly, reduction of cation **4.46** gives 1,3,2,4-dithiadiazolyl radical **4.43**. Cation **4.46** can be prepared by a 4 + 2 cycloaddition of a nitrile with S_2N^+.[133]

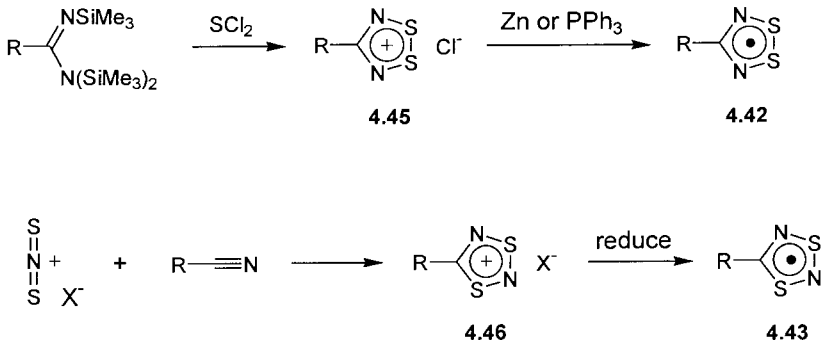

4.45 **4.42**

4.46 **4.43**

Scheme 4.14. Synthesis of isomeric dithiadiazolyl radicals **4.42** and **4.43**.

The 1,2,3,5-dithiadiazolyls (**4.42**), with a range of R groups, have a propensity to form diamagnetic π-dimers in the solid state.[134] An exception to this is Rawson's dithiadiazolyl radical **4.47** that forms discrete monomeric radicals in the solid state.[135]

The radical is interesting because it magnetically orders at an unprecedented critical temperature (T_c) of 36 K.[136] To date this is the highest T_c reported for a purely organic based radical.

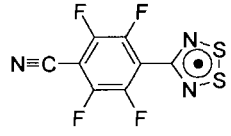

4.47

The ESR spectra for 1,2,3,5-dithiadiazolyls (**4.42**) normally show a five line pattern as a result of the electron coupling to the two equivalent nitrogen atoms ($a(^{14}N)$ = 5.0 G). Coupling to the R substituents is negligible due to a nodal plane passing through the ring carbon atom (see SOMO in Figure 4.12 for **4.42**). Triplets are most often observed in the ESR spectra for the 1,3,2,4-dithiadiazolyl radicals **4.43**, arising from coupling to the nitrogen at the 2-position. In agreement with the SOMO for **4.43** (Figure 4.12), coupling to the nitrogen atom at the 4-position is small.

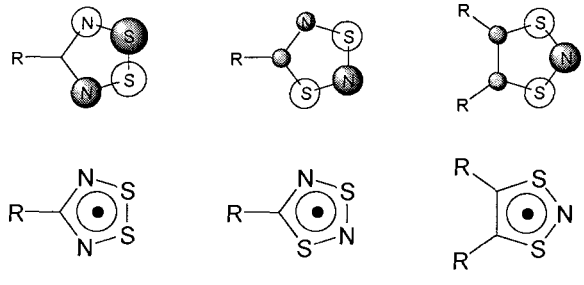

4.42 **4.43** **4.44**

Figure 4.12. π SOMOs of radicals **4.42**, **4.43**, and **4.44**.

When R is *tert*-butyl for **4.43** the radical is stable indefinitely at room temperature,[137] whereas the methyl derivative is prone to polymerization, and only persists while in dilute solution.[138]

One method to prepare 1,3,2-dithiazolyls (**4.44**) is by the condensation of SNS^+ with an alkyne (Scheme 4.15).[133] Many derivatives of **4.44** with varying R groups have been prepared and structurally characterized. For example, when R is a cyano (CN) group, the radicals dimerize in a face-to-face manner.[139] However, discrete monomeric radicals have been observed in the solid state for 1,3,2-dithiazolyls fused to aromatic groups (e.g., quinoxaline and naphthalene).[140] Coupling of the unpaired electron to the nitrogen atom at the 3-position in 1,3,2-dithiazolyls (**4.44**) results in an ESR spectrum with three prominent lines separated by approximately 11 G.

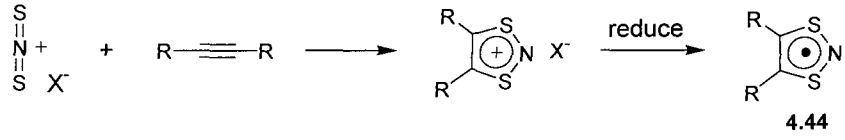

4.44

Scheme 4.15. Synthesis of 1,3,2-dithiazolyl radicals (**4.44**).

4.3 Aims and Objectives for Part II

A survey of the more common classes of radicals reveals that three common strategies can be employed in achieving radical stability: (a) delocalization of the spin onto electron-rich heteroatoms (e.g., sulfur, nitrogen, and oxygen); (b) delocalization of the spin onto substituents; and (c) sterically protecting the radical center with bulky substituents. The latter technique has been most heavily used, but for practical applications is the least desirable. Most applications require radicals to be able to interact (e.g., chemically, magnetically, etc.) with other species or themselves. Too much steric protection can suppress or even prevent these interactions. For example, solid state radicals typically exhibit their highest degrees of magnetic or conductive responses when neighboring radicals can strongly interact in a cooperative fashion without self-associating to closed-shell species. Although these association modes can often be avoided by placing very bulky substituents around the radical center, this usually leads to poor magnetic or conductive exchange interactions between the neighboring spins as they are now too far apart. An alternative approach is to use main group elements (e.g., sulfur, nitrogen, and oxygen), for which we have already seen are highly effective at stabilizing radicals without the need for steric protection. In this vein, nitroxides, nitronyl nitroxides, and verdazyls all experience good stability, while relying little if any on steric protection.

Table 4.1. Comparison of some acyclic radicals (above) and their corresponding resonance delocalized cyclic counterparts (below).

Acyclic Radical	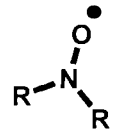 **Nitroxide**	 **Hydrazyl**	 **Thioaminyl**	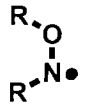 **Alkoxyaminyl**
Cyclic Radical	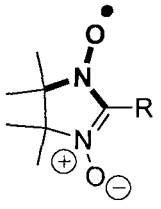 **Nitronyl Nitroxide**	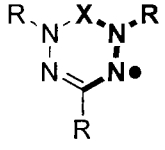 **Verdazyl**	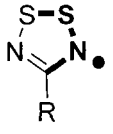 **Dithiadiazolyl**	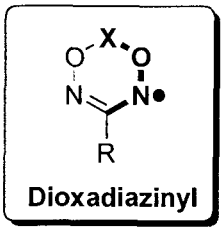 **Dioxadiazinyl** ***Unknown***

The most stable organomain group radicals to date are based on nitronyl nitroxides, verdazyls, and cyclic sulfur-nitrogen compounds (see Table 4.1). All of these radicals have the inherent properties of their corresponding acyclic counterparts, but in addition are further stabilized by resonance delocalization through their cyclic frameworks. One class of radicals that was not mentioned in this chapter are the *N*-alkoxyaminyl radicals, which are isoelectronic with thioaminyls. *N*-alkoxyalkylaminyl radicals have been studied as a class of persistent radicals, but are generally not isolable.[141] Recently, however, Miura *et al.* have overcome this by preparing a range of isolable and air stable *N*-alkoxyarylaminyl radicals (**4.48-4.50**).[142] Several of these derivatives could be characterized by X-ray crystallography. The radicals are stabilized by delocalization within the NO bridge and also onto the aryl substituents. The

incorporation of bulky *ortho* substituents (e.g., *tert*-butyl or aryl) on the *N*-aryl groups also aid in sterically protecting the radicals.

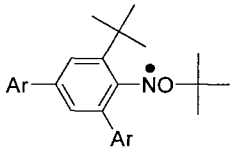

4.48

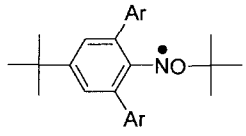

4.49

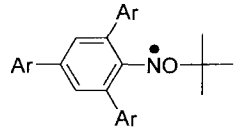

4.50

Surprisingly, there are no known cyclic analogs of alkoxyaminyl radicals (see Table 4.1). In this regard, the unknown 6-membered ring dioxadiazinyl radicals should serve as effective resonance-delocalized alkoxyaminyls. Dioxadiazinyls are anticipated to show good stability based on many factors. Firstly, they are similar to alkoxyaminyls, but now have an added degree resonance delocalization through the cyclic framework. Secondly, these radicals are stabilized by delocalization on electron-rich NO groups as is the case for nitroxides, nitronyl nitroxides, and alkoxyaminyls. Lastly, the dioxadiazinyls are anticipated to be electronically similar to the exceptionally stable verdazyl radicals (see Chapter 5). All of these attributes make dioxadiazinyl radicals worth pursuing as a new class of stable radicals. Most of the well known classes of stable radicals have been prepared accidentally (e.g., recall Gomberg's triphenylmethyl radical or Kuhn and Trischmann's parent verdazyl), and many of the newer ones are simply derivatives of these. A less common theme is to *design* entirely new stable radicals from scratch, and thus it is the intention of the remainder of this thesis to describe rational synthetic routes to dioxadiazinyl radicals.

Chapter 5

Exploratory Syntheses Toward Dioxadiazinyl Radicals

5.1 Introduction

The purpose of this chapter is to describe the synthetic efforts put forth to prepare a series of 3- and 6-substituted dioxadiazinyl radicals **5.1**. New heterocyclic chemistry will need to be developed as there are no paramagnetic or even diamagnetic examples of the O_2N_2CE (**5.1**) ring system. This structure is desired because it closely resembles that of verdazyl radicals, which are known to exhibit excellent stability.[143] Our group is actively involved in the systematic study of how skeletal atom substitutions at the 3- and 6-positions influence the stability and electronic properties of verdazyl radicals **5.2** (see Chapter 4). To extend this work, we became interested in placing divalent oxygen substituents at the 1- and 5-positions, and similarly want to examine how these modifications will influence structure-property relationships.

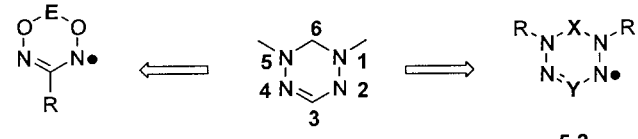

5.1 **5.2**

The electronic structure of dioxadiazinyl radicals is anticipated to be qualitatively similar to that of verdazyls based on the DFT calculations performed by Dr. Robin Hicks (Figure 5.1). Both contain 7π electrons in a planar ring system, and the SOMO of each is a delocalized π orbital spanning four heteroatoms. However, differences between the spin distributions and the SOMO energies can be seen by examination of Figure 5.1. These

structural differences and the anticipated stability make dioxadiazinyl radicals worth pursuing as a new class of neutral radicals.

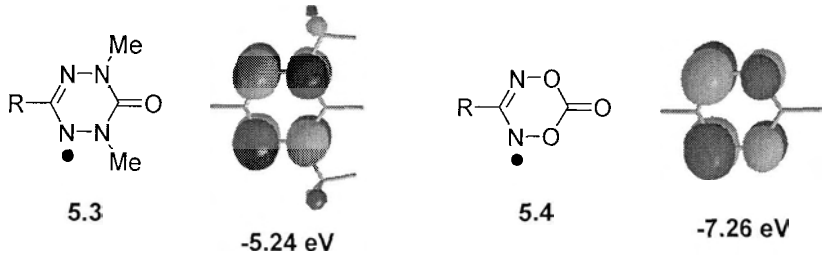

Figure 5.1. π-SOMOs of verdazyl radical **5.3** and dioxadiazinyl radical **5.4** calculated at the UB3LYP/6-31G* level.

Section *5.2.1* highlights the initial efforts of Greg Patenaude (a previous graduate student in our group) toward preparing dioxadiazine heterocycles by condensing oxyamidoximes with either carbon or main group based substrates. The challenges he encountered while attempting to synthesize the O_2N_2CE ring system (radical or precursor) motivated the development of two new synthetic strategies that are specific to this chapter. The first of these, as described in section *5.3.1*, involves studying the condensation reactions of *O*-silylated chloroximes with hydroxylamine, with the intent to prepare 6-siladioxadiazine heterocycles. The second strategy (section *5.3.2*) examines the possibility of preparing various 3-substituted dioxadiazanes by condensing bis(hydroxylamino) compounds with substituted aldehydes.

5.2 Background

5.2.1 Synthetic Strategy I – Condensation Reactions of Oxyamidoximes

In the early 1960s, Kuhn and Trischmann found that formazans could be functionalized with primary alkyl halides to give tetrazines (Scheme 5.1).[119] The tetrazines are then air-oxidized to the corresponding verdazyl radicals. Using a similar approach, Patenaude sought to prepare a series of unknown dioxadiazines (**5.6** and **5.7**) by condensing oxyamidoximes (**5.5**) with a wide range of either carbon (e.g., aldehydes

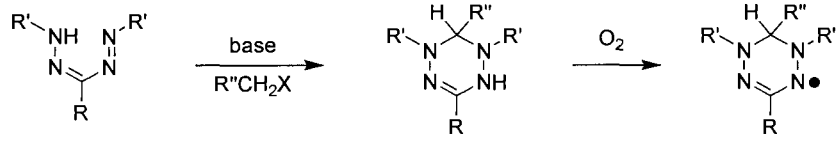

Scheme 5.1. Preparation of verdazyl radicals by the alkylation of formazans.

and ketones) or main group dihalide (e.g., $RBCl_2$, R_2SiCl_2, $RPCl_2$, etc.) based substrates (Scheme 5.2).[144] Compounds **5.6** and **5.7** could then be converted, in principle, to

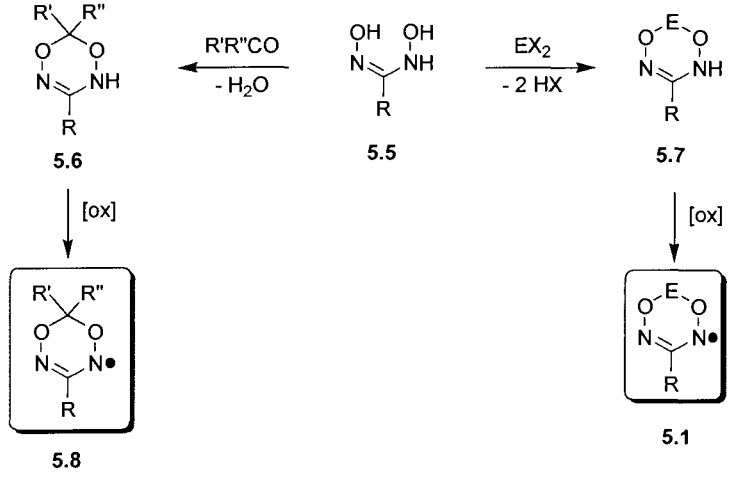

Scheme 5.2. Proposed syntheses of dioxadiazinyl (**5.8**) and heterodioxadiazinyl (**5.1**) radicals.

dioxadiazinyl radicals **5.8** and **5.1** by oxidation. Oxyamidoximes themselves are typically synthesized in one of two ways: (a) the reaction of amidoximes with hydroxylamine hydrochloride, or (b) by treating nitrile oxides with free hydroxylamine (Scheme 5.3).[145] Oxyamidoximes prepared by the latter method are primarily restricted to aryl substituents attached to the carbon position, because alkyl nitrile oxides undergo rapid dimerization to give furoxan byproducts.

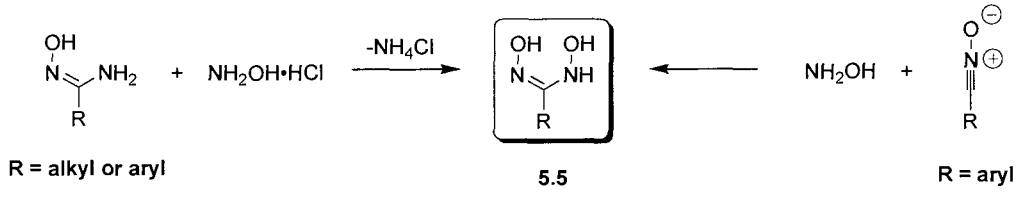

Scheme 5.3. Synthetic pathways to oxyamidoximes (**5.5**).

Greg Patenaude prepared a *p*-tolyl substituted oxyamidoxime according to Scheme 5.4.[144] The first step involves the chlorination of oxime **5.9** to afford the hydroximinoyl chloride **5.10**. Dehydrochlorination of **5.10** with one equivalent of hydroxylamine in DMF gave the intermediate nitrile oxide **5.11**, which was reacted *in situ* with a second equivalent of hydroxylamine to provide the desired oxyamidoxime **5.12** in 36%. The low yield is largely due to competing furoxan (**5.13**) formation via dimerization of the intermediate nitrile oxide.

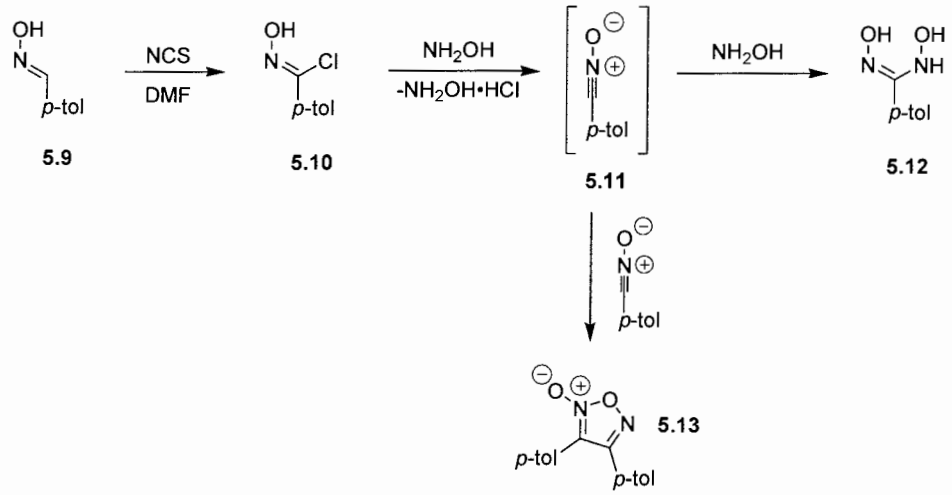

Scheme 5.4. Synthesis of *p*-tolyl substituted oxyamidoxime (**5.12**).

Cyclization reactions of **5.12** with several electrophiles were attempted by Patenaude, but isolation of the proposed 6-membered dioxadiazine ring system was frustrated as unidentifiable product mixtures had formed in each case (Scheme 5.5).[144]

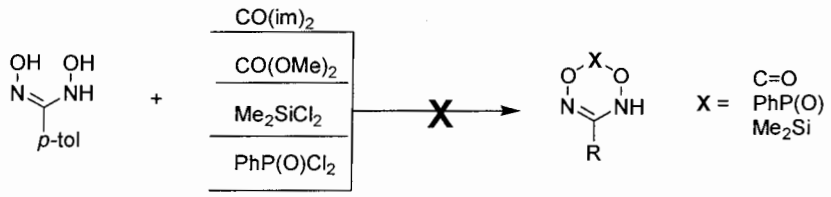

Scheme 5.5. Attempted syntheses of various 6-substituted dioxadiazines.

Desherces *et al.* reported on the cyclization reactions of oxyamidoximes with aldehydes; however, in all instances, *N*-hydroxy-1,2,4-oxadiazolines (**5.15** – **5.16**) were formed (Scheme 5.6).[146] Similarly, Patenaude isolated **5.17** and **5.18** while attempting to condense **5.12** with either *p*-tolualdehyde or propionaldehyde in the presence of catalytic

acid. Presumably the 5-membered ring forms by attack of the NH group on intermediate **5.14** (Scheme 5.6).[144]

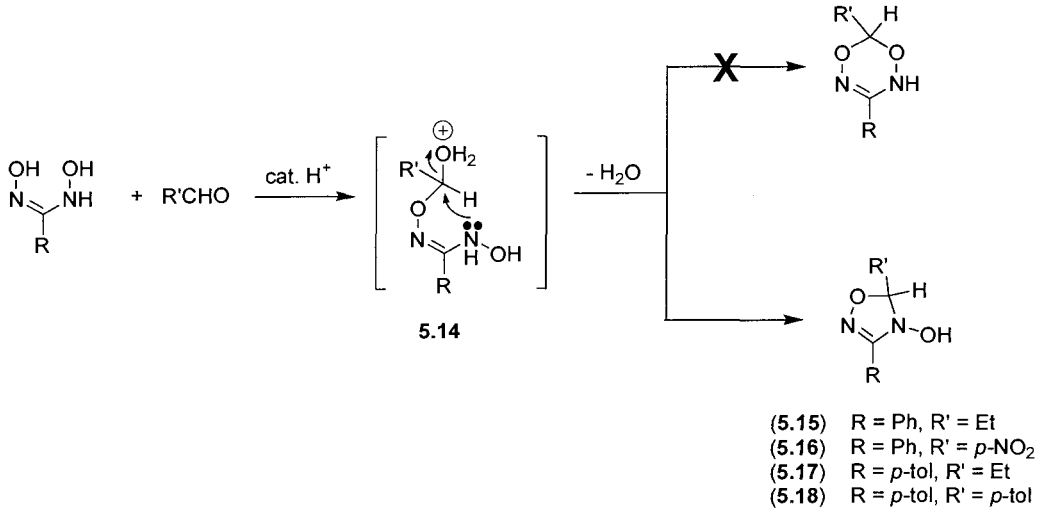

Scheme 5.6. Formation of the 5-membered ring *N*-hydroxy-1,2,4-oxadiazolines (**5.15** - **5.18**).

5.3 Results and Discussion

5.3.1 Synthetic Strategy II – Condensation Reactions of Functionalized Chloroximes

In 1993, Neugebauer and co-workers developed a route to 6-oxo and 6-thioxoverdazyl radicals (Scheme 5.7).[121] The reaction of hydrazones **5.19** with phosgene or thiophosgene gave the corresponding carbamoyl chlorides **5.20**. Ring closure is achieved by treating **5.20** with either alkyl or aryl hydrazines in the presence of an

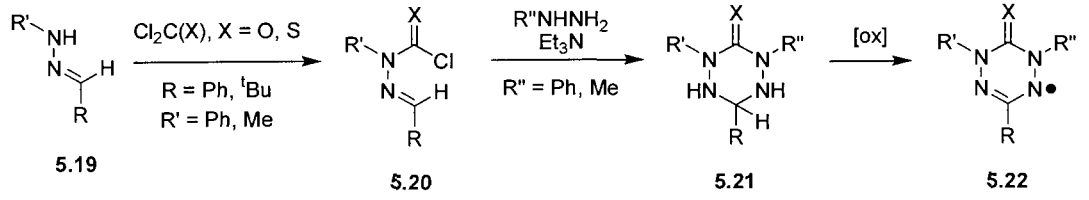

Scheme 5.7. Neugebauer's synthesis of 6-oxo and 6-thioxoverdazyl radicals.

auxiliary base to afford the tetrazanes (**5.21**). Conversion of **5.21** to verdazyl radicals **5.22** is then effected by oxidation.

In light of the difficulties encountered during attempts to synthesize the dioxadiazine ring system by Strategy I, an alternative synthetic pathway, which closely resembles Neugebauer's oxoverdazyl synthesis, has been devised. A retrosynthetic analysis suggests that the target dioxadiazine ring structure, with a silicon group in the 6-position, might be directly accessible by ring-closure of a dihalogenated intermediate **E** with hydroxylamine (Scheme 5.8). It was anticipated that **E** could be prepared directly by chlorinating the Si-H group of **D**. Compound **D** itself could be formed by either selective halogenation of **B** at the imine C-H group, or by reacting chloroxime **C** with a dialkylchlorosilane (e.g., R'_2SiHCl). Direct *O*-silylation of oxime **A** with R'_2SiHCl should give hydrosilane **B**. It is also worth noting that dichlorination of **B** might proceed directly to compound **E** in a one-pot procedure.

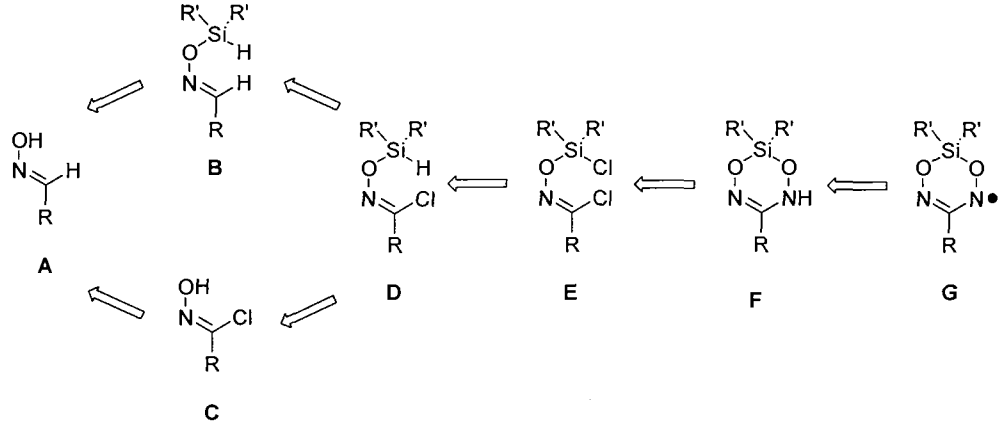

Scheme 5.8. Retrosynthetic analysis of the 6-siladioxadiazinyl radical **G**.

As a first step, the functionalization of *p*-tolualdehyde oxime with simple chlorosilane reagents was tested. Thus, treatment of oxime **5.9** with chlorotrimethylsilane in the presence of triethylamine and 4-(dimethylamino)-pyridine in CH_2Cl_2 furnished the silylated oxime **5.23** in 68% (Scheme 5.9). Oxime **5.9** could also be silylated with chlorodimethylsilane in Et_2O to give the required hydrosilane **5.24** in 87%. Since the latter compound is of the type **B** in the retrosynthetic scheme, the next step was to prepare **D**. Although oximes themselves can be easily chlorinated at room temperature,[147] no reaction between NCS and *O*-silyloxime **5.23** was observed in chloroform or DMF, even at elevated temperatures. No attempts were made to chlorinate the hydrosilane (**5.24**) because (a) it was anticipated that its C-H group would also be non-reactive towards NCS, and (b) a successful synthesis of **D** was independently discovered by way of intermediate **C** (see below).

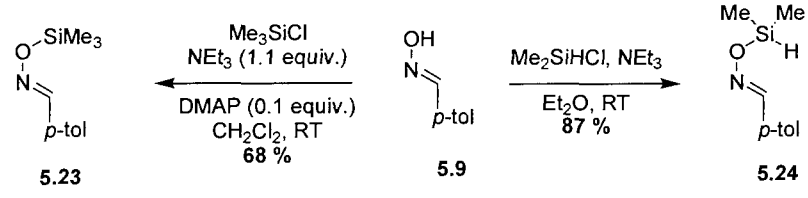

Scheme 5.9. Syntheses of *O*-silylated oximes **5.23** and **5.24**.

Instead of functionalizing the C-H group after the *O*-silylation (i.e., **B**→**D**), the silylation of a chloroxime was alternatively investigated. Thus, treatment of a chloroxime with a chlorosilane in the presence of an auxiliary base would be expected to give **5.25** (Scheme 5.10). Under these conditions, however, direct *O*-silylation probably does not occur, but rather the silylation proceeds via the formation of an intermediate nitrile oxide.

The nitrile oxide is rapidly formed by the action of base on the chloroxime. Regardless of the silylation pathway, the outcome remains the same as long as chlorosilanes are used in conjunction with chloroximes.

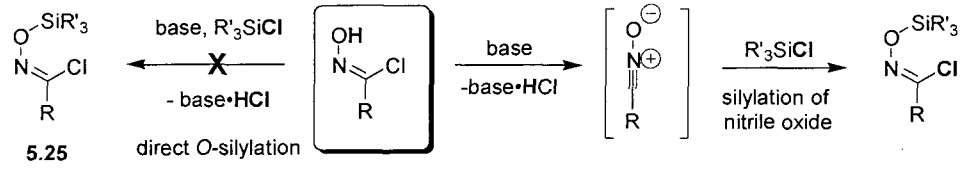

Scheme 5.10. Direct *O*-silylation versus silylation of a nitrile oxide.

Reactions of alkyl or aryl nitrile oxides with silanes are not unknown, but in most instances careful conditions are required such that competing dimerization to furoxans is avoided. Alkyl nitrile oxides are particularly prone to dimerization; for instance, acetonitrile oxide has been reported to exist for less than one minute at 18 °C.[148] Cunico *et al.* have shown that the cycloreversion of dimethylfuroxan by flash vacuum pyrolysis (630 °C, 0.05 mmHg) provides acetonitrile oxide, which can be subsequently condensed at -78 °C and allowed to react with a wide range of silanes at -25 °C in Et_2O (Scheme 5.11).[149] Aryl nitrile oxides have considerably longer lifetimes (minutes to several days) than their alkyl counterparts, but are still subject to dimerization.[150] Nevertheless, Cunico

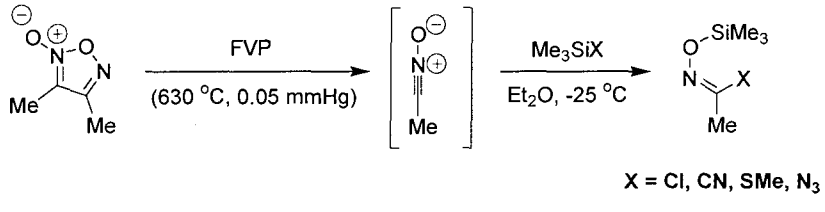

Scheme 5.11. Silylation of acetonitrile oxide.

reported that *O*-(trimethylsilyl)benzohydroxamoyl chloride **5.26** could be prepared from chlorotrimethylsilane and benzonitrile oxide, but the publication lacked specific experimental details (Scheme 5.12).[151]

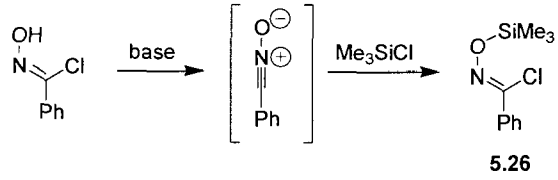

5.26

Scheme 5.12. Silylation of benzonitrile oxide.

The *p*-tolyl substituted nitrile oxide was used in subsequent chemistry because its rate of dimerization (5 – 7 days) is substantially slower than that of benzonitrile oxide (30 – 60 minutes).[152] The dehydrochlorination of **5.10** was achieved by treatment with triethylamine in Et_2O, and the resulting nitrile oxide (**5.11**) was quenched with a slight excess of chlorotrimethylsilane (Scheme 5.13). Removal of the salt byproducts by filtration and concentration of the filtrate provided the desired product in almost pure form. The crude product can then be vacuum distilled to give an analytically pure sample of **5.27** in 85%. The proton decoupled ^{29}Si NMR in CD_2Cl_2 of **5.27** shows a single resonance at 29.34 ppm. In a similar manner, nitrile oxide **5.11** could be trapped with chlorodimethylsilane to afford the hydrosilane **5.28** in 84% after distillation. The ^1H NMR spectrum of **5.28** is shown in Figure 5.2. The most important feature is the 6H doublet at 0.42 ppm, resulting from the coupling ($^3J_{HH}$ = 3 Hz) of the methyl hydrogen atoms to the hydrogen atom directly attached to silicon. The corresponding 1H septet ($^3J_{HH}$ = 3 Hz) is observed at 4.88 ppm. All other peaks are consistent with the proposed

structure. Compound **5.28** is of the form **D** in our retrosynthetic analysis, and so the next step was to perform the conversion to the dihalogenated derivative **E**.

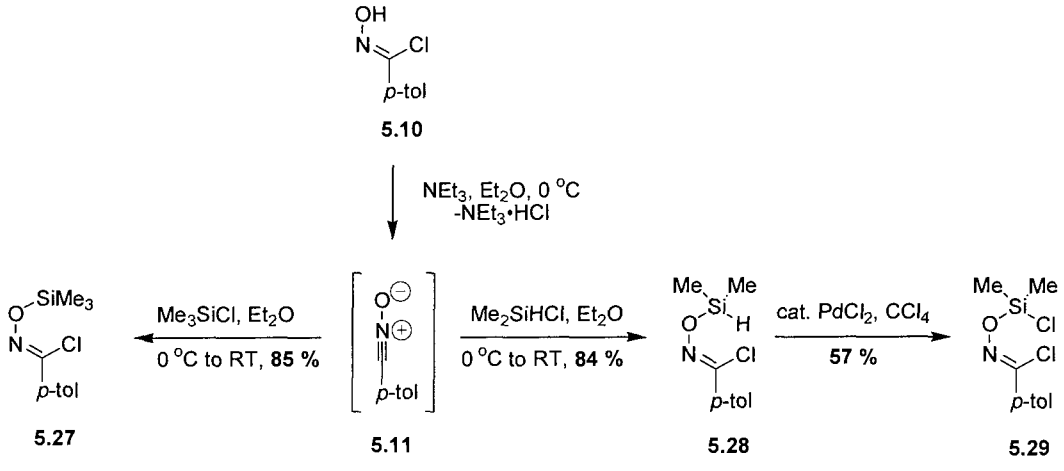

Scheme 5.13. Syntheses of *O*-silylated chloroximes (**5.27** and **5.28**) and chlorosilane **5.29**.

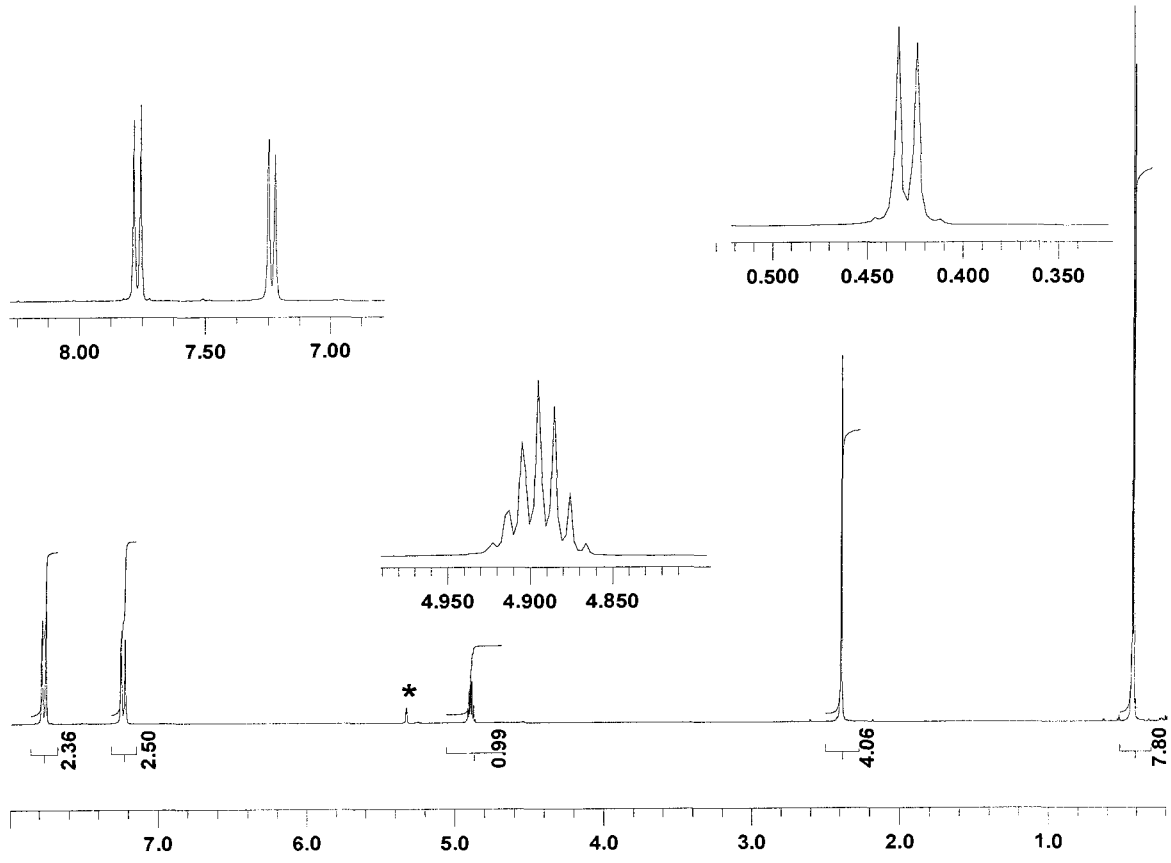

Figure 5.2. ^{1}H NMR spectrum of **5.28** in CD_2Cl_2. The peak with an asterisk is due to $CHDCl_2$.

Catalytic palladium dichloride in carbon tetrachloride was used to chlorinate hydrosilane **5.28** (Scheme 5.13). The chlorosilane **5.29** could be obtained in 57% as a clear and colorless oil after distillation. The ^{1}H NMR of **5.29** is shown in Figure 5.3. The most notable feature is the loss of the doublet and septet from the starting hydrosilane, and the onset of a 6H singlet centered at 0.69 ppm for the chlorosilane.

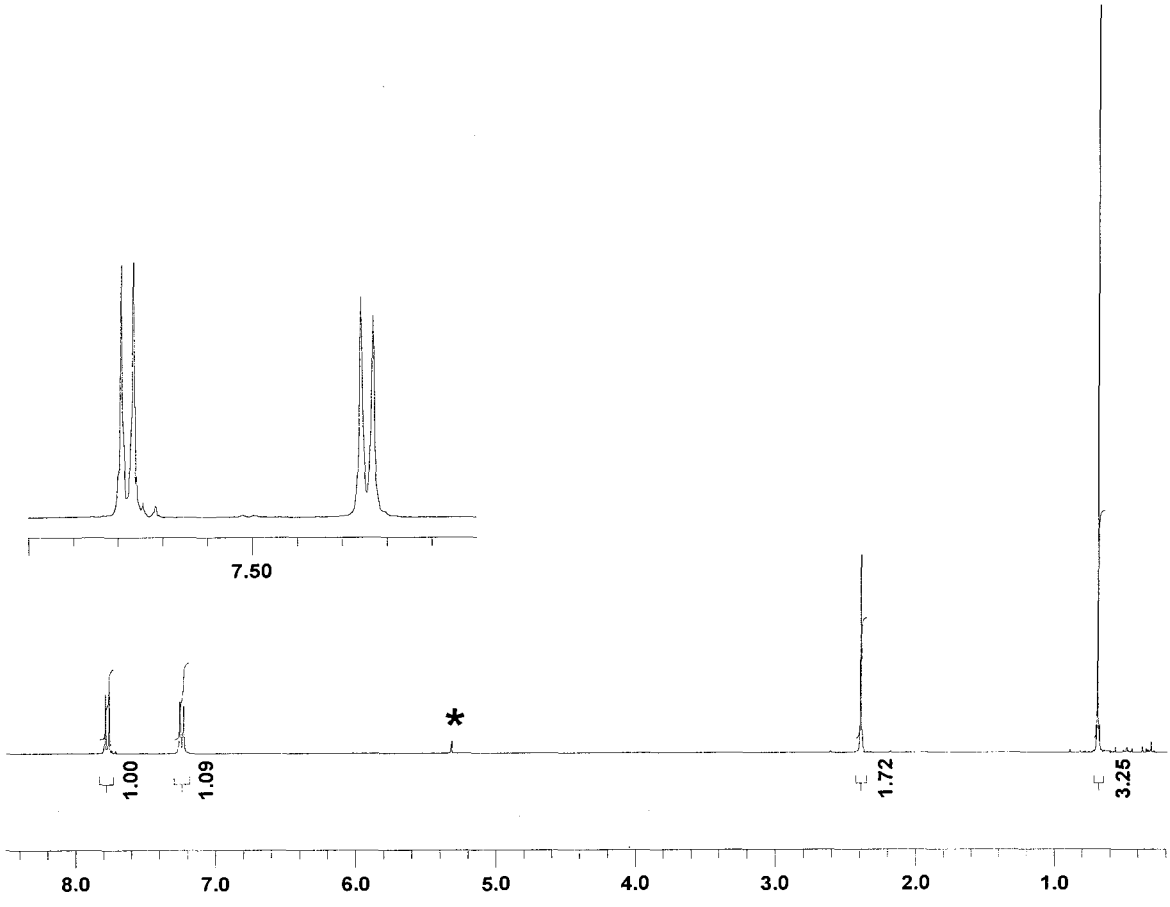

Figure 5.3. ^{1}H NMR spectrum of **5.29** in CD_2Cl_2. The peak with an asterisk is due to $CHDCl_2$.

The next step was to perform the ring closure to dioxadiazine **F** via the dihalogenated precursor **E**. Based on the oxophilic nature of silicon, it is anticipated that the reaction of silylated chloroxime **5.29** with free hydroxylamine will give the Si-O isomer **5.31** rather than the Si-N isomer **5.30** (Scheme 5.14). Most other examples of analogues reactions have shown that chlorosilanes react preferentially with hydroxylamine to provide the Si-O bound isomer.[153] For example, it has been shown that *O*-trimethylsilyl hydroxylamine can be prepared by the mono-silylation of hydroxylamine with one equivalent of chlorotrimethylsilane in dichloromethane.[154]

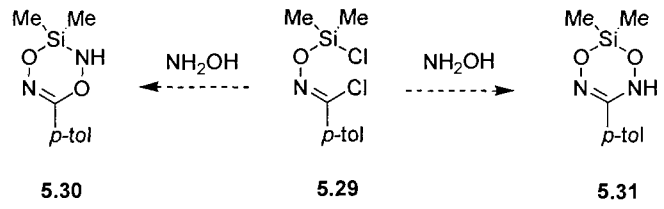

5.30 **5.29** **5.31**

Scheme 5.14. Possible outcomes for the reaction of **5.29** with hydroxylamine.

Due to the fact that neat hydroxylamine is known to decompose at room temperature and that it has been reported to explode at elevated temperatures,[155] it was alternatively prepared *in situ* by the dehydrochlorination of hydroxylamine hydrochloride with triethylamine in THF. Silylated chloroxime **5.29** was then allowed to react with an equivalent of free hydroxylamine and two equivalents of triethylamine in THF for 24 hours at room temperature (Scheme 5.15). Surprisingly, the major product formed was the known *p*-tolyl substituted oxyamidoxime **5.12**. Compound **5.12** could also be

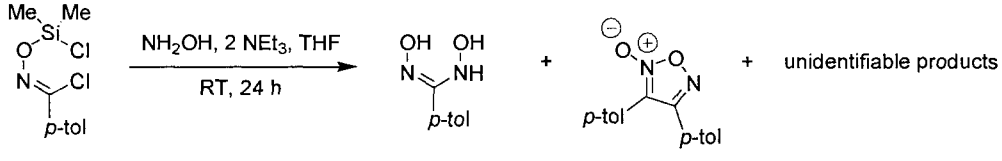

5.29 **5.12** (67%) **5.13** (11%)

Scheme 5.15. Reaction of **5.29** with hydroxylamine to give **5.12** and **5.13**.

generated by subjecting **5.27** to an analogous reaction with hydroxylamine (Scheme 5.16), suggesting that the chlorine attached to silicon in **5.29** is not required for the desilylation.

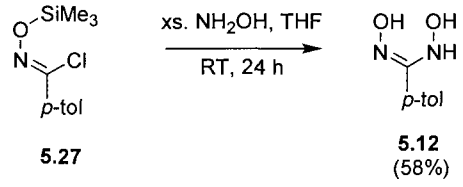

Scheme 5.16. Reaction of **5.27** with hydroxylamine to give oxyamidoxime **5.12**.

One possibility is that compound **5.12** is formed according to Scheme 5.17. The first step could involve addition of hydroxylamine at the imine carbon, followed by subsequent elimination of chloride ion. The chloride ion could then attack silicon, resulting in the loss of chlorotrimethylsilane or dichlorodimethylsilane. It does, however, seem counterintuitive that chloride ion can cleave an exceptionally strong silicon-oxygen (452 kJ mol^{-1}) bond. Closer examination of the crude product mixture from Scheme 5.15

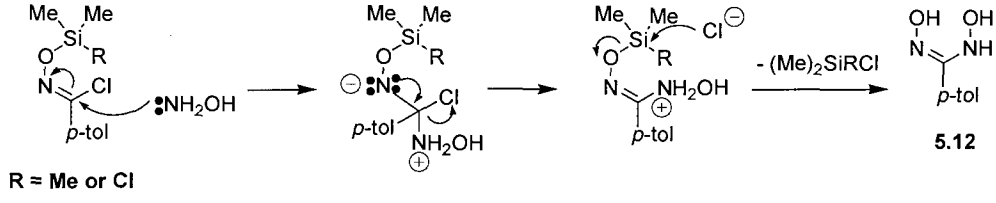

Scheme 5.17. One possible mechanism for the formation of **5.12**.

revealed that furoxan **5.13** had also formed. Therefore, it seems more likely that **5.12** is forming via nitrile oxide **5.11** (Scheme 5.18), rather than the initially suggested mechanism. The first step might involve the loss of the silicon group upon interaction of **5.27** or **5.29** with base to yield oxime **5.10** (Scheme 5.18). The base initiated

dehydrochlorination of **5.10** would provide the necessary nitrile oxide. Compounds **5.12** and **5.13** would then form analogously to Scheme 5.4.

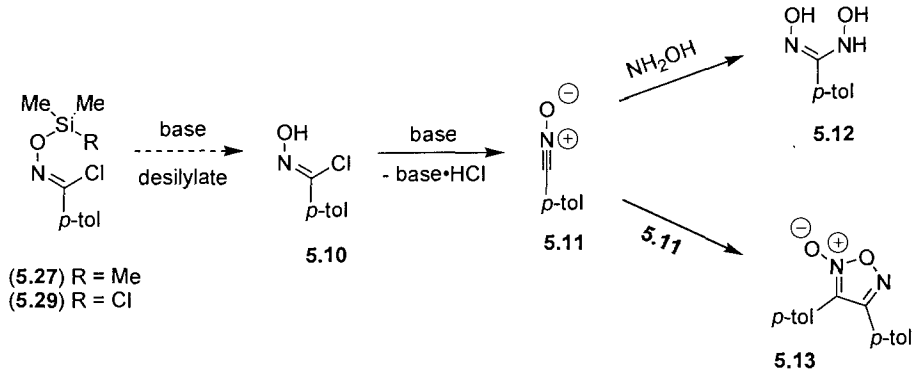

Scheme 5.18. Alternative pathway to oxyamidoxime **5.12** and furoxan **5.13**.

Silyloxime **5.23** and an excess of hydroxylamine were combined in THF and stirred at room temperature for 24 hours (Scheme 5.19). No reaction was observed, signifying that hydroxylamine is not a general desilylating reagent, and that a chlorine group must be attached to the imine carbon of an *O*-silylated oxime for the desilylation to occur.

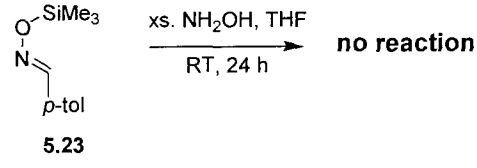

Scheme 5.19. Attempted reaction of silyloxime **5.23** with excess hydroxylamine.

Although a clear understanding as to why hydroxylamine initiates the desilylation of **5.27** and **5.29** is lacking, the protection of silicon with bulky substituents might help to suppress this undesirable reaction. Thus, the targeted compound is of the form **E** in the retrosynthetic analysis (Scheme 5.8) with R = *p*-tolyl and R' = *tert*-butyl. Unfortunately, the synthesis of the necessary precursor **5.32** failed by the standard method (Scheme 5.20). It is believed that the silane is too bulky to react with the nitrile oxide. The only product formed was furoxan **5.13** as evidenced by ^{1}H NMR spectroscopy.

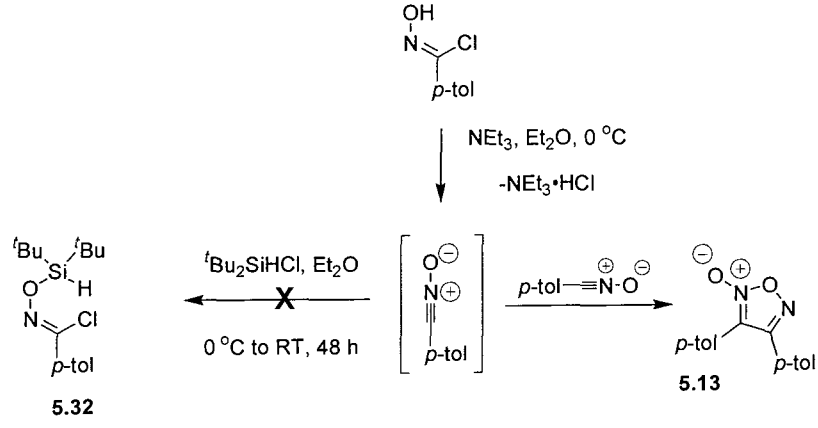

Scheme 5.20. Attempted synthesis of a bulky silylated chloroxime **5.32**.

5.3.2 *Synthetic Strategy III – Condensation Reactions of Bis(hydroxylamino) Compounds*

In 1980, Neugebauer *et al.* found that 6-oxoverdazyl radicals **5.35** could alternatively be prepared by oxidation of tetrazanes **5.34** (Scheme 5.21).[156] Reaction of four equivalents of methylhydrazine with phosgene gas at low temperature gives 2,4-dimethylcarbohydrazide (**5.33**). The tetrazanes (**5.34**) are then prepared by the condensation of **5.33** with aldehydes. This strategy allows for functionality at the 3-position of the tetrazane ring system by treating the intermediate hydrazides with appropriate electrophiles.

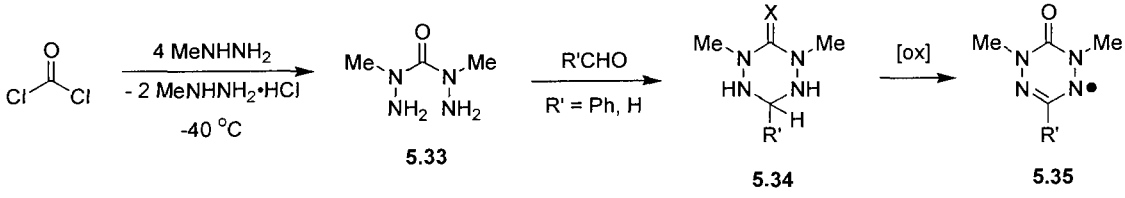

Scheme 5.21. Alternative synthesis of 6-oxoverdazyl radicals (**5.35**).

Using an approach similar to the one outlined in Scheme 5.21, preparation of the analogous dioxadiazane ring system **5.37** by condensation reactions of various bis(hydroxylamino) (**5.36**) derivatives with aldehydes was envisioned (Scheme 5.22).

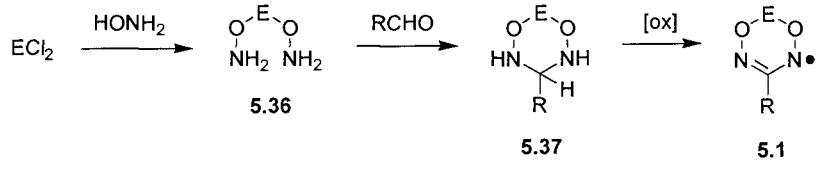

Scheme 5.22. Condensations of **5.36** with aldehydes to dioxadiazanes **5.37**.

The dioxadiazinyl radicals could then, in principle, be prepared by oxidations of **5.37**. A few examples of mono(*O*-hydroxylamines) (**5.38**) have appeared in the literature, and are typically prepared by reactions of hydroxylamine with main group substrates (E-Cl; E = P or Si) (Scheme 5.23).[157] In the case of phosphorus, *O*-(diphenylphosphinyl)-hydroxylamine ($Ph_2P(O)ONH_2$) has been extensively used as a powerful aminating reagent to a wide range of nucleophiles (nu:).[158] However, in the presence of carbonyl containing compounds, such as ketones or aldehydes, mono(*O*-hydroxylamines) condense to give oximes **5.39**.[159]

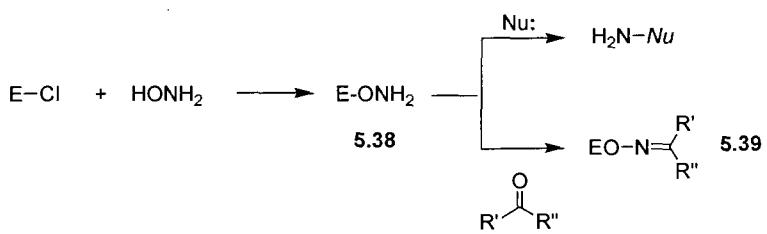

Scheme 5.23. Reaction of mono(*O*-hydroxylamines) (**5.38**) with nucleophiles or carbonyl compounds.

Recently, Klingebiel and co-workers reported the synthesis of a stable *O,O'*-bis(hydroxylamino)silane **5.40** (Scheme 5.24).[160] Compound **5.40** should serve as an intermediate to a 6-siladioxadiazinyl radical by analogy to Scheme 5.22. Unfortunately, we have been unable to reproduce the synthesis of **5.40** by the literature protocol or by

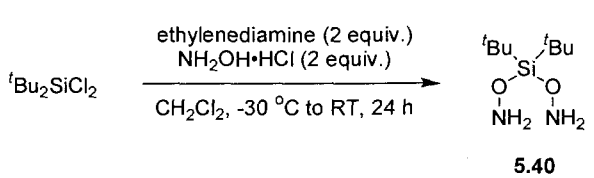

Scheme 5.24. Literature synthesis of $^tBu_2Si(ONH_2)_2$ (**5.40**).

modifications of it. According to the literature procedure, the first step involves the dehydrochlorination of hydroxylamine hydrochloride by using ethylenediamine as the acceptor base. This results in the formation of hydroxylamine, which is then allowed to react with di-*tert*-butyldichlorosilane at -30 °C. The mixture was then warmed to room temperature and stirred overnight. After removal of the insoluble salt byproducts, the authors claim that "compound [**5.40**] was isolated as crystals at room temperature." It seemed puzzling that no specific details were given on how the compound was actually crystallized. All attempts to crystallize the crude product from various solvents failed, but later it was found that a white semicrystalline material could be obtained by vacuum sublimation at room temperature. However, all of the spectral data obtained for either the crude or sublimed materials were found to be inconsistent with those reported in the literature for **5.40**. Most striking is that the sublimed material has its melting point at 148 °C, whereas literature compound **5.40** melts at 66 °C. In addition, the ^{1}H NMR of our material in C_6D_6 lacks the expected NH_2 resonance at 4.81 ppm, and also no signal is observed in the ^{15}N NMR, providing evidence that the hydroxylamino groups are absent. Regardless as to whether the reaction is performed according to the literature procedure in CH_2Cl_2 with ethylenediamine or in THF with triethylamine as base, the isolated material is qualitatively the same. The challenges associated with repeating the literature synthesis of **5.40**, and our inability to assign a structure using the spectral data obtained for our isolated product(s), has forced this chemistry to be abandoned.

To the best of our knowledge, the only other bis(hydroxylamino) compound that exists in the literature is *O,O'*-bis(hydroxylamino)methane **5.43**. Reaction of the sodium salt of ethyl acetohydroximate with methylene iodide gives the *N*-protected *O,O'*-bis(ethylacethydroximate)methane **5.41** (Scheme 5.25).[161] Deprotection is then achieved by acid hydrolysis of **5.41**, resulting in the formation of the bis(hydrochloride) salt **5.42**.[162] Although **5.42** has been converted to its freebase form **5.43**, isolation of the latter compound in its pure form was avoided because it is known to be shock sensitive with a tendency to explode (in fact **5.43** was developed by the United States of America Air Force to be used as an oxidizing agent for rocket fuels).[162]

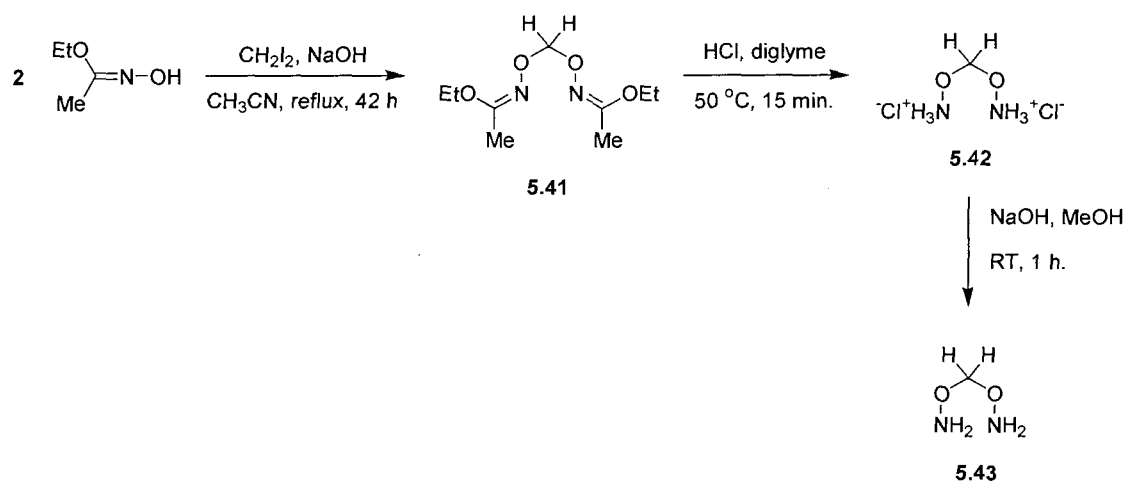

Scheme 5.25. Synthesis of methylene dioxyamine **5.43**.

It was found that **5.43** could alternatively be generated *in-situ* by treating **5.42** with triethylamine in methanol. Intermediate **5.43** was then subjected to reactions with aldehydes for the purpose of making 3-substituted dioxadiazanes. When a dilute methanol solution of *p*-tolualdehyde is slowly added to a concentrated solution of **5.43** and allowed to reflux for 15 hours, the only product isolated is bis(imine) **5.44** (Scheme

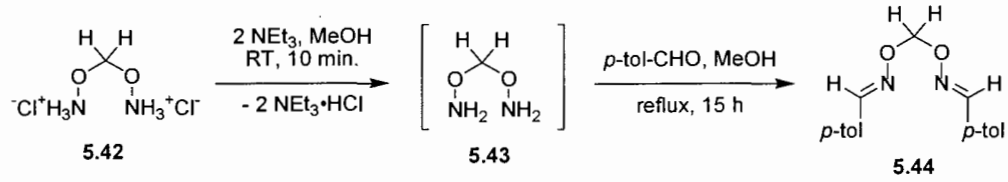

5.42 5.43 5.44

Scheme 5.26. Condensation of methylene dioxyamine (**5.43**) with *p*-tolualdehyde.

5.26). This was not entirely surprising, as the analogous bis(hydrazides) are also prone to bis(imine) formation when reacted with aldehydes. For example, Patenaude found that the reaction of **5.45** with benzaldehyde gave bis(imine) **5.46** exclusively (Scheme 5.27).[144] Attention was then directed to aldehydes that contain strongly electron-

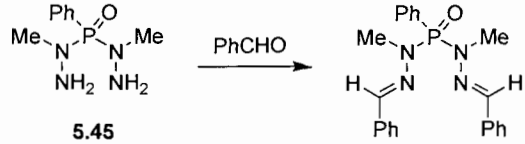

5.45 5.46

Scheme 5.27. Condensation of **5.45** with benzaldehyde to give bis(imine) **5.46**.

withdrawing groups (EWGs). This type of substitution should make the imine carbon of intermediate **5.47** more electrophilic, thereby facilitating the attack of the NH_2 group (Scheme 5.28).

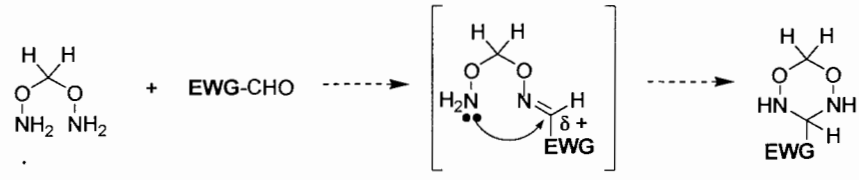

5.47

Scheme 5.28. Proposed synthesis of dioxadiazanes using electron-withdrawing aldehydes.

Given our group's previous success in preparing pyridyl substituted tetrazanes,[163] an attempt to condense **5.43** with 2-pyridinecarboxaldehyde was made (Scheme 5.29). In this case, the targeted dioxadiazane **5.48** was not formed, but rather a mixture of bis(imine) **5.49** and mono(imine) **5.50**. The two compounds could be isolated by

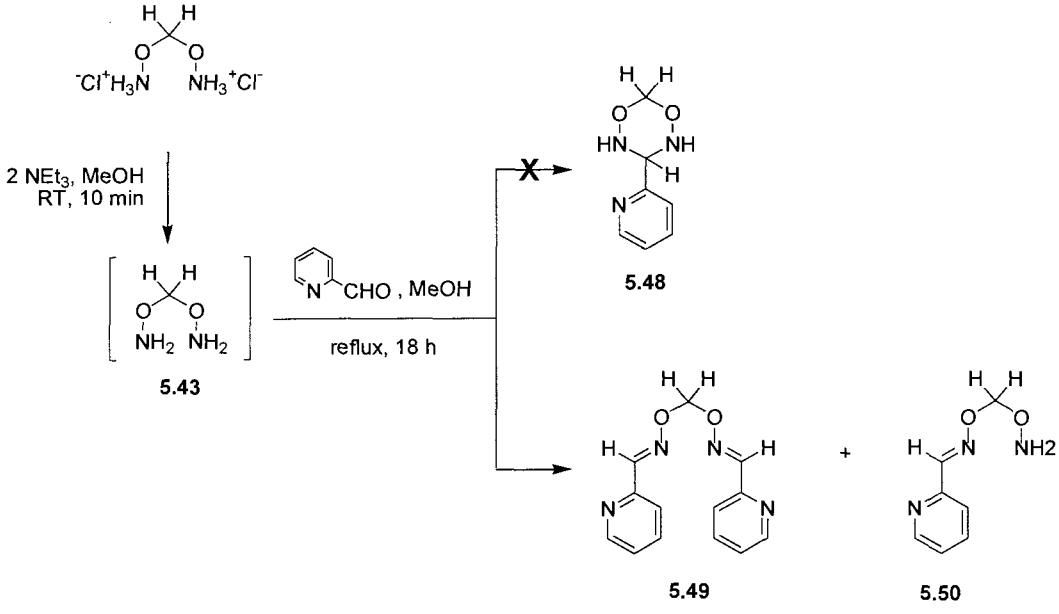

Scheme 5.29. Condensation of **5.43** with 2-pyridinecarboxaldehyde.

separation on a basic alumina column. The ^{1}H NMR spectra for **5.49** and **5.50** are presented in Figures 5.4 and 5.5, respectively. The only notable difference between the spectra of **5.49** and **5.50**, is that the latter exhibits an amine (NH_2) resonance at 5.69 ppm. Unexpectedly, intramolecular ring-closure to **5.48** did not occur, despite the fact that the necessary precursor **5.50** is forming in the reaction mixture. NMR scale reactions of neat **5.50** in either CD_3OD, DMSO, or d_8-toluene were subsequently performed with intent to effect the ring-closure to **5.48**. In all cases however, **5.50** remained unchanged even after refluxing for 72 hours. Nevertheless, compound **5.50** could be isolated pure and does

remain a potentially important intermediate to a pyridyl substituted dioxadiazane ring system.

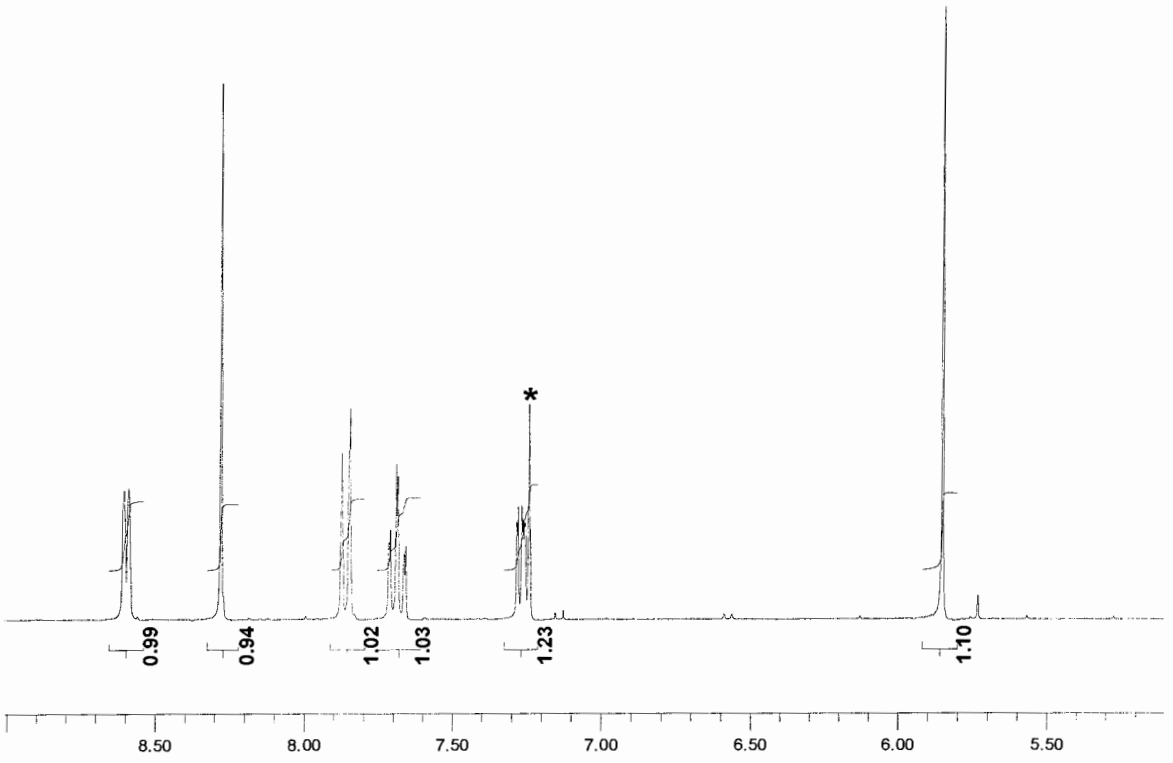

Figure 5.4. ^{1}H NMR spectrum of bis(imine) **5.49** in $CDCl_3$. The peak with an asterisk is due to $CHCl_3$.

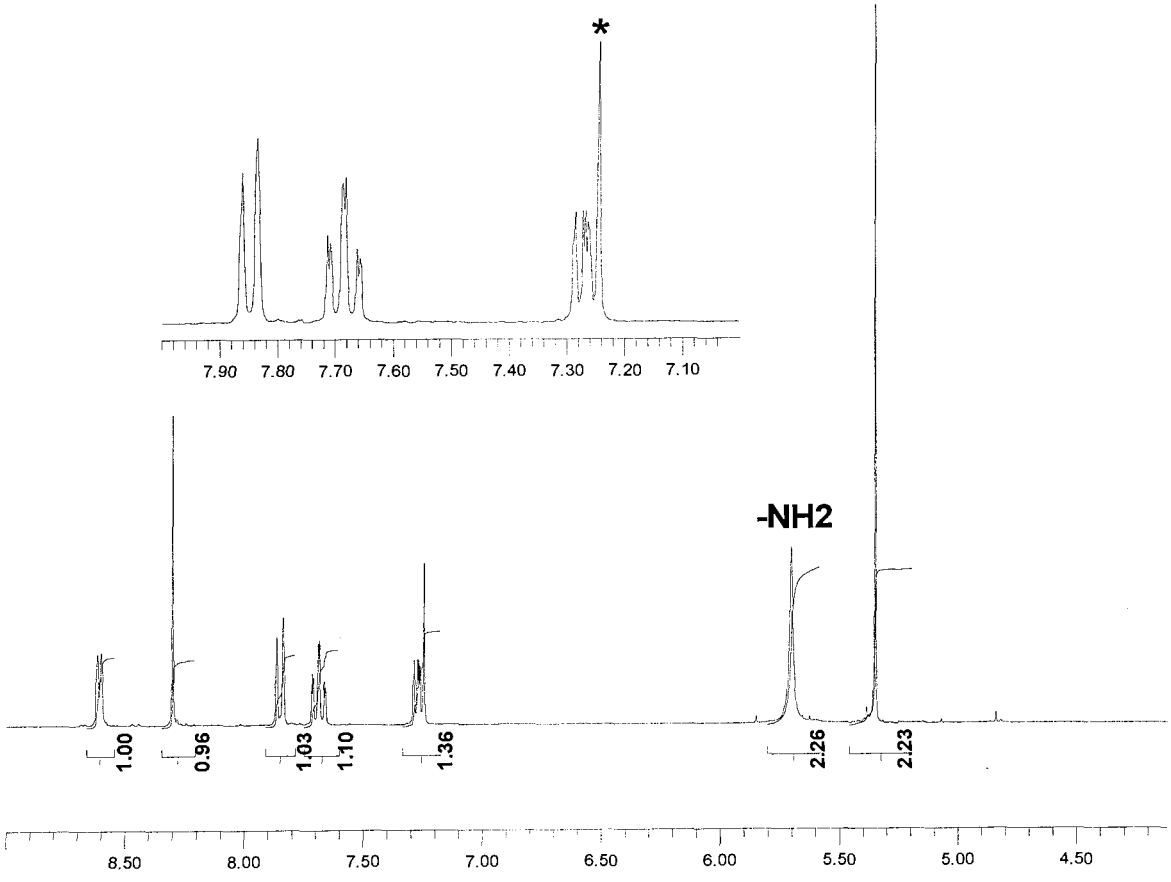

Figure 5.5. ^{1}H NMR spectrum of mono(imine) **5.50** in $CDCl_3$. The peak with an asterisk is due to $CHCl_3$.

5.4 Conclusions and General Remarks for Part II

The main objective for the second part of this thesis was to prepare a new series of various 3- and 6-substituted dioxadiazinyl radicals, which are expected to show good stability by analogy to verdazyls. Two synthetic pathways were explored.

Given Neugebauer's success with preparing tetrazanes **5.21** by ring-closure reactions of carbamoyl chlorides with substituted hydrazines, a similar approach to dioxadiazines was implemented. Thus, *O*-silylated chloroxime **5.29** was prepared and its reactions with hydroxylamine were studied. Interestingly, the targeted 6-siladioxadiazine was not formed, but rather *N*-hydroxy-*p*-toluamidoxime **5.12** was isolated as the major product. It is believed that **5.12** is being formed via nitrile oxide **5.11**, because small amounts of another product that is also known to form from this intermediate can be isolated, namely di-*p*-tolylfuroxan **5.13**. The exact details for how the nitrile oxide is being generated from the starting *O*-silylated chloroxime **5.29** remain unclear, and additional experiments will be required to resolve this.

Another method for preparing verdazyl radicals is by oxidation of tetrazanes. It was described earlier that tetrazanes themselves can be readily made by condensations of bis(hydrazides) with aldehydes. By analogy, reactions of bis(hydroxylamino) substrates with aldehydes should afford dioxadiazanes. Although *O,O'*-bis(hydroxylamino)silane **5.40** has been reported to exist, attempts to replicate its synthesis by the literature procedure, or by modifications of it, failed. This compound would have been useful as an intermediate to various 3-substituted 6-siladioxadiazinyl radicals; however, the difficulties associated with preparing **5.40** denied the possibility for this chemistry to be further explored. Fortunately, the synthesis of *O,O'*-bis(hydroxylamino)methane **5.43**

works remarkably well, and so the chemistry of this intermediate with several aldehydes was investigated. The only product obtained from the condensation of **5.43** with *p*-tolualdehyde was bis(imine) **5.44**. Attention was then directed at using a more electron-deficient aldehyde, namely 2-pyridinecarboxaldehyde, which should render the imine-carbon of **5.47** more electrophilic, thereby facilitating the nucleophilic attack of the pendant amine group (Scheme 5.28). In this experiment the desired 3-pyridyl substituted dioxadiazane ring system was not formed, but rather a mixture of bis(imine) **5.49** and mono(imine) **5.50**. The latter compound is interesting because it still remains a useful intermediate to dioxadiazane **5.48**. Solution NMR scale experiments have been performed in attempts to thermally induce the intramolecular cyclization of **5.50** to **5.48**, but in all cases the starting substrate remained unchanged. Indirect strategies will need to be developed and explored for the synthesis of **5.48**, some of which are described in the section to follow.

5.5 Future Directions for Part II

This chapter has shown that the designed synthesis of stable radicals, and even their precursor molecules, can be challenging. The synthesis of a dioxadiazine (radical or otherwise) ring system was unsuccessful, but it is important to stress that some interesting and fundamental science has been revealed during these attempts. These fundamental results should provide a benchmark to those who wish to further embark on this chemistry. Based on all of the observations from this chapter, it is felt that these alternative avenues (vide infra) to the dioxadiazinyl radical hold some promise.

N-protected hydroxylamines have proven to be valuable precursors for the selective preparation of *O*-substituted hydroxylamines. This strategy was applied to the successful synthesis of **5.43** via the deprotection of methylene-*O,O'*-bis(ethylacethydroximate) **5.41**. In this vein, the analogous silicon derivative **5.51** has been prepared, but its deprotection chemistry has yet to be explored (Scheme 5.30). Other carbon and phosphorus derivatives are also possible by treating ethyl acetohydroximate

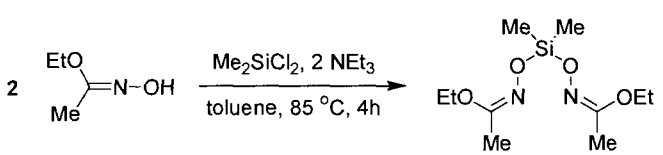

5.51

Scheme 5.30. Synthesis of dimethyl-*O,O'*-bis(ethylacethydroximate)silane **5.51**.

with appropriate electrophiles (e.g., R_3PCl_2, $RP(O)Cl_2$, $Cl_2C(O)$, triphosgene, etc.) (Scheme 5.31). Deprotection and subsequent freebasing of **5.52** to **5.54** should afford the *O,O'*-bis(hydroxylamino) compounds **5.36**. The resulting bis(hydroxylamino) compounds with varying main group element linkers might exhibit different reactivity

towards aldehydes than *O,O'*-bis(hydroxylamino)methane **5.43**. These changes may facilitate the ring-closure to the targeted dioxadiazane ring structure (Scheme 5.31).

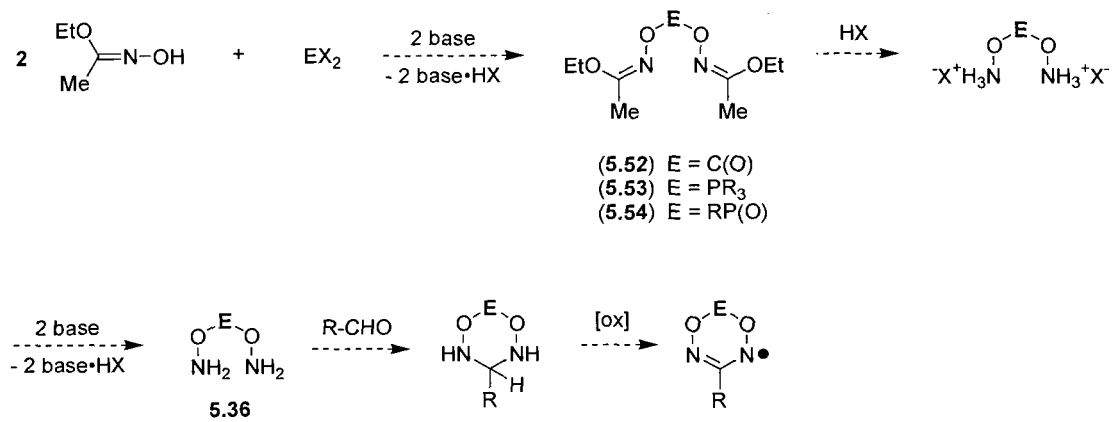

Scheme 5.31. Proposed syntheses of other substituted *O,O'*-bis(hydroxylamino) compounds (**5.36**) and their condensation reactions with aldehydes.

The closest we have come to a dioxadiazane ring structure is compound **5.50**. Since all of the direct routes to the O_2N_2CE ring system have not yet been successful, other indirect ones should be explored. One possibility here is to place a halogen group at the imine carbon, which may facilitate the nucleophilic attack of the amine group (Scheme 5.32). Subsequent ring-closure of either **5.55** or **5.56** might afford the dioxadiazinyl radical precursor **5.57**. Pyridyl substituted dioxadiazinyl radicals (**5.58**) are particularly exciting because they offer the potential to be used as ligands for metal complexes, much like the coordination chemistry of verdazyls.[164]

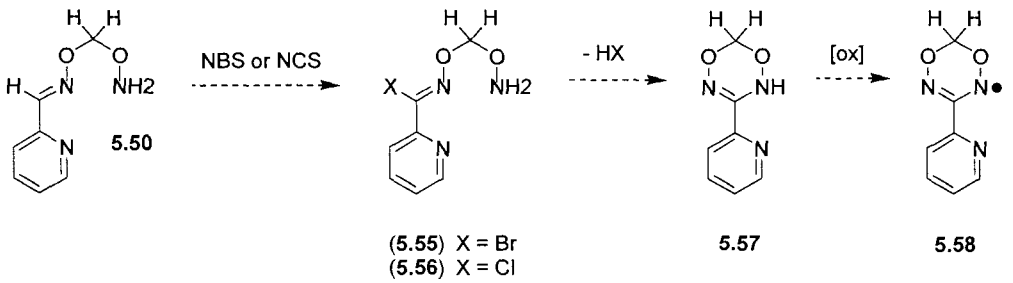

Scheme 5.32. Proposed halogenation of **5.50**, followed by ring-closure to **5.57**.

5.6 Experimental Section

General Experimental

General experimental details can be found in §2.4. Experimental details that are unique to this chapter are described below.

$^{29}Si\{^{1}H\}$ NMR spectra were recorded on a Bruker AMX 360 instrument (71.55 MHz) and are referenced relative to tetramethylsilane. Infrared spectra were recorded as Nujol mulls on KBr plates or as KBr pressed pellets by using a Perkin Elmer One FT-IR spectrometer.

Carbon tetrachloride was distilled over phosphorus pentoxide. All reagents were purchased from Aldrich and used as received except as otherwise stated. Triethylamine was distilled over calcium hydride and hydroxylamine hydrochloride was dried under vacuum for 24 h prior to use.

***p*-Tolualdehyde oxime (5.9).** This compound was prepared by the literature route.[147] To a mixture of *p*-tolualdehyde (59 mL, 0.5 mol) in 300 mL of ice-water and 125 mL of ethanol was added hydroxylamine hydrochloride (42 g, 0.6 mol) in one portion. To this was slowly added 12.5 M NaOH (100 mL) as to not allow the reaction mixture temperature to exceed 30 °C. The addition of base took approximately 1 h. After the addition, the mixture was stirred for a further 1 h at room temperature. The mixture was then extracted with Et_2O (2 x 250 mL) to remove any neutral impurities, and the remaining aqueous phase was made acidic by the slow addition of concentrated hydrochloric acid (70 mL). Ice was added to the mixture during the acidification to ensure the internal temperature did not exceed 30 °C. The aqueous phase was then

extracted with Et_2O (3 x 250 mL), and the combined organic extracts were dried over anhydrous calcium sulfate. After filtration of the drying agent, the solvent was removed from the filtrate by rotary evaporation to leave a white crystalline solid of *p*-tolualdehyde oxime, yield 51 g (75 %). ^{1}H NMR (CD_2Cl_2): δ 8.19 (s, 1H), 7.42 (d, J = 8 Hz, 2H), 7.15 (d, J = 8 Hz, 2H), 2.38 (s, 3H). This compound was used without further purification.

***p*-Tolualdehyde chloroxime (5.10).** Prepared by a modification of the literature method.[147] *p*-Tolualdehyde oxime (8.1 g, 60.0 mmol) was dissolved in anhydrous DMF (100 mL) and a large excess of NCS (12.0 g, 90.0 mmol) in DMF (60 mL) was added rapidly via syringe. The resulting pale yellow solution was stirred at room temperature for 24 h. The mixture was poured into water (200 mL) and this was extracted with Et_2O (3 x 60 mL). The combined organic extracts were washed with water (3 x 100 mL) to remove any remaining DMF and then dried over anhydrous sodium sulfate. After filtration of the drying agent, the solvent was removed from the filtrate by rotary evaporation to leave a pale yellow solid. This solid was suspended in pentane (50 mL) to remove the colored impurities. The solid was filtered and washed with cold pentane (3 x 15 mL) to provide the title compound as a white solid, yield 7.4 g (73 %). ^{1}H NMR ($CDCl_3$): δ 8.30 (s, 1H), 7.63 (d, J = 8 Hz, 2H), 7.19 (d, J = 8 Hz, 2H), 2.39 (s, 3H).

***O*-Trimethylsilyl-*p*-tolualdehyde oxime (5.23).** To a solution of *p*-tolualdehyde oxime **5.9** (1.00 g, 7.40 mmol) in CH_2Cl_2 (10 mL) was sequentially added triethylamine (1.13 mL, 8.15 mmol), 4-(dimethylamino)pyridine (90 mg, 0.74 mmol), and chlorotrimethylsilane (0.94 mL, 7.4 mmol) at room temperature. A white precipitate

formed immediately and the reaction mixture was stirred for an additional 2 h. The precipitate was removed by gravity filtration and the solid was washed with CH_2Cl_2 (3 x 5 mL). The filtrate was concentrated to a gummy white solid, which was purified by column chromatography (neutral alumina, 1:1 hexanes/chloroform). The product was isolated as a colorless oil, yield 1.05 g (68 %). ^{1}H NMR (CD_2Cl_2): δ 8.13 (s, 1H), 7.47 (d, J = 8 Hz, 2H), 7.17 (d, J = 8 Hz, 2H), 2.37 (s, 3H), 0.26 (s, 9H). ^{13}C NMR (125 MHz, CD_2Cl_2): δ 153.91, 140.77, 130.46, 129.89, 127.51, 21.73, -0.49. ^{29}Si NMR (CD_2Cl_2): δ 25.22. HRMS (EI) for $C_{11}H_{17}NOSi$ [M^+]: Calcd: 207.1079. Found: 207.1082.

***O*-Dimethylsilyl-*p*-tolualdehyde oxime (5.24).** A stirred mixture of triethylamine (1.80 mL, 13.0 mmol), *p*-tolualdehyde oxime **5.9** (1.35 g, 10.0 mmol), and chlorodimethylsilane (1.44 mL, 13.0 mmol) in Et_2O (40 mL) was stirred at room temperature for 24 h. The white precipitate of triethylamine hydrochloride was filtered off, washed with Et_2O (3 x 10 mL), and the solvent was flash distilled from the filtrate to leave a pale yellow oil. Vacuum distillation at 48 °C/10^{-3} Torr afforded the title compound as a colorless oil, yield 1.68 g (87 %) ^{1}H NMR (CD_2Cl_2): δ 8.12 (s, 1H), 7.50 (d, J = 8 Hz, 2H), 7.21 (d, J = 8 Hz, 2H), 4.83 (septet, $^3J_{HH}$ = 3 Hz, 1H), 2.37 (s, 3H), 0.36 (d, $^3J_{HH}$ = 3 Hz, 6H). ^{13}C NMR (CD_2Cl_2): δ 154.62, 141.06, 130.05, 129.94, 127.63, 21.74, -1.88. ^{29}Si NMR (CD_2Cl_2): δ 12.32. HRMS (EI) for $C_{10}H_{15}NOSi$ [M^+]: Calcd: 193.0923. Found: 193.0926. Anal. Calcd for $C_{10}H_{15}NOSi$: C, 62.13; H, 7.82; N, 7.25%. Found: C, 62.58; H, 7.42; N, 7.07%.

***O*-(Trimethylsilyl)-*p*-toluhydroxamoyl chloride (5.27).** *p*-Tolualdehyde chloroxime **5.10** (3.00 g, 17.7 mmol) was dissolved in Et_2O (80 mL) and the solution was then cooled to 0 °C. Triethylamine (2.94 mL, 21.2 mmol) was added rapidly via syringe, which resulted in the formation of a thick-white precipitate. Immediately after was added chlorotrimethylsilane (2.70 mL, 21.3 mmol). After stirring at 0 °C for 1 h, the white slurry was allowed to warm to room temperature and stirred overnight. The white precipitate of triethylamine hydrochloride was filtered off, washed with Et_2O (3 x 20 mL), and the solvent was flash distilled from the filtrate to leave a viscous yellow oil. Vacuum distillation at 75 °C/10^{-3} Torr afforded the title compound as a colorless oil, yield 3.64 g (85 %). ^{1}H NMR (CD_2Cl_2): δ 7.75 (d, J = 8 Hz, 2H), 7.22 (d, J = 8 Hz, 2H), 2.38 (s, 3H), 0.32 (s, 9H). ^{13}C NMR (125 MHz, CD_2Cl_2): δ 142.13, 141.68, 130.78, 129.64, 127.77, 21.64, -0.52. ^{29}Si NMR (CD_2Cl_2): δ 29.34. HRMS (EI) for $C_{11}H_{16}ClNOSi$ [M^+]: Calcd: 241.0690. Found: 241.0685. Anal. Calcd for $C_{11}H_{16}ClNOSi$: C, 54.64; H, 6.67; N, 5.79%. Found: C, 54.76; H, 6.46; N, 5.81%.

***O*-(Dimethylsilyl)-*p*-toluhydroxamoyl chloride (5.28).** *p*-Tolualdehyde chloroxime **5.10** (3.00 g, 17.7 mmol) was dissolved in Et_2O (80 mL) and the solution was then cooled to 0 °C. Triethylamine (2.94 mL, 21.2 mmol) was added rapidly via syringe, which resulted in the formation of a thick-white precipitate. Immediately after was added chlorodimethylsilane (2.40 mL, 21.6 mmol). After stirring at 0 °C for 1 h, the white slurry was allowed to warm to room temperature and stirred overnight. The white precipitate of triethylamine hydrochloride was filtered off, washed with Et_2O (3 x 20 mL), and the solvent was flash distilled from the filtrate to leave a viscous yellow oil. Vacuum

distillation at 80 °C/10^{-3} Torr afforded the title compound as a colorless oil, yield 3.38 g (84 %). ^{1}H NMR (CD_2Cl_2): δ 7.76 (d, J = 8 Hz, 2H), 7.22 (d, J = 8 Hz, 2H), 4.88 (septet, $^{3}J_{HH}$ = 3 Hz, 1H), 2.39 (s, 3H), 0.42 (d, $^{3}J_{HH}$ = 3 Hz, 6H). ^{13}C NMR (125 MHz, CD_2Cl_2): δ 143.21, 141.93, 130.47, 129.68, 127.82, 21.64, -1.91. ^{29}Si NMR (CD_2Cl_2): δ 15.18. HRMS (EI) for $C_{10}H_{14}ClNOSi$ [M^+]: Calcd: 227.0533. Found: 227.0538. Anal. Calcd for $C_{10}H_{14}ClNOSi$: C, 52.73; H, 6.20; N, 6.15%. Found: C, 52.53; H, 5.80; N, 6.46%.

***O*-(Chlorodimethylsilyl)-*p*-toluhydroxamoyl chloride (5.29).** To a solution of **5.28** (3.0 g, 13.2 mmol) in carbon tetrachloride (50 mL) was added catalytic palladium dichloride (234 mg, 10 mol %) at room temperature. An exothermic reaction immediately took place resulting in a dark brown reaction mixture. After the exothermic reaction ceased, the mixture was then heated to reflux for 24 h. The mixture was cooled to room temperature, and the solvents were removed by flash distillation leaving a dark black residue. Vacuum distillation at 85 °C/10^{-3} Torr afforded the title compound as a colorless oil, yield 1.97 g (57 %). ^{1}H NMR (CD_2Cl_2): δ 7.77 (d, J = 8 Hz, 2H), 7.24 (d, J = 8 Hz, 2H), 2.39 (s, 3H), 0.69 (s, 6H). ^{13}C NMR (125 MHz, CD_2Cl_2): δ 145.44, 142.44, 130.05, 129.76, 128.01, 21.69, 1.74. ^{29}Si NMR (CD_2Cl_2): δ 24.05. HRMS (EI) for $C_{10}H_{13}Cl_2NOSi$ [M^+]: Calcd: 261.0143. Found: 261.0139. Anal. Calcd for $C_{10}H_{13}Cl_2NOSi$: C, 45.81; H, 5.00; N, 5.34%. Found: C, 46.22; H, 5.13; N, 5.25%.

Reaction of 5.29 with hydroxylamine. To a stirred slurry of hydroxylamine hydrochloride (168 mg, 2.42 mmol) in THF (8 mL) was added triethylamine (0.30 mL, 2.16 mmol) via syringe. After stirring at room temperature for 24 h, the resulting

triethylamine hydrochloride salt was filtered off and washed with THF (3 x 4 mL). To the filtrate containing free hydroxylamine was added triethylamine (0.55 mL, 3.97 mmol), and the solution was then cooled to -30 °C. A solution of **5.29** (0.50 g, 1.91 mmol) in THF (10 mL) was added to the above via cannula, which resulted in the immediate precipitation of a white solid. This was stirred at -30 °C for 30 min, and then the mixture was warmed to room temperature and left to stir overnight. The white precipitate was filtered off, washed with THF (3 x 5 mL), and the filtrate was concentrated *in vacuo* to leave a viscous yellow oil. Addition of dichloromethane (10 mL) to this oil resulted in the precipitation of a white solid. The white solid was filtered, washed with cold CH_2Cl_2 (3 x 5 mL), and dried, yield 280 mg (67%). All spectral data match an authentic sample of *N*-hydroxy-*p*-toluamidoxime (**5.12**). ^{1}H NMR (DMSO): δ 10.21 (s, 1H), 8.36 (s, 1H), 8.11 (s, 1H), 7.43 (d, J = 8 Hz, 2H), 7.18 (d, J = 8 Hz, 2H), 2.30 (s, 3H). Mp: 90 °C (Lit.[144] mp 88 – 89 °C). The filtrate from above was concentrated by rotary evaporation to provide a sticky yellow solid. Column chromatography (neutral alumina, chloroform) provided a second component, which appears to be furoxan **5.13**, yield 55 mg (11 %). ^{1}H NMR (CD_2Cl_2): δ 7.38 (d, J = 8 Hz, 2H), 7.35 (d, J = 8 Hz, 2H), 7.21 (d, J = 8 Hz, 2H), 7.18 (d, J = 8 Hz, 2H), 2.39 (s, 3H), 2.37 (s, 3H). Mp: 143 °C (Lit.[165] mp 142 – 143 °C).

Reaction of 5.27 with hydroxylamine. To a slurry of hydroxylamine hydrochloride (730 mg, 10.5 mmol) in THF (15 mL) was added triethylamine (1.30 mL, 9.38 mmol) by syringe. After stirring at room temperature for 21 h, the solution containing free hydroxylamine was transferred with filtration to a solution of **5.27** (573 mg, 2.37 mmol) in THF (20 mL). After being left to stir overnight, the precipitate of hydroxylamine

hydrochloride was filtered off and washed with THF (2 x 10 mL). The filtrate was then concentrated *in vacuo* to provide a sticky white solid. To this was added CH_2Cl_2 (10 mL), which resulted in a powdery white solid. The solid was filtered, washed with CH_2Cl_2 (2 x 10 mL), and dried to afford *N*-hydroxy-*p*-toluamidoxime (**5.12**), yield 200 mg (58 %). ^{1}H NMR (DMSO): δ 10.21 (s, 1H), 8.36 (s, 1H), 8.11 (s, 1H), 7.43 (d, J = 8 Hz, 2H), 7.18 (d, J = 8 Hz, 2H), 2.30 (s, 3H).

Representative reaction for the attempted synthesis of 5.40. To a slurry of hydroxylamine hydrochloride (730 mg, 10.5 mmol) in THF (15 mL) was added triethylamine (1.30 mL, 9.38 mmol) by syringe. After stirring for 22.5 h, the resulting triethylamine hydrochloride was filtered off and washed with THF (2 x 5 mL). The filtrate was cooled to 0 °C and di-*tert*-butyldichlorosilane (0.5 mL, 2.37 mmol) was added dropwise by syringe. The mixture was warmed to room temperature and left to stir overnight. The insoluble byproducts were filtered and washed with THF (2 x 10 mL). The filtrate was concentrated to a sticky white solid, which was subsequently sublimed *in vacuo* (10^{-3} Torr) onto a cold finger at room temperature, yield 280 mg. Mp: 148 °C. ^{1}H NMR (C_6D_6): δ 1.18 (s, 4H), 1.08 (s, 1H). ^{13}C NMR (C_6D_6): δ 28.36, 27.86, 20.91, 20.37. ^{29}Si NMR (C_6D_6): δ -6.04, -9.05. MS (EI): *m/z* 196 (20%), 181 (8%), 134 (28%), 119 (39%), 105 (29%), 92 (30%), 77 (100%), 57 (32%). IR (KBr): 3439 (br, s), 3321 (br, s), 2967 (s), 2948 (s), 2934 (s), 2893 (s), 2860 (s), 1597 (w), 1477 (s), 1468 (s), 1390 (w), 1363 (m), 1216 (w), 1172 (w), 1055 (m), 1012 (m), 938 (m), 827 (s), 802 (s), 656 (m), 569 (w) cm^{-1}.

***O,O'*-Bis(ethylacethydroximate)methane (5.41).** This compound was prepared by the literature route.[161] A mixture of powdered NaOH (7.75 g, 0.19 mol) and ethyl acetohydroximate (20.0 g, 0.19 mol) in CH_3CN (300 mL) were brought to reflux. To this was added methylene iodide (8.6 mL, 0.10 mol) dropwise by syringe, and the solution was left to stir at reflux for 42 h. After which time the dark brown mixture was cooled to room temperature, and the volatiles were removed by rotary evaporation. Dichloromethane (250 mL) was added to the resulting brown sludge and the sodium iodide was filtered off. Removal of the solvent from the filtrate afforded a yellow oil, which was subsequently vacuum distilled (58 °C, 10^{-3} Torr) to provide the title compound as a colorless liquid, yield 12.0 g (58 %). ^{1}H NMR ($CDCl_3$): δ 5.28 (s, 2H), 4.05 (q, J = 7 Hz, 4H), 1.95 (s, 6H), 1.24 (t, J = 7 Hz, 6H).

Bis(hydrochloride) salt of *O,O'*-bis(hydroxylamino)methane (5.42). This compound was prepared by the literature route.[162] To a solution of **5.41** (10.0 g, 45.8 mmol) in diglyme (100 mL) was added concentrated hydrochloric acid (8.4 mL). The mixture was then heated to 60 °C for 20 min, and then cooled to room temperature. The resulting white precipitate was filtered off, washed with Et_2O (3 x 80 mL), and dried. Yield: 6.5 g (94 %). Mp: 150 °C (Lit.[162] 154 – 155 °C). Anal. Calcd $CH_8Cl_2N_2O_2$: C, 7.95; H, 5.34; N, 18.55%. Found: C, 7.93; H, 5.38; N, 18.19%.

Reaction of *O,O'*-bis(hydroxylamino)methane (5.43) with *p*-tolualdehyde. To a solution of the bis(hydrochloride) salt **5.42** (906 mg, 6.00 mmol) in MeOH (20 mL) was added triethylamine (1.66 mL, 12.0 mmol) rapidly by syringe. The mixture was then heated to a gentle reflux, and a solution of *p*-tolualdehyde (0.71 mL, 6.02 mmol) in

methanol (200 mL) was added dropwise over 5 h. After which time the mixture was left to reflux for an additional 15 h. The mixture was cooled to room temperature and the volatiles were removed by rotary evaporation. The remaining white solid was redissolved in $CHCl_3$ (80 mL) and washed with water (5 x 50 mL) to remove the triethylamine hydrochloride byproduct. The organic layer was collected, dried over $MgSO_4$, and evaporated under reduced pressure. The residue was subjected to column chromatography on silica gel using hexanes/ethyl acetate (1:1 v/v) as eluent to give a white semicrystalline solid of bis(imine) **5.44**, as the only isolable product. Yield: 480 mg (28%). ^{1}H NMR ($CDCl_3$): δ 8.20 (s, 2H), 7.43 (d, J = 8 Hz, 4H), 7.16 (d, J = 8 Hz, 4H), 5.68 (s, 2H), 2.28 (s, 6H). ^{13}C NMR ($CDCl_3$): δ 151.38, 140.68, 129.60, 129.16, 127.58, 99.58, 21.70. IR (Nujol): ν(C=N) 1608 (s) cm^{-1}. HRMS (EI) for $C_{17}H_{18}N_2O_2$ [M^+]: Calcd: 282.1368. Found: 282.1376.

Reaction of *O,O'*-bis(hydroxylamino)methane (5.43) with 2-pyridinecarboxaldehyde. To a solution of the bis(hydrochloride) salt **5.42** (2.70 g, 17.9 mmol) in MeOH (25 mL) was added triethylamine (4.98 mL, 35.9 mmol) rapidly by syringe. The mixture was then heated to a gentle reflux, and a solution of 2-pyridinecarboxaldehyde (1.70 mL, 17.9 mmol) in methanol (300 mL) was added dropwise over 5 h. After which time the mixture was left to reflux for an additional 18 h. The mixture was cooled to room temperature and the volatiles were removed by rotary evaporation. Diethyl ether (80 mL) was added to the residue, and the white solid of triethylamine hydrochloride was filtered off. Removal of the solvent from the filtrate gave a yellow oil, which was purified by column chromatography on basic alumina. The first component (R_f = 0.61) was eluted

with $CHCl_3$/EtOAc (4:1 v/v) to provide bis(imine) **5.49** as a white solid, yield 830 mg, (18%). ^{1}H NMR ($CDCl_3$): δ 8.58 (d, J = 3.7 Hz, 2H), 8.27 (s, 2H), 7.85 (d, J = 7.4 Hz, 2H), 7.67 (td, J = 7.4, 1.5 Hz, 2H), 7.24 (dd, J = 7.7, 5.1 Hz, 2H), 5.83 (s, 2H). ^{13}C NMR ($CDCl_3$): δ 152.20, 151.37, 149.94, 136.68, 124.59, 121.58, 100.02. IR (Nujol): ν(C=N) 1583 (s), 1561 (s) cm^{-1}. HRMS (EI) for $C_{13}H_{12}N_4O_2$ [M^+]: Calcd: 256.0960. Found: 256.0969. The second component (R_f = 0.39) was then eluted with EtOAc to provide mono(imine) **5.50** as a pale yellow liquid, yield 1.40 g (47%). ^{1}H NMR ($CDCl_3$): δ 8.60 (d, J = 4.4 Hz, 1H), 8.29 (s, 1H), 7.84 (d, J = 8.1 Hz, 1H), 7.68 (td, J = 7.4, 1.5 Hz, 1H), 7.27 (dd, J = 7.7, 5.1 Hz, 1H), 5.69 (s, 2H), 5.35 (s, 2H). ^{13}C NMR ($CDCl_3$): δ 151.84, 151.46, 149.93, 136.68, 124.55, 121.41, 101.59. IR (Neat): ν(NH) 3313 (s), 3241 (m), ν(C=N) 1583 (s), 1563 (s) cm^{-1}. HRMS (EI) for $C_7H_9N_3O_2$ [M^+]: Calcd: 167.0695. Found: 167.0697.

***O,O'*-Bis(ethylacethydroximate)dimethylsilane (5.51).** A stirred mixture of triethylamine (14.8 mL, 106.8 mmol), ethyl acetohydroximate (10.0 g, 97.0 mmol), and dichlorodimethylsilane (6.0 mL, 49.5 mmol) in toluene (300 mL) was heated at 85 ^{0}C for 4 h. After which time, the resulting thick-white suspension was cooled to room temperature and stirred overnight. The white precipitate of triethylamine hydrochloride was filtered off, washed with toluene (3 x 20 mL), and the solvent was flash distilled from the filtrate to leave an orange oil. Vacuum distillation at 50 ^{0}C/10^{-3} Torr afforded the title compound as a colorless oil, yield 12.2 g (94 %). ^{1}H NMR (C_6D_6): δ 4.00 (q, J = 7 Hz, 4H), 1.98 (s, 6H), 1.05 (t, J = 7 Hz, 6H), 0.57 (s, 6H). ^{13}C NMR (C_6D_6): δ 166.44, 62.74, 14.74, 13.94, -2.92. ^{29}Si NMR (C_6D_6): δ 4.89. IR (neat): 2980 (m), 2943 (w), 2902

(w), 1646 (s), 1397 (w), 1376 (s), 1302 (vs), 1255 (s), 1118 (w), 1095 (w), 1060 (m), 1011 (s), 979 (s), 926 (s), 873 (m), 828 (m), 805 (m), 665 (m) cm^{-1}. HRMS (EI) for $C_{10}H_{22}N_2O_4Si$ [M^+]: Calcd: 262.1349. Found: 262.1358. Anal. Calcd for $C_{10}H_{22}N_2O_4Si$: C, 45.78; H, 8.45; N, 10.68%. Found: C, 45.27; H, 8.33; N, 10.41%.

References

1. a) Fuchigami, H.; Tsumura, A.; Koezuka, H. *Appl. Phys. Lett.* **1993**, *63*, 1372. b) Garnier, F.; Peng, F. Z.; Horowitz, G.; Fichou, D. *Adv. Mater.* **1990**, *2*, 592. c) Garnier, F.; Hajlaoui, R.; Yassar, A.; Srivastava, P. *Science* **1994**, *265,* 1684.

2. a) Shirota, Y.; Kobata, T.; Noma, N. *Chem. Lett.* **1989**, 1145. b) Naito, K.; Miura, A. *J. Phys. Chem.* **1993**, *97*, 6240. c) Stolka, M.; Yanus, J. F.; Pai, D. M. *J. Phys. Chem.* **1984**, *88*, 4707. d) Tang, C. W.; VanSlyke, S. A. *Appl. Phys. Lett.* **1987**, *51*, 913. e) Shi, J.; Tang, C. W. *Appl. Phys. Lett.* **1997**, *70*, 1665.

3. a) Marsella, M. J.; Swager, T. M. *J. Am. Chem. Soc.* **1993**, *115*, 12214. b) Marsella, M. J.; Carroll, P. J.; Swager, T. M. *J. Am. Chem. Soc.* **1994**, *116*, 9347. c) Marsella, M. J.; Newland, R. J.; Carroll, P. J.; Swager, T. M. *J. Am. Chem. Soc.* **1995**, *117*, 9842. d) Marsella, M. J.; Carroll, P. J.; Swager, T. M. *J. Am. Chem. Soc.* **1995**, *117*, 9832.

4. a) Chiang, C. K.; Druy, M. A.; Gau, S. C.; Heeger, A. J.; Louis, E. J.; MacDiarmid, A. G.; Park, Y. W.; Shirakawa, H. *J. Am. Chem. Soc.* **1978**, *100*, 1013. b) Chiang, C. K.; Park, Y. W.; Heeger, A. J.; Shirakawa, H.; Louis, E. J.; MacDiarmid, A. G. *J. Chem. Phys.* **1978**, *69*, 5098. c) Chiang, C. K.; Fincher, C. R.; Park, Y. W.; Heeger, A. J.; Shirakawa, H.; Louis, E. J.; Gau, S. C.; MacDiarmid, A. G. *Phys. Rev. Lett.* **1977**, *39*, 1098. d) Shirakawa, H.; Louis, E. J.; MacDiarmid, A. G.; Chiang, C. K.; Heeger, A. J. *J. Chem. Soc., Chem. Commun.* **1977**, 578.

5. Deits, W.; Cukor, P.; Rubner, M.; Jopson, H. *J. Electron. Mater.* **1981**, *10*, 683.

6. Patil, A. O.; Heeger, A. J.; Wudl, F. *Chem. Rev.* **1988**, *88*, 183.

7. Deits, W.; Cukor, P.; Rubner, M.; Jopson, H. *Ind. Eng. Chem. Prod. Res. Dev.* **1981**, *20*, 696.

8. Roncali, J. *Chem. Rev.* **1992**, *92*, 711.

9. Sato, M.; Tanaka, S.; Kaeriyama, K. *J. Chem. Soc., Chem. Commun.* **1985**, 713.

10. a) Sato, M.; Tanaka, S.; Kaeriyama, K. *J. Chem. Soc., Chem. Commun.* **1986**, 873. b) Jen, K. Y.; Miller, G. G.; Elsenbaumer, R. L. *J. Chem. Soc., Chem. Commun.* **1986**, 1346.

11. a) McCullough, R. D.; Lowe, R. D.; Jayaraman, M.; Anderson, D. L. *J. Org. Chem.* **1993**, *58*, 904. b) McCullough, R. D.; Lowe, R. D. *J. Chem. Soc., Chem. Commun.* **1992**, 70.

12. Sotzing, G. A.; Reynolds, J. R.; Steel, P. J. *Chem. Mater.* **1996**, *8*, 882.

13. Akoudad, S.; Roncali, J. *Synth. Met.* **1999**, *101*, 149.

14. MacDiarmid, A. G. *Angew. Chem. Int. Ed.* **2001**, *40*, 2581.

15. a) Chiang, J. C.; Macdiarmid, A. G. *Synth. Met.* **1986**, *13*, 193. b) MacDiarmid, A. G.; Epstein, A. J. *Faraday Discuss.* **1989**, 317.

16. Cornil, J.; Beljonne, D.; Brédas, J. L. *J. Chem. Phys.* **1995**, *103*, 842.

17. a) Miller, L. L.; Mann, K. R. *Acc. Chem. Res.* **1996**, *29*, 417. b) Hong, Y. L.; Yu, Y.; Miller, L. L. *Synth. Met.* **1995**, *74*, 133.

18. *Electronic Materials: The Oligomer Approach.* Müllen, K.; Wegner, G. Wiley-VCH: Weinheim, 1998.

19. Kiehl, A.; Eberhardt, A.; Adam, M.; Enkelmann, V.; Müllen, K. *Angew. Chem. Int. Ed. Engl.* **1992**, *31*, 1588.

20. a) Horowitz, G.; Garnier, F.; Yassar, A.; Hajlaoui, R.; Kouki, F. *Adv. Mater.* **1996**, *8*, 52. b) Dodabalapur, A.; Torsi, L.; Katz, H. E. *Science* **1995**, *268*, 270. c) Dodabalapur, A.; Katz, H. E.; Torsi, L.; Haddon, R. C. *Science* **1995**, *269*, 1560.

21. a) Noda, T.; Shirota, Y. *J. Am. Chem. Soc.* **1998**, *120*, 9714. b) Noda, T.; Ogawa, H.; Shirota, Y. *Adv. Mater.* **1999**, *11*, 283.

22. Bäuerle, P.; Segelbacher, U.; Gaudl, K. U.; Huttenlocher, D.; Mehring, M. *Angew. Chem. Int. Ed. Engl.* **1993**, *32*, 76.

23. a) Fichou, D. *J. Mater. Chem.* **2000**, *10*, 571. b) Horowitz, G. *Adv. Mater.* **1998**, *10*, 365.

24. a) Guay, J.; Diaz, A.; Wu, R. L.; Tour, J. M.; Dao, L. H. *Chem. Mater.* **1992**, *4*, 254. b) Guay, J.; Kasai, P.; Diaz, A.; Wu, R. L.; Tour, J. M.; Dao, L. H. *Chem. Mater.* **1992**, *4*, 1097.

25. Hill, M. G.; Mann, K. R.; Miller, L. L.; Penneau, J. F. *J. Am. Chem. Soc.* **1992**, *114*, 2728.

26. a) Nakanishi, H.; Sumi, N.; Ueno, S.; Takimiya, K.; Aso, Y.; Otsubo, T.; Komaguchi, K.; Shiotani, M.; Ohta, N. *Synth. Met.* **2001**, *119*, 413. b) Apperloo, J. J.; Groenendaal, L.; Verheyen, H.; Jayakannan, M.; Janssen, R. A. J.; Dkhissi, A.; Beljonne, D.; Lazzaroni, R.; Brédas, J. L. *Chem. Eur. J.* **2002**, *8*, 2384. c) Nessakh, B.; Horowitz, G.; Garnier, F.; Deloffre, F.; Srivastava, P.; Yassar, A. *J. Electroanal. Chem.* **1995**, *399*, 97. d) Bäuerle, P.; Fischer, T.; Bidlingmeier, B.; Stabel, A.; Rabe, J. P. *Angew. Chem. Int. Ed. Engl.* **1995**, *34*, 303.

27. Bäuerle, P.; Segelbacher, U.; Maier, A.; Mehring, M. *J. Am. Chem. Soc.* **1993**, *115*, 10217.

28. Fichou, D.; Xu, B.; Horowitz, G.; Garnier, F. *Synth. Met.* **1991**, *41*, 463.

29. van Haare, J.; Havinga, E. E.; van Dongen, J. L. J.; Janssen, R. A. J.; Cornil, J.; Brédas, J. L. *Chem. Eur. J.* **1998**, *4*, 1509.

30. a) Graf, D. D.; Campbell, J. P.; Miller, L. L.; Mann, K. R. *J. Am. Chem. Soc.* **1996**, *118*, 5480. b) Graf, D. D.; Duan, R. G.; Campbell, J. P.; Miller, L. L.; Mann, K. R. *J. Am. Chem. Soc.* **1997**, *119*, 5888.

31. Merz, A.; Kronberger, J.; Dunsch, L.; Neudeck, A.; Petr, A.; Parkanyi, L. *Angew. Chem. Int. Ed.* **1999**, *38*, 1442.

32. Kozaki, M.; Yonezawa, Y.; Okada, K. *Org. Lett.* **2002**, *4*, 4535.

33. Tabakovic, I.; Maki, T.; Miller, L. L.; Yu, Y. A. *Chem. Commun.* **1996**, 1911.

34. Wakamiya, A.; Nishinaga, T.; Komatsu, K. *Chem. Commun.* **2002**, 1192.

35. Nishinaga, T.; Wakamiya, A.; Yamazaki, D.; Komatsu, K. *J. Am. Chem. Soc.* **2004**, *126*, 3163.

36. Gao, Y.; Liu, C. G.; Jiang, Y. S. *J. Phys. Chem. A* **2002**, *106*, 5380.

37. Noma, N.; Kawaguchi, K.; Imae, I.; Nakano, H.; Shirota, Y. *J. Mater. Chem.* **1996**, *6*, 117.

38. Engelmann, G.; Kossmehl, G.; Heinze, J.; Tschuncky, P.; Jugelt, W.; Welzel, H. P. *J. Chem. Soc., Perkin Trans. 2* **1998**, 169.

39. Miller, L. L.; Yu, Y. *J. Org. Chem.* **1995**, *60*, 6813.

40. Yu, Y.; Gunic, E.; Zinger, B.; Miller, L. L. *J. Am. Chem. Soc.* **1996**, *118*, 1013.

41. Tabakovic, I.; Maki, T.; Miller, L. L. *J. Electroanal. Chem.* **1997**, *424*, 35.

42. a) Nodwell, M. B. *Masters of Science Thesis*. University of Victoria **1999**. b) Hicks, R. G.; Nodwell, M. B. *J. Am. Chem. Soc.* **2000**, *122*, 6746.

43. Tour, J. M.; Jones, L.; Pearson, D. L.; Lamba, J. J. S.; Burgin, T. P.; Whitesides, G. M.; Allara, D. L.; Parikh, A. N.; Atre, S. V. *J. Am. Chem. Soc.* **1995**, *117*, 9529.

44. a) Creager, S.; Yu, C. J.; Bamdad, C.; O'Connor, S.; MacLean, T.; Lam, E.; Chong, Y.; Olsen, G. T.; Luo, J. Y.; Gozin, M.; Kayyem, J. F. *J. Am. Chem. Soc.* **1999**, *121*, 1059. b) Seminario, J. M.; Zacarias, A. G.; Tour, J. M. *J. Am. Chem. Soc.* **1998**, *120*, 3970. c) Bumm, L. A.; Arnold, J. J.; Cygan, M. T.; Dunbar, T. D.; Burgin, T. P.; Jones, L.; Allara, D. L.; Tour, J. M.; Weiss, P. S. *Science* **1996**, *271*, 1705. d) Dhirani, A. A.; Zehner, R. W.; Hsung, R. P.; GuyotSionnest, P.; Sita, L. R. *J. Am. Chem. Soc.* **1996**, *118*, 3319.

45. a) Reed, M. A.; Zhou, C.; Muller, C. J.; Burgin, T. P.; Tour, J. M. *Science* **1997**, *278*, 252. b) Yaliraki, S. N.; Kemp, M.; Ratner, M. A. *J. Am. Chem Soc.* **1999**, *121*, 3428. c) Samanta, M. P.; Tian, W.; Datta, S.; Henderson, J. I.; Kubiak, C. P. *Phys. Rev. B* **1996**, *53*, R7626.

46. Purcell, S. T.; Garcia, N.; Binh, V. T.; Jones, L.; Tour, J. M. *J. Am. Chem. Soc.* **1994**, *116*, 11985.

47. Smoes, S.; Vanderau, A; Drowart, J.; Mandy, F. *Bull. Soc. Chim. Belg.* **1972**, *81*, 45.

48. Seminario, J. M.; Zacarias, A. G.; Tour, J. M. *J. Am. Chem. Soc.* **1999**, *121*, 411.

49. Fan, F. R. F.; Yao, Y. X.; Cai, L. T.; Cheng, L.; Tour, J. M.; Bard, A. J. *J. Am. Chem. Soc.* **2004**, *126*, 4035.

50. Wolf, M. O. *Adv. Mater.* **2001**, *13*, 545.

51. MacDiarmid, A. G. *Rev. Mod. Phys.* **2001**, *73*, 701.

52. a) Brady, D. G. *J. Appl. Polym. Sci.* **1976**, *20*, 2541. b) Brady, D. G. *J. Appl. Polym. Sci.* **1981**, *36*, 231. c) Cheng, S. Z. D.; Wu, Z. Q.; Wunderlich, B. *Macromolecules* **1987**, *20*, 2802.

53. Ikeda, Y.; Ozaki, M.; Arakawa, T. *J. Chem. Soc., Chem. Commun.* **1983**, 1518.

54. Berlin, A.; Pagani, G. A.; Sannicolo, F. *J. Chem. Soc., Chem. Commun.* **1986**, 1663.

55. Groenendaal, L.; Zotti, G.; Aubert, P. H.; Waybright, S. M.; Reynolds, J. R. *Adv. Mater.* **2003**, *15*, 855.

56. a) Murray, M. M.; Kaszynski, P.; Kaisaki, D. A.; Chang, W. H.; Dougherty, D. A. *J. Am. Chem. Soc.* **1994**, *116*, 8152. b) Stickley, K. R.; Blackstock, S. C. *J. Am. Chem. Soc.* **1994**, *116*, 11576. c) Wienk, M. M.; Janssen, R. A. J. *J. Am. Chem. Soc.* **1997**, *119*, 4492.

57. Wienk, M. M.; Janssen, R. A. J. *J. Am. Chem. Soc.* **1996**, *118*, 10626.

58. van Haare, J.; van Boxtel, M.; Janssen, R. A. J. *Chem. Mater.* **1998**, *10*, 1166.

59. Smith, M. B.; March, J. *March's Advanced Organic Chemistry.* 5th Ed. John Wiley and Sons, New York. **2001**.

60. Tour, J. M.; Wu, R. L. *Macromolecules* **1992**, *25*, 1901.

61. Chinchilla, R.; Najera, C.; Yus, M. *Chem. Rev.* **2004**, *104*, 2667.

62. Reddinger, J. L.; Reynolds, J. R. *J. Org. Chem.* **1996**, *61*, 4833.

63. Hassan, J.; Sevignon, M.; Gozzi, C.; Schulz, E.; Lemaire, M. *Chem. Rev.* **2002**, *102*, 1359.

64. Steinkopf, W.; Leitsmann, R.; Hofmann, K. *Lieb. Ann. Chem.* **1941**, *546,* 180.

65. Greving, B.; Waterman, A; Kauffman, T. *Angew. Chem. Int. Ed. Engl.* **1974**, *13*, 467.

66. Nakayama, J.; Konishi, T.; Murabayashi, S.; Hoshino, M. *Heterocycles* **1987**, *26*, 1793.

67. Stille, J. K. *Angew. Chem. Int. Ed. Engl.* **1986**, *25*, 508.

68. a) Littke, A. F.; Fu, G. C. *Angew. Chem. Int. Ed.* **1999**, *38*, 2411. b) Littke, A. F.; Fu, G. C. *Angew. Chem. Int. Ed.* **2002**, *41*, 4176.

69. Tamao, K.; Kodama, S.; Nakajima, I.; Kumada, M.; Minato, A.; Suzuki, K. *Tetrahedron* **1982**, *38*, 3347.

70. Nakayama, J.; Katano, N.; Shimura, Y.; Sugihara, Y.; Ishii, A. *J. Org. Chem.* **1996**, *61*, 7608.

71. Torres-Nieto, J.; Arevalo, A.; Garcia-Gutierrez, P.; Acosta-Ramirez, A.; Garcia, J. J. *Organometallics* **2004**, *23*, 4534.

72. Jong, F. D.; Janssen, M. J. *J. Org. Chem.* **1971**, *36*, 1645.

73. a) Rulkens, R.; Gates, D. P.; Balaishis, D.; Pudelski, J. K.; McIntosh, D. F.; Lough, A. J.; Manners, I. *J. Am. Chem. Soc.* **1997**, *119*, 10976. b) Li, X. C.; Sirringhaus, H.; Garnier, F.; Holmes, A. B.; Moratti, S. C.; Feeder, N.; Clegg, W.; Teat, S. J.; Friend, R. H. *J. Am. Chem. Soc.* **1998**, *120*, 2206.

74. Mitchell, R. H.; Lai, Y. H.; Williams, R. V. *J. Org. Chem.* **1979**, *44*, 4733.

75. a) Meng, H.; Perepichka, D. F.; Bendikov, M.; Wudl, F.; Pan, G. Z.; Yu, W. J.; Dong, W. J.; Brown, S. *J. Am. Chem. Soc.* **2003**, *125*, 15151. b) Meng, H.; Perepichka, D. F.; Wudl, F. *Angew. Chem. Int. Ed. Engl.* **2003**, *42*, 658.

76. Chisholm, M. H.; Corning, J. F.; Huffman, J. C. *Inorg. Chem.* **1984**, *23*, 754.

77. Jones, E.; Moodie, I. M. *Organic Syntheses*. Wiley: New York, **1988**; Coll. Vol. 6, 979.

78. Wu, R. L.; Schumm, J. S.; Pearson, D. L.; Tour, J. M. *J. Org. Chem.* **1996**, *61*, 6906.

79. Zhu, S. S.; Swager, T. M. *J. Am. Chem. Soc.* **1997**, *119*, 12568.

80. Turbiez, M.; Frere, P.; Blanchard, P.; Roncali, J. *Tetrahedron Lett.* **2000**, *41*, 5521.

81. Casado, J.; Navarrete, J. T. L. *Unpublished Results*.

82. Hill, M. G.; Penneau, J. F.; Zinger, B.; Mann, K. R.; Miller, L. L. *Chem. Mater.* **1992**, *4*, 1106.

83. a) Casado, J.; Hicks, R. G.; Hernandez, V.; Myles, D. J. T.; Delgado, M. C. R.; Navarrete, J. T. L. *J. Chem. Phys.* **2003**, *118*, 1912. b) Casado, J.; Zgierski, M. Z.; Hicks, R. G.; Myles, D. J. T.; Orti, E.; Hernandez, V.; Navarrete, J. T. L. *Manuscript in Preparation.*

84. Connelly, N. G.; Geiger, W. E. *Chem. Rev.* **1996**, *96*, 877.

85. Chahma, M.; Hicks, R. G.; Myles, D. J. T. *Macromolecules* **2004**, *37*, 2010.

86. Heeger, A. J. *Angew. Chem. Int. Ed.* **2001**, *40*, 2591.

87. a) Jen, K. Y.; Benfaremo, N.; Cava, M. P.; Huang, W. S.; MacDiarmid, A. G. *J. Chem. Soc., Chem. Commun.* **1983**, 633. b) Cava, M. P.; Lakshmikantham, M. V.; Jen, K. Y.; Benfaremo, N.; Huang, W. S.; MacDiarmid, A. G. *Abstr. Pap. Am. Chem. Soc.* **1983**, *185*, 152.

88. Chahma, M.; Hicks, R. G. *Can. J. Chem.* **2004**, *82*, 1629.

89. Power, P. P. *Chem. Rev.* **2003**, *103*, 789.

90. a) Rajca, A. *Chem. Rev.* **1994**, *94*, 871. b) Miller, J. S.; Epstein, A. J. *Angew. Chem. Int. Ed. Engl.* **1994**, *33*, 385. c) Barclay, T. M.; Cordes, A. W.; Haddon, R. C.; Itkis, M. E.; Oakley, R. T.; Reed, R. W.; Zhang, H. *J. Am. Chem. Soc.* **1999**, *121*, 969. d) Itkis, M. E.; Chi, X.; Cordes, A. W.; Haddon, R. C. *Science* **2002**, *296*, 1443.

91. a) Keana, J. F. W. *Chem. Rev.* **1978**, *78*, 37. b) Borbat, P. P.; Costa-Filho, A. J.; Earle, K. A.; Moscicki, J. K.; Freed, J. H. *Science* **2001**, *291*, 266. c) Yordanov, A. T.; Yamada, K.; Krishna, M. C.; Mitchell, J. B.; Woller, E.; Cloninger, M.; Brechbiel, M. W. *Angew. Chem. Int. Ed.* **2001**, *40*, 2690. d) Reddy, T. J.; Iwama, T.; Halpern, H. J.; Rawal, V. H. *J. Org. Chem.* **2002**, *67*, 4635.

92. a) Studer, A. *Chem. Eur. J.* **2001**, *7*, 1159. b) Fischer, H. *Chem. Rev.* **2001**, *101*, 3581. c) Georges, M. K.; Veregin, R. P. N.; Kazmaier, P. M.; Hamer, G. K. *Macromolecules* **1993**, *26*, 2987. d) Hawker, C. J.; Bosman, A. W.; Harth, E. *Chem. Rev.* **2001**, *101*, 3661.

93. Sullivan, P. J.; Koski, W. S. *J. Am. Chem. Soc.* **1963**, *85*, 384.

94. Griller, D.; Ingold, K. U. *Acct. Chem. Res.* **1976**, *9*, 13.

95. Mendenha, G; Griller, D.; Lindsay, D.; Tidwell, T. T.; Ingold, K. U. *J. Am. Chem. Soc.* **1974**, *96*, 2441.

96. Gomberg, M. *J. Am. Chem. Soc.* **1901**, *22*, 757.

97. McBride, J. M. *Tetrahedron* **1974**, *30*, 2009.

98. a) Sabacky, M. J.; Johnson, C. S.; Smith, R. G.; Gutowsky, H. S.; Martin, J. C. *J. Am. Chem. Soc.* **1967**, *89*, 2054. b) Muller, E.; Moosmayer, A.; Rieker, A.; Scheffle, K. *Tetrahedron Lett.* **1967**, 3877. c) Neugebauer, F. A.; Hellwinkel, D.; Aulmich, G. *Tetrahedron Lett.* **1978**, 4871.

99. Andersen, P.; Klewe, B. *Acta Chem. Scand.* **1967**, *21*, 2599.

100. Schlenk, W.; Brauns, M. *Chem. Ber.* **1915**, *48*, 661.

101. Rajca, A.; Utamapanya, S. *J. Am. Chem. Soc.* **1993**, *115*, 2396.

102. Rajca, A.; Wongsriratanakul, J.; Rajca, S.; Cerny, R. *Angew. Chem. Int. Ed.* **1998**, *37*, 1229.

103. Rajca, A. *Chem. Eur. J.* **2002**, *8*, 4834.

104. Reid, D. H. *Tetrahedron* **1958**, *3*, 339.

105. Goto, K.; Kubo, T.; Yamamoto, K.; Nakasuji, K.; Sato, K.; Shiomi, D.; Takui, T.; Kubota, M.; Kobayashi, T.; Yakusi, K.; Ouyang, J. Y. *J. Am. Chem. Soc.* **1999**, *121*, 1619.

106. Koutentis, P. A.; Chen, Y.; Cao, Y.; Best, T. P.; Itkis, M. E.; Beer, L.; Oakley, R. T.; Cordes, A. W.; Brock, C. P.; Haddon, R. C. *J. Am. Chem. Soc.* **2001**, *123*, 3864.

107. Pal, S. K.; Itkis, M. E.; Reed, R. W.; Oakley, R. T.; Cordes, A. W.; Tham, F. S.; Siegrist, T.; Haddon, R. C. *J. Am. Chem. Soc.* **2004**, *126*, 1478.

108. Zheng, S. J.; Lan, J.; Khan, S. I.; Rubin, Y. *J. Am. Chem. Soc.* **2003**, *125*, 5786.

109. Fremy, E. *Ann. Chim. Phys.* **1845**, *15*, 459.

110. Forrester, A. R.; Hay, J. M.; Thomson, R. H. *Organic Chemistry of Stable Free Radicals.* Academic Press, London. **1968.**

111. Neiman, M. B.; Rozantsev, E. G.; Mamedova, Yu. G. *Nature London.* **1963**, *200*, 256.

112. Delpierre, G. R.; Lamchen, M. *Quart. Rev.* **1965**, *19*, 329.

113. Adams, J. Q.; Nicksic, S. N.; Thomas, J. R. *J. Chem. Phys.* **1966**, *45*, 654.

114. Forrester, A. R.; Thomson, R. H. *Nature* **1964**, *203*, 74.

115. a) Keana, J. F. W.; Lex, L.; Mann, J. S.; May, J. M.; Park, J. H.; Pou, S.; Prabhu, V. S.; Rosen, G. M.; Sweetman, B. J.; Wu, Y. *Pure Appl. Chem.* **1990**, *62*, 201. b) Volodarsky, L. B. *Pure Appl. Chem.* **1990**, *62*, 177.

116. Osiecki, J. H.; Ullman, E. F. *J. Am. Chem. Soc.* **1968**, *90*, 1078.

117. a) Goldschmidt, S. *Ber.* **1920**, *53*, 44. b) Goldschmidt, S.; Renn, K. *Ber.* **1922**, *55*, 628-647. c) Goldschmidt, S.; Graef, F. *Ber.* **1928**, *61*, 1858.

118. Holt, P. F.; Hughes, B. P. *J. Chem. Soc.* **1955**, 1320.

119. Kuhn, R.; Trischmann, H. *Angew. Chem. Int. Ed. Engl.* **1963**, *2*, 155.

120. Williams, D. E. *Acta Crystallogr.* **1973**, *B29*, 96.

121. a) Neugebauer, F. A.; Fischer, H.; Krieger, C. *J. Chem. Soc. Perkin Trans. 2* **1993**, 535. b) Brook, D. J. R.; Fox, H. H.; Lynch, V.; Fox, M. A. *J. Phys. Chem.* **1996**, *100*, 2066.

122. Hicks, R. G.; Hooper, R. *Inorg. Chem.* **1999**, *38*, 284.

123. Hicks, R. G.; Ohrstrom, L.; Patenaude, G. W. *Inorg. Chem.* **2001**, *40*, 1865.

124. Barclay, T. M.; Hicks, R. G.; Ichimura, A. S.; Patenaude, G. W. *Can. J. Chem.* **2002**, *80*, 1501.

125. Heal, H. G. *Adv. Inorg. Chem. Radiochem.* **1972**, *15*, 375.

126. Hassanzadeh, P.; Andrews, L. *J. Am. Chem. Soc.* **1992**, *114*, 83.

127. a) Miura, Y.; Asada, H.; Kinoshita, M. *Bull. Chem. Soc. Jpn.* **1977**, *50*, 1855. b) Miura, Y.; Yamamoto, A.; Katsura, Y.; Kinoshita, M. *J. Org. Chem.* **1980**, *45*, 3875. c) Miura, Y.; Asada, H.; Kinoshita, M. *Bull. Chem. Soc. Jpn.* **1980**, *53*, 720.

128. a) Miura, Y.; Kitagishi, Y.; Ueno, S. *Bull. Chem. Soc. Jpn.* **1994**, *67*, 3282. b) Miura, Y.; Tanaka, A.; Hirotsu, K. *J. Org. Chem.* **1991**, *56*, 6638. c) Miura, Y.; Katsura, Y.; Kinoshita, M. *Bull. Chem. Soc. Jpn.* **1979**, *52*, 1121.

129. a) Miura, Y.; Yamamoto, A.; Katsura, Y.; Kinoshita, M. *J. Org. Chem.* **1982**, *47*, 2618. b) Nakatsuji, M.; Miura, Y.; Teki, Y. *J. Chem. Soc. Perkin Trans. 2* **2001**, 738.

130. Oakley, R. T. *Can. J. Chem.* **1993**, *71*, 1775.

131. a) Aherne, C. M.; Banister, A. J.; Gorrell, I. B.; Hansford, M. I.; Hauptman, Z. V.; Luke, A. W.; Rawson, J. M. *J. Chem. Soc. Dalton Trans.* **1993**, 967. b) Cordes, A. W.; Haddon, R. C.; Oakley, R. T.; Schneemeyer, L. F.; Waszczak, J. V.; Young, K. M.; Zimmerman, N. M. *J. Am. Chem. Soc.* **1991**, *113*, 582. c) Cordes, A. W.; Chamchoumis, C. M.; Hicks, R. G.; Oakley, R. T.; Young, K. M.; Haddon, R. C. *Can. J. Chem.-Rev. Can. Chim.* **1992**, *70*, 919. d) Beer, L., Cordes, A.W., Myles, D.J.T., Oakley, R.T., and Taylor, N.J. *CrystEngComm* **2000**, *20*, 109.

132. Boeré, R. T.; Hicks, R. G.; Oakley, R. T. *Inorg. Synth.* **1996**, *36*, 94.

133. Parsons, S.; Passmore, J.; Schriver, M. J.; Sun, X. P. *Inorg. Chem.* **1991**, *30*, 3342.

134. a) Banister, A. J.; Hansford, M. I.; Hauptman, Z. V.; Wait, S. T.; Clegg, W. *J. Chem. Soc. Dalton Trans.* **1989**, 1705. b) Vegas, A.; Perezsalazar, A.; Banister, A. J.; Hey, R. G. *J. Chem. Soc. Dalton Trans.* **1980**, 1812. c) Andrews, M. P.; Cordes, A. W.; Douglass, D. C.; Fleming, R. M.; Glarum, S. H.; Haddon, R. C.; Marsh, P.; Oakley, R. T.; Palstra, T. T. M.; Schneemeyer, L. F.; Trucks, G. W.; Tycko, R.; Waszczak, J. V.; Young, K. M.; Zimmerman, N. M. *J. Am. Chem. Soc.*

1991, *113*, 3559. d) Cordes, A. W.; Haddon, R. C.; Hicks, R. G.; Oakley, R. T.; Palstra, T. T. M.; Schneemeyer, L. F.; Waszczak, J. V. *J. Am. Chem. Soc.* **1992**, *114*, 5000.

135. Banister, A. J.; Bricklebank, N.; Clegg, W.; Elsegood, M. R. J.; Gregory, C. I.; Lavender, I.; Rawson, J. M.; Tanner, B. K. *J. Chem. Soc. Chem. Commun.* **1995**, 679.

136. Banister, A. J.; Bricklebank, N.; Lavender, I.; Rawson, J. M.; Gregory, C. I.; Tanner, B. K.; Clegg, W.; Elsegood, M. R. J.; Palacio, F. *Angew. Chem. Int. Ed. Engl.* **1996**, *35*, 2533.

137. Brooks, W. V. F.; Burford, N.; Passmore, J.; Schriver, M. J.; Sutcliffe, L. H. *J. Chem. Soc. Chem. Commun.* **1987**, 69.

138. Maclean, G. K.; Passmore, J.; Rao, M. N. S.; Schriver, M. J.; White, P. S.; Bethell, D.; Pilkington, R. S.; Sutcliffe, L. H. *J. Chem. Soc. Dalton Trans.* **1985**, 1405.

139. Wolmershauser, G.; Kraft, G. *Chem. Ber.* **1990**, *123*, 881.

140. Barclay, T. M.; Cordes, A. W.; George, N. A.; Haddon, R. C.; Oakley, R. T.; Palstra, T. T. M.; Patenaude, G. W.; Reed, R. W.; Richardson, J. F.; Zhang, H. Z. *Chem. Commun.* **1997**, 873.

141. a) Danen, W. C.; Neugebauer, F. A. *Angew. Chem. Int. Ed. Engl.* **1975**, *14*, 783. b) Danen, W. C.; West, C. T.; Kensler, T. T. *J. Am. Chem. Soc.* **1973**, *95*, 5716. c) Kaba, R. A.; Ingold, K. U. *J. Am. Chem. Soc.* **1976**, *98*, 7375. d) Woynar, H.; Ingold, K. U. *J. Am. Chem. Soc.* **1980**, *102*, 3813. e) Ahrens, W.; Wieser, K.; Berndt, A. *Tetrahedron Lett.* **1973**, 3141. f) Balaban, A. T.; Frangopo.Pt; Frangopo.M; Negoita, N. *Tetrahedron* **1967**, *23*, 4661. g) Negoita, N.; Baican, R.; Balaban, A. T. *Tetrahedron Lett.* **1973**, 1877.

142. a) Miura, Y.; Nishi, T.; Teki, Y. *J. Org. Chem.* **2003**, *68*, 10158. b) Miura, Y.; Tomimura, T.; Matsuba, N.; Tanaka, R.; Nakatsuji, M.; Teki, Y. *J. Org. Chem.* **2001**, *66*, 7456. c) Miura, Y.; Matsuba, N.; Tanaka, R.; Teki, Y.; Takui, T. *J. Org. Chem.* **2002**, *67*, 8764.

143. Neugebauer, F. A. *Angew. Chem. Int. Ed. Engl.* **1973**, *12*, 455.

144. Patenaude, G. W. *Ph.D. Dissertation.* University of Victoria **2002**.

145. a) Armand, J. *Bull. Soc. Chim. Fr.* **1966**, 1658. b) Eloy, F.; Lenears, R. *Chem. Rev.* **1962**, *62*, 155.

146. Desherces, S.; Barrans, J.; Roubaty, J. L. *Rev. Roum. Chim.* **1978**, *23*, 203.

147. Liu, K. C.; Shelton, B. R.; Howe, R. K. *J. Org. Chem.* **1980**, *45*, 3916.

148. Mitchell, W. R.; Paton, R. M. *Tetrahedron Lett.* **1979**, 2443.

149. Cunico, R. F.; Bedell, L. *J. Organomet. Chem.* **1985**, *281*, 135.

150. Grundmann, C; Dean, J. M. *J. Org. Chem.* **1965**, *30*, 2809.

151. Cunico, R. F.; Bedell, L. *J. Org. Chem.* **1983**, *48*, 2780.

152. Grundmann, C.; Grünanger, P. *The Nitrile Oxides*, Springer-Verlag, New York, **1971**.

153. a) Mitzel, N. W.; Blake, A. J.; Rankin, D. W. H. *J. Am. Chem. Soc.* **1997**, *119*, 4143. b) Losehand, U.; Mitzel, N. W. *J. Chem. Soc. Dalton Trans.* **1998**, 2537. c) Mitzel, N. W.; Losehand, U. *J. Am. Chem. Soc.* **1998**, *120*, 7320. d) Losehand, U.; Mitzel, N. W. *Inorg. Chem.* **1998**, *37*, 3175. e) Wolfgramm, R.; Muller, T.; Klingebiel, U. *Organometallics* **1998**, *17*, 3222. f) West, R.; Boudjouk, P. *J. Am. Chem. Soc.* **1973**, *95*, 3987.

154. Bottaro, J. C.; Bedford, C. D.; Dodge, A. *Synth. Commun.* **1985**, *15*, 1333.

155. Lecher, H.; Hofmann, J. *Chem. Ber.* **1992**, *55*, 912.

156. Neugebauer, F. A.; Fischer, H. *Angew. Chem. Int. Ed. Engl.* **1980**, *19*, 724.

157. a) Bernardi, P.; Dembech, P.; Fabbri, G.; Ricci, A.; Seconi, G. *J. Org. Chem.* **1999**, *64*, 641. b) Smulik, J. A.; Vedejs, E. *Org. Lett.* **2003**, *5*, 4187.

158. Harger, M. J. P. *J. Chem. Soc. Perkin Trans. 1* **1981**, 3284.

159. Tamura, Y.; Minamikawa, J.; Ikeda, M. *Synthesis* **1977**, 1.

160. Ebker, C.; Diedrich, F.; Klingebiel, U.; Noltemeyer, M.; Schmatz, S. *Organometallics* **2003**, *22*, 2594.

161. McDowell, C. S.; Barnes, M. W. *United States Patent 3,709,920,* **1973**.

162. McDowell, C. S.; Merill, C. *United States Patent 3,714,199*, **1973**.

163. a) Barr, C. L.; Chase, P. A.; Hicks, R. G.; Lemaire, M. T.; Stevens, C. L. *J. Org. Chem.* **1999**, *64*, 8893. b) Barclay, T. M.; Hicks, R. G.; Lemaire, M. T.;

Thompson, L. K. *Inorg. Chem.* **2003**, *42*, 2261. c) Barclay, T. M.; Hicks, R. G.; Lemaire, M. T.; Thompson, L. K. *Inorg. Chem.* **2001**, *40*, 6521.

164. a) Barclay, T. M.; Hicks, R. G.; Lemaire, M. T.; Thompson, L. K. *Inorg. Chem.* **2001**, *40*, 5581. b) Barclay, T. M.; Hicks, R. G.; Lemaire, M. T.; Thompson, L. K. *Chem. Commun.* **2000**, 2141. c) Hicks, R. G.; Lemaire, M. T.; Thompson, L. K.; Barclay, T. M. *J. Am. Chem. Soc.* **2000**, *122*, 8077. d) Barclay, T. M.; Hicks, R. G.; Lemaire, M. T.; Thompson, L. K.; Xu, Z. Q. *Chem. Commun.* **2002**, 1688. e) Hicks, R. G.; Lemaire, M. T.; Ohrstrom, L.; Richardson, J. F.; Thompson, L. K.; Xu, Z. Q. *J. Am. Chem. Soc.* **2001**, *123*, 7154.

165. Wiley, R. H.; Wakefield, B. J. *J. Org. Chem.* **1960**, *25*, 546.